An Experimental Approach in Reconstructing "Invisible" Knapping Variables in the Early Pleistocene Archaeological Record

Dissertation

der Mathematisch-Naturwissenschaftlichen Fakultät

der Eberhard Karls Universität Tübingen

zur Erlangung des Grades eines

Doktors der Naturwissenschaften

(Dr. rer. nat.)

vorgelegt von

Li Li

aus Peking, China

Tübingen

2022

Gedruckt mit Genehmigung der Mathematisch-Naturwissenschaftlichen Fakultät der Eberhard Karls Universität Tübingen.

Tag der mündlichen Qualifikation:	27.06.2022
Dekan:	Prof. Dr. Thilo Stehle
1. Berichterstatter/-in:	Dr. Claudio Tennie
2. Berichterstatter/-in:	Prof. Dr. Nicolas J. Conard

For my parents

致父母

Acknowledgments

Above all, I would like to express my sincere gratitude to my advisor Shannon McPherron for his continued support throughout the duration of my Ph.D., and for his patience, motivation, enthusiasm, and immense knowledge. Thank you Shannon for encouraging me to pursue this experimental line of lithic research and for adopting me as your student. Thank you for challenging me with new questions and training me to become a better archaeologist. Thank you for always listening to my questions so patiently and offering wise feedback. Thank you for supporting me, and pushing me to finish my project during the pandemic. Your help has made this journey much less scary and much more manageable. I look forward to the many experiments we will do together in the future.

I would also like to thank my other thesis advisors: Claudio Tennie, Sam Lin, and Jonathan Reeves. Thank you Claudio for welcoming me to Tübingen and sharing your expertise with me so selflessly. Thank you for always being so supportive and encouraging. I am grateful to be a member of your lab, and for the opportunity to get out of my comfort zone when learning about cumulative culture and primate tool use. Thank you Sam for your guidance and help throughout my Ph.D. journey. Thank you also for supporting me through the abrupt change in my Ph.D. study plans, and for always having my back. Thank you for brainstorming experiment ideas with me and continuing to patiently help me with my writing. Thank you for adjusting to the time difference during all our meetings. Thank you Jon for your guidance and help in formulating my thesis project and in my application for the Leakey Research Grant. Thank you for your incredibly insightful feedback and constant encouragement that has pushed me to keep marching along this journey. Thank you for your help too with my data collection in Nairobi, without which I could not have gotten all the data I need to complete my thesis. I could not have imagined having a better team of thesis advisors, truly.

My gratitude also goes to my TAC committee member Oliver Betz for his generous help and insightful feedback during all my TAC meetings. I would also like to thank Nick Conard for welcoming me to our department and for being generously supportive of my study. Thank you Nick for reminding me to stay focused and produce good work. I am also grateful to David Braun for granting me access to the

collections at Nairobi National Museum and for having insightful scientific discussions with me. I would also like to thank Mima, for helping me with administrative matters with great patience and kindness in the past three years.

I am indebted to Nicolas Zwyns, Teresa Steele, and Tim Weaver for introducing me to the field of paleoanthropology and archaeology. Thank you for kindly welcoming me to your research group at the University of California, Davis. Without your kindness and help, I would not be able to pursue my dreams in archaeology.

I would like to say a special thank you to the late Harold Dibble. Although I was only a Harold's student for one short year, I have learned so much from him, not only during his lectures, but also office hours and at lunches. His passion for science will forever encourage me to go forward.

I have been very lucky to work with wonderful lab mates over the past three years – thank you Alba, Elisa, Jordy, and Will for your help. Thank you Will for helping me with translating the abstract to German. It is a shame that we could not spend more time together in the lab because of the pandemic. I would also like to thank the EVEREST members for their support. Thank you too to Aylar, Giulia, and Kim for being the best Ph.D. buddies and friends one could ask for. I am so lucky and honored to be able to do my Ph.D. with you, and grateful for all the laughter and tears that we have shared along our journeys. Thank you Mingxi, Jing, Geyu, Anna, Eunha, and Harry for your precious friendship. I cannot tell you how much your love and support have brightened up this journey.

Finally, I would like to thank my parents. This thesis is dedicated to my Mom and Dad, who have always been my biggest advocates. Thank you Mom and Dad for your unconditional love and support. Thank you for sending me abroad after high school, for broadening my horizons and supporting me as I pursued what I love. Thank you for teaching me to be brave and trust myself and for never questioning my decisions. I owe everything I have accomplished to my parents.

Abstract

Stone artifacts are the most prevalent pieces of evidence for studying prehistoric hominin behaviors. The emergence and development of stone tool technology delineate the trajectory of human evolution and are argued to represent a distinctive form of hominin culture in comparison with other species. Reconstructing hominins' technical decisions from the archaeological record of stone tools is an important approach for studying their behavior and cognition. Much has been learned in this regard using approaches such as reconstructing reduction sequences, analyzing the morphological characteristics of the stone artifacts, identifying raw material procurement patterns, and analyzing use-wear patterns. However, how early hominins managed various force delivery variables, in other words how they struck off flakes, is still not well understood because these variables are difficult to directly measure from the archaeological record.

This thesis sets out to investigate one such force delivery variable, namely the angle of blow (i.e., the angle at which the hammer strikes the core's platform for flake removal) using an experimental approach. Controlled flaking experiments have increasingly become crucial in lithic studies by virtue of their ability to quantify knapping behaviors into measurable lithic attributes. Controlled experiments are improving and evolving to create a robust framework for archaeologists to form and test different hypotheses related to the production and use of stone tools while generating reproducible results.

The structure of this thesis is threefold. First, I review and synthesize what we know about flake formation from previous controlled flaking experiments (Chapter 2). Second, I design a controlled experiment guided by principles coming from fracture mechanics to study the effect of the angle of blow on flake formation and to establish a way to measure it on flakes (Chapter 3). The experimental results show that the angle of blow is visible and measurable on a feature of the bulb of percussion that I name the bulb angle. Third, I use the bulb angle measurement coming from the controlled experiment to measure flakes from a series of Early Pleistocene assemblages to investigate how early hominins managed their angles of blow during knapping (Chapter 4). I find evidence that early hominins began to appreciate the

impact of angle of blow through the application of a more systematic control over the angle of blow towards the Oldowan-Acheulean transition.

The experimental approach applied here illustrates how important insights can be gained to complement the more traditional technological approaches for studying hominins' technical capabilities. The results of this thesis 1) show the usefulness of controlled experimentation in lithic studies and the importance of designing experiments that can effectively link knapping behaviors to measurable lithic attributes, drawing on information from fracture mechanics; 2) show a temporal progression in early hominins' understanding and control over the angle of blow through time; and thereby 3) provide insights into the evolution of early hominin behavior and cognition, which in turn has the potential to help clarify debates over the onset of cumulative culture in human prehistory.

Abstrakt

Steinartefakte sind das häufigste Beweismittel für die Untersuchung prähistorischer homininer Verhaltensweisen. Die Entstehung und die Entwicklung der Steinwerkzeugtechnologie zeichnen den Weg der menschlichen Evolution nach und werden als eine besondere Form der Homininkultur im Vergleich zu anderen Spezies dargestellt. Die Rekonstruktion der technischen Entscheidungen von Homininen anhand des archäologischen Befundes von Steinwerkzeugen ist eine wichtige Herangehensweise zur Untersuchung ihres Verhaltens und ihrer Kognition. Durch die Rekonstruktion von Reduktionssequenzen, die Analyse morphologischer Merkmale der Steinartefakte, die Identifizierung von Rohstoffbeschaffungsmustern und die Analyse von Gebrauchs- und Abnutzungsmustern hat man in dieser Hinsicht schon viel gelernt. Jedoch ist es immer noch nicht gut verstanden wie frühe Homininen mit verschiedenen Variablen der Kraftübertragung umgingen, d.h. wie sie die Splitter abschlugen, , da diese Variablen in dem archäologischen Befund nur schwer direkt zu messen sind.

In dieser Arbeit soll ein wichtiger Aspekt der Krafteinwirkung untersucht werden, nämlich der Schlagwinkel (d.h. der Winkel, in dem der Hammer auf die Plattform des Kerns auftrifft, um die Steinabschläge abzuschlagen), wobei ein experimenteller Ansatz verfolgt wird. Kontrollierte Abschlagsexperimente sind in der Lithologie immer wichtiger geworden, da sie die Möglichkeit bieten, das Verhalten der Knapper in messbare lithische Eigenschaften umzuwandeln. Kontrollierte Experimente verbessern und entwickeln sich weiter, um einen robusten Rahmen für Archäologen zu schaffen, in dem sie verschiedene Hypothesen über die Herstellung und Verwendung von Steinwerkzeugen aufstellen und testen können, während sie gleichzeitig reproduzierbare Ergebnisse liefern.

Die Struktur dieser Arbeit ist dreifach. Erstens fasse ich zusammen, was wir aus früheren kontrollierten Abschlagsexperimenten über die Abschlagbildung wissen (Kapitel 2). Zweitens entwerfe ich ein kontrolliertes Experiment, das sich an den Grundsätzen der Bruchmechanik orientiert, um die Auswirkung des Schlagwinkels auf die Entstehung von Steinabschlägen zu untersuchen und eine Möglichkeit zu finden, ihn an Abschlägen zu messen (Kapitel 3). Die experimentellen Ergebnisse

zeigen, dass der Schlagwinkel an einem Merkmal des Schlagbuckels sichtbar und messbar ist, das ich den Buckelwinkel nenne. Drittens verwende ich die aus dem kontrollierten Experiment stammende Messung des Buckelwinkels zur Vermessung von Abschlägen aus einer Reihe frühpleistozäner Assemblagen, um zu untersuchen, wie frühe Homininen ihre Schlagwinkel handhabten (Kapitel 4). Ich finde Beweise dafür, dass frühe Homininen den Einfluss des Schlagwinkels zu schätzen begannen, indem sie gegen den Übergang vom Oldowan zum Acheulean eine systematischere Kontrolle über den Schlagwinkel ausübten.

Diehier angewandte experimentelle Herangehensweise veranschaulicht, wie wichtige Erkenntnisse gewonnen werden können, um die eher traditionellen technologischen Herangehensweisen zur Untersuchung der technischen Fähigkeiten von Homininen zu ergänzen. Die Ergebnisse dieser Arbeit zeigen 1) die Nützlichkeit kontrollierter Experimente in lithologischen Studien und die Wichtigkeit der Entwicklung von Experimenten, die das Steinschlagsverhalten effektiv mit messbaren lithischen Attributen verknüpfen können, indem sie auf Informationen aus der Bruchmechanik zurückgreifen; 2) zeigen eine zeitliche Entwicklung des Verständnisses und der Kontrolle des Schlagwinkels durch frühe Homininen im Laufe der Zeit; und dadurch 3) bieten sie Einblicke in die Entwicklung des Verhaltens und der Kognition früher Homininen, was wiederum das Potenzial hat, Debatten über den Beginn der kumulativen Kultur in der menschlichen Vorgeschichte zu klären.

Table of Contents

CHAPTER 1 General introduction 1

1 General overview of the thesis objective 1

2 The need for experimentation in lithic studies 2

3 Controlled experiments in lithic studies 3

3.1 Replicative experiments 3

3.2 Controlled experiments 4

4 A general flake formation model derived from the controlled flaking experiments to date 7

4.1 The EPA-PD model 7

4.2 Application of the EPD-PD model in the archaeological record 8

4.3 Limitations of the EPA-PD model 9

5 The role of fracture mechanics in controlled flaking experiments 10

6 Thesis aims 11

6.1 The overall thesis aim 11

6.2 Paper one: A synthesis of the Dibble et al. controlled experiments into the mechanics of lithic production 12

6.3 Paper two: Quantifying knapping actions: a method for measuring the angle of blow on flakes 14

6.4 Paper three: Did early hominins control their hammer strike angles when making stone tools? 16

7 Open science 20

CHAPTER 2 A synthesis of the Dibble et al. controlled experiments into the mechanics of lithic production 21

Abstract 22

1 Introduction 22

1.1 A brief review of the history of experimentation in lithic studies 23

1.2 Philosophy behind experimentation in lithic studies 24

1.3 Strategies of the Dibble experiments 28

2 Experimental variables 30

2.1 Exterior platform angle and platform depth are the primary factors driving flake size 30

2.2 Force does not have a significant effect on the flaking outcome 33

2.2.1 Direct percussion and pressure flaking produce equivalent flakes 34

2.2.2 Hitting the core harder does not matter because force is a function of flake mass and flake mass is a function of EPA-PD 35

2.3 The effect of platform beveling on the EPA-PD relationship remains poorly understood 38

2.4 Core surface morphology has an impact on flake shape and size 42

2.5 Hammer type and shape affect several flake attributes 43

2.5.1 Soft hammers produce platform lipping and impact flake shape. Hard hammers can also produce platform lipping 43

2.5.2 Hammer shape and size do not affect flake size and shape 45

2.6 The angle of blow affects flake size 46

2.6.1 The zero or positive angle of blow affects the size but not the overall shape of the flake 46

2.6.2 Negative angles of blow may change flake size 48

2.7 Striking on the platform edge changes the flake shape 49

3 Limitations of the Dibble experiments to date 50

3.1 The EPA-PD model only works in a highly controlled setting 51

3.2 The collinearity and equifinality of the experimental variables should be taken into consideration in the data analysis 53

3.4 The range of flake attributes analyzed should be broadened 55

4 Future directions of the controlled flaking experiments 56

4.1 The fracture mechanics theory 56

4.2 Force and energy 57

4.3 Something other than plain platforms 58

4.4 Platform width in addition to platform depth 59

4.5 Core morphology 60

4.6 Flake terminations 61

5 Conclusions 62

Acknowledgments 63

CHAPTER 3 Quantifying knapping actions: a method for measuring the angle of blow on flakes 64

Abstract 65

1 Introduction 65

2 Material and Methods 71

2.1 Experimental design 71

2.2 Measuring the bulb angle 74

2.3 Statistical comparison 76

3 Results 78

3.1 Drop tower dataset 78

3.3 MPI dataset 81

3.4 Linear modeling 83

4 Discussion 85

5 Conclusions 89

Acknowledgments: 90

CHAPTER 4 Did early hominins control their hammer strike angles when making stone tools? 92

Abstract 93

1 Introduction 93

2 Materials and Methods 100

2.1 An overview of the study sites 102

2.1.1 The Early Pleistocene assemblages 102

2.1.2 Roc de Marsal 103

2.2 Attribute measurements 103

2.3 Statistical comparison 105

3 Results 106

3.1 The Early Pleistocene assemblages 107

3.2 Roc de Marsal 111

4 Discussion 112

5 Conclusions 116

Acknowledgments **116**

CHAPTER 5 General discussion **118**

1 Summary of findings **118**

1.1 The EPA-PD flake formation model 118

1.2 Reconstructing the angle of blow from flake attributes 119

1.3 Investigating early hominins' control over the angle of blow from the archaeological record 120

2 Implications for the evolution of hominin behavior **121**

3 Limitations **123**

4 Conclusions **124**

5 Outlook **126**

Bibliography **129**

Appendix I Chapter 2 Supplementary Information **156**

1 Statistical analysis **156**

1.1 EPA-PD linear model 156

1.1.1 Summary statistics of the EPA-PD model 156

1.1.2 Summary statistics of the EPA-PD-AOB model: 156

2 Figures from the Dibble experiments **157**

2.1 Dibble and Rezek (2009) 157

2.2 Rezek et al. (2011) 161

2.3 Magnani et al. (2014) 162

2.4 Leader et al. (2017) 166

2.5 Dogandžić et al. (2020) 174

3 A description of each of the variables in the controlled experiment dataset **178**

3.1 Experimental design 178

3.2 The independent variables tested in the experiments 178

3.3 Results 181

Appendix II Chapter 3 Supplementary Information **183**

1 The drop tower setup **183**

2 Supplementary figures 183

3 Supplementary tables 184

4 Statistical analysis 185

4.1 The drop tower dataset 185

4.2 The Dibble dataset 186

4.3 The MPI dataset 188

4.4 The EPA-PD model comparison 188

Appendix III Chapter 4 Supplementary Information 189

1 Supplementary figures 189

List of Figures

Chapter 1

Fig. 1-1 Illustration of the mechanics of exterior platform angle (EPA) and platform depth (PD), increasing either or both variables increase flake size..... 8
Fig. 1-2 Illustration of the angle of blow (AOB), (a) shows when the hammer directly strikes the core or when the angle of blow is zero (perpendicular to the platform), (b) shows when the hammer strikes into the core or when the angle of blow is positive, (c) shows when the hammer strikes towards the core or when the angle of blow is negative. The red dot represents the point of percussion..... 14
Fig. 1-3 Schematic illustration of bulb angle on a flake from its profile view, the dark grey triangle represents the Hertzian cone, and the orange arc marks the bulb angle 15

Chapter 2

Fig. 2-1 Illustration of a semispherical glass core redrawn from Dibble and Rezek (2009)..... 30
Fig. 2-2 The Super Igor machine. This experimental setup was used in Dogandžić et al. (2020). The device marked by the orange square was used to hold the core during the flake removal process. This same device was used in previous experiments conducted with the Igor machine (Dibble and Rezek, 2009; Leader et al., 2017; Magnani et al., 2014; Rezek et al., 2011)..... 30
Fig. 2-3 Schematic illustration of the relationship between EPA-PD and flake size in profile view (redrawn from Dibble and Pelcin, 1995). The dotted lines represent the flaking outcome. (a) When the exterior platform angle is held at a constant, increasing platform depth will result in larger flakes. (b) When platform depth is held at a constant, increasing exterior platform angle will result in larger flakes 31
Fig. 2-4 Relationship between platform depth and flake mass grouped by exterior platform angle. The cube root of flake mass is used here to standardize its dimension with platform depth (Dibble and Rezek, 2009) 32
Fig. 2-5 Relationship between flake mass and striking force. The minimum force required to remove a flake with a certain mass is tightly related to its mass (Dibble and Rezek, 2009). Force is expressed as a function of flake mass 36

Fig. 2-6 Relationship between platform depth, exterior platform angle and flake mass (cube root) for flakes made of four different types of raw material (Dogandžić et al., 2020). 38
Fig. 2-7 The three types of beveled cores examined in Leader et al. (2017). (a) and (b) show the platform surface; (c) shows the core exploitation surface. The striped areas represent portions of the core removed to produce the bevel 40
Fig. 2-8 Relationships between different flake attributes and platform depth for beveled and unbeveled flakes (Leader et al., 2017). Both flat and concave bevels were cut at a 6 mm depth from the original flake exterior surface, and the lateral bevels were cut at 45 degrees relative to the platform surface. (a) shows the relationship between the cube root of flake mass and platform depth, (b) shows the relationship between flake length and platform depth, (c) shows the relationship between flake width and platform depth, and (d) shows the relationship between platform width and platform depth 41
Fig. 2-9 (a) The relationship between platform depth and flake mass for different core morphologies when exterior platform angle is 65 degrees. (b) Flake elongation (length/width) grouped by the core morphology for different core morphologies (Rezek et al., 2011) 43
Fig. 2-10 Angle of blow as the angle between the hammer and the perpendicular of the platform. (a) shows a positive angle of blow between the hammer and the core, (b) shows a zero angle of blow between the hammer and the core, and (c) shows a negative angle of blow between the hammer and the core 47
Fig. 2-11 Box plots showing changes in flake mass and other dimensions on angles of blow ranging from 0 to 50 degrees. (a) Flake mass (cube root) standardized by platform depth on flakes produced from angles of blow ranging from (b) Flake length relative to flake width. All flakes have an exterior platform angle of 65 degrees..... 48
Fig. 2-12 Predicted flake mass to actual flake mass. (a) The predicted flake mass is calculated from the basic EPA-PD model, (b) the predicted flake mass is calculated from the updated EPA-PD model with the addition of the angle of blow 53

Chapter 3

Fig. 3-1 Schematic illustration of how the angle of blow is measured as the angle between the hammer's striking direction and the perpendicular of the platform from

the profile view of a flake removal. (a) shows a positive (oblique) angle of blow, (b) shows a zero (direct) angle of blow, and (c) shows a negative (oblique in the other direction) angle of blow 67
Fig. 3-2 Schematic illustration of the bulb angle on a flake from its profile view. The Hertzian cone generated from the hammer blow is represented by the triangle beneath the hammer, α refers to the Hertzian cone angle, which is approximately 136 degrees in soda lime glass. The bulb angle is the angle between the flake's platform and the extruding side of its Hertzian cone, as is marked in orange. (a) Showing that the Hertzian cone's central line remains perpendicular to the platform when angle of blow is zero, the theoretical bulb angle should be 158 degrees; (b) showing the case when the Hertzian cone is completely pushed to the platform, the theoretical bulb angle should be 136 degrees; (c) showing the case when the Hertzian cone is tilted into the core, the theoretical bulb angle should be greater than 158 degrees 70
Fig. 3-3 The drop tower setup used in this study; the laser level is not shown in the photo 72
Fig. 3-4 Illustration of how the bulb angle is measured on a flake with a goniometer. (a) shows how the goniometer is placed on the flake to measure bulb angle, (b) and (c) present a zoomed-in view of the bulb angle on a flake. Note that the 3D model of the flake used in the illustration is from the Dibble dataset, and it is for illustration purposes only. 75
Fig. 3-5 Illustration of the two measurement methods on a 3D flake model from the Dibble dataset. (a) In the vector calculation method, bulb angle on the flake is defined as the angle between vectors P_0P_1 and P_0P_2. (b) In the virtual goniometer method with the Virtual Goniometer plugin for MeshLab loaded (Yezzi-Woodley et al., 2021), bulb angle is defined as the angle between the red and blue patches marked on the flake model 76
Fig. 3-6 Boxplot showing that bulb angle decreases as angle of blow (AOB) increases for flakes in the drop tower dataset 79
Fig. 3-7 Boxplot summarizing the relationship between bulb angle and angle of blow for flakes in the Dibble dataset. Flakes measured with the vector calculation method are colored in grey. Flakes measured with the virtual goniometer method are colored in yellow. 80

Fig. 3-8 Comparison of the flake bulb angles in the Dibble dataset as measured by the vector calculation method and by the virtual goniometer method. The line represents a 1:1 correspondence. 81
Fig. 3-9 Histogram showing the distribution of bulb angle with overlaying density curve for all flakes analyzed in the MPI dataset. 82
Fig. 3-10 Boxplot showing the result of the angle of blow blind test with the MPI dataset. 83
Fig. 3-11 Comparison of the actual flake mass and modeled flake mass in the Dibble dataset, n = 53. (a) Actual to predicted flake mass using the basic EPA-PD model, (b) actual to predicted flake mass using the EPA-PD-AOB model, (c) actual to predicted flake mass using the EPA-PD-BA (vector calculation) model, and (d) actual to predicted flake mass using the EPA-PD-BA (virtual goniometer) model..... 85

Chapter 4

Fig. 4-1 Schematic illustration of the effect of the angle of blow (AOB) on flaking. The angle of blow is measured as the angle between the hammer striking direction and the perpendicular of the platform surface (marked by the black arc in b), the red dot refers to the point of percussion. (a) Shows the scenario when the angle of blow is perpendicular to the platform (equal to zero), (b) shows the scenario when the angle of blow is oblique (or is positive) 95
Fig. 4-2 Schematic illustration of bulb angle on a flake from its profile view, bulb angle is marked by the orange arc and α refers to the Hertzian cone angle. (a) shows the orientation of the Hertzian cone when the angle of blow is zero, the theoretical bulb angle is $90° + 0.5\alpha$; (b) shows the case when the Hertzian cone is completely pushed onto the platform by an oblique (positive) angle of blow, the theoretical bulb angle is equal to α 98
Fig. 4-3 Locations of the assemblages analyzed in the study. The Oldowan assemblages are colored and labeled in blue, the Karari assemblages are colored and labeled in yellow, and the Acheulean assemblages are colored and labeled in red 101
Fig. 4-4 Profile view of the flake made from different angles of blow, bulb angle is marked by the orange arc and the Hertzian cone is represented by the dark grey triangle. (a) Shows the case when the flake is made with a direct angle of blow and

has a big bulb angle, (b) shows the case when the flake is made with an oblique angle of blow and has a small bulb angle 107
Fig. 4-5 Boxplot showing the bulb angle distribution of the four Early Pleistocene groups, the red dot in each boxplot indicates the average bulb angle. The groups on the y axis are in chronological order from young to old (top to bottom) 108
Fig. 4-6 3D scatterplots of the regression results using exterior platform angle (EPA) and platform depth (PD) to predict bulb angle for flakes from Early Pleistocene assemblages grouped by technological industry. The regression plane for flakes from the Acheulean assemblages is displayed 109
Fig. 4-7 Boxplots of the relationship between platform depth and bulb angle for flakes from the Early Pleistocene assemblages. The red dot represents the average bulb angle within each platform depth interval 110
Fig. 4-8 Boxplots of the relationship between bulb angle and flake mass for flakes from the Early Pleistocene assemblages grouped by the technological industry. The red dot represents the average flake mass within each bulb angle interval 111
Fig. 4-9 Boxplot of the relationship between platform depth and bulb angle for flakes from RDM. The average bulb angle within each platform depth interval is represented by the red dot 112

Chapter 5

Fig. 5-1 Illustration of bulb angle from a flake's profile view, the dark grey triangle represents the Hertzian cone, and the orange arc marks the bulb angle. (a) Shows when the hammer strike is direct, (b) shows when the hammer strikes the platform at an angle 120

Appendix I

Fig.Appx-I. 1 Relationship between flake mass and PD (cubed) 158
Fig.Appx-I. 2 Box plot showing relationship between flake mass standardized by PD (cubed) and EPA 158
Fig.Appx-I. 3 Boxplot showing changes in flake shape (left: length to width, right: area to thickness) as affected by different values of EPA 159
Fig.Appx-I. 4 Relationship between flake mass and PD (cubed) for different AOBs 159

Fig.Appx-I. 5 Boxplot showing relationship between flake mass standardized by PD (cubed) for different AOBs 160
Fig.Appx-I. 6 Boxplot showing changes in flake shape (left: length to width, right: area to thickness) as affected by different AOBs 160
Fig.Appx-I. 7 Flake mass as a function of force 161
Fig.Appx-I. 8 Graphs of both intra- and inter-Core variability on flake surface area, either controlling for PD (graph A) or EPA (graph B) and length/width (graphs C and D) 162
Fig.Appx-I. 9 Scatter diagrams and correlations between flake weight and platform depth cubed by hammer material (EPA = 65, AOB = 5, both platform surface-struck and edge-struck flakes are included) 164
Fig.Appx-I. 10 Correlations between flake weight and platform depth cubed for lipped and unlipped flakes, both platform-struck and edge-struck flakes are included. AOB = 5, EPA = 65, R^2 and adjusted R^2 are displayed on each plot 165
Fig.Appx-I. 11 Flake weight relative to platform depth cubed by angle of blow (EPA = 65, copper hammer). Note that the means of weight/platform depth cubed between edge-struck and platform-struck are not significantly different, except in the case of AOB = 5 165
Fig.Appx-I. 12 Scatter plot of flake weight and platform depth cubed for combined sample of flat-beveled flakes and unbeveled flakes produced with EPA of 75 and 90. In the bevel field, GRINDER represents concave bevel, SANDER represents flat bevel, and NONE represents either no bevel or lateral bevel 167
Fig.Appx-I. 13 Boxplot of the ratio of flake weight to platform depth cubed for flat-beveled flakes compared with unbeveled flakes with EPA of 75 and 90 167
Fig.Appx-I. 14 Scatter plot of flake weight and platform depth cubed for combined sample of concave-beveled flakes and unbeveled flakes produced with EPA of 75 and 90 168
Fig.Appx-I. 15 Boxplots of the ratio of flake weight to platform depth with unbeveled flakes with EPA of 75 and 90 168
Fig.Appx-I. 16 Scatter plot of flake weight and initial platform depth cubed for flat-beveled flakes of different bevel depths and unbeveled flakes produced with EPA = 75 169
Fig.Appx-I. 17 Boxplot of the ratio of flake weight to initial platform depth cubed for flat-beveled flakes compared with unbeveled flakes, EPA = 75 and 90 169

Fig.Appx-I. 18 Scatterplot of flake weight and initial platform depth cubed for concave-beveled flakes of different bevel depths and unbeveled flakes produced with EPA = 75 and 90 169
Fig.Appx-I. 19 Boxplot of the ratio of flake weight to initial platform depth cubed for concave-beveled flakes compared with unbeveled flakes, with EPA = 75 and 90 . 170
Fig.Appx-I. 20 Boxplot of the ratio of flake weight to platform depth cubed for various classes of laterally-beveled flakes compared with unbeveled flakes with EPA = 75 170
Fig.Appx-I. 21 Boxplots showing ratios of (A) flake weight to platform depth and (B) flake weight to initial platform depth for various classes of bevels 171
Fig.Appx-I. 22 Scatterplots showing (A) platform width to platform depth for all bevel depths of flat-beveled flakes, (B) platform width vs. initial platform depth for each bevel depth of flat- beveled flakes 171
Fig.Appx-I. 23 Scatter plots showing (A) platform width to platform depth for each bevel depth of concave-beveled flakes, (B) platform width vs. initial platform depth for all bevel depths of concave-beveled flakes..... 172
Fig.Appx-I. 24 Boxplots of ratios of platform width to both platform depth and initial platform depth. (A) Platform width to platform depth, flat-beveled flakes; (B) Platform width to initial platform depth, flat-beveled flakes; (C) Platform width to platform depth, concave-beveled flakes; (D) Platform width to initial platform depth, concave-beveled flakes..... 172
Fig.Appx-I. 25 Relationship between platform width and platform depth for unbeveled cores, laterally-beveled cores with 1 mm and 10 mm platform surface, and cores with single lateral bevels. All bevel angles at 45° relative to the platform surface 173
Fig.Appx-I. 26 Relationship between platform width and platform depth for unbeveled cores and laterally-beveled cores with bevel angles at 30°, 45°, and 60° relative to platform surface. All platform surfaces of the beveled cores have a width of 10 mm..... 173
Fig.Appx-I. 27 Boxplots of ratio of platform width to platform depth for all of major bevel classes described above..... 174
Fig.Appx-I. 28 Box plots of ratio of flake length to platform depth for all major bevel classes described above..... 174

Fig.Appx-I. 29 Volume (cube root) as a function of platform depth for each EPA group, by raw material 175
Fig.Appx-I. 30 Dotplot showing the effect of EPA on flake volume (cube root of volume is standardized by platform depth) for different raw materials 175
Fig.Appx-I. 31 Dotplot showing the effect of EPA on flake length (standardized by platform depth) for different raw materials 176
Fig.Appx-I. 32 Dotplot showing the effect of EPA on flake width (standardized by platform depth) for different raw materials 176
Fig.Appx-I. 33 Dotplot showing the effect of EPA on flake thickness (standardized by platform depth) for different raw materials 177
Fig.Appx-I. 34 Relationship of force required to remove flakes by weight (log transformed) for different raw materials and varying EPAs 177

Appendix II

Fig.Appx-II. 1 Histogram of bulb angle standard error for flakes from the Early Pleistocene dataset 189
Fig.Appx-II. 2 Boxplots of the relationship between platform depth and bulb angle, using 15 mm as the upper cutoff to standardize platform depth. The red dot represents the average platform depth within each bulb angle group 189
Fig.Appx-II. 3 Boxplots of the relationship between bulb angle and flake mass, using 100 g as the upper cutoff to standardize flake mass. The red dot represents the average flake mass within each bulb angle group 190

Appendix III

Fig.Appx-III. 1 Histogram of bulb angle standard error for flakes from the Early Pleistocene dataset 189
Fig.Appx-III. 2 Boxplots of the relationship between platform depth and bulb angle, using 15 mm as the upper cutoff to standardize platform depth. The red dot represents the average platform depth within each bulb angle group 189
Fig.Appx-III. 3 Boxplots of the relationship between bulb angle and flake mass, using 100 g as the upper cutoff to standardize flake mass. The red dot represents the average flake mass within each bulb angle group 190

List of Tables

Table 3-1 Summary statistics of the different EPA-PD models. 85
Table 4-1 Summary of flakes with bulb angle measured from the 13 archaeological localities in chronological order from young to old. 105
Table 4-2 Summary statistics of the bulb angle distribution for the Early Pleistocene dataset. 108

Appendix I

Table.Appx-I. 1 Dataset overview, breakdown of the number of flakes by core morphology and EPA 161
Table.Appx-I. 2 Presence or absence of lipping by hammer material. Includes EPA = 55, 65, and 75, all values of AOB, and both locations of force (strikes both on the platform surface and the exterior edge of the platform) 162
Table.Appx-I. 3 Presence or absence of lipping by EPA, including flakes struck with both copper and steel hammers, both force locations, and a full range of AOBs. The lack of association with EPA holds even if AOB or location of force is controlled... 162
Table.Appx-I. 4 Presence or absence of lipping by location of force. All flakes were produced with the copper hammer, EPA = 65, a full range of AOBs are included . 163
Table.Appx-I. 5 Presence or absence of lipping by AOB. All flakes were produced with copper hammer and EPA = 65. Flakes produced by both locations of force (on edge or on platform) are included 163
Table.Appx-I. 6 Relationship between location of force and the ratio of platform area to flake area, broken down by the presence or absence of lipping (EPA = 65, AOB = 5, all hammer types included) 163
Table.Appx-I. 7 Mean values and sample size (N) of various dimension ratios by shape and size of the hammer (EPA = 65, AOB = 0, steel hammers). The first three entries of the table refer to the hammers with rounded tips..... 163
Table.Appx-I. 8 Basic descriptive statistics and tests among different both platform depth and initial platform depth..... 166
Table.Appx-I. 9 Averages of bevel width, G2 refers to the 2mm bevel, G4 refers to the 4mm bevel, G4-8 refers to the narrow 4mm bevel, G4-30 refers to the wide 4mm bevel, G6 refers to the 6mm bevel..... 166

Table.Appx-I. 10 Sample size by raw material and by EPA 174

Appendix II

Table.Appx-II. 1 Summary statistics of bulb angle by angle of blow for the drop tower dataset (n = 103) 184
Table.Appx-II. 2 Summary of bulb angle by angle of blow based on the measurement method, VG refers to the virtual goniometer method and VC refers to the vector calculation method (the Dibble dataset, n = 70)..... 185
Table.Appx-II. 3 Summary of angle blow prediction for all flakes in the MPI dataset 185

CHAPTER 1 General introduction

1 General overview of the thesis objective

The production and use of stone tools is an essential trait of the hominin lineage (Davidson and McGrew, 2005; Shea, 2017; Stout et al. 2011). One of the earliest definitive pieces of evidence for technology and culture in human history dates to more than two million years ago, known as the Oldowan (Schick and Toth, 1994, 2006; Toth, 1985). The Oldowan industry was discovered and named by Louis Leakey in the 1930s (Gowlett, 1990; Leakey, 1934; Schick and Toth, 2006), preceding the Acheulean industry that is characterized by the prevalence of different forms of biface, handaxe, and large cutting tools (De la Torre, 2016; de la Torre, 2011; Gowlett et al., 2014; Gowlett, 2015; Kleindienst, 1962). Although subsequent research conducted in Africa and Eurasia since the 1930s revealed the complexity of the Oldowan form (e.g., Barsky, 2009; Braun et al., 2019; Braun and Harris, 2003; Harris, 1983; Isaac, 1976; Leakey, 1971; Schick and Toth, 1993, 1994; Titton et al, 2020; Toth, 1985; Toth and Schick, 2006), the Oldowan is still generally defined by simple flake and core forms made with hard-hammer percussion techniques with a least-effort strategy to produce sharp edges (Schick and Toth, 1994, 2006; Toth, 1985).

The sheer quantity of stone artifacts from the Oldowan record that span a wide geographic and temporal range allows researchers to study the origin of human uniqueness from early hominins' biomechanics, cognitive, and technological capabilities (Hayden, 2008; Hovers, 2012; Plummer, 2004; Stout et al., 2019; Toth and Schick, 2018). Using a controlled experimental approach, this thesis aims to reconstruct an important knapping variable, namely the angle at which knappers strike the core for flake detachment, a hitherto archaeologically invisible aspect of flaking. Results from this thesis shed light on how hominins' behavior and cognition evolve through time from the archaeological record.

2 The need for experimentation in lithic studies

Stone artifacts are one of the most widely occurring bits of material evidence for studying hominin behavior owing to their virtually indestructible nature. Compared to organic remains, lithic remains are much less prone to post-depositional degradation and preserve well over time in the archaeological record. However, despite their ubiquity across time and space, our knowledge of how and why prehistoric knappers made the great variety of stone artifacts that we discover today remains relatively limited.

One of the biggest obstacles in using stone artifacts as a proxy for past hominin behavior is a lack of modern analogs for understanding the prehistoric stone tool technology. There is some documentation of the use of stone tools in very specialized technology in the recent past, such as gunflints for muskets (Bjarke Ballin, 2014; de Lotbiniere, 1984; Kenmotsu, 1990; Quinn, 2004; White, 1975), cutting-edge inserts on threshing sledges (Whallon Jr, 1978; Whittaker, 1996; Whittaker et al., 2009), and liners in steel drums for porcelain production (Tsirk, 2014, and see citations within). There are also ethnographic studies of the few living groups that still use stone tools on a more regular basis. These studies have proven to be invaluable for helping researchers conceptualize the stone tool technology beyond the limits of their modern and post-industrial experiences. For example, the ethnographic records of stone tool use among the modern hunter-gatherers provide much insight into a wide range of processes and considerations that underlie the production, selection, and use of stone tools (Allen, 1996; Gallagher, 1977; Hayden, 2015; Hayden and Nelson, 1981; Shott, 1986, 1989; Stout et al., 2002). However, the above-mentioned examples only represent a subset of the lithic technology that operated under very specific cultural contexts and time scales. As such, it is better to treat them as a source of information for generating hypotheses rather than as explanatory analogs for direction interpretation of the archaeological stone artifacts (Ascher, 1961; Lin et al., 2018).

Besides these examples of recent stone tool use, experimentation plays an important role in lithic research as it allows researchers to verify hypotheses and develop inferences about past lithic technology based on the experimental findings (Eren et al., 2016; Lin et al., 2018). The uniformitarian nature of the stone material's

fracture mechanics allows researchers to study past lithic technologies by replicating the forms of stone artifacts observed in the archaeological record with rather good confidence.

Systematic documentation of the experimental approach to lithic studies started in the late 19th century. This early experimental work emphasized replicating the exact form of artifacts with what was believed to be the "original" method (Johnson et al., 1978). While it continued to be a part of archaeology throughout, it was not until the 1960s that the experimental approach was brought into the spotlight by prominent archaeologists and knappers such as Bordes, Crabtree, Tixier, and others (Bordes, 1969; Callahan, 1985; Crabtree, 1970; Frison, 1979; Shea et al., 2001; Sheets and Muto, 1972). Since this time there has been increasing interest in using experimental approaches to investigate questions regarding the production and use of stone tools from a variety of perspectives including raw material selection and procurement, technological and functional organization, cognitive capacities, biomechanical characteristics, and so forth (Andrefsky, 2006; Bradbury and Carr, 1995; Buchanan et al., 2016; Eren et al., 2011; Key and Dunmore, 2018; Moore and Perston, 2016; Pargeter et al., 2019; Rugg and Mullane, 2001; Stout and Khreisheh, 2015; Toth and Schick, 2018; Tringham et al., 1974). Today, experimentation is an indispensable component of lithic research.

3 Controlled experiments in lithic studies

3.1 Replicative experiments

Here I divide lithic experimentation into two categories: replicative and controlled. In replicative experiments, (modern) human knappers usually aim to either re-produce the forms of artifacts as discovered in the archaeological record or replicate what they believe were the methods used by the past knappers, or sometimes, both (Amick and Mauldin, 1989; Flenniken, 1978; Franklin and Simek, 2008; Scerri et al., 2016). Replicative experiments often emphasize the importance of using specific techniques and methods to create the different forms of artifacts that are discovered from the archaeological record (Bordes, 1950, 1969; Crabtree, 1966; Flenniken, 1978). Replicative experiments allow researchers to explore the different ways by

which past hominins could have created the various forms of stone artifacts we discover in the archaeological record today (Andrefsky Jr, 2004; Johnson et al., 1978). Replicative experiments play a key role in a wide range of topics in lithic studies such as reduction sequence (Bradbury and Carr, 1995; Bradley and Sampson, 1986; Buchanan et al., 2016; Eren et al., 2005), knapping technique (Callahan, 1979, 1985; Crabtree, 1966; Crabtree and Davis, 1968; Driscoll and García-Rojas, 2014; Flenniken, 1978; Karavanić and Šokec, 2003; Pelegrin, 2006), retouch intensity (Andrefsky, 2006; Hiscock and Clarkson, 2005a, 2005b, 2009; Kuhn, 1990), edge production efficiency (Eren et al., 2008; Jennings et al., 2010; Prasciunas, 2007; Sheets and Muto, 1972), and use- and edge-wear analysis (Odell, 1979; Schoville et al., 2016; Stevens et al., 2010).

While replicative knapping experiments have informed us greatly about how different knapping techniques and methods work to generate flake outcomes, they still come with some inevitable limitations. It is not uncommon for experienced knappers to consistently produce desirable and to sometimes even quite accurately predict specific flaking outcomes (Bril et al., 2010; Nonaka et al., 2010). But even experienced knappers might not be able to unambiguously identify all variables that are responsible for driving the different patterns they observe on their knapping products (Amick and Mauldin, 1989). Knapping is a motor skill that involves a complex interaction of different body parts (Bril et al., 2012; Geribàs et al., 2010; Vernooij et al., 2015), it is extremely difficult for a knapper to isolate and control a specific variable or gesture during the knapping process. The change of one knapping variable is often accompanied by changes in other variables. For example, when knappers switch between soft and hard hammers, they might also simultaneously change how they swing and where they strike the platform, oftentimes unconsciously. As a result, the inter-knapper variability can be high in replicative experiments because it is hard for one knapper to perform an exact replication of another knapper's action or strategy.

3.2 Controlled experiments

Here I define controlled flaking experiments as studies that use a mechanical knapping apparatus and standardized knapping materials to conduct the

experimental work. Controlled experimentation highlights the control over individual knapping variables and focuses on testing their effect on visible flake attributes. The use of a mechanical flaking apparatus allows precise control of variation in both knapping technique and material that may occur during the knapping process and thus offers a highly consistent setup. Glass is a commonly used material in controlled experiments because of its high resemblance in the fracture mechanics with actual archaeological materials such as basalt and flint. In addition, glass can be rather easily molded into different shapes, which is advantageous for varying and standardizing core shapes. Both the mechanical flaking apparatus and homogeneous testing material (in most cases glass) ensure a high internal validity for the controlled experiments – that the results are robust and reproducible under a controlled setting (Lin et al., 2018).

The first wave of systematic controlled flaking experiments started in the 1970s (Bonnichsen, 1977; Cotterell et al., 1985; Cotterell and Kamminga, 1987, 1992; Faulkner, 1972, 1973; Speth, 1972, 1974, 1975). These earlier studies rely heavily on fracture mechanics theories to study the flake initiation, propagation, and termination process (Cotterell et al., 1985; Cotterell and Kamminga, 1987, 1992; Speth, 1972). Hereafter I will refer to these earlier experiments as fracture-mechanics-based because both the experimental setup and the research questions are heavily driven by the basic fracture mechanics of flaking. Despite these fracture-mechanics-based experiments focused on a rigorous investigation of the different flaking phases, it has remained difficult to connect the experimental results with the archaeological record. In particular, it is often difficult to directly apply results from these fracture-mechanics-based experiments to the archaeological record because the experiments can involve variables not easily obtained from the artifacts themselves such as hammer strike angle, hammer size and velocity, and striking force.

To better integrate the experimental results with archaeological observations, later controlled experiments shifted the focus to quantifying the effect of flaking variables that are under the direct control of knappers on measurable flake attributes (e.g., Dibble and Pelcin, 1995; Dibble and Rezek, 2009; Dibble and Whittaker, 1981). This change allows for a better understanding of the role played by flaking mechanics in knappers' decisions. I will refer to these experiments as knapper-guided as they are

designed to understand the flaking process from a knapper's perspective. To better simulate the knapping process and produce more realistic flake outcomes, Dibble and colleagues upgraded the experimental design and conducted a series of knapper-guided experiments (henceforth referred to as the Dibble experiments) to test a variety of variables. Up to now, knapper-guided controlled experiments have investigated a number of variables such as exterior platform angle, platform depth, angle of blow, core and platform morphology, hammer size and shape, hammer material, hammer velocity, and raw material properties (Dibble and Pelcin, 1995; Dibble and Rezek, 2009; Dogandžić et al., 2020; Leader et al., 2017; Magnani et al., 2014; Pelcin, 1997a, 1997b; Rezek et al., 2011).

Despite the adjustments and improvements made in the Dibble experiments to better apply the experimental results to the archaeological record, or in other words, to improve their external validity (Braun et al., 2019; Dibble, 1997; Dogandžić et al., 2020; Lin et al., 2015; Režek et al., 2018), controlled flaking experiments are still sometimes critiqued for their rather artificial setup and a lack of generalization to the archaeological data. For one, while a mechanical flaking apparatus offers a precise force delivery and easy documentation of the process, for now these setups do not generate a strike in the same way that a human knapper does. Second, the use of glass as the testing material has long been subject to criticism. Obsidian is practically volcanic glass and is common in some archaeological records, but other raw materials were more frequently used in most cases in the past. Opponents of using glass in controlled experiments argue that the differences between glass and these other archaeological materials will cause fundamental differences in the knapping outcomes, thus questioning the external validity of the controlled experiments based on glass. Dogandžić et al. (2020) addressed this critique by using some more common archaeological materials in the controlled setup and found few differences (see Chapter 2), but it is also true that more work needs to be done in this area. Third, although the core shape in the Dibble experiments greatly improve over the plate glass and other glass forms used in prior controlled experiments, the artificial shape of these cores is still criticized for its lack of resemblance to cores coming from the archaeological record. This criticism is also currently being addressed with new technologies that allow experimental core forms to be machine tooled to replicate archaeological examples. In this regard, it is worth

noting that a major advantage to using glass is that it is easily shaped into different forms, which then effectively widens the range of core morphologies that can be used in the controlled experiments.

4 A general flake formation model derived from the controlled flaking experiments to date

4.1 The EPA-PD model

Controlled flaking experiments offer a platform to generate and test hypotheses of how stone tools are produced and used. One of the key findings from the knapper-guided controlled experiments is that exterior platform angle and platform depth play a significant role in determining flake size. Increasing either or both exterior platform angle and platform depth will result in a larger flake (Dibble and Pelcin, 1995; Dibble and Rezek, 2009; Dibble and Whittaker, 1981; Dogandžić et al., 2020; Leader et al., 2017; Magnani et al., 2014; Pelcin, 1996; Rezek et al., 2011, see also Fig.1-1). Changes in platform depth also have a greater effect on flake size at higher values of exterior platform angle (Dibble and Rezek, 2009). A flake formation model is subsequently derived from the experimental results to predict flake size with exterior platform angle and platform depth. I will refer to this model as the EPA-PD model (Dibble and Pelcin, 1995; Dibble and Rezek, 2009; Dibble and Whittaker, 1981; Dogandžić et al., 2020; Li et al., Under Review; McPherron et al., 2020).

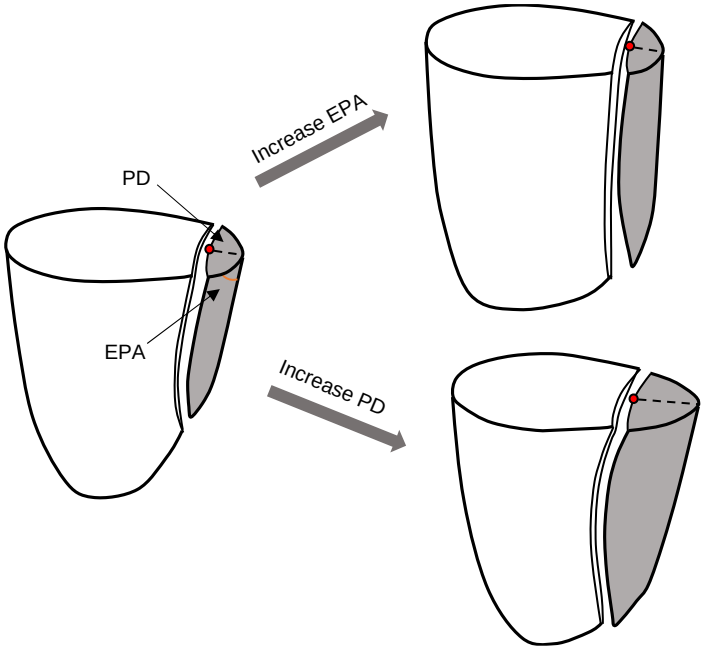

Fig. 1-1 Illustration of the mechanics of exterior platform angle (EPA) and platform depth (PD), increasing either or both variables increase flake size

4.2 Application of the EPD-PD model in the archaeological record

With the EPA-PD relationship at its core, variants of the EPA-PD model have been applied to interpret variation observed in archaeological assemblages (Braun et al., 2019; Clarkson and Hiscock, 2011; Dibble, 1997; Dogandžić et al., 2020, 2015; Lin et al., 2013; Režek et al., 2018; Shott et al., 2000; Shott and Seeman, 2017). One application of the EPA-PD model is to predict the original flake size (in the form of flake mass or sometimes volume), which is important for measuring mass loss and studying curation and reduction in stone tools. For example, a number of studies have attempted to use different platform attributes such as exterior platform angle, platform depth, platform width, platform area, and platform shape to predict flake size and shape (Archer et al., 2018; Clarkson and Hiscock, 2011, 2011; Davis and Shea, 1998; Dibble, 1997; Dogandžić et al., 2015; Shott et al., 2000; Shott and Seeman, 2017).

Another important application of the EPA-PD model is to investigate how manipulating exterior platform angle and platform depth varies flake outcomes. For instance, the EPA-PD model has been used to explain variability in sharp edge

production in lithic assemblages. Obtaining a sharp edge is a key component in stone tool manufacture because it increases the economization of the raw material. The sharp edge efficiency of a flake can be quantified as the ratio of its usable edge per unit mass or volume (Eren et al., 2008; Lin et al., 2013; Muller and Clarkson, 2016). Using results from the controlled experiments, Lin et al. (2013) found that exterior platform angle and platform depth could drive different flake characteristics to increase the edge efficiency of unretouched flakes. Specifically, they discovered that increasing exterior platform angle while decreasing platform depth will produce flakes that are more economical, i.e., have a higher ratio of usable edge per flake mass. Lin et al. (2013) looked at this strategy in archaeological assemblages and discovered that hominins from different technological groups have distinct choices of exterior platform angle and platform depth, suggesting that different production strategies were employed by the different groups of hominins to economize raw materials.

Režek et al. (2018) furthered Lin et al. (2013)'s study by tracking the change in the interaction between exterior platform angle and platform depth of flakes from sites that cover wide temporal and geographical ranges. Režek et al. (2018) discovered that both the amount of and variability in sharp edge production increased from the Early Pleistocene to the Late Pleistocene. They argued that this trend reflects the intense interrelations between hominins' use and management of stone tools, which are dependent on both their social and environmental contexts. The work of Režek et al. (2018) demonstrated that the experimentally-derived EPA-PD model allows us to examine a global lithic variability that was not previously recognized.

4.3 Limitations of the EPA-PD model

Although the EPA-PD model has been proven useful in investigating long-term patterns in the archaeological record (Režek et al., 2018), it is a very incomplete model of flake formation and does not account for other common knapper guided variations such as platform morphology (e.g., beveling), striking force, hammer velocity, and hammer strike angle. The main difficulty relating these many variables stem from the fact that the EPA-PD model is not well connected to the fundamental of flaking mechanics. Several studies have shown that a major limitation of the

application of the EPA-PD model is that flake mass is not well predicted on a case-by-case basis (Clarkson and Hiscock, 2011; Davis and Shea, 1998; Dogandžić et al., 2015; Shott et al., 2000; Shott and Seeman, 2017; Wilson and Andrefsky, 2008). Several variants of the EPA-PD model using additional independent variables such as platform area and platform width have also been tested on different archaeological and experimental lithic assemblages (e.g., Clarkson and Hiscock, 2011; Dogandžić et al., 2015; Shott, 2000). But there is still some considerable over- or under-estimation of flake size using these varied EPA-PD models.

In addition to exterior platform angle and platform depth, the hammer strike angle (or the angle of blow) also plays a significant role in flake formation (Dibble and Rezek, 2009; Magnani et al., 2014). Li et al. (Under Review) show that including the angle of blow can significantly improve the EPA-PD model's performance. However, it is difficult to simply add the angle of blow to the EPA-PD model when assessing archaeological assemblages because this variable cannot be easily extracted from the stone artifacts. How to address the limitations of the EPA-PD model and improve its performance is further discussed in detail in Chapter 2 and also Chapter 3 of this thesis.

5 The role of fracture mechanics in controlled flaking experiments

The field of fracture mechanics offers rich literature on the basic principles of fracture initiation and propagation in brittle solids. In particular, Hertzian fracture, which is the key feature in conchoidal flaking, has been extensively studied in fracture mechanics (Chaudhri, 2015; Gorham and Salman, 2005; Kocer and Collins, 1998; Marimuthu et al., 2016; Zeng et al., 1992a). Stone knapping variables such as a raw material's mechanical properties, initial core size, platform surface roughness, hammer size and velocity, and hammer strike angle have all been discussed regarding their role in the initiation and propagation of Hertzian fracture (Frank and Lawn, 1967; Gorham and Salman, 2005; Kocer and Collins, 1998; Langitan and Lawn, 1969; Salman and Gorham, 2000; Swain and Lawn, 1976). The fracture-mechanics-related lithic research on conchoidal flaking offers a rather detailed explanation of some important aspects of flaking mechanics including the flake initiation and termination, fracture propagation, and bulb formation (Baker, 2003, 2004; Cotterell et al., 1985; Cotterell

and Kamminga, 1987; Speth, 1972; Tsirk, 2014). While these fracture-mechanics-based studies tried to incorporate laws of fracture mechanics into the different flake formation phases to predict the growth of the crack path, they were not successful in generating a model that can be conveniently applied to archaeological assemblages. As previously discussed, this is because it is difficult if not impossible to measure variables (such as striking angle, force angle, hammer size, and velocity) used to predict the crack path in the fracture mechanics-based studies on actual artifacts. Few follow-up studies have been conducted to bridge this gap between the fundamental flaking mechanics and its practical application to the lithic record.

The knapper-guided controlled experiments up to date focus on establishing the empirical relationships between different flake attributes (Dibble and Pelcin, 1995; Dibble and Rezek, 2009; Dibble and Whittaker, 1981). While this approach is effective in isolating individual lithic attributes and studying their effect on flaking, it leaves an inevitable gap between the basic flaking mechanics and the knapping behaviors that generate the observed variation in lithic assemblages. As a result, the EPA-PD model generated from these knapper-guided experiments is sensitive to changes introduced to the controlled setting because of a lack of connection to the fundamental physics of flaking. By introducing fracture mechanics to the experimental design and hypotheses formulation, the knapper-guided controlled experiments can be improved to provide a more robust framework to quantify knapping behaviors based on the basic flaking mechanics that stay invariant regardless of changes in the external environment. The experimental results can then be generalized to a much broader context, guaranteeing both a high internal and external validity (Lin et al., 2018).

6 Thesis aims

6.1 The overall thesis aim

Many lithic studies have greatly advanced our understanding of how early hominins knapped by reconstructing their technical decisions throughout reduction sequences (Braun and Harris, 2009; Braun et al., 2008b; Delagnes and Roche, 2005; Roche et al., 1999), but some knapping parameters related to force delivery still need further

investigation. These variables, such as the amount of force used by the hominins to remove a flake, the hammer velocity at the point of impact, the angle at which the hammer strikes the cores, and the hammer size and shape, cannot be directly detected from the archaeological record, making them invisible to the modern observers. Yet these archaeologically invisible variables are important for an understanding of the biomechanical and technological capacities of hominins. Studying the effect of these knapping variables on flake formation will not only allow us to reconstruct hominins' knapping strategies more accurately but also enhance our understanding of how their behavior and cognition evolved through time.

This thesis contains three publishable articles that have been submitted or are ready to be submitted. The overall goal of this thesis is to use controlled experiments to connect one of the currently invisible aspects of stone tool production – the angle of blow, with measurable lithic attributes to explore one aspect of technical decisions made by early hominins. More specifically, this thesis addresses the question of whether and how early hominins controlled their angles of blow to produce the tools that we see in the archaeological record. After examining what we know of flake production from controlled experiments and identifying the importance of including the angle of blow in the current flake formation model (Chapter 2), I conduct a series of controlled flaking experiments guided by fracture mechanics to investigate and quantify the effect of the angle of blow on measurable flake attributes (Chapter 3). I then apply the experimental results to selected Oldowan and Acheulean assemblages to reconstruct and track changes in knapper strategies of Early Pleistocene hominins (Chapter 4).

6.2 Paper one: A synthesis of the Dibble et al. controlled experiments into the mechanics of lithic production

This paper is an effort to synthesize what we have learned from the previous Dibble experiments and to discuss the limitations and future directions of controlled flaking experiments. We also included the complete dataset produced from the controlled experiments by Dibble and colleagues in this paper. We first review and summarize what we have learned about flake formation and flake variability from the Dibble experiments. The Dibble experiments looked at a wide range of knapping variables

including platform morphology, core surface morphology, hammer strike position and angle, hammer size and material, and raw material properties, all of which were found to affect the flake outcome (Dibble and Rezek, 2009; Dogandžić et al., 2020; Leader et al., 2017; Magnani et al., 2014; Rezek et al., 2011). Among the variables that have been studied, three have the most significant impact on determining the flake size and shape: exterior platform angle, platform depth, and the angle of blow. Exterior platform angle (EPA) refers to the angle between a flake's platform and its exterior surface. Platform depth (PD) refers to the distance between a flake's point of percussion and its exterior surface (Fig.1-1). The angle of blow refers to the angle at which the hammer strikes the platform (Fig.1-2). As previously mentioned, the prominent effect of exterior platform angle and platform depth has led to the creation of an EPA-PD model to predict flake size (in the form of flake mass) (Li et al., Under Review; McPherron et al., 2020). The angle of blow, however, was dropped from the EPA-PD model due to the difficulty of obtaining it from stone artifacts.

We then discuss the limitations and future directions of the Dibble controlled experiments. For one, although the EPA-PD model has been applied to both experimental and archaeological assemblages (Braun et al., 2019; Dibble, 1997; Dogandžić et al., 2020, 2015, 2015; Li et al., Under Review, Under Reviewb; McPherron et al., 2020), it only explains a portion of the variability in flake formation. Any change that causes the model to deviate from a "standard" experimental setting will greatly reduce its explanatory power (Clarkson and Hiscock, 2011; Davis and Shea, 1998; Dogandžić et al., 2015; Shott et al., 2000; Shott and Seeman, 2017). Second, knapping variables such as platform and core surface morphology, striking force, and flake termination all require further investigation to better understand their effect on flake formation. Third, we argue for the importance of bringing fracture mechanics back into controlled flaking experiments to fill the gap between the basics of flaking mechanics and the knapping behaviors that underlie the archaeological record.

Using the experimental dataset from the Dibble experiments, we find that adding the angle of blow can significantly improve the EPA-PD model's performance. However, as previously mentioned, the angle of blow has remained an archaeologically invisible variable until now so it cannot be included in the EPA-PD model when it is applied to interpret the archaeological assemblages. In Chapter 3 (paper two) of this

thesis, I conducted a series of controlled experiments guided by fracture mechanics to reconstruct the angle of blow from measurable flake attributes, providing an opportunity to finally include it in the EPA-PD model.

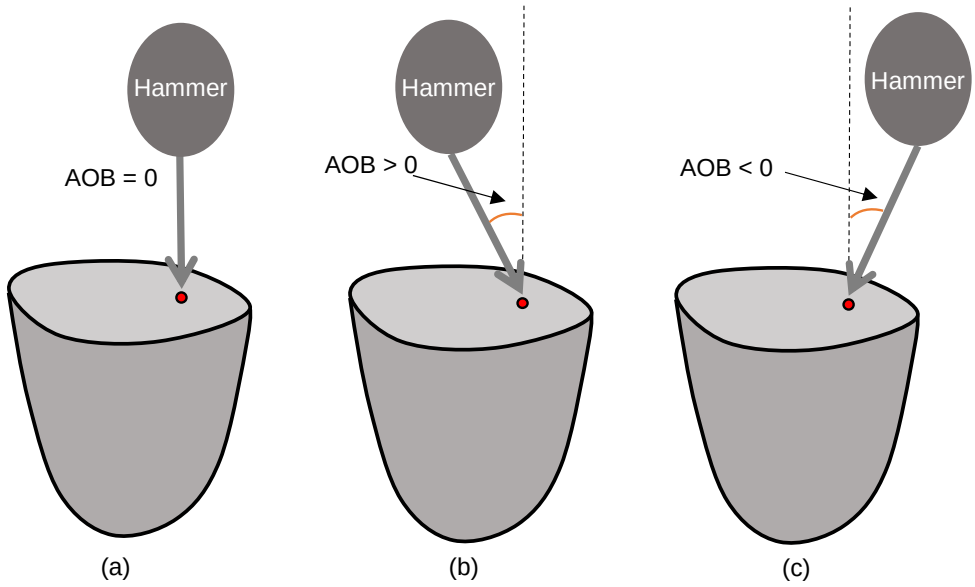

Fig. 1-2 Illustration of the angle of blow (AOB), (a) shows when the hammer directly strikes the core or when the angle of blow is zero (perpendicular to the platform), (b) shows when the hammer strikes into the core or when the angle of blow is positive, (c) shows when the hammer strikes towards the core or when the angle of blow is negative. The red dot represents the point of percussion

6.3 Paper two: Quantifying knapping actions: a method for measuring the angle of blow on flakes

In paper two, I conducted a series of controlled flaking experiment using a drop tower and plate glass setup to investigate the effect of the angle of blow on flaking, specifically focusing on reconstructing the angle of blow from features of a flake's bulb of percussion. Drop tower is a classic setup used among earlier controlled flaking experiments (Dibble and Pelcin, 1995; e.g., Dibble and Whittaker, 1981; Pelcin, 1996; Speth, 1974) that simulates the knapping process by dropping hammers (steel ball bearings) at fixed distances onto cores held in a fixed position. Despite its simplicity, the drop tower setup can effectively control both the striking

force and location during flake removal. The drop tower used in my experiments was built in the metal workshop at the University of Tübingen.

The drop tower experiment conducted in this paper is guided by the fracture mechanics of Hertzian cone formation. The Hertzian cone is a key feature in conchoidal flaking, it is generated from the hammer blow and extends to form the bulb of percussion on a flake. Fracture mechanics studies have shown that the angle of blow has an impact on the Hertzian cone orientation (Akimune, 1990; Chaudhri, 2015; Chaudhri and Chen, 1989; Salman et al., 1995). I investigate how changes in the angle of blow affect the Hertzian cone orientation in the form of a new flake attribute, namely the bulb angle. Bulb angle refers to the angle between a flake's platform and the extruding side of the Hertzian cone before it extends to form the bulb (Fig.1-3).

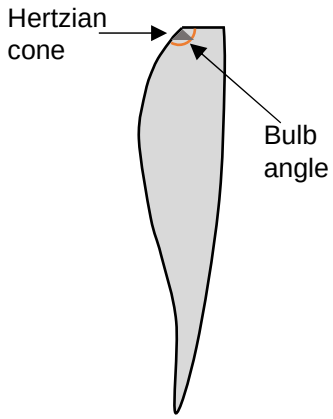

Fig. 1-3 Schematic illustration of bulb angle on a flake from its profile view, the dark grey triangle represents the Hertzian cone, and the orange arc marks the bulb angle

Results from the drop tower experiment show that bulb angle, within limits, reflects changes in the angle of blow. The relationship between bulb angle and the angle of blow is further tested in two additional datasets, one from the previous Dibble experiments (Dibble and Rezek, 2009; Dogandžić et al., 2020; Leader et al., 2017; Magnani et al., 2014; Rezek et al., 2011) and another from a replicative experiment. Overall, all three datasets yield the same result that bulb angle can be used as a proxy for the angle of blow, allowing us to measure this archaeologically invisible knapping variable from flakes from the first time.

6.4 Paper three: Did early hominins control their hammer strike angles when making stone tools?

In paper three, I use the bulb angle method developed in paper two to measure the angle of blow used by early hominins using flakes from sites dated from 1.95 to 1.4 Ma with the goal to investigate changes in their knapping strategies over this period of time.

The dataset used in this paper consists of 12 Early Pleistocene assemblages and one Middle Paleolithic assemblage with Levallois technology as a control. A map of the sites can be found in Chapter 4. The reason for choosing the Early Pleistocene assemblages is because studying these early archaeological materials provides an opportunity to track changes in early hominins' control over their angles of blow and in their understanding of aspects of flaking mechanics related to the angle of blow. More specifically, we are interested in looking at whether there is a change in early hominins' knapping strategies towards the Oldowan-Acheulean transition, namely, whether early hominins developed a more comprehensive understanding of different knapping variables including the angle of blow through time. We also include one Middle Paleolithic site, Roc de Marsal, France, to use Neandertals, who were more competent knappers, to help us contextualize changes observed in the Early Pleistocene assemblages.

Our results show that early hominins begun to adjust their angle of blow according to platform attributes such as platform depth and exterior platform angle towards the Oldowan-Acheulean transition. In particular, hominins from the younger Early Pleistocene assemblages preferred to strike more directly at the platform when making larger flakes.

6.4.1 Site descriptions of the Early Pleistocene assemblages

The 12 Early Pleistocene assemblages are currently curated at Nairobi National Museum in Kenya, including five Oldowan assemblages (FwJj20, FxJj1, FxJj3, FxJj10, FxJj82), four Karari assemblages (FxJj16, FxJj18IH, FxJj20E, FxjJ50), and three Acheulean assemblages (FxJj37, FxJj63, FxJj65). These assemblages are also grouped based on the technological industry they belong to in the analysis.

FwJj 20 belongs to the Upper Burgi Member (Mbr.) and is dated to around 1.94 Ma (Braun et al., 2010). It is located in the II Dura sub-region of the Turkana Basin and was in a well-watered environment when the artifacts were deposited (Bamford, 2011; Braun et al., 2010). Although FwJj covers an area of 130 m^2, its artifact layer is only about 15 cm thick, indicating a fast burial of the archaeological material with good preservation. All artifacts analyzed from FwJj 20 thus came from one single layer (Archer et al., 2014; Braun et al., 2010).

FxJj 1, FxJj 3, FxJj 10, and FxJj 82 belong to the KBS Mbr. in the Karari region (Braun and Harris, 2009, 2003) and are dated to between 1.87 and 1.6 Ma (Braun and Harris, 2009; Brown et al., 2006; Isaac and Behrensmeyer, 1997; Lepre and Kent, 2010; Toth, 1985). FxJj 1, FxJj 3, and FxJj 10 were excavated in the 1970s, FxJj 10 was excavated again in 2003, and FxJj 82 was excavated in the 2000s (Braun and Harris, 2009; Isaac and Harris, 1997).

FxJj 1 is located on the northern slopes of the Aberegaya Ridge, northeast of Lake Turkana. It is known for being the first site discovered in the Koobi Fora Formation (Fm.). A total of 138 *in situ* artifacts were discovered at the site and the majority of these came from one layer. The site was occupied during a period when the environment was wet (Isaac and Harris, 1997). FxJj 3 is located southwest of FxJj 1 and shares a very similar context with FxJj 1. The main excavation at FxJj 3 yielded 122 *in situ* artifacts from one single layer (Braun and Harris, 2009; Isaac and Harris, 1997).

FxJj 10 is located in the Karari Ridge region and was occupied during a dry period of time (Braun and Harris, 2009). The initial excavations at FxJj 10 yielded 294 *in situ* artifacts and a large collection of surface pieces from an area of roughly 19 m^2. The new excavations yielded 161 *in situ* artifacts and much fewer surface pieces from an area of 89 m^2, suggesting that a large region was occupied and has been under erosion since the initial excavations (Braun and Harris, 2009; Isaac and Harris, 1997). The site stratigraphy is divided into five layers, with most artifacts coming from Layers 2 and 1. FxJj 82 is also located in the Karari Ridge region and was occupied during a period of time when the environment was varying but on the drier end. The excavations at FxJj 82 yielded 541 *in situ* artifacts from four layers (Braun and Harris, 2009).

FxJj 16, FxJj 18IH, FxJj 20E, and FxJj 50 are from the Lower Okote Mbr. and are dated between 1.6 Ma and 1.5 Ma (Bunn, 1997; Isaac and Behrensmeyer, 1997). FxJj 16 is located at the western face of the Karari Escarpment and was likely situated in a floodplain context when it was occupied (Harris, 1978). The excavation conducted in 1972 yielded a total of 173 *in situ* artifacts from one layer (Harris, 1978; Isaac and Harris, 1997).

FxJj 18IH belongs to the FxJj 18 site complex that is located in the Karari ridge region. The FxJj 18 site complex covers an area of approximately 7,200 m^2 and consists of four localities: FxJj 18 GL, FxJj 18NS, FxJj 18GU, FxJj 18IH (Harris, 1978; Isaac and Harris, 1997; Kaufulu, 1983). FxJj 18IH (Ingrid Herbich Site) is in the northern part of the site complex and is the youngest site in the stratigraphic sequence (Harris, 1978; Kaufulu, 1983). The excavation of FxJj 18IH in 1973 yielded a high artifact density: a total of 3272 *in situ* artifacts including 889 whole flakes from about an area of 11 m^2 (Harris, 1978; Isaac and Harris, 1997). FxJj 18IH was in close proximity to a floodplain at the time it was occupied (Harris, 1978). Because the excavation at FxJj 18IH yielded a large number of artifacts, we randomly sampled the complete and unretouched flakes with a clear bulb angle to reach a sample size of at least 40.

FxJj 20E (East) belongs to the FxJj 20 site complex that is located on the western side of the Karari Escarpment. The site complex consists of four sites: FxJj 20S, FxJj 20M, FxJj 20E, and FxJj 20AB. Both FxJj 20M (Main) and FxJj 20E underwent extensive excavations in the 1970s (Harris, 1978; Isaac and Harris, 1997; Kaufulu, 1983). FxJj 20E is known for the discovery of KNM-ER 3230, a mandible attributed to *Australopithecus boisei* (Harris, 1978; Isaac and Harris, 1997). The excavations at FxJj 20E yielded a total of 1773 *in situ* artifacts from 130 m^2 (Harris, 1978; Isaac and Harris, 1997). The site stratigraphy indicates that FxJj 20E was located in a channel near a floodplain during its occupation by the hominins (Harris, 1978; Isaac and Harris, 1997; Kaufulu, 1983).

FxJj 50 is located in the southern part of the Karari region and was excavated in the 1970s. The excavations yielded a total of 1438 *in situ* artifacts including 562 whole flakes. In addition, both the stone artifacts and bones had a rather high success rate for refitting (Isaac and Harris, 1997). The site stratigraphy is divided into six

excavation units (EU) with most of the findings coming from EU II (Bunn et al., 1980; Isaac and Harris, 1997). The archaeological materials were deposited on a floodplain next to a channel (Isaac and Harris, 1997). The overall broad horizontal distribution and good preservation of the findings at FxJj 50 provide researchers a great opportunity to test various hypotheses regarding the activities carried out by the early hominins at the site (Braun and Harris, 2009; Bunn et al., 1980; Isaac and Harris, 1997).

FxJj 37, FxJj 63, and FxJj 65 belong to the Upper Okote Mbr. and are dated to around 1.4 Ma (Isaac and Harris, 1997; Presnyakova et al., 2018; Presnyakova, 2019). FxJj 37 was excavated in the 1970s (Isaac and Harris, 1997; Liljestrand, 1980). Evidence from the lithology of the site deposits and artifact disposition indicates that the archaeological materials at FxJj 37 were discovered in a secondary context. The excavations yielded a total of 604 artifacts including 257 whole flakes (Isaac and Harris, 1997).

FxJj 63 is located on the east side of the Karari Escarpment. The majority of the archaeological materials at FxJj 63 were deposited on a channel with a high energy flow (Isaac and Harris, 1997; Kaufulu, 1983). The excavations yielded a total of 1036 *in situ* artifacts including 446 whole flakes (from one layer) and 1224 surface pieces (Isaac and Harris, 1997). FxJj 65 is located approximately 500 m northwest of FxJj 63, sharing a very similar depositional context with FxJj 63. FxJj 65 was excavated in 2010 and 2011, the excavations yielded a total of 675 *in situ* artifacts (Presnyakova, 2019).

6.4.2 Site description of the Middle Paleolithic assemblage

Roc de Marsal (henceforth RDM) is a small cave site located in the tributary valley of the Vézère River, southwest of Les Eyzies, France. RDM was initially excavated by Jean Lafille from 1953 to 1971 (Bordes and Lafille, 1962; Turq, 1979). A more recent series of excavations were carried out by a large collaborative team from 2004 to 2009 (Aldeias et al., 2012; Sandgathe et al., 2011a, 2011b; Turq et al., 2008). The recent excavations recognized 13 stratigraphic layers (Layers 1 through 13), all of which are Middle Paleolithic (Sandgathe et al., 2011b). The lower layers (Layer 9-5)

are characterized by Levallois blank production, and the upper layers (4-2) show a change in the production mode to Quina technology (Lin et al., 2015; Sandgathe et al., 2011b).

7 Open science

Open science aims to promote transparency, accessibility, and reproducibility in scientific research (Munafò, 2016; Vicente-Saez and Martinez-Fuentes, 2018; Wilkinson et al., 2016). To promote open science, all data and code used to generate results in my thesis will be made publicly available once the manuscripts are accepted. This thesis has greatly benefited from the open science practice. For one, all software used to conduct the analyses, such as R, Python, and Meshlab (Cignoni et al., 2011; R Core Team, 2020; Van Rossum and Drake, 2011), are open-source. Throughout the development of this thesis, I draw on open-source datasets and software to help formulate my research hypotheses and test preliminary research questions (Pelcin, 1996; Režek et al., 2018; Yezzi-Woodley et al., 2021). By making our data and code publicly available, my collaborators and I welcome and encourage the scientific community to test and reproduce our findings, and furthermore, advocate for establishing good reliability and reproducibility of the scientific research (Hoffman, 2016; Marwick, 2017). We also welcome anyone to make use of our data and exchange ideas. I believe that promoting open science will not only broaden the audience of this thesis but also make resources from this thesis available for teaching purposes.

CHAPTER 2 A synthesis of the Dibble et al. controlled experiments into the mechanics of lithic production

This chapter includes the following manuscript is accepted with minor revisions by the *Journal of Archaeological Method and Theory*:

Li, L., Lin, S.C., McPherron, S.P., Abdolahzadeh, A., Chan, A., Dogandžić, T., Iovita, R., Leader, G.M., Magnani, M., Rezek, Z., Dibble, H.L. (*under review in the Journal of Archaeological Method and Theory*). A synthesis of the Dibble et al. controlled experiments into the mechanics of lithic production.

Author contributions

Conceptualization: Li Li, Sam C. Lin, Shannon P. McPherron, Harold L. Dibble

Data curation: Aylar Abdolahzadeh, Annie Chan, Harold L. Dibble, Tamara Dogandžić, Radu Iovita, George M. Leader, Li Li, Sam C. Lin, Matthew Magnani, Zeljko Rezek

Data organization: Li Li, Shannon P. McPherron

Writing – original draft: Li Li, Sam C. Lin, Shannon P. McPherron

Writing – review and editing: Aylar Abdolahzadeh, Annie Chan, Tamara Dogandžić, Radu Iovita, George M. Leader, Matthew Magnani, Zeljko Rezek

Abstract

Archaeologists have explored a wide range of topics regarding archaeological stone tools and their connection to past human lifeways through experimentation. Controlled experimentation systematically quantifies the empirical relationships among different flaking variables under a controlled and reproducible setting. This approach offers a platform to generate and test hypotheses about technological decisions of past knappers from the perspective of basic flaking mechanics. Over the past decade Harold Dibble and colleagues have run a number of controlled flaking experiments to better understand flake variability using mechanical flaking apparatuses and standardized cores. Results of their studies underscore the dominant impact of exterior platform angle and platform depth on flake size and shape, but the results also illustrate the complexity of the flake formation process through the influence of other parameters such as core surface morphology and force application. Here we review the work of Dibble and colleagues on controlled flaking experiments by summarizing their findings to date. Our goal is to synthesize what was learned about flake variability from these controlled experiments to better understand the flake formation process.

1 Introduction

From the 1980s until his death in 2018, Harold Dibble built and ran an experimental lab in his department at the University of Pennsylvania designed to better understand stone tool production through controlled experimentation. This effort resulted in the construction of two flaking apparatuses, nicknamed Igor and Super Igor, that represented a culmination of his experimental interests dating back to his dissertation work in the 1970s when he built a drop tower apparatus to generate insights that he then applied to the Tabun lithic assemblages house at the University of Arizona. He maintained interests in the approach over the subsequent years, eventually partnering with his graduate student Andy Pelcin to restart the drop tower experiments in the 1990s (Dibble and Pelcin, 1995; Pelcin, 1997a, 1997b, 1996). Dibble was assured that controlled experimentation, where individual variables could be isolated and systematically manipulated, was superior to the more common replication experiments that characterize lithic studies. The renewed drop tower experiments with Pelcin also convinced Dibble of the need to upgrade the

experimental design, and this led to a difficult but ultimately successful effort to obtain National Science Foundation funding (BCS-0649673 and BCS-1153192) to build a new lab. This upgrade was largely motivated by an experimental desire to not only test more variables than the drop tower setup allowed but also to produce flake outcomes that more closely resembled the archaeological record (Rezek et al., 2016). And thereby, the new setup could perhaps convince more archaeologists of the validity of the approach and of the results for understanding the decisions and actions of past flintknappers. For Dibble, the validity of the empirical models derived from the drop tower experiments for the archaeological record was never in doubt; in fact, the scraper reduction model for which his early career is best known was a direct result of this work. However, he also well understood that the burin spall-like flakes produced in those early experiments from plate glass inhibited a greater appreciation of the underlying, general process of flake production they were revealing.

The Dibble and colleagues experiments (hereafter called the Dibble experiments) produced a series of papers examining many aspects of flake production. However, while there is continuity in these papers, a coherent flaking model did not emerge, making it difficult to take stock of where this line of research currently stands. At the time of his passing, it was Dibble's intention to produce a paper pulling together and summarizing the results to date, and here we do our best to complete this effort in his absence. In addition to trying to integrate his papers, we also discuss some of the limitations of the experimental design and highlight areas and approaches that could be constructively explored in subsequent experiments. With this summary, we also include a complete database coming from these experiments (see Appendix I for field descriptions).

1.1 A brief review of the history of experimentation in lithic studies

Because the physical properties of stone and the ways through which they fracture are uniformitarian and invariant across time and space, we can assume that processes associated with stone fracture observed today also operated in the past (Eren et al., 2016; Lin et al., 2018). Based on this premise, archaeologists verify hypotheses and develop inferences about past lithic technology by replicating the forms of stone artifacts observed in the archaeological record.

Systematic documentation of the experimental approach in lithic research appeared as early as the late 19th century. These early efforts mainly focused on reproducing "primitive" tools with "primitive methods" and were not considered as a major component in archaeological research (Johnson et al., 1978). From the 1960s onwards, the flintknapping work of Bordes, Crabtree, Tixier, and others began to draw more attention to the use of replicative flintknapping to investigate past knapping procedures (Bordes, 1969; Crabtree, 1970; Frison, 1979; Shea et al., 2001; Sheets and Muto, 1972). Lithic experiments flourished in the following decades as increasingly researchers used flintknapping as an experimental means to examine different questions concerning stone tool production, including the effect of different percussion techniques, reduction sequences, and raw material types (Dogandžić et al., 2020; Eren et al., 2011; Eren and Lycett, 2012; Magnani et al., 2014; Moore and Perston, 2016; Tabarev, 1997). Today, experiment is arguably a core aspect of stone tool research that is routinely employed to examine a wide variety of issues surrounding the technological and functional nature of past stone tools (Eren et al., 2016; Lin et al., 2018, 2013; Režek et al., 2018), as well as broader socio-cultural, biomechanical, and cognitive domains associated with lithic technology (Moore and Perston, 2016; Pargeter et al., 2019; Stout et al., 2015).

1.2 Philosophy behind experimentation in lithic studies

The inferential power of lithic experiments for explaining past hominin behavior depends on the validity of the experimental design. The inferential validity of an experiment has been discussed in the form of "internal" and "external" validity (Eren et al., 2016; Lin et al., 2018). Internal validity refers to the quality of the causal relationships between the independent variables and the experimental outcome within an experimental framework (Eren et al., 2016; Lin et al., 2018). External validity refers to the ability to apply the experimental conclusions to settings beyond the condition in which the experiment was conducted (Lin et al., 2018; Lycett and Eren, 2013). The inferential validity of an experiment is governed by hypothesis construction and variable control (Lin et al., 2018). Like in any other science, experimentation in archaeology should be guided with clear and testable hypotheses (Eren et al., 2016). A good hypothesis should finely balance the relationship between its underlying uniformitarian assumptions and how these assumptions are treated to

avoid being non-testable or un-falsifiable (Lin et al., 2018). Once a hypothesis is formulated, it is realized through a concrete experimental design that allows control over independent variables relevant for testing the hypothesis. This is to avoid possible confounding factors that may complicate the interaction between these independent variables, thus ensuring the internal validity of an experiment (Lin et al., 2018).

With these concepts of validity in mind, we can categorize lithic experiments into two groups: replicative and controlled. Lithic experimentation has traditionally centered around replication. Specifically, in replicative experiments, human knappers use what is believed to be the actual methods and materials to replicate forms of stone artifacts discovered in the archaeological record (Flenniken, 1978; Franklin and Simek, 2008; Johnson et al., 1978; Scerri et al., 2016). This type of lithic experimentation allows researchers to look beyond the form of the artifacts and explore the dynamic ways through which past people made and used different forms of stone tools (Johnson et al., 1978). Today, replicative experimentation plays a central role in the technological approach of analyzing lithic artifacts (Bordes, 1953, 1969, 1971; Brenet et al., 2009; Crabtree, 1970; Frison, 1979; Geneste, 1985, 1988; Pelegrin, 1990; Roussel et al., 2009; Shea et al., 2001), with a particular focus on reconstructing the sequences and techniques of past stone tool production. However, a major issue surrounding replicative experimentation is its heavy reliance on the subjective observation and experience of the modern knapper. Knapping is a skill that involves the coordination of multiple bodily movements (Bril et al., 2012; Geribàs et al., 2010; Rein et al., 2013; Vernooij et al., 2015). Yet, mastering the knapping process with the ability to consistently produce a desirable flaking outcome does not necessarily imply that the knapper is fully aware of the variables at work and their respective effects on the flaking outcome (Dibble and Rezek, 2009). In fact, while experienced knappers can often predict the flaking result of different knapping actions with a relatively high degree of accuracy (Bril et al., 2010; Nonaka et al., 2010), it is still extremely difficult to isolate and quantify the exact effect of a particular variable during the flaking process (Dibble and Rezek, 2009). This in turn results in a poor internal validity of the experimental outcome, meaning that it is difficult to be certain if the observed flaking outcome is truly caused by the manipulated knapping variable instead of other confounding factors. To mitigate the

degree of subjectivity in replicative experimentation, recent studies have argued that a greater amount of attention needs to be paid to the design of replicative experiments, particularly as a tool for hypothesis testing and model building (Eren et al., 2016; Lin et al., 2018).

In contrast to replicative flintknapping, a number of studies in the 1970s and ‘80s began to employ mechanical flaking apparatuses to investigate the underlying mechanics of flake formation under a more controlled experimental setting (Bonnichsen, 1977; Cotterell et al., 1985; Cotterell and Kamminga, 1987, 1992; Faulkner, 1972, 1973; Speth, 1974, 1975, 1981). The primary focus of the controlled experimental approach is on isolating the impact of different knapping parameters on flake attributes through variable control. By maintaining all of the relevant test variables in an experiment while only varying the one in question, a controlled experimental setting can best guarantee the internal validity of its outcome. This means that researchers can have greater confidence in the causal relationships between the tested variables (i.e., independent variables) and the flaking outcome examined within the scope of an experiment (Eren et al., 2016; Lin et al., 2018).

The early controlled experiments focused on testing ideas drawn from fracture mechanics (Cotterell et al., 1985; Cotterell and Kamminga, 1992; Speth, 1972, 1974, 1975, 1981). While they provided some in-depth discussions on flake initiation, formation, and termination, the results of these studies were difficult to apply to the interpretation of archaeological assemblages and did not gain much traction in mainstream lithic research. In part, this lack of traction comes from the variables examined in these fracture mechanics-based experiments being difficult, if not impossible, to measure on lithic artifacts (e.g., mechanical properties and size of the hammerstone, contact time of the hammer strike). Starting from the work of Dibble and Whittaker (1981), Dibble and colleagues made an explicit shift away from fracture mechanics and instead to investigate variables under the direct control of knappers (e.g. platform configurations) (Dibble and Pelcin, 1995; Dibble and Rezek, 2009; Dogandžić et al., 2020; Leader et al., 2017; Magnani et al., 2014; Rezek et al., 2011). These knapper-based controlled experiments are guided by knappers’ observations of what they think matters in flake production. By directly testing variables that knappers can manipulate, this approach arguably touches more directly on stone knapping as a technological process than experiments that focus

explicitly on how fracture mechanics works. Moreover, this focus on knapper control also meant that Dibble's experiments were largely driven by the attributes he observed among the archaeological lithics that he primarily studied in his field research, namely Middle Paleolithic and Middle Stone Age flakes from Europe, southwest Asia, and northern Africa. At the same time, however, it is perhaps worth noting that Dibble himself was quite skeptical of the validity of some apparent truisms derived from modern knapper experience. He questioned, for instance, the relative importance that knappers typically place on core surface morphology and on hammer type to determine flaking outcomes. Thus, an implicit goal of the Dibble experiments was to systematically test what could be described as modern knapper "folk wisdom".

The effort to exert experimental control necessarily requires breaking down the stone knapping process into individual parameters that can then be controlled and manipulated during the experimental process. Controlled flaking experiments often feature a highly artificial setup, such as the drop tower, and flaking products that can have limited resemblance to actual archaeological flakes (Rezek et al., 2016). This lack of "realism" is one of the main critiques that have been leveled against a controlled experimental approach, leading to questions about the external validity of the study outcomes (i.e., the degree to which the experimental findings can be applied to real-world settings). As an effort to address this realism critique, Dibble and colleagues developed a new experimental design to increase the external validity of the experiments by adopting a more realistic core design and hammer delivery process (Dibble and Rezek, 2009; Dogandžić et al., 2020). We will discuss these changes made in the new experimental design in detail in the next section. In addition, it has been argued that the ability to generalize experimental findings to archaeological settings does not necessarily depend on the realism of the experimental design but rather on the ability to confidently determine the causal effects of fundamental parameters (i.e., high in internal validity) (Lin et al., 2018; Magnani et al., 2014). From this perspective, if we can confidently establish the cause-effect of key knapping variables such as platform shape and hammer hardness on flake attributes, we should expect the same cause-effect from these key variables to operate in lithic fracture irrespective of where, when, or how these flakes were made (Magnani et al., 2014).

1.3 Strategies of the Dibble experiments

As mentioned above, many of the earlier controlled experiments employed a drop tower setup that drops a steel ball bearing onto the narrow edge of plate glass to produce flakes. The resulting flakes have a morphology similar to a burin spall. In order to make more “realistic” flakes, Dibble and Rezek (2009) introduced a new controlled experimental design for studying flake formation with two primary changes. First, instead of using plate glass with angular shapes, soda-lime glass cores were molded to have a curved flaking surface with lateral and longitudinal convexity (Fig.2-1). This core geometry, which was referred to as a “semispherical” core in the Dibble experiments, produced flakes that, in terms of both size and shape, looked similar to archaeological flakes. In later experiments, other core shapes were molded or cut to test the effect of core surface morphology on flaking outcomes. Glass was chosen as the core material because it fractures conchoidally and is easily molded to standardized shapes. To these standardized core shapes, different platform morphologies were achieved by using saws and grinding wheels. A purpose-built core mount allowed the core to be flexibly positioned for different hammer striking conditions.

The second important change in these experiments was the use of a pneumatic cylinder to apply a direct compressive load on the core to initiate flake fracture. The use of a steel ball bearing in previous drop tower experiments inevitably meant that the ball “hammer” can bounce back after coming into contact with the core, a phenomenon that is the opposite of the common practice among modern flintknappers of “following through” with a hammer blow after the initial impact (Whittaker, 1994). With the new Dibble experimental machine (“Igor”), hammers of different materials and shapes are mounted to the piston of the cylinder. Upon activation, the cylinder extends the hammer downward over a fixed distance to strike the core underneath, thereby simulating a hammer blow with “follow through” upon impact. A load cell is positioned between the hammer and the cylinder to record the amount of force exerted for each flake removal (Dibble and Rezek, 2009). The experiments ran from 2009 to 2017 used a pneumatic cylinder that allowed for forces up to 1,500 lbs (Dibble and Rezek, 2009; Leader et al., 2017; Magnani et al., 2014; Rezek et al., 2011). In 2017, a second machine (“Super Igor”) with a more powerful

Servohydraulic press (Fig. 2-2) was built to increase the amount of force that could be exerted for flake removal up to 20,000 lbs. This new machine allowed raw materials other than glass to be tested (Dogandžić et al., 2020). Compared to the previous drop tower setup, the new design allowed for a finer control over the hammer percussion process, with the ability to manipulate force application parameters such as the displacement speed and the hammer travel distance. The hammer displacement speed on the second machine is adjusted by the controllers attached to the Servohydraulic testing press (Dibble and Rezek, 2009; Dogandžić et al., 2020).

Using the new experimental design, Dibble and colleagues examined a range of fundamental aspects of flaking by summarizing the empirical relationships among test variables using regression models (Dibble and Rezek, 2009; McPherron et al., 2020; Rezek et al., 2016). With this approach, Dibble's research group studied the effect of a number of flaking variables, including platform attributes such as platform depth and exterior platform angle, core surface morphology, the application of force (i.e., hammer type, angle of blow, location of hammer strike), and raw materials (Dibble and Rezek, 2009; Dogandžić et al., 2020; Leader et al., 2017; Magnani et al., 2014; Rezek et al., 2011). Results from these experiments demonstrate the complexity of the flake formation process, which involves simultaneous interactions of different variables that are difficult to understand in isolation. In the next section, we will review in detail the experimental variables that were controlled as independent variables in the Dibble experiments and how they contribute to variability in flaking outcomes.

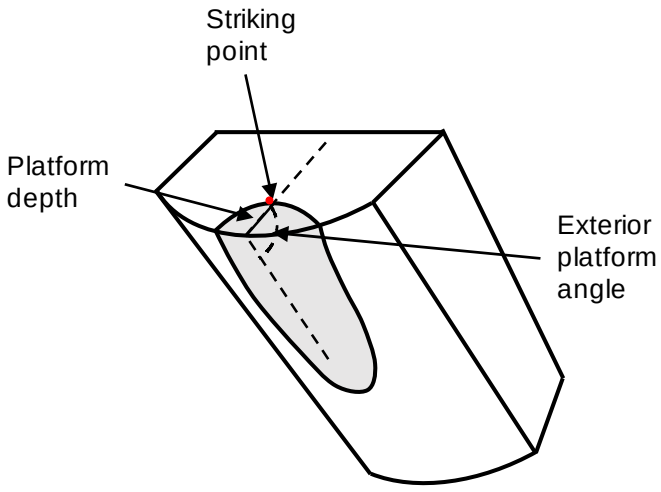

Fig. 2-1 Illustration of a semispherical glass core redrawn from Dibble and Rezek (2009)

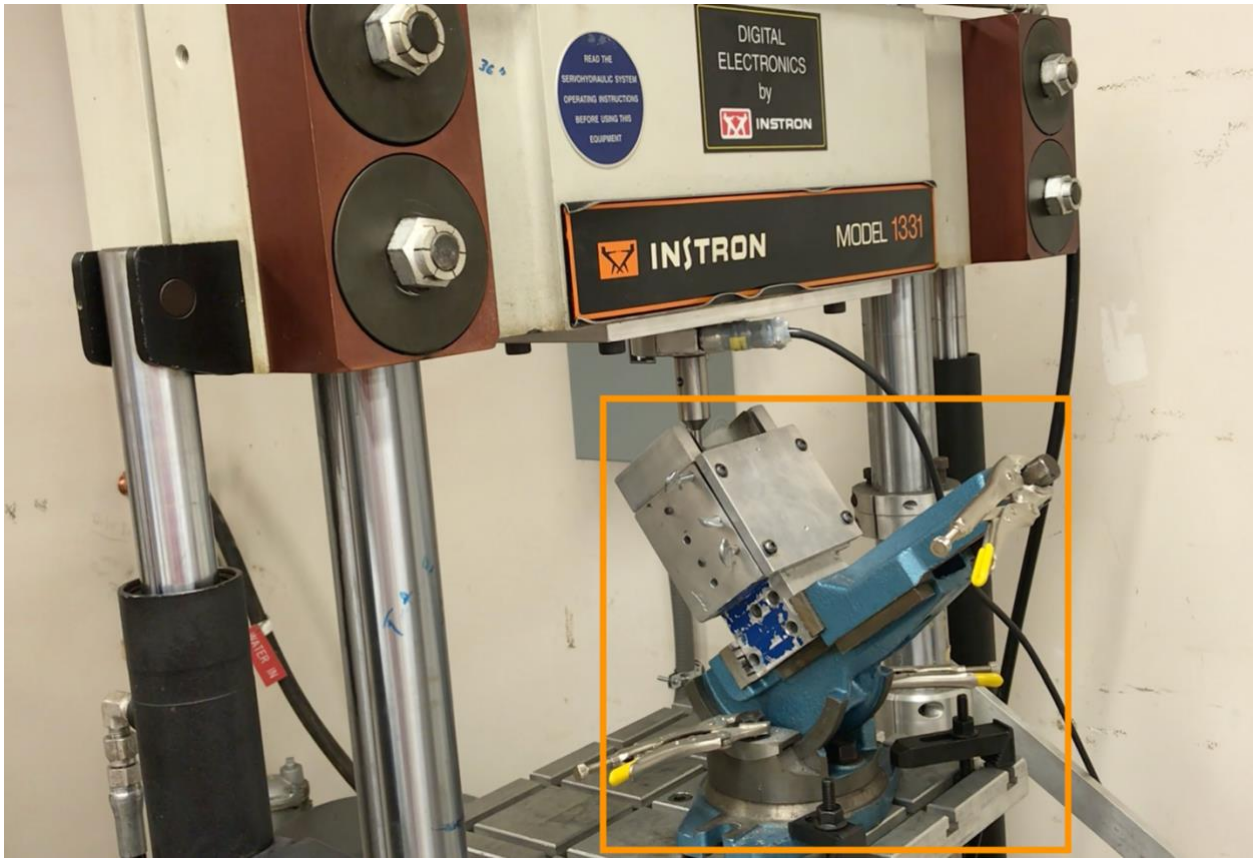

Fig. 2-2 The Super Igor machine. This experimental setup was used in Dogandžić et al. (2020). The device marked by the orange square was used to hold the core during the flake removal process. This same device was used in previous experiments conducted with the Igor machine (Dibble and Rezek, 2009; Leader et al., 2017; Magnani et al., 2014; Rezek et al., 2011)

2 Experimental variables

2.1 Exterior platform angle and platform depth are the primary factors driving flake size

The exterior platform angle (EPA) is the angle between the platform surface and the exterior surface of the core. Platform depth (PD, also sometimes referred to as platform thickness) is the distance from the point of percussion to the core edge (Fig.2-1). Prior to the Dibble experiments, drop tower experiments repeatedly demonstrated the importance of these two platform parameters in determining flake

size and shape (Dibble, 1997; Dibble and Pelcin, 1995; Dibble and Whittaker, 1981; Pelcin, 1996, 1997a, 1997b) (see also Fig.2-3). Increasing either or both exterior platform angle and platform depth results in larger and heavier flakes. The first paper from the Dibble experiments (Dibble and Rezek, 2009) replicated this finding by showing a clear positive correlation between EPA-PD and flake mass. Thus, with a given exterior platform angle, greater platform depths result in heavier flakes. Likewise, the slope of the relationship between platform depth and flake mass increases with exterior platform angle, such that higher exterior platform angles result in increasingly heavier flakes for the same platform depth (Fig.2-4) (Dibble and Rezek, 2009). The flake shape is impacted by exterior platform angle but not by platform depth. For a given platform depth, a higher exterior platform angle produces flakes that are relatively thinner (i.e., higher surface area to thickness ratio) and more elongated (i.e., higher length to width ratio) than those produced with a lower exterior platform angle (Dibble and Rezek, 2009; Lin et al., 2013).

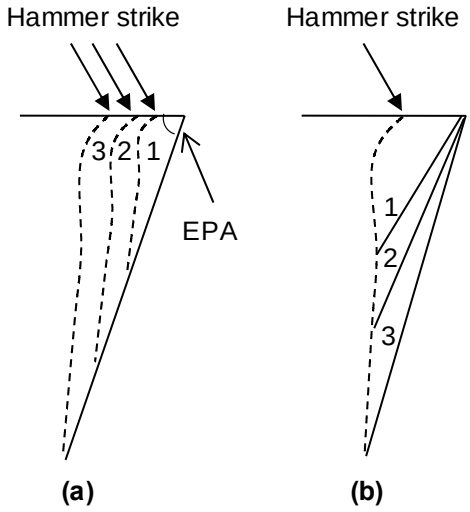

Fig. 2-3 Schematic illustration of the relationship between EPA-PD and flake size in profile view (redrawn from Dibble and Pelcin, 1995). The dotted lines represent the flaking outcome. (a) When the exterior platform angle is held at a constant, increasing platform depth will result in larger flakes. (b) When platform depth is held at a constant, increasing exterior platform angle will result in larger flakes

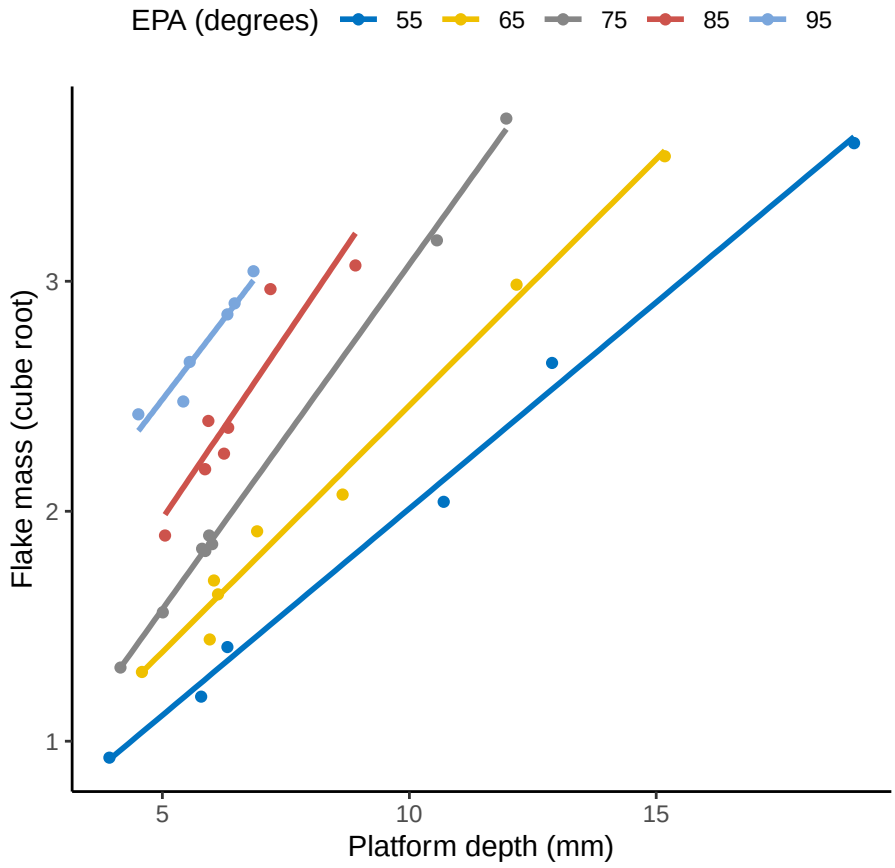

Fig. 2-4 Relationship between platform depth and flake mass grouped by exterior platform angle. The cube root of flake mass is used here to standardize its dimension with platform depth (Dibble and Rezek, 2009)

One of the most important findings of the Dibble experiments is that in comparison to other knapping variables such as core morphology, hammer type, and platform configuration, the effect of EPA-PD on flake size and shape is by far the strongest and the most consistent (Dibble and Rezek, 2009; Dibble and Whittaker, 1981; Dogandžić et al., 2020; Leader et al., 2017; Magnani et al., 2014; Rezek et al., 2011). This relationship has also been demonstrated in actual flake collections, though in each case the strength of the relationship is less strong than in the controlled experiments (Braun et al., 2019; Davis and Shea, 1998; Dibble, 1997; Dogandžić et al., 2020; Lin et al., 2013; Režek et al., 2018; Shott et al., 2000). The repeated success of these two variables in multiple contexts leads to the creation of an EPA-PD model wherein flake mass is a function of exterior platform angle and platform depth. This EPA-PD model arguably captures a fundamental relationship

between platform geometry and flake morphology in the flake formation process, though it is important to note that there is still a considerable amount of flake variability that cannot be explained by the EPA-PD model, especially when other factors (for instance, platform beveling and the angle of blow) are included in the experimental setting. We will discuss the EPA-PD model in greater detail later in this paper.

2.2 Force does not have a significant effect on the flaking outcome

Some of the more counter-intuitive and perhaps controversial findings of the Dibble experiments involve force. Here, the striking force refers to the push of the hammer when it hits the core to remove a flake. In the Dibble experiments, the striking force is measured by a load cell attached to the hammer. In the drop tower setup, the striking force is controlled by changes in hammer mass and/or speed (i.e., drop height). It is a common conception among modern knappers that a harder blow, meaning a greater striking force, will generate a bigger flake. In this respect, however, previous controlled experiments have produced equivocal outcomes. Some showed that changes in striking force result in variation in flake dimensions and termination types (Dibble and Whittaker, 1981; Speth, 1974), while others showed that changing the striking force does not exert any sizable impact on the detached flakes (Dibble and Pelcin, 1995; Pelcin, 1996). For example, Dibble and Whittaker (1981) varied striking force by changing the mass of the steel ball bearings used in their drop tower experiment. The results show that, while increasing the size of the ball bearing does allow larger flakes to be made, force operates as a threshold variable – that is, for a given force, flake size is dependent on the combined effect of exterior platform angle and platform depth. Or, stated alternatively, given a particular platform configuration, a certain level of force is required to remove a flake, and exceeding this level of force does not change the flake outcome in terms of size or shape.

It is worth noting that these earlier drop tower experiments varied striking force in different ways. Speth (1974) varied the drop height of the ball bearing, which in turn changed the travel distance/time of the hammer and hence speed at contact while holding hammer mass and morphology constant. On the other hand, Dibble and Whittaker (1981) held speed constant but changed the size of the ball bearing, which

in turn altered the mass and size (i.e., diameter) of the hammer. Importantly, it is not clear whether these alternative approaches to changing force are experimentally equivalent. It is known, for instance, that hammer size impacts Hertzian cone characteristics (Fischer-Cripps, 2007; Frank and Lawn, 1967; Roesler, 1956), but how these characteristics may change flake outcomes is still not well understood.

2.2.1 Direct percussion and pressure flaking produce equivalent flakes

From an experimental perspective, one way to think about the speed component of force in stone knapping is to consider two extremes in the distinction between static and dynamic loading. The former represents a process whereby the pressure mounts slowly (slow hammer speed), such as in pressure flaking, while the latter represents a quick delivery (fast hammer speed) of pressure in direct hammer percussion. It is commonly noted in replicative flintknapping that flakes produced through direct hammer percussion versus pressure flaking share distinct differences in shape, such that pressure flaked flakes are said to be thinner, more elongated, and more evenly shaped (e.g., Mourre et al., 2010). However, direct percussion and pressure flaking are typically applied in very different contexts in flintknapping, and these actualistic experiments leave many important variables, especially related to platform preparation, uncontrolled.

This point, namely whether and how percussive and pressure flakes vary, is essential to the Dibble experimental setup and the applicability of the conclusions drawn from it. Dibble was convinced that, for the variables he examined, the difference between static (pressure) and dynamic (percussive) loads was minimal, if not irrelevant. This conviction was based on three sets of data. First, the Dibble and Pelcin drop tower experiments showed that force does not seem to matter beyond achieving the threshold force for flake initiation (Dibble and Pelcin, 1995). Second, the flakes from the new controlled experiments (static loading) showed the same patterns already observed in the drop tower experiments (dynamic loading). Third, in two studies using the new experimental setup with varying hammer displacement speeds (0.01, 0.05, 650, 10000 inches per minute), Dibble and colleagues observed no discernable variation in flake mass and dimensions (Dibble and Rezek, 2009; Magnani et al., 2014). Note that the upper value, 10000 inches per minute or approximately 4.3 meters per second, is roughly equivalent to the speed at which knappers strike a core (Bril et al., 2010).

2.2.2 Hitting the core harder does not matter because force is a function of flake mass and flake mass is a function of EPA-PD

Using the new mechanical flaking apparatus, the Dibble experiments revisited this issue of percussive force by using a load cell to record the exact amount of force necessary to remove a flake. Importantly, the high-resolution load cell data shows a picture in line with what was previously proposed by Dibble and Whittaker (1981) based on the drop tower experiments. Specifically, the load cell data show that force increases to the level required for flake detachment and then declines immediately once the flake is removed. The amount of force required for successful flake removal is related to the mass of the flake, as the load recorded by the load cell correlates tightly with flake mass irrespective of variation in other variables such as exterior platform angle, platform depth, and angle of blow (Fig.2-5). Thus, the minimum force required to remove a flake is a function of the flake's mass, which itself is a function of platform depth and exterior platform angle. Applying more force by hitting the core harder would not change the outcome, although Van Peer (2021) argued that flake mass starts to increase at a slower rate relative to the striking force once the force surpasses a certain threshold. However, we note that this particular conclusion is based more on the drop tower experiments than on the new experimental design, because with the use of cylinder compressive load it was not possible to apply forces in excess of what was minimally required to remove a flake.

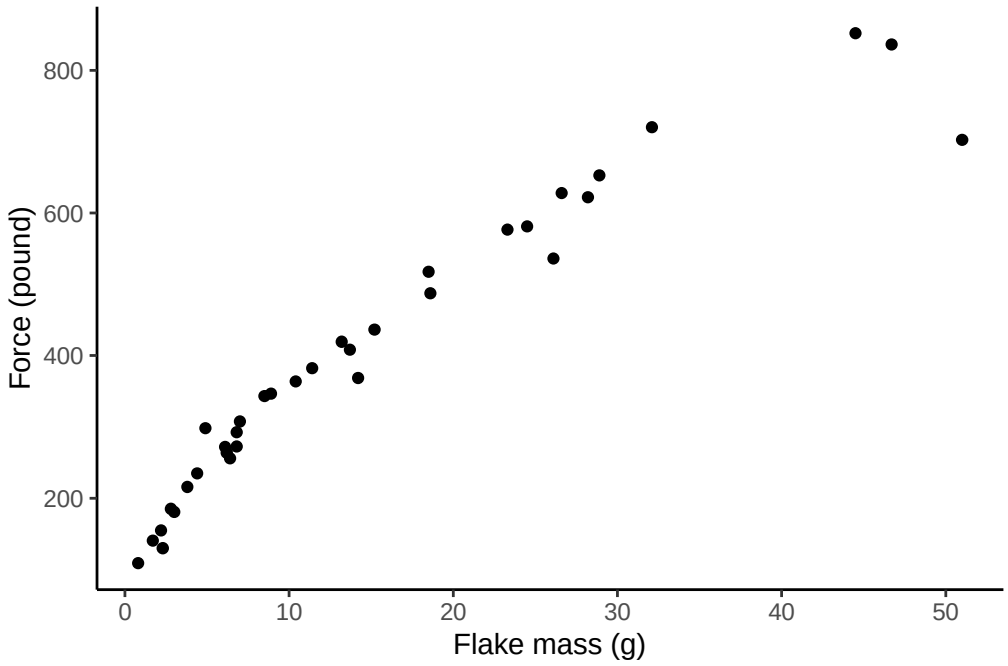

Fig. 2-5 Relationship between flake mass and striking force. The minimum force required to remove a flake with a certain mass is tightly related to its mass (Dibble and Rezek, 2009). Force is expressed as a function of flake mass

2.2.3 Raw material type affects the force required but not the flaking outcome

One of the main critiques of the controlled flaking experiments to date is the sole reliance on glass as the flaking medium. While the new experimental design introduced by Dibble and Rezek (2009) has greatly improved the resemblance of the experimental flakes to actual lithic artifacts, the use of glass cores still raised concerns regarding the applicability of the experimental results to flakes made on different raw material types. Raw material variability features prominently in explanations of archaeological stone tool variability, especially in relation to discussions of lithic technological organization in terms of the quality and supply of lithic raw materials in a given region (Andrefsky, 1994). Thus, the sole reliance on glass among controlled experiments inhibits further considerations of cost-benefit analyses in stone flake production based on raw material variability. However, a number of replicative flintknapping studies have indicated that raw material differences, at least among relatively fined-grained stone types, have minimal to no effect on the general morphology of the detached flakes (Clarkson and Hiscock,

2011; Eren et al., 2014; Kimura, 2002). Thus, how various raw materials respond to the knapping process under controlled conditions was important to evaluate.

To address this, Dogandžić et al. (2020) compared the glass flaking results to flakes made on three other raw material types (basalt, flint, obsidian). All cores were made to an identical form that features a central ridge and longitudinal convexity. The results show that, in nearly every comparison of flake volume and linear dimensions, the flakes show no discernable variation among the four raw material types. Instead, the experimental flakes exhibit the same EPA-PD relationship whereby increasing either platform parameter causes flake size to rise in almost identical ways (Dogandžić et al., 2020) (see also Fig.2-6). The only measurable difference among the flaking outcomes of different raw material types is the amount of force required for successful flake detachment – more force is required to remove flakes from the flint and basalt cores than from the glass or obsidian cores. The results demonstrate that the general flaking patterns observed in glass can indeed be extended to some raw materials that were commonly used in the past for lithic production (Dogandžić et al., 2020). Of course, there are likely many other raw material types that may respond differently to fracture than those tested in this study, especially those that are more heterogeneous. However, given the consistency in flake formation across multiple stone types as shown in Dogandžić et al. (2020), it is more reasonable to assert that the same fundamental fracture patterns also apply to less amorphous raw materials, though the relationship may be more variable or “noisy” due to heterogeneities such as flaws and inclusions.

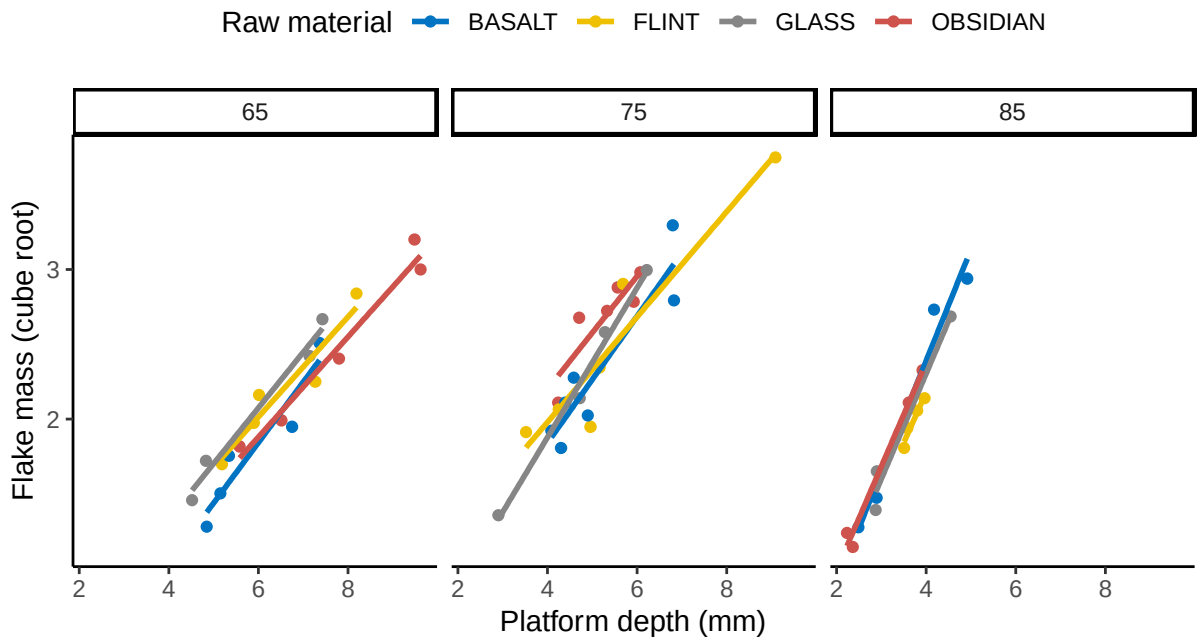

Fig. 2-6 Relationship between platform depth, exterior platform angle and flake mass (cube root) for flakes made of four different types of raw material (Dogandžić et al., 2020).

2.3 The effect of platform beveling on the EPA-PD relationship remains poorly understood

At the outset of the new experimental program, Dibble already knew that the combination of EPA-PD had a strong determining factor in flake outcomes, an observation that was later confirmed and strengthened with subsequent experimental outcomes. At the same time, however, Dibble also knew that, while the EPA-PD model worked well on plane, symmetrical, unobstructed and unmodified platforms, platform preparation (e.g., trimming behind the platform, faceting the platform surface, isolating the platform, etc.) altered the EPA-PD model in ways that were not all understood. For instance, previous controlled experiments (Pelcin, 1996) on plate glass tested the influence of different platform bevels (material removed from behind or from the sides of the platform) and found that flakes with beveled platforms are generally longer than those made with unbeveled platforms while showing no clear difference in mass. In these earlier experiments, the bevel morphologies also changed the bulb thickness. To explain this finding, Pelcin (1996) proposed that platform beveling likely causes flake mass to be redistributed across

the core morphology to produce longer flakes without changing the overall flake mass.

Given that one of the guiding principles of the Dibble experiments was to understand the ways in which knappers can control flaking outcomes (as opposed to creating a general model of fracture mechanics) and given that platform preparation is an important aspect of flake variability in the archaeological record, an experiment was designed to investigate the effect of platform beveling on the EPA-PD model's ability to predict flake mass (Leader et al., 2017). In this experiment, the platform surface was beveled in three ways: flat exterior bevel, concave exterior bevel, and lateral bevel (Fig.2-7). The flat bevel was thought to simulate trimming behind the platform, while the concave bevel represented striking a flake from a core immediately behind a previously struck flake. The lateral bevel, on the other hand, was meant to represent uneven platform surfaces, including the faceted types where the point of percussion was intentionally isolated. Each of these bevel types is found in the archaeological record and is thought to represent techniques used to control the flake outcome. The impact of beveling could be compared across bevel types and to the same cores without bevels.

The results show that beveling significantly changes the EPA-PD model. For instance, flat and concave beveled cores produced larger flakes in their linear dimensions and heavier than those made from the laterally beveled and unbeveled cores (Fig.2-8). However, if instead of using the actual platform depth of these flakes in the EPA-PD model, the platform depth is calculated from the original edge of the core (prior to the bevel) (see Fig.2-7a and Fig.2-7b), the relationship between EPA-PD and flake mass remains the same across the different bevel types. The study concluded that platform beveling changes the relationship between platform depth and flake attributes through the geometry of the platform surface configuration, such that the influence of platform beveling on flake variation changes depending on the position, curvature, angle, and depth of the bevel (Leader et al., 2017). For instance, for flakes with concave platform beveling, the depth of the bevel significantly affects the resulting flake mass—a deeper bevel depth leads to greater flake mass relative to the actual platform depth. However, for flakes with flat platform beveling, a deeper bevel depth leads to a smaller flake mass relative to platform depth.

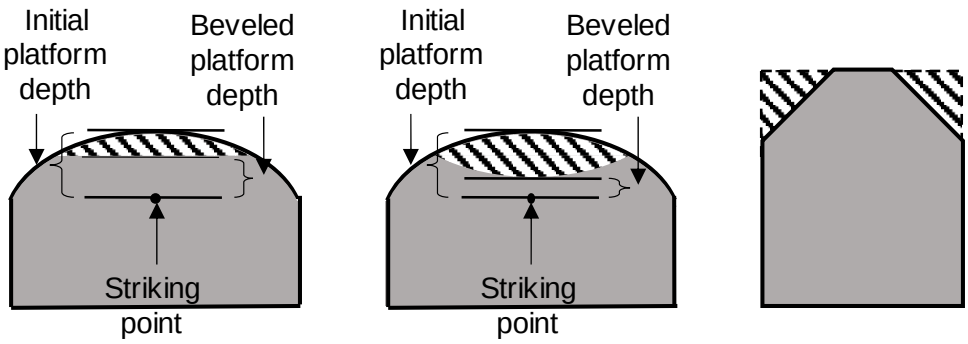

(a) Flat bevel **(b)** Concave bevel **(c)** Lateral bevel

Fig. 2-7 The three types of beveled cores examined in Leader et al. (2017). (a) and (b) show the platform surface; (c) shows the core exploitation surface. The striped areas represent portions of the core removed to produce the bevel

One possible explanation for why the EPA-PD model is skewed by platform beveling is that the relationship between platform depth and platform width is changed. Leader et al. (2017) found that all three types of platform beveling have some influence over platform width. When the platform surface is unbeveled, the resulting platform width of the flake is simply a function of platform depth (see also McPherron et al., 2020). Platform beveling changes this simple linear relationship between platform width and platform depth. For instance, among the flakes made on a concave beveled platform, a deeper bevel resulted in significantly wider platforms for a given value of platform depth. Similarly, flakes made with laterally beveled platforms show a greater platform width when compared to their unbeveled counterparts of the same platform depth (as shown in Fig.2-8d). However, these changes of platform width caused by platform beveling cannot be conveniently translated to a refined EPA-PD model that produces a consistent outcome. While both flat and concave bevel platforms result in larger and heavier flakes (Fig.2-8a-c), the laterally beveled platform actually causes the flakes to become relatively shorter than the unbeveled flakes (Fig.2-8b) (Leader et al., 2017).

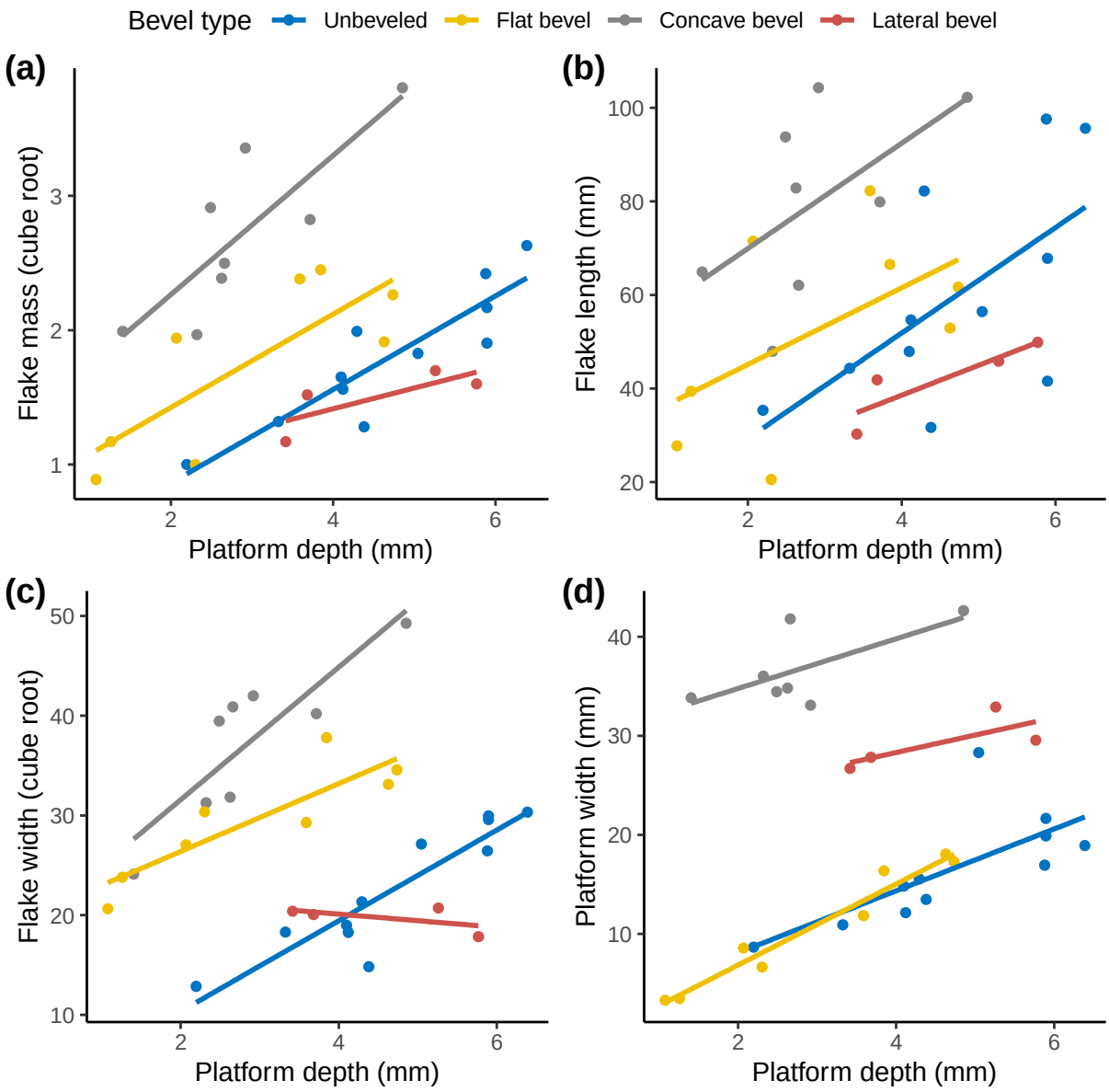

Fig. 2-8 Relationships between different flake attributes and platform depth for beveled and unbeveled flakes (Leader et al., 2017). Both flat and concave bevels were cut at a 6 mm depth from the original flake exterior surface, and the lateral bevels were cut at 45 degrees relative to the platform surface. (a) shows the relationship between the cube root of flake mass and platform depth, (b) shows the relationship between flake length and platform depth, (c) shows the relationship between flake width and platform depth, and (d) shows the relationship between platform width and platform depth

Combined with the results of the prior drop tower experiment (Pelcin, 1996), the Leader et al. (2017) platform beveling experiment showed that the EPA-PD model only applies to a certain class of flakes (such as those without platform

modifications) and pointed to platform depth as the weaker part of the model (because platform depth varies by bevel type). In addition, the experimental findings indicate that some of the flake variability unexplainable by the EPA-PD model may be attributable to platform beveling. For instance, typically in the analysis of archaeological flakes, all of the flakes shown in Fig.8a would be considered together as one group in an EPA-PD model to predict mass, as such the result would have much more variation compared to the unbeveled flakes alone. McPherron et al. (2020) introduced a new variable called platform surface interior angle (PSIA) – the angle between the two vectors formed from the point of percussion to the two lateral platform points. They found that PSIA plays a key role in improving the EPA-PD model. Specifically, by substituting the actual platform depth with a predicted platform depth calculated from PSIA and platform width, the updated EPA-PD model is able to account for a large portion of the underestimation of flake mass that happens on beveled flakes, resulting in a more accurate prediction of flake mass (McPherron et al., 2020).

2.4 Core surface morphology has an impact on flake shape and size

Core surface morphology has long been considered an important factor in constraining flake initiation, propagation, and termination, as well as the size and morphology of the produced flake (Cotterell and Kamminga, 1987; Pelcin, 1997a; Rezek et al., 2011). The Rezek et al. (2011) experiment tested the effect of core surface morphology on flake variation by modifying the exterior surface of the original semispherical design. Four designs were used: a center ridge form (resembling a blade core), a parallel form (resembling a prismatic blade core), a convergent form (resembling a Levallois point core), and a divergent form (see Rezek et al., 2011). The experimental results show that core morphologies do affect, but not always, flake size and shape (Fig.2-9) (see also Van Peer, 2021). For example, independently of EPA-PD, flake elongation (flake length to width ratio) shows variation among some of the core morphologies but not others (Fig.2-9b). A geometric morphometric analysis on the two-dimensional outline of the flakes shows that, while core morphology does exert some effect on flake morphology, much of the variation in flake shape, especially elongation, is in fact controlled by the EPA-PD relationship. Because of this relationship, flakes from distinct core forms can, in

some instances, share very similar size and shape, while flakes from the same core type can vary considerably due to platform configurations alone. This set of results led Rezek et al. (2011) to conclude that core surface morphology is not as important of a factor in affecting flake variation, especially when compared to the effect of EPA-PD, such that the shape of a flake cannot be predicted solely by the geometry of the core. This conclusion, while in agreement with that of Pelcin (1997a), highlights the complexity of the interaction between core morphological variation and the platform attributes in flake variation. Probably a better way of expressing this is that core morphology has a smaller effect on flake morphology than EPA-PD does and that the addition of core morphology to the EPA-PD model would help explain additional variability in flake size and shape, which is suggested by Fig.2-9b.

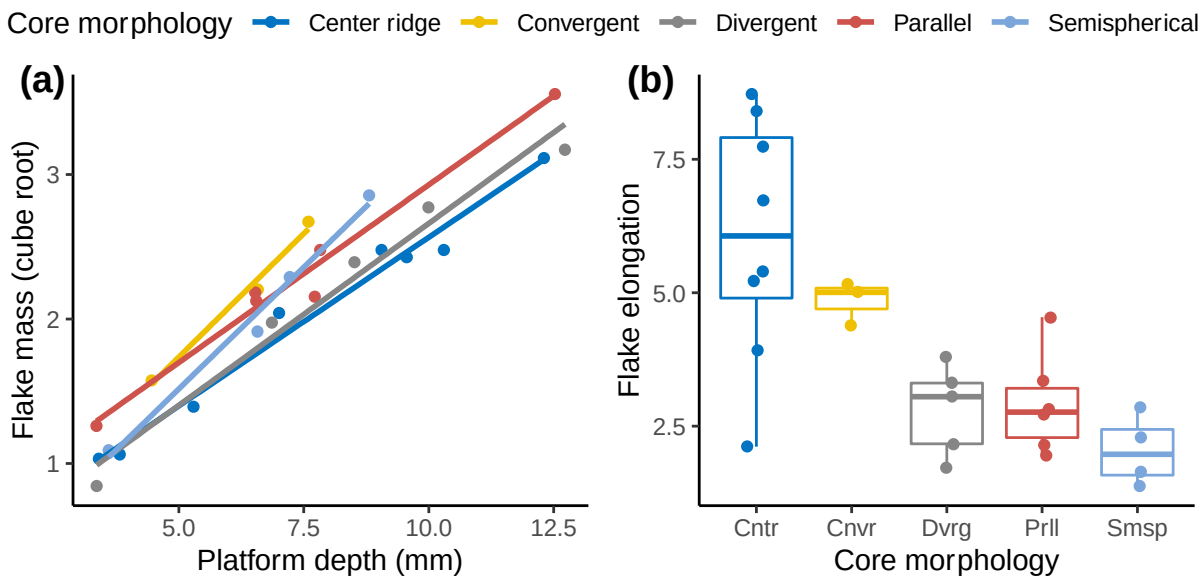

Fig. 2-9 (a) The relationship between platform depth and flake mass for different core morphologies when exterior platform angle is 65 degrees. (b) Flake elongation (length/width) grouped by the core morphology for different core morphologies (Rezek et al., 2011)

2.5 Hammer type and shape affect several flake attributes

2.5.1 Soft hammers produce platform lipping and impact flake shape. Hard hammers can also produce platform lipping.

Replicative knapping experiments have shown that hard versus soft hammers can affect various flake attributes, including flake mass, linear flake dimensions, platform

attributes, flake initiation, and flake termination (Bradbury and Carr, 1995; Buchanan et al., 2016; Damlien, 2015; Driscoll and García-Rojas, 2014; Schindler and Koch, 2012). These differences in flake outcomes are often attributed to differences in force propagation mechanisms. For hard hammer percussion, it is often said that a conchoidal fracture takes place where the force propagates directly from the point of percussion to the termination (Cotterell and Kamminga, 1987). This process results in a clear point of initiation and a well-formed bulb of percussion. On the other hand, a bending fracture is often said to take place with soft hammer percussion (Cotterell and Kamminga, 1987), where the fracture initiates some distance away from the point of hammer contact, leading to flakes having a more diffused bulb, a smaller platform surface and a pronounced “lip” on the interior platform edge. In fact, platform lipping in particular is often used as an indicator of soft hammer percussion in the analysis of archaeological stone tools (Hayden and Hutchings, 1989; Sharon and Goren-Inbar, 1999; Sullivan and Rozen, 1985). However, prior controlled experiments by Bonnichsen (1977) and Pelcin (1997b) showed no clear differences in the occurrence of platform lipping between hard and soft hammer percussion. Pelcin (1997b) postulated that this discrepancy could be because human knappers tend to change percussion techniques, either consciously or unconsciously, when switching between hard and soft hammer use (Hayden and Hutchings, 1989). As such, the presence of flake features such as platform lipping may be related to knapping factors other than hammer type.

To test this proposition, the Magnani et al. (2014) experiment examined the effect of three different hammer materials: steel, copper and synthetic bone. To ensure consistency, these hammers were milled to an identical ball bearing shape the same size as the tip of the mechanical indenter normally used in the experiments. These hammers were then used to strike the platform surface at varying platform depths and exterior platform angles. The results showed that flakes produced by the synthetic bone hammer have smaller bulbs and are longer and thinner than flakes produced by the steel and copper hammers. This outcome is consistent with Pelcin’s (1997b) earlier observation.

Results of the Magnani et al. (2014) experiment showed that platform lipping is much more prevalent (over 95%) among the flakes produced by soft hammer percussion than those made with the steel (under 40%) and copper hammers (under 60%). This

finding suggests that the use of a softer hammer material increases the chance for platform lipping to occur. In the case of lipped flakes made by harder hammers, the angle of blow and where the platform was struck affected the outcome. A negative angle of blow (hitting “inward” to the core) or striking the platform on its edge (as opposed to the surface) increases the chance of lip formation. Thus Magnani et al. (2014:40) concluded that “the presence or absence of lipping in general has little or no predictive value regarding the kind of hammer that was used.” While this statement is true on a flake-by-flake basis, it is also clear that at an assemblage level an elevated percentage of lipped flakes can indicate the use of soft hammer given that negative angles of blow and flakes struck on platform edges are likely to be relatively infrequent knapping strategies. Further, the ability to infer the hammer type on a flake-by-flake basis could be improved if the angle of blow or where the platform was struck can be measured on an archaeological flake.

The Magnani et al. (2014) experiment also showed an important trade-off in knapping success with the use of a soft hammer. When the exterior platform angle of the core is greater, the synthetic bone hammer had a higher chance of failing during the experiment as the hammer tip was not able to sustain the impact pressure and instead crushed against the platform surface. Magnani et al. (2014) thus suggested that the common co-occurrence of other knapping techniques, such as on-edge strikes with soft hammers, may reflect strategies for mitigating the heightened probability of unsuccessful flake detachment with soft hammer percussion when striking directly on platform surfaces.

According to Magnani et al. (2014), the correlation between platform depth and flake mass for a given exterior platform angle is weaker for flakes with platform lipping than for flakes without platform lipping. This outcome might be caused by the bending fracture process associated with the formation of platform lipping. Specifically, because fracture appears to have initiated some distance away from the point of percussion on these flakes, there is likely noise in the platform depth to flake mass relationship because the actual platform depth could not be measured from the point of percussion.

2.5.2 Hammer shape and size do not affect flake size and shape

In addition to hammer material, Magnani et al. (2014) also tested the influence of hammer size and shape by adopting five different steel hammer designs that varied

in their tip shape and diameter. They concluded that when other variables are held at constant, neither the size nor shape of the hammer shows an effect on flake morphology. However, according to the fracture mechanics theory of conchoidal (Hertzian) fracture, the size of the Hertzian cone is related to several variables such as the mechanical properties of both the hammer and the core, the size of the hammer, and the striking force (Frank and Lawn, 1967; Lawn, 1967; Lawn et al., 1974). Changes made on the hammers used in the Dibble experiments might not have been big enough to influence the overall size and shape of the flakes produced.

2.6 The angle of blow affects flake size

2.6.1 The zero or positive angle of blow affects the size but not the overall shape of the flake

The angle of blow is the angle at which the hammer comes into contact with the platform surface. Dibble and Rezek (2009) measured this angle between the hammer impact trajectory and the perpendicular of the platform. A perpendicular hammer impact has an angle of blow of zero, a positive angle indicates an oblique blow striking “outward” towards the core surface, and a negative angle of blow describes a strike directed “inward” to the core volume (Fig.2-10). In his drop tower experiment, Speth (1972) argued that the angle of blow affects the size of the bulb of percussion, whereby a greater angle of blow (a more oblique impact) results in a less prominent bulb. In a later study, Speth (1975) also showed that flakes produced with a large angle of blow were slightly shorter than those produced with a smaller angle of blow. According to Speth (1972, 1975), higher angles of blow limit the stress applied on the platform, thus resulting in a more reduced flake length and a less prominent bulb under otherwise identical striking conditions. However, Dibble and Whittaker (1981) found limited variation among flake attributes in relation to the angle of blow. They explained the discrepancy between their work and Speth (1975)’s in two ways. The first is that the range of variation in the angle of blow was set at 25 degrees in Dibble & Whittaker (1981), which is considerably smaller than the 45-degree interval used in Speth (1975). As such, the 25-degree range of variation may not have been sufficient to observe the effect of angle of blow on flake dimensions. The second reason is that the effect of the angle of blow could have been overshadowed by the more dominant impact of platform depth and exterior

platform angle. It could also be the case that the response to the angle of blow is not linear across all possible angles and where the range of angles tested falls may impact the results. In a later study, Pelcin (1996) went further to argue that the angle of blow does not exert any direct influence on flake attributes, though he did not provide further detailed discussion of this perspective.

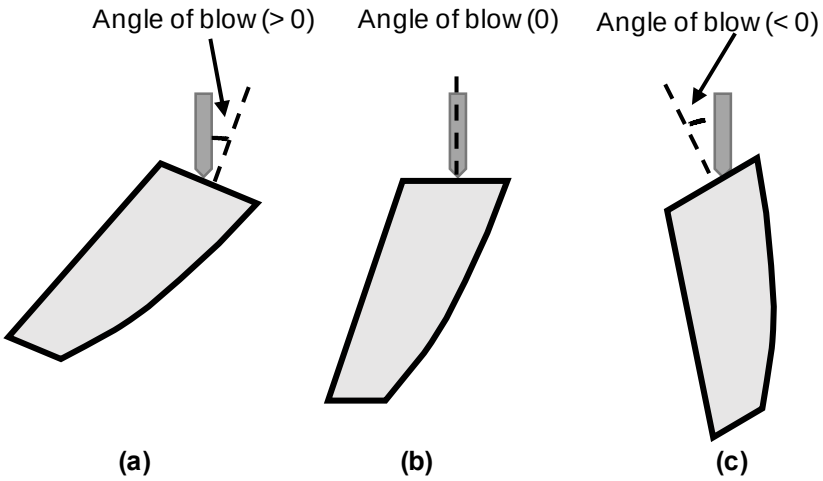

Fig. 2-10 Angle of blow as the angle between the hammer and the perpendicular of the platform. (a) shows a positive angle of blow between the hammer and the core, (b) shows a zero angle of blow between the hammer and the core, and (c) shows a negative angle of blow between the hammer and the core

The initial Dibble and Rezek (2009) experiment explored the influence of the angle of blow at intervals up to 50 degrees. The results showed that the angle has a negative effect on flake mass (standardized by platform depth). Put simply, for a particular EPA and PD, a more perpendicular blow produces a heavier flake than a more oblique strike (Fig.2-11a). This may be because the percussive force applied to the platform surface is more concentrated when the hammer blow is more direct (Dibble and Rezek, 2009). Later, Magnani et al. (2014) showed that a more perpendicular angle of blow also produces flakes that are longer, wider, and thicker (when both platform depth and exterior platform angle are held constant), as was reported in Speth (1975). In addition, Van Peer (2021) showed that changes in the combination of the angle of blow and exterior platform angle could also affect flake morphology. However, the angle of blow does not influence the overall shape in terms of the

length and width ratio of the detached flake (Fig.2-11b), nor does it alter the minimum force required for successful flake removals (Dibble and Rezek, 2009; Magnani et al., 2014).

Although the angle of blow has been shown to have an impact on various flake attributes in several controlled experiments (Dibble and Rezek, 2009; Magnani et al., 2014; Speth, 1975), it is not included in the current EPA-PD model derived from the Dibble experiments. This is because the angle of blow has remained an unmeasurable knapping variable up to now. In the next section we will discuss in detail the addition of angle of blow to the EPA-PD model.

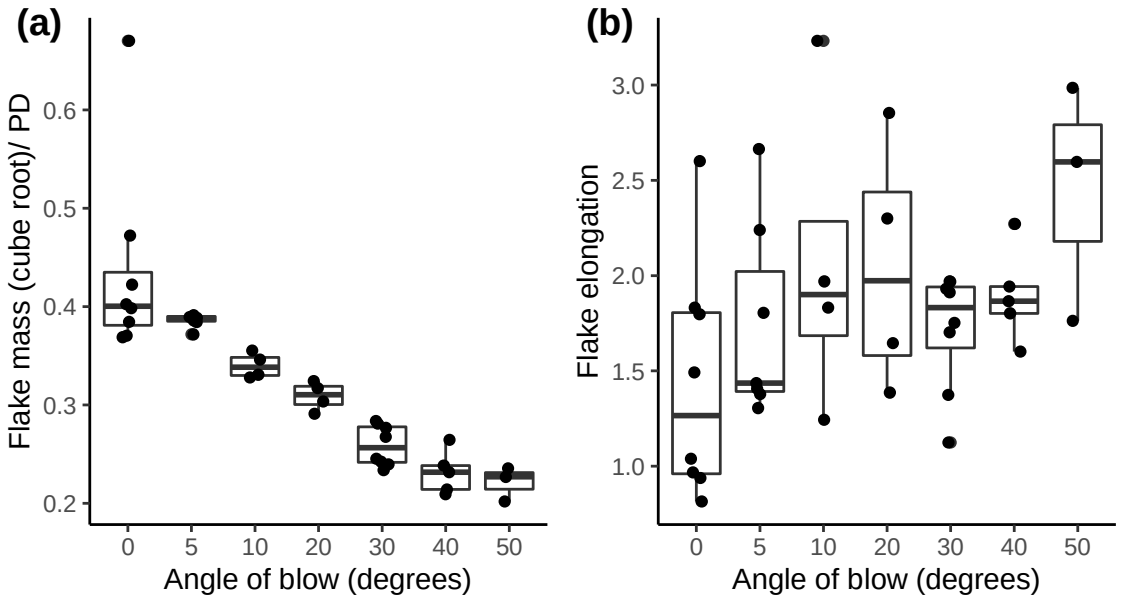

Fig. 2-11 Box plots showing changes in flake mass and other dimensions on angles of blow ranging from 0 to 50 degrees. (a) Flake mass (cube root) standardized by platform depth on flakes produced from angles of blow ranging from (b) Flake length relative to flake width. All flakes have an exterior platform angle of 65 degrees

2.6.2 Negative angles of blow may change flake size

The Magnani et al. (2014) experiment revisited the angle of blow in the context of force application and examined the effect of negative angles of blow (i.e., striking “inward” into the core, as in biface thinning, see also Fig.2-10c). Looking only at platform surface-struck flakes, the experimental findings are largely consistent with those reported in the prior study of Dibble and Rezek (2009), where the angle of

blow has a negative effect on flake size (as measured by mass). That is, flakes made on lower angles of blow, including those with negative impact angles (Fig.2-11c), are consistently heavier than those made on more oblique angles. Interestingly, when negative angle of blow flakes are included, the experimental results show that the angle of blow has a significant influence on both the mass and linear dimensions such as the length and width of flakes. Specifically, flakes made with negative angles of blow are consistently heavier and larger (in both length and width) than the flakes made on positive angles of blow when holding EPA and PD constant (Magnani et al., 2014). This finding, however, needs to be interpreted with caution due to possible confounding variables. To be specific, because decreasing the angle of blow also increases the relative occurrence of platform lipping and hence bending fracture (Magnani et al., 2014), it is currently unclear whether the greater flake length and width associated with negative angle of blows actually reflect the greater propensity of bending fracture when the hammer is struck “inward” into the core.

2.7 Striking on the platform edge changes the flake shape

The Magnani et al. (2014) experiment also explored the influence of different hammer strike locations on the resulting flake variability in the context of their force application experiment. They produced flakes by having the hammer strike either on the platform surface some distance away from the core exterior surface (platform strikes) or directly on the exterior platform edge (on-edge strikes). The latter simulates the common knapping technique used in biface thinning, often in association with the use of a soft hammer. Interestingly, the experimenters found that for on-edge strikes, they had to lightly abrade the platform edge to reduce the chance of the core edge shattering upon hammer impact, especially when a steel hammer was used. This observation is consistent with the common flintknapping practice of edge abrasion in biface thinning, which is thought to make the edge more resistant to on-edge hammer impact (Sheets, 1973).

The Magnani et al. (2014) experiment showed that edge-struck flakes tend to be longer and wider compared to flakes made from platform strikes. This difference is particularly pronounced when the angle of blow is negative. Put simply, for a given platform depth, flakes made by striking the core edge at an inward angle are

substantially longer and wider than those made by striking the platform surface at an outward angle. However, as with angle of blow and hammer type discussed earlier, on-edge strikes also increase the occurrence of platform lipping and, hence bending fracture. It is thus unclear whether on-edge strikes directly increase the dimensions of the detached flakes or whether the increase in flake length and width is associated with the occurrence of bending fracture that is more prevalent with on-edge percussion. If it is the latter, the EPA-PD model will not perform well on the lipped flakes because these flakes are not produced from conchoidal fracture, which is the premise for all of the Dibble experiments.

3 Limitations of the Dibble experiments to date

A major departure of the Dibble experiments from the earlier controlled flaking experiments (e.g., Cotterell et al., 1985; Cotterell and Kamminga, 1987; Speth, 1972, 1974, 1975) is their explicit shift away from fracture mechanics. Rather, the Dibble experiments were designed to test the empirical effects of various knapper-controlled variables on flake variability. As discussed in the section above, this approach has allowed the researchers to effectively evaluate the cause-and-effect of different knapping factors. While some of the results from the Dibble experiments support conventional views shared among replicative flintknappers, many findings illustrate a more nuanced and complex picture of the knapping process, where flake attributes are simultaneously influenced by multiple knapping variables at varying levels. Clarifying the complex relationships of these variables remains a challenging task for future research.

The knapper controlled variables that the Dibble experiments examined also broadly fall into two categories: those that are directly observable and measurable on flakes and cores and those that are not. For instance, Dibble focused on exterior platform angle and platform depth because these variables are measurable on actual flakes. So too are platform preparations and to an extent core surface morphology. However, variables like hammer hardness, strike force, and angle of blow cannot be easily derived from flakes up to now. Dibble's hope was that the measurable attributes would have the largest impact on flaking outcomes and that the unmeasurable attributes would play at best only a minor role. If the opposite were true, then the whole set of experimental results and its applicability to the

archaeological record would be questionable. The results summarized here seem to suggest that a mix of variables is at work. On the one hand, the EPA-PD model stands out as a clear finding. Knappers can alter their flaking outcomes by manipulating these two variables. It is also clear that measurable platform modifications like trimming and shaping are also impacting flake outcomes, but it is unclear how they can be incorporated into the EPA-PD model to clearly quantify their impact on flake size and shape. The fact that the angle of blow also clearly has an impact on the EPA-PD relationship but remains unmeasurable on archaeological flakes makes it even more difficult to quantify the relationship between different variables. These two aspects together likely to a large extent account for the limits of the EPA-PD model in predicting flake size in archaeological collections.

In the following section, we consider this and some of the other limitations of the Dibble experiments, and we follow this by considering some future directions for experimentation.

3.1 The EPA-PD model only works in a highly controlled setting

The current EPA-PD model based on the Dibble experiments is derived from the dominant EPA-PD relationship in determining flake size and shape (Dibble, 1997; Dibble and Pelcin, 1995; Dibble and Rezek, 2009; Dibble and Whittaker, 1981; Lin et al., 2013; McPherron et al., 2020). In addition to the results outlined above, the prominence of the EPA-PD relationship in accounting for flake variability has also been repeatedly verified in both experimentally flintknapped materials and archaeological assemblages (Dibble, 1997; Dogandžić et al., 2020, 2015; Lin et al., 2013; Režek et al., 2018). However, the EPA-PD model only performs well under a strictly controlled setting. That is, the model works best with flakes made by hard-hammer percussion on the platform surface and from cores with no platform beveling or core edge asymmetry (Dibble and Rezek, 2009; Leader et al., 2017; Magnani et al., 2014; Rezek et al., 2011). As discussed in the previous section, any change made to the striking condition that deviates from the “standardized” setting described in Dibble and Rezek (2009) has the potential to skew the EPA-PD model.

From the Dibble experiments, we summarized three major factors that can cause the EPA-PD model to break. The first factor is platform beveling. The addition of platform

beveling changes the EPA-PD relationship with flake mass by altering the relationship between platform depth and platform width. Beveled flakes have a wider platform width relative to platform depth compared to unbeveled flakes (Leader et al., 2017; McPherron et al., 2020). This change is subsequently translated into how exterior platform angle and platform depth work to determine the final flake mass. The second factor is the hammer strike location. Results from the Magnani et al. (2014) experiment showed that the EPA-PD model does not work well in predicting flake mass when applied to flakes produced from on-edge strikes. The third factor is the angle of blow, the Dibble and Rezek (2009) experiment showed that flakes become lighter as the angle of blow increases, even when exterior platform angle is held at a constant. In addition, the Magnani et al. (2014) experiment found that negative angles of blow also affected the EPA-PD relationship with flake mass.

Separately, McPherron et al. (2020) used the Dibble experimental dataset to show that platform surface interior angle (or PSIA) is related to the Hertzian cone angle (itself a constant that varies with raw material type) and this angle can help explain why the EPA-PD model works less well in some instances (particularly in the case of beveled flakes). PSIA is measurable but it is not yet clear how it could be directly incorporated into the EPA-PD model. Alternatively, including the angle of blow can dramatically improve the EPA-PD model's performance. For instance, in the Dibble experimental dataset, where the angle of blow is known, adding it to the EPA-PD model increases the adjusted R-square from 0.80 to 0.91. It can also be seen in Fig.2-12 that the predicted flake mass from the updated EPA-PD-AOB model plots more tightly against the actual flake mass. Thus, efforts to explain flake variation need to consider the effect of the angle of blow. Yet, because the angle of blow remains unmeasurable on archaeological flakes, the variable has been left out of the EPA-PD model. If some way to bring PSIA and the angle of blow into the EPA-PD model can be found, then we will have a much better summary of how knappers control and adjust these variables to vary their flake outcomes.

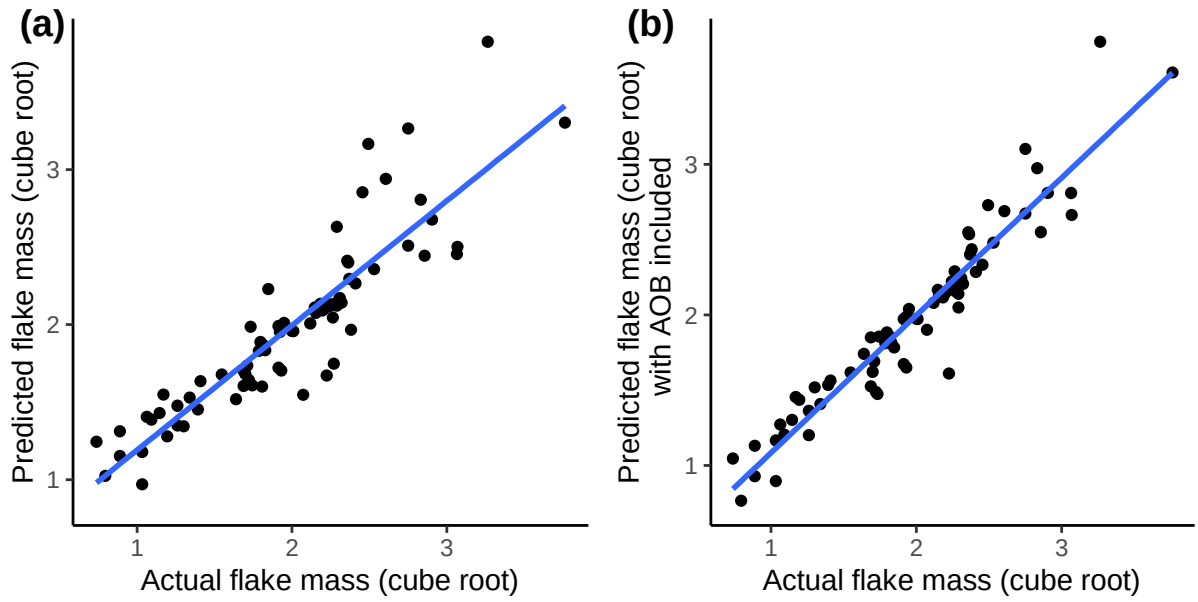

Fig. 2-12 Predicted flake mass to actual flake mass. (a) The predicted flake mass is calculated from the basic EPA-PD model, (b) the predicted flake mass is calculated from the updated EPA-PD model with the addition of the angle of blow

3.2 The collinearity and equifinality of the experimental variables should be taken into consideration in the data analysis

The Dibble experiments are specifically designed to control and isolate knapping variables so that only one of them is tested at a time. This ideally will allow researchers to record only the interactions between the tested independent variables and the dependent variables of interest. However, interactions among the various independent and dependent variables are far more complex and difficult to be disentangled.

The interaction between platform width and platform depth on beveled flakes is an example of collinearity of the experimental variables. Platform beveling has been shown to cause the current EPA-PD model to underestimate flake mass on beveled flakes by changing the simple linear relationship between platform width and platform depth (Leader et al., 2017; McPherron et al., 2020). Although adding PSIA helps correct the EPA-PD model, it is still unclear whether platform width is acting independently or under the influence of platform depth (Lin et al., 2022). Equifinality is another commonly encountered issue when analyzing experimental variables. In the Magnani et al. (2014) experiment, factors such as hammer material, strike

location, and the angle of blow are all found to possibly contribute to the variability in the EPA-PD model. In addition, Magnani et al. (2014) suggested that platform lipping may also introduce noise to the EPA-PD model because lipped flakes are generated from bending fracture, which is different from the conchoidal fracture that the EPA-PD model is built on. However, the presence of platform lipping can be influenced by changes in hammer material, strike location, and the angle of blow. It is thus difficult to identify the actual variable(s) responsible for lowering the correlation between EPA-PD and flake mass. These findings highlight the issue of equifinality in flake formation and caution against attempts to unambiguously infer a particular knapping technique on the basis of particular flaking attributes.

Up to now, most of the analyses in the Dibble experiments were done to examine the effect of individual variables on different flake attributes. These analyses are usually done in the form of linear correlations of the experimental variables and the various flake attributes, leading to the current EPA-PD model (Dibble and Rezek, 2009; Dogandžić et al., 2020; Leader et al., 2017; Magnani et al., 2014; Rezek et al., 2011). Although this approach shows that EPA-PD can account for a large portion of flake variability (Braun et al., 2019; Dibble, 1997; Dogandžić et al., 2020; Lin et al., 2013; Režek et al., 2018), the effect of many other variables that were examined in the Dibble experiments is left unexplained. For instance, variables such as core surface morphology, platform width, hammer material, the angle of blow, hammer strike location, and raw material type are all found to influence the flake size and/or shape, but they are not included in the EPA-PD model because: 1) the effect of these variables is overshadowed by EPA-PD and 2) it is difficult to quantify the effect of some variables in the form of linear regression. Multivariate approaches such as general linear modeling (as conducted in Dogandžić et al., 2015) and principal component analysis (as conducted in Rezek et al., 2011) should be applied more to the Dibble experimental dataset to better understand the influence of the various experimental variables and to create a more comprehensive model of flake formation.

3.3 The current experimental design does not allow certain flaking variables to be examined as independent variables

The high-resolution load cell attached to the mechanical striker allowed the amount of force needed to remove a flake to be measured in the Dibble experiments (Dibble and Rezek, 2009; Dogandžić et al., 2020). During the flaking process, as the hammer comes into contact with the core, the load cell begins to register an increasing amount of load exerted onto the platform surface until flake detachment. However, this experimental setting does not allow control over the striking force. It only allows the load cell to record the minimum force needed to remove a flake with a given exterior platform angle and platform depth. Therefore, the experimental setting makes it difficult to manipulate force as an independent variable at varying set levels. As a result, although Dibble and Rezek (Dibble and Rezek, 2009) observed a positive correlation between flake mass and force that is up to the amount required to detach such mass (Dogandžić et al., 2020; Mraz et al., 2019), the individual effect of force on flaking is not well understood due to limitations in the experimental setup.

Platform width is another variable that cannot be easily controlled as an independent variable in the current experimental setting. Several studies have shown that platform width can account for some variability observed in flake mass and other linear dimensions in addition to EPA-PD (Davis and Shea, 1998; Dibble, 1997; Dogandžić et al., 2015; McPherron et al., 2020; Pelcin, 1998; Shott et al., 2000). However, platform width has traditionally been treated as a variable that is highly dependent on platform depth in the previous Dibble experiments. The core designs do not allow platform width to vary independently of platform depth. Hence, the effect of platform width on flaking is yet to be explored.

3.4 The range of flake attributes analyzed should be broadened

The Dibble experiments have examined a number of flake attributes, but the range of these attributes is limited – they mostly describe the flake dimensions (e.g., flake mass, length, width, and thickness, platform depth and width, and exterior platform angle). While these variables describe some key features of a flake, attributes related to the interior of the flake, such as the bulb of percussion, the curvature of the flake, and core surface morphology have largely been overlooked. Dibble deemphasized these attributes because knappers do not control them directly during knapping. However, these attributes might also give some insight into practices that

the knappers were, in fact, doing to influence the flaking outcome, and they might help us determine which models should best apply. Examples of this include platform lipping and the presence/absence of a bulb. Platform lipping gives some indication, though weak, of the type of hammer used, which in turn does have an impact on flake outcomes, and the absence of a bulb may suggest that predictive models based on conchoidal fracture are not applicable.

4 Future directions of the controlled flaking experiments

As mentioned already, controlled flaking experiments have long been criticized for their artificial setup. In this respect, the new generation of controlled experiments carried out by Dibble and colleagues has significantly improved the external validity of the experimental results owing to the more controlled setup. Moreover, contrary to the previous controlled flaking studies that focused almost exclusively on building theoretical models of fracture mechanics, Dibble and colleagues explicitly focused on establishing the empirical relationships of tangible knapping variables and their cause-and-effect on flake attributes (Dibble and Pelcin, 1995; Dibble and Rezek, 2009; Dibble and Whittaker, 1981; Dogandžić et al., 2020; Leader et al., 2017; Magnani et al., 2014; Rezek et al., 2011). While this approach has certainly proven to be effective in characterizing and quantifying the effect of particular lithic attributes on empirical lithic variability, the results have not yet led to the development of a general model of flake formation that comprehensively integrates the various experimental variables. We will discuss the importance of bringing fracture mechanics back into controlled flaking experiments below. In addition, while the Dibble experiments have clarified the cause-effect of many key knapping factors, there are many variables commonly discussed in replicative flintknapping that remain to be fully investigated by the new controlled experimental approach. We will also briefly discuss some of these variables below.

4.1 The fracture mechanics theory

McPherron et al. (2020) argued that the controlled experimental program can benefit from a return to a greater incorporation of fracture mechanics theory that can help provide a guiding framework to integrate the various test parameters and generate

further test hypotheses (Speth, 1972). Indeed, the flake formation process (especially crack initiation and propagation) is governed by laws of fracture mechanics that are invariant regardless of changes in the external environment (Eren et al., 2016; Lin et al., 2018). The field of fracture mechanics offers a rich literature on the basic principles of fracture initiation and propagation in brittle solids. In particular, numerous studies investigate the formation of Hertzian cones – a key component in conchoidal flaking (Gorham and Salman, 2005; Kocer and Collins, 1998; Marimuthu et al., 2016; Zeng et al., 1992a). The effect of different force delivery parameters such as speed and mechanical properties of the hammer on fracture initiation and propagation is well studied in fracture mechanics. However, there are few studies that connect the fundamental mechanics of flaking to the knapping behavior underlying the lithic record. Incorporating fracture mechanics in the current experimental design will provide a more robust framework to quantify different knapping behaviors (e.g., striking force and the angle of blow) into tangible flake attributes and will help us move beyond the current EPA-PD model.

4.2 Force and energy

While the Magnani et al. (2014) experiment examined several force application variables, many aspects of force application and delivery have yet to be fully explored. In particular, not much attention has been given to the amount of force needed to remove a flake from a core despite its implication for understanding the potential strength of the tool makers. The Dibble experiments show that there is a positive correlation between force and flake mass (Dibble and Rezek, 2009; Dogandžić et al., 2020; Mraz et al., 2019), though the individual effect of force on flaking is not well understood due to limitations in the experimental setup as discussed in the previous section. Since striking force cannot be controlled as an independent variable, it remains to be verified whether the delivery of force in excess of the minimum required threshold indeed produces no effect on the resulting flake form. From a knapper's perspective, it is still unclear how some of the force delivery variables are related to and maybe interact with each other during knapping. For example, to generate more striking force for flake removal, knappers would hit a core at a higher velocity. In doing so, they might (subconsciously) try to hit further in on the platform to avoid missing the target, thereby also increasing platform depth.

Consequently, it is difficult to disentangle the effect of the increased force and platform depth to determine which one (or both) causes the flake size to rise.

At a more fundamental level, there is a need to reevaluate the ways in which the concept of “force” is used in the lithic experimental literature. The load cell used in the Dibble experiments measures how big the “push” of the hammer is when it hits the core to remove a flake. The potential hammer impact energy (kinetic) can be estimated using hammer mass and its velocity at the point of impact. Part of this impact energy is transferred from the hammer to the core during the hammer blow. The hammer momentum refers to how much the motion is of a moving object, which is calculated as the product of the hammer’s mass and velocity. Theoretically, we can calculate the hammer striking force based on the change in its momentum from the point of impact to zero, provided that we know the contact time between the hammer and the platform. This means increasing the hammer velocity at the point of impact is an important factor in increasing striking force. Clarifying these concepts is critical for improving the mechanical flaking design, particularly to refine the control of the hammer delivery process.

4.3 Something other than plain platforms

While the Dibble experiments focused heavily on platform depth and exterior platform angle as independent knapping variables, there are many aspects of the striking platform that have yet to be fully interrogated in a controlled experimental context. A number of studies have repeatedly highlighted the importance of platform shape and size in relation to flake size (Clarkson and Hiscock, 2011; Davis and Shea, 1998; Dibble, 1997; Pelcin, 1998; Shott et al., 2000). For example, the Clarkson and Hiscock (2011) replicative experiment demonstrated that there is a systematic difference in the size of flakes with distinct platform types (focalized vs. dihedral vs. plain). Thus, while platform size and exterior platform angle can help predict variation in flake size within these platform shape categories (Clarkson and Hiscock, 2011; Muller and Clarkson, 2014), it is clear that the overall geometry of the striking platform plays an important role in controlling flake variation during knapping. The challenge with examining this property using a controlled experimental approach is that the large number of variables that need to be controlled can quickly become difficult to operationalize. For example, in their platform beveling experiment (Leader

et al., 2017), Dibble and colleagues had to hold constant the exterior platform angle of the cores as well as the angle at which the bevel intersects the platform surface in order to keep the number of flaking trials feasible. Thus, additional experiments are required in the future to continue this line of research by exploring other variable combinations to better clarify the relationship between platform morphology and the resulting flake variability.

4.4 Platform width in addition to platform depth

Related to platform morphology, another platform variable commonly discussed in the lithic literature is platform width. Studies have shown that, in addition to platform depth and exterior platform angle, platform width can also help explain flake variation (Davis and Shea, 1998). For example, Dibble (1997) showed that flakes of different platform depth intervals all have a positive relationship between platform width and flake mass. In a more recent study, Dogandžić et al. (2015) demonstrated that, when the effects of platform depth and exterior platform angle are controlled, platform width contributes significantly to variation in flake mass, surface area, and edge length. However, controlled experiments to date have not focused much on platform width and instead have treated the variable largely as a by-product of platform depth (Dibble and Rezek, 2009; Pelcin, 1998). In part this is because these controlled studies have held the core morphologies constant, meaning that there is minimal variation in the relationship between platform depth and platform width. The focus on platform depth over platform width is also explained by Dibble's emphasis on investigating variables under knapper control. While knapping decisions can secondarily impact the eventual platform width, how far in from the core edge the knapper strikes is under the direct control and was, therefore, a primary focus for Dibble and colleagues.

The Leader et al. (2017) experiment has shown that the relationship between platform depth and platform width does in fact vary by the type of beveling. Thus, platform width may potentially represent a useful proxy for tracking the influence of platform morphology on flake attributes. In addition, McPherron et al. (2020) showed that platform width can be calculated as a function of platform depth and PSIA. Lin et al. (2022) argue for a mediating effect of platform width on flake mass and flake width. They examine the relationship between EPA-PD (as the independent variable)

and flake size (as the dependent variable) with platform width as a mediator. Their results show that platform width facilitates the direct effect of EPA-PD on size, meaning that flakes with a wider platform (a larger platform width to platform depth ratio) are generally wider and heavier. Future experiments are needed to investigate how different independent variables interact to form platform width in the flake formation process, and how they help determine flake width and mass.

4.5 Core morphology

Although the core surface morphology experiment conducted by Dibble and colleagues (the Rezek et al., 2011 experiment) showed that EPA-PD has a stronger effect on flake variability, the experiment outcomes also indicated that that core surface morphology does nevertheless have an impact on the resulting flake shape (e.g., surface area and length to width ratio, see also Van Peer, 2021). As noted by Rezek et al. (2011), however, the different core surface morphologies examined in their study may not have been distinctive enough, particularly with respect to the general curvature, to overcome the effect of exterior platform angle and platform depth on flake variability. It may be that, with more pronounced variation in ridge configurations, the impact of core surface morphology on flake size and shape would become more dominant. Another aspect of core surface morphology that has yet to be explored is the longitudinal or distal convexity. So far, all of the core designs used by Dibble and colleagues share a similar longitudinal curvature profile. It is commonly noted among flintknappers that the distal curvature and dorsal ridge configuration strongly dictates the point of flake termination, and hence the resulting flake length (Whittaker 1994). In fact, these core morphology elements represent key factors in the discussion of particular reduction techniques such as Levallois and blade technologies (Boëda, 1993). Finally, we also note that core size is not well tested. Speth (1981) showed that the initial core size has an impact on the flake size, but how specific core dimensions (such as core length, width, edge angle, etc.) affect flake dimensions is unclear. Thus, the general topic of core morphology remains an important area to explore in future controlled experimental studies.

4.6 Flake terminations

Flake formation can be divided into three stages: initiation, propagation, and termination (Cotterell and Kamminga, 1987). The Dibble experiments have largely focused on the initiation and propagation stage. Thus, the formation of different flake terminations remains a largely unexplored topic in controlled flaking experiments. Dibble and Whittaker (1981)'s controlled experiment showed a relationship between exterior platform angle and flake termination: flakes with feather termination had a lower average exterior platform angle (41.8 degrees) than hinged (61.5 degrees) and overshot flakes (76.7 degrees). They suggested that exterior platform angles might affect flake termination by changing the converging configuration of the core surface. One of the controlled experiments conducted in Pelcin (1997a) similarly showed that exterior platform angle and platform depth have an influence on both flake initiation and termination. That is, for a given interval of exterior platform angles, flake termination progressively changes from feathered to hinged before the flakes eventually exhibit bending initiations as platform depths increase. However, in the Dibble studies summarized here, only flakes with feather terminations were included. This is because the size and dimensions of flakes with feathered termination were considered to be a more accurate representation of the "true" flakes associated with the knapping conditions in question. However, though in low frequencies, flakes with stepped and hinged terminations were occasionally produced in the controlled flaking condition. The cause for these non-feather terminations has yet to be explored.

There are several existing hypotheses regarding flake termination that are worth examining through a controlled experimental approach. First, it is commonly noted that a possible cause for hinge and step termination relates to the angle and trajectory of the hammer blow. As Whittaker (1994) explained, when the hammer blow follows an arc, the vector of the force trajectory is separated into two directions, a downward shearing force that drives the fracture into the core and an outward opening force that opens the crack. When the hammer is swung in such a way where the outward force is too great, the flake is "pulled" away from the core too rapidly and hence snaps. Another hypothesis is that hinge and step terminations are results of insufficient percussive force. As a result, the fracture propagation "follows a shorter path to the core surface" (1994:109) by hinging the termination. Both of these

hypothetical causes can be tested by using a controlled experimental approach, though a flaking apparatus different from the one used by Dibble and colleagues would be required to allow for an arc hammer swing and the delivery of a variable force blow.

5 Conclusions

Controlled flaking experimentation allows us to study the variation observed in lithic assemblages from the fundamental perspectives of flaking, that is, by understanding how a single flake is made (Rezek et al., 2016). It serves as a bridge between the basic flaking principles and the knapping behaviors behind the archaeological record. The Dibble experiments have greatly advanced our understanding of the effect of various knapping variables that knappers directly control (Dibble and Rezek, 2009; Dogandžić et al., 2020; Leader et al., 2017; Magnani et al., 2014; Rezek et al., 2011). They provide a means to quantify knapping actions into different combinations of measurable flake and core attributes, which will ultimately inform us of what knappers can do to change flake characteristics. These experiments also demonstrate the power and precision of a highly controlled experimental design in studying the effect of single independent variables on flaking. Through variable control, this approach allows the construction of fundamental knapping properties based on internally consistent cause-effect relationships that can then be applied to examine variability in the archaeological stone artifact record on a global scale.

The EPA-PD model summarized from the Dibble experiments allows different assemblages to be compared on an objective and continuous scale of flake variability, as demonstrated in Lin et al. (2013) and Režek et al. (2018). However, the EPA-PD model's ability to predict the flaking outcome depends largely on the standardized setup in the Dibble experiment, any deviation from the "normal" condition (e.g., changes in core and platform configuration, hammer size and morphology, angle of blow) may negatively impact the model's performance. It is thus important for us to understand the role of other equally important knapping parameters besides exterior platform angle and platform depth so that these variables can be properly included in the EPA-PD model to improve its power in explaining flake variability in different scenarios. Despite its inherent limitations (Leader et al., 2017; McPherron et al., 2020; Rezek et al., 2011), the controlled

experimental setting provides a powerful and effective pathway forward for lithic researchers to evaluate hypotheses and construct experimental inferences.

Acknowledgments

This paper is an effort to review and draw a synthesis of the controlled flaking experiments conceptualized and led by Harold Dibble since 2009. It was his intention to wrap up this phase of his experimental program with a synthesis paper, but sadly he passed away before he could see it through. Without his work there would not be such a dataset generated from a controlled setting that allows us to synthesize models of flake formation. The experiments that generate the dataset were funded by the National Science Foundation (BCS-0649673 and BCS-1153192), University of Pennsylvania Museum of Archaeology and Anthropology and School and Arts and Sciences, the European Union's Framework Programme for Research and Innovation Horizon 2020 under the Marie Skłodowska-Curie grant agreement No. 751125, and the Institutional Strategy of the University of Tübingen (Deutsche Forschungsgemeinschaft, ZUK 63). We dedicate this paper to Harold.

CHAPTER 3 Quantifying knapping actions: a method for measuring the angle of blow on flakes

This chapter includes the following manuscript under review in *Archaeological and Anthropological Sciences*:

Li, L., Reeves, J.S., Lin, S.C., Tennie, C., McPherron, S.P., (*under review in Archaeological and Anthropological Sciences*). Quantifying knapping actions: a method for measuring the angle of blow on flakes.

Author contributions

Conceptualization: Li Li, Sam C. Lin, Jonathan S. Reeves, Shannon P. McPherron, Claudio Tennie

Data curation: Li Li

Writing – original draft: Li Li, Sam C. Lin, Jonathan S. Reeves, Shannon P. McPherron

Writing – review and editing: Li Li, Sam C. Lin, Jonathan S. Reeves, Shannon P. McPherron, Claudio Tennie

Abstract

Stone artifacts are critical for investigating the evolution of hominin behavior – they are among our only proxies for hominin behavior in deep time. Hominin cognition and skill are often inferred by reconstructing the technical decisions hominins made throughout the knapping process. However, despite the great advancements made in understanding how hominins knapped, some of the key factors involved in past flake production cannot be easily/readily derived from stone artifacts. In particular, the angle at which the knapper strikes the hammer against the core to remove the flake, or the angle of blow, is a key component of the knapping process that has up to now remained unmeasurable on archaeological assemblages. In this study, we introduce a new method for estimating angle of blow from the ventral surface of flakes. This method was derived from a controlled experiment that explicitly connects fracture mechanics to flake variability. We find that a feature of the flake's bulb of percussion, what we call the bulb angle, is a measurable indicator for the angle of blow. Our experimental finding is further validated in two additional datasets from controlled and replicative knapping experiments. These results demonstrate the utility of continuing to link flake variation with technical decision-making to fracture mechanics. In addition, they also provide a useful and relatively simple means to capture a currently invisible aspect of hominin stone tool production behavior.

1 Introduction

Much of what is known about the evolution of hominin cognition and behavior is derived from the study of stone tools. Today, researchers routinely employ a wide array of analytical approaches to reconstruct the technical decisions and processes underlying hominin knapping strategies in the past (Boëda, 1995; Delagnes and Roche, 2005; Pelegrin, 1993; Roche et al., 1999; Texier and Roche, 1995). Knapping is without a doubt a complex motor process that involves interactions of different body parts (Biryukova and Bril, 2008; Bril et al., 2010; Geribàs et al., 2010; Nonaka et al., 2010; Rein et al., 2013; Susman, 1998; Williams et al., 2012), and archaeologists have come to recognize the importance of understanding this dynamic process by combining methods such as replicative experiments, refitting and other technological approaches (Eren et al., 2016). A key aspect of these

technological approaches is in underlining the importance of manual gestures and knapping actions in lithic reduction (Forestier, 1992; Pelegrin, 1993; Roche et al., 1999; Texier and Roche, 1995). Knappers need to flexibly apply different manual gestures along the knapping sequence to effectively navigate the changing interactions among different functional parameters, including configurations of the striking platform and various force application variables like the hammer striking speed and angle (Baena et al., 2017; Cueva-Temprana et al., 2019; Geribàs et al., 2010; Rein et al., 2013; Roussel et al., 2009; Vernooij et al., 2015). Studies of modern knappers suggest that these gestural skills and 'know-hows' may be acquired through learning and practice, highlighting the significance of cultural transmission in hominin stone tool-making (Lycett, 2013; Lycett et al., 2016; Morgan et al., 2015; Pargeter et al., 2019). Moreover, because knapping actions ultimately depend on the biomechanics of the human musculoskeletal structure, increasingly researchers have focused on examining the relationship between stone percussive activities and hominin skeletal morphologies (Macchi et al., 2021; Marzke, 2013; Rolian et al., 2011).

One component of knapping gestures that has been repeatedly observed to be critical in controlling the flaking process is the angle at which the hammer strikes the core, or the angle of blow (e.g., Hellweg, 1984, Fig.3-1). It has been said that striking a hammer perpendicularly straight into the core runs the risk of crushing the platform and generating step fractures and incipient cones, while increasing the angle of blow by tilting the platform and swinging the hammer in an arc helps facilitate flake detachment (Whittaker, 1994: 95). Importantly, variation in the angle of blow has been shown to be one of the main parameters that separate novice from expert knappers (Vernooij et al., 2015). For instance, experimental studies carried out by Geribàs et al. (2010) and Cueva-Temprana et al. (2019) both showed that novices tend to prefer striking the hammer in a more direct angle of blow, while experts can effectively control different striking angles to achieve a desired result (Cueva-Temprana et al., 2019; Geribàs et al., 2010; Rein et al., 2013). The importance of controlling the angle of blow also varies with the knapping strategy and goals. For instance, the ability to apply appropriate angles of blow has been shown to be critical in biface production, especially during biface thinning (Shipton, 2018).

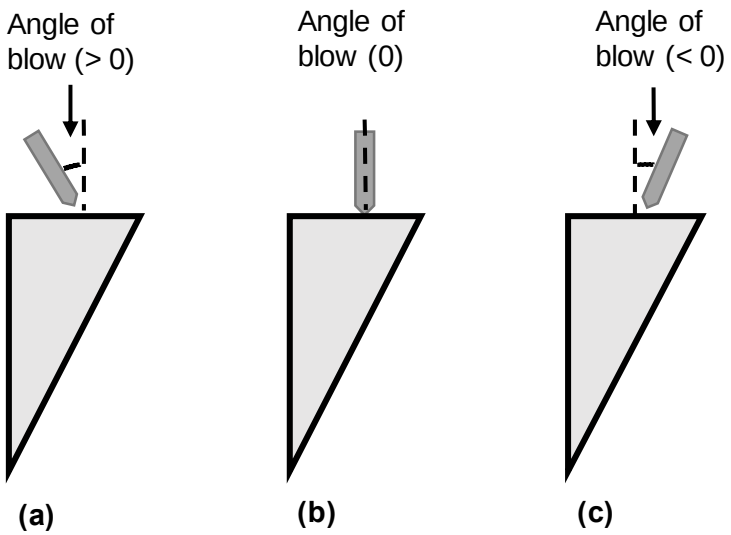

Fig. 3-1 Schematic illustration of how the angle of blow is measured as the angle between the hammer's striking direction and the perpendicular of the platform from the profile view of a flake removal. (a) shows a positive (oblique) angle of blow, (b) shows a zero (direct) angle of blow, and (c) shows a negative (oblique in the other direction) angle of blow

Varying the angle of blow also appears to affect various characteristics of a detached flake such as its linear dimensions, bulb of percussion, and the presence of platform lipping. The controlled flaking experiment by Speth (1975, 1972) described that flakes made with larger angles of blow are generally shorter and have a less prominent bulb of percussion than those produced under a more direct hammer strike (Soriano et al., 2007). Several studies have also shown that in addition to producing a less prominent bulb of percussion, a more oblique hammer strike may increase the chance of platform lipping (Bataille and Conard, 2018; Schmid et al., 2019, 2021). Speth (1972) argued that this might be due to the limited stress exerted on the platform by the higher angles of blow. Similarly, Hellweg (1984) noted that increasing the striking angle during knapping would lead to the detachment of shorter flakes. In a later experiment using a similar controlled flaking setup, Dibble and Whittaker (1981) found no obvious impact of angle of blow on

flake dimensions, though the authors suggested that the negative outcome may be related to confounding variables in the experimental design. More recently, using a more developed mechanical flaking apparatus, Dibble and Rezek (2009) showed that flakes produced from higher angles of blow are indeed smaller in mass. The same pattern was reported by Magnani et al. (2014). They found that linear dimensions such as flake length and width, relative to platform depth, decreased as angle of blow increased. In other words, two identically prepared cores struck in identical locations with identical hammers will produce two different flakes depending on the angle of blow.

Starting in the 1980s, Dibble and colleagues designed a series of controlled experiments to understand the flaking process from a knapper's perspective (Dibble and Pelcin, 1995; Dibble and Rezek, 2009; Dibble and Whittaker, 1981; Dogandžić et al., 2020; Leader et al., 2017; Magnani et al., 2014; Rezek et al., 2011). These knapper-guided controlled experiments focused on investigating the effect of various variables under the direct control of a knapper on the flaking outcome. The most important finding from the knapper-guided controlled experiments by far is the dominant effect of exterior platform angle (EPA) and platform depth (PD) on flake size and shape. An EPA-PD model of flake formation, where flake mass is a function of the combined effect of exterior platform angle and platform depth, was subsequently derived from the controlled experiments led by Dibble and colleagues. This EPA-PD model has proven valid in both experimental and archaeological assemblages (Braun et al., 2019; Dogandžić et al., 2020; Lin et al., 2013; Režek et al., 2018).

Despite its effect on various flake attributes as previously discussed, the angle of blow was not included in the EPA-PD flaking model because there has been no direct way of measuring this angle from the lithic artifacts themselves. Crabtree (1972a) suggested the angle of blow could be reconstructed by the interior platform angle of the detached flake, yet Dibble and Whittaker (1981) showed that this is not the case in their controlled experiment. More recently, Magnani et al. (2014) described the angle of blow as archaeologically invisible and suggested that any inference about the angle of blow will have to be derived from its effect on flake attributes such as bulb size and flake shape. However, these attributes are also under the influence of other independent knapping factors such as the exterior

platform angle and platform depth, and so reconstructing the angle of blow from these attributes will be difficult.

To address the challenge of measuring the angle of blow directly from archaeological flakes, we turned to fracture mechanics and the basic principles of brittle solid fracture to study the visible traces that the angle of blow produces on the detached flake. In the fracture mechanics literature, it has been repeatedly shown that an oblique hammer blow (i.e., a non-zero angle of blow) will *tilt* the Hertzian cone so that its central line is no longer perpendicular to the platform (Chaudhri, 2015; Chaudhri and Chen, 1989; Lawn et al., 1984; Salman et al., 1995; Suh et al., 2006). Modern knappers have also noted the possible relationship between the angle of blow and the angle of the Hertzian cone (Hellweg, 1984; Whittaker, 1994). As shown in Fig.3-2, the Hertzian cone is tilted relative to the platform surface when the hammer strike is not perpendicular to the platform. Because the Hertzian cone initiates the formation of the bulb of percussion, it should be possible to detect the change in the Hertzian cone's orientation, brought on by varying hammer strike angles, in the initial angle of the bulb of percussion on a flake's interior surface. Specifically, this angle, which we refer to hereafter as the bulb angle, is measured immediately at the intersection between a flake's platform and the protruding side of the Hertzian cone before it bends back to form the bulb of percussion (Fig.3-2). Defined this way, a bulb angle of 90 degrees indicates a flat interior surface of the flake with no visible bulb of percussion. As this angle increases from 90 degrees, the Hertzian cone becomes more apparent, and the bulb becomes more prominent. Note that the bulb angle is different from the interior platform angle, which has been defined as the angle between the platform and the flake ventral surface *without* considering the curvature of the bulb of percussion (Dibble and Whittaker, 1981).

Key here is that Hertzian cone angles are constants within each raw material type. In the case of soda-lime glass, it has been shown experimentally that the Hertzian cone angle is approximately 136 degrees (Kocer and Collins, 1998; Lawn et al., 1974; Roesler, 1956). That means, when the central line of the Hertzian cone is perpendicular to the platform, the angle between either edge of the cone and the platform is 22 degrees (180 degrees in a flat platform, minus a 136-degree cone, divided by the two sides the cone intersects a plane). Theoretically then, a flake detached with a zero angle of blow from a soda-lime glass core should have a bulb

angle of 158 degrees (i.e., 136 degrees from the Hertzian cone plus 22 degrees between inner edge of the cone and the platform surface; see Fig.3-2a). Based on observations made in previous fracture mechanics studies (Chaudhri, 2015; Chaudhri and Chen, 1989; Lawn et al., 1984; Salman et al., 1995; Suh et al., 2006), we hypothesize that as the angle of blow increases, the Hertzian cone will pivot outward towards the core's flaking surface, causing the bulb angle to decrease. Take the hypothetical scenario illustrated in Fig.3-2b as an example, here the greater angle of blow causes the Hertzian cone to pivot into the flake to the point that the inner edge of the cone becomes aligned with the platform surface. In this scenario, we would expect the flake to exhibit a bulb angle that equals the Hertzian cone angle (i.e., 136 degrees). If, on the other hand, the hammer strike is into the core (i.e., negative angles of blow, Fig.3-2c), the Hertzian cone will tilt away from the flake and into the core instead. In this case, we should see a more prominent blub of percussion and a bulb angle that is greater than 158 degrees.

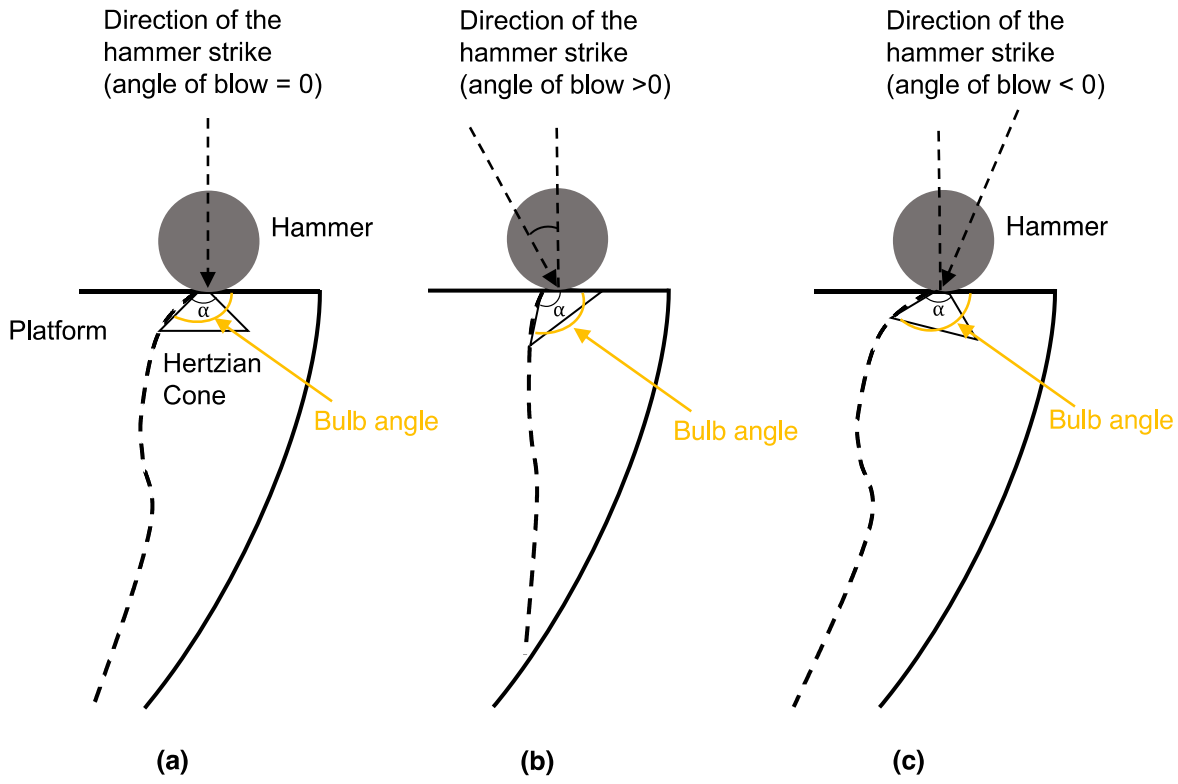

Fig. 3-2 Schematic illustration of the bulb angle on a flake from its profile view. The Hertzian cone generated from the hammer blow is represented by the triangle

beneath the hammer, α refers to the Hertzian cone angle, which is approximately 136 degrees in soda lime glass. The bulb angle is the angle between the flake's platform and the extruding side of its Hertzian cone, as is marked in orange. (a) Showing that the Hertzian cone's central line remains perpendicular to the platform when angle of blow is zero, the theoretical bulb angle should be 158 degrees; (b) showing the case when the Hertzian cone is completely pushed to the platform, the theoretical bulb angle should be 136 degrees; (c) showing the case when the Hertzian cone is tilted into the core, the theoretical bulb angle should be greater than 158 degrees

2 Material and Methods

2.1 Experimental design

To test our hypothesis of the relationship between bulb angle and angle of blow, we first conducted a controlled experiment using a 'drop tower' setup to systematically investigate the effect of angle of blow on bulb angle. This experiment is henceforth referred to as the *drop tower experiment*. Drop tower setups were used in controlled flaking experiments from the 1970s to the 1990s (Dibble and Pelcin, 1995; Dibble and Whittaker, 1981; Speth, 1972, 1975). This type of setup is effective for controlling both the striking location and angle of blow for a flaking event. As shown in Fig.3-3, the drop tower used in our experiment adopts the design from these previous studies. Additionally, a commercially available self-leveling two-way (up and down) gravity-controlled laser (Huepar 621CR) was used to ensure precision of the strike location. A steel ball bearing with a diameter of 16 mm was used as the hammer. We were able to achieve a strike location precision of about 2 mm. This precision impacts mainly our ability to control the platform depth. For each set of angles of blow, we varied platform depth from around 7 mm (±2 mm) up to 20 mm (±2 mm). Plate (soda-lime) glass with a thickness of 10 mm was used as the core material. The plate glass was cut with a diamond blade wet saw to prepare an exterior platform angle of 65 degrees for all cores. A total of 103 flakes (henceforth the *drop tower dataset*) were made using the plate glass cores with angles of blow ranging from -20 to 60 degrees in 10-degree intervals. To control the angle of blow, glass cores were secured in a clamping vice which allowed for the relative position of

the core platform to be altered (Fig.3-3). In other words, in this type of setup, the angle of blow is altered by pivoting the core platform surface relative to a horizontal plane. We positioned a digital angle gauge on the flake platform to measure the angle between the flake platform and the horizontal, which is equal to the angle of blow. More information regarding the setup is provided in Appendix I. We measured the bulb angle (see below) and platform depth on each of the flakes coming from this experiment.

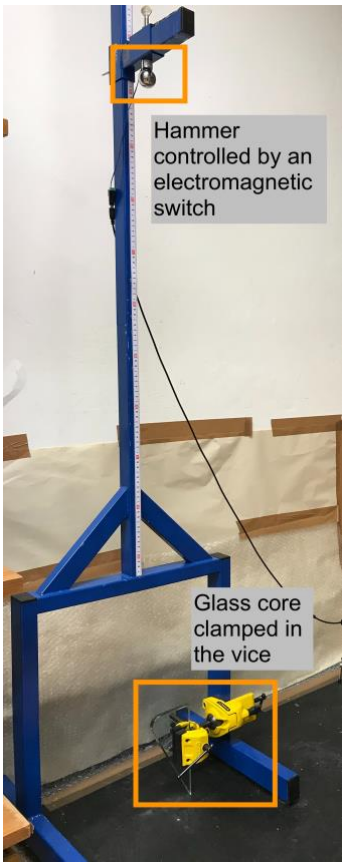

Fig. 3-3 The drop tower setup used in this study; the laser level is not shown in the photo

To verify the results from the drop tower experiment, we measured the bulb angle on 3D models of glass flakes produced with known angles of blow by Dibble and colleagues in previous controlled experiments (Dibble and Rezek, 2009; Dogandžić et al., 2020; Leader et al., 2017; Magnani et al., 2014; Rezek et al.,

2011). This dataset is henceforth referred to as the *Dibble dataset*. Flakes from this dataset were selected to have no broken platforms, clear bulbs of percussion, and no platform lipping, and were made with a steel hammer. These flakes were scanned and landmarked following protocols outlined in Archer et al. (2018). Low quality scans, here defined as having a file size of less than 5 MB, were excluded because the detail of the platform was insufficient to make a reliable measurement of the bulb angle. In total, we obtained reliable data on 53 flakes from the Dibble collection with angles of blow of 0, 5, 10, 20, 30, and 40 degrees. These flakes were made on cores with exterior platform angles varying from 65 to 95 degrees with a 10-degree interval, though the majority of flakes have either a 65- or 75-degree exterior platform angle. Note that these angle of blow intervals in the Dibble dataset are different from that used in the drop tower experiment.

To test whether the bulb angle was sensitive to changes in the angle of blow in a less controlled setting, we conducted a blind test on a small set of flintknapped flakes produced at the Max Planck Institute for Evolutionary Anthropology. This dataset is henceforth referred to as the *MPI dataset*. To produce this dataset, two knappers (SPM and JR) each produced two sets of flakes using hard hammer percussion on two flint nodules from the Bergerac region of southwest France. Cobble hammerstones of varying sizes were used. The first set (n = 16) was made by the knappers consciously tilting the core to strike with the highest angle of blow that resulted in a flake removal. The second set (n = 16) was made with a deliberate effort to strike as directly or perpendicularly as possible into the platform (i.e., a zero angle of blow). In total, 64 flakes were produced between the two knappers, and each flake was given a random ID number along with the name of the knapper and the intended level of angle of blow as either “High” or “Low”. After excluding flakes with visible multiple Hertzian cones near the point of percussion, broken platforms, and broken bulbs near the point of percussion, 44 of the 64 flakes were selected for analysis. Of these 44 flakes, 14 were made from a nodule of black flint and 30 flakes were made from a yellow flint nodule. Without prior knowledge of the associated knapper and angle of blow designation (high or low), one of us (LL) measured the bulb angle on the 44 flakes. These bulb angle values were merged with the MPI dataset using the random ID number once all of the flakes had been measured.

2.2 Measuring the bulb angle

For the flakes in the drop tower and MPI datasets, the bulb angle was measured with a manual goniometer with 1-degree precision as the angle between the platform surface and the extruding side of the Hertzian cone before it extends and integrates into the bulb of percussion. To make this measurement, the joint of the goniometer is positioned at the point of percussion, one leg of the goniometer lies on the flake's platform surface and the other leg is positioned against the extruding side of the Hertzian cone, which is at the very beginning of the flake's bulb of percussion (Fig.3-4). It should be noted that the measurement can be prone to measurement error due to the extremely small size of the Hertzian cone (the typical length of a Hertzian cone observed on the glass flakes in the drop tower dataset is about 1 mm to 2 mm), the platform curvature, and the overall curvature of the flake interior surface. To minimize measurement error and bias, the bulb angle on each of the flakes in the drop tower dataset was measured on three separate occasions, and the bulb angle on each of the flakes in the MPI dataset was measured on four separate occasions (with no prior knowledge of the previous measurement results). The average of these measures was used in the final analysis. We also calculated the standard error of bulb angle (the standard deviation of bulb angle divided by the square root of the count of the total bulb angle measurements) for each flake in the two datasets. This bulb angle standard error captures the likely discrepancy between the actual average bulb angle calculated from the three measurements and the theoretical average bulb angle to be calculated from an infinite number of measurements, thus helping us estimate how accurately bulb angle is measured using a goniometer.

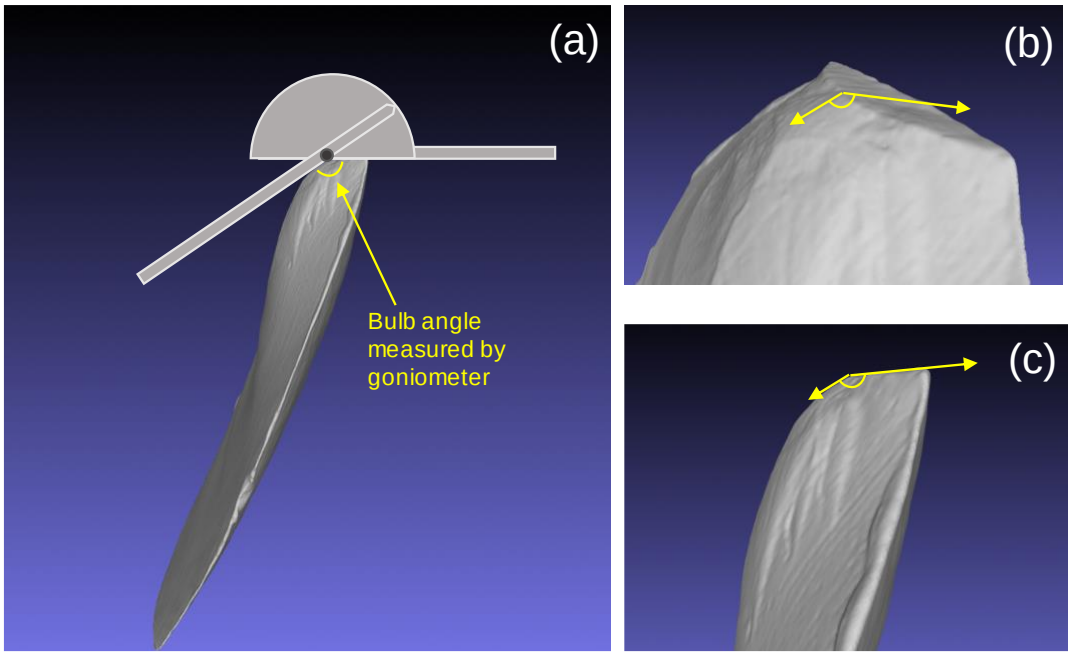

Fig. 3-4 Illustration of how the bulb angle is measured on a flake with a goniometer. (a) shows how the goniometer is placed on the flake to measure bulb angle, (b) and (c) present a zoomed-in view of the bulb angle on a flake. Note that the 3D model of the flake used in the illustration is from the Dibble dataset, and it is for illustration purposes only.

Two methods were used to measure the bulb angle from the 3D flake models in the Dibble dataset. The first method is referred to as the vector calculation method and uses scripts written in Python (Van Rossum and Drake, 2011) and R (R Core Team, 2020). In this method, first, we reorient each flake mesh such that the point of percussion (P_0) is positioned at the origin point (0, 0, 0), the platform is coincident with the XY plane, the profile (longitudinal) section of the flake is perpendicular to the YZ plane, and the flake extends into negative Z space (Fig.3-5a). Second, we extract the profile section (YZ) and intersect it with a circle centered at (0, 0) with a radius of 1 mm. The points where the circle intersects the flake profile are labeled $P_1$and P_2 (as marked in Fig.3-5a). The bulb angle is then the angle between the vectors P_0P_1 and P_0P_2. The vector calculation method returns bulb angle with a precision of 0.01 degrees. The second method that we used for measuring the bulb angle, which is referred to as the virtual goniometer method, uses the Meshlab (Cignoni et al., 2008) Virtual Goniometer Plugin developed by Yezzi-Woodley et al. (2021). To use the

virtual goniometer, we first aligned the flake mesh following the above procedure described in step one of the vector calculation method. After that, we loaded the aligned flake mesh into Meshlab (Cignoni et al., 2008) and specified a patch centered at the flake's point of percussion using the Virtual Goniometer Plugin with a 1 mm radius (Fig.3-5b). As shown in Fig.3-5b, the patch was then automatically divided by the platform edge of the flake: one half of the patch on the flake's platform (colored in blue) and the other half on the flake's bulb of percussion (colored in red). The bulb angle was measured as the angle between these two sub-patches by the Virtual Goniometer Plugin with a precision of 1 degree.

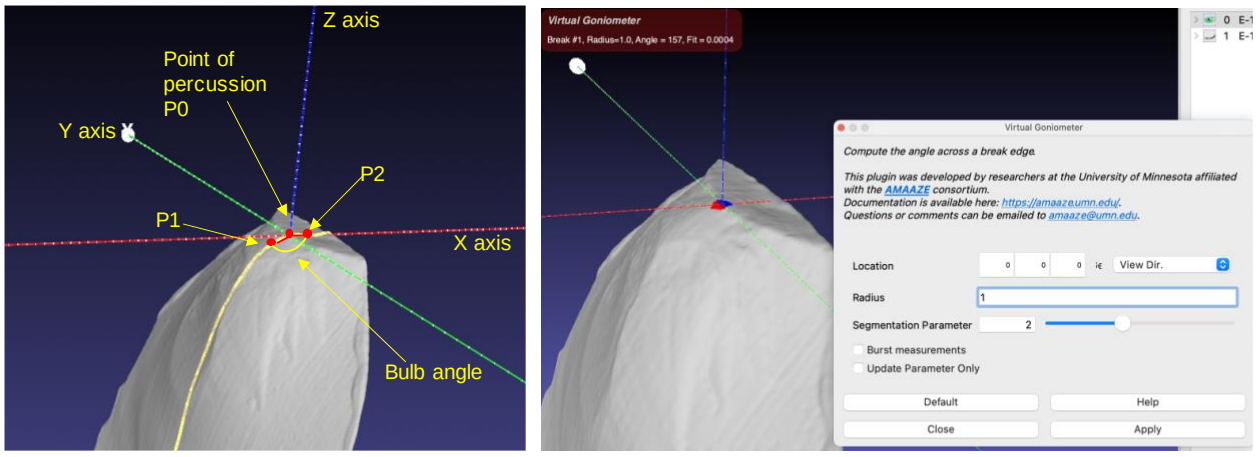

(a) (b)

Fig. 3-5 Illustration of the two measurement methods on a 3D flake model from the Dibble dataset. (a) In the vector calculation method, bulb angle on the flake is defined as the angle between vectors P_0P_1 and P_0P_2. (b) In the virtual goniometer method with the Virtual Goniometer plugin for MeshLab loaded (Yezzi-Woodley et al., 2021), bulb angle is defined as the angle between the red and blue patches marked on the flake model

2.3 Statistical comparison

The experimental data were analyzed in two parts. First, we considered the relationship between the measured bulb angle values and their associated hammer angle of blow across the three datasets. We used the Kruskal-Wallis test (also

known as the one-way ANOVA on ranks), which assumes no particular distribution of the data, to examine whether there is a significant difference in bulb angle between the angle of blow groups. Then, we use the linear regression model (Ordinary Least Squares) to examine in addition to the angle of blow, whether changes in exterior platform angle and platform depth have a significant effect on bulb angle. For the drop tower dataset, only platform depth is included as the independent variable since exterior platform angle is a constant of 65 degrees. For the Dibble dataset, both exterior platform angle and platform depth are included as the independent variables. Bulb angle is the response variable in both linear models.

We also apply linear regression to evaluate the usefulness of the bulb angle as an independent flake attribute for explaining variation in flake size, namely mass. Previous studies have shown that the mass of a flake can in part be explained by the exterior platform angle (EPA) and platform depth (PD). Based on this relationship, which is referred henceforth as the EPA-PD model, we construct three sets of linear regression models using the data obtained from the Dibble dataset. The first model is a baseline EPA-PD model that includes only EPA and PD as the independent variables, with flake mass as the response variable. The second model builds on the baseline model by including the known angle of blow as an additional predictor into the model. This model establishes the additional explanatory power of the angle of blow when accounting for variation in flake mass. Then, to evaluate how well the bulb angle acts as a proxy for the angle of blow, a third set of linear models are constructed by substituting the bulb angle measurements in place of the angle of blow as a predictor variable. Two separate models are constructed for the two different methods of measuring the bulb angle from the 3D flake models. Based on the three sets of models, we examine two questions. First, by comparing the first and second linear models, we examine whether the inclusion of the angle of blow helps improve the performance of the baseline EPA-PD model in predicting flake mass. Second, by comparing the second and third set of linear models, we assess if the bulb angle can serve as a reliable proxy measurement for the angle of blow.

For all linear models, the response variable, flake mass, was transformed to its cube root so that its dimensionality is comparable to the independent variables. As explained in Dibble and Rezek (2009), compared to the single-dimensional flake attribute platform depth, flake mass is a three-dimensional attribute similar to flake

volume. It is thus important to bring these two variables to the same dimensionality for conducting analysis using linear models. Models were examined for their residual distribution, leverage, Cook's distance, and variance inflation factor. Model comparison was done using the ANOVA test. All other data analyses in this study are conducted in R (R Core Team, 2020).

3 Results

3.1 Drop tower dataset

For the drop tower dataset, the average standard error of bulb angle is 0.77 degrees. That is, the overall possible discrepancy between the measured bulb angle and the theoretical bulb angle is less than one degree (Fig.Appx-II.1 in Appendix II). The overall standard deviation of bulb angle within each grouping of angle of blow is less than three degrees (Table Appx-II.1 in Appendix II). There is a significant difference in bulb angle between the angle of blow groups (Fig.3-6, Kruskal-Wallis test, H = 84.709, $p < 0.01$). The flakes produced by the zero angle of blow have an average bulb angle of 152.1 (±1.91) degrees, which is not far off from the 158 degrees that we initially predicted based on Hertzian cone formation when the hammer strikes perpendicularly to the platform surface in soda-lime glass (Fig.3-2a). As the angle of blow increases (i.e., the hammer strikes more obliquely), the bulb angle becomes smaller. As the angle of blow tilts to 40 degrees or more, the average bulb angle appears to stabilize at around 137 degrees. Again, this minimum bulb angle fits well with our predicted value of 136 degrees for when the Hertzian cone tilts to the point where one side of the cone is aligned with the platform surface (Fig.3-2b). The regression model used to predict bulb angle with the angle of blow and platform depth can be found in Appendix I. While the overall regression was statistically significant ($R^2 = 0.78$, $F(2, 98) = 173.9$, $p < 0.001$), only the angle of blow significantly predicted bulb angle ($p < 0.001$).

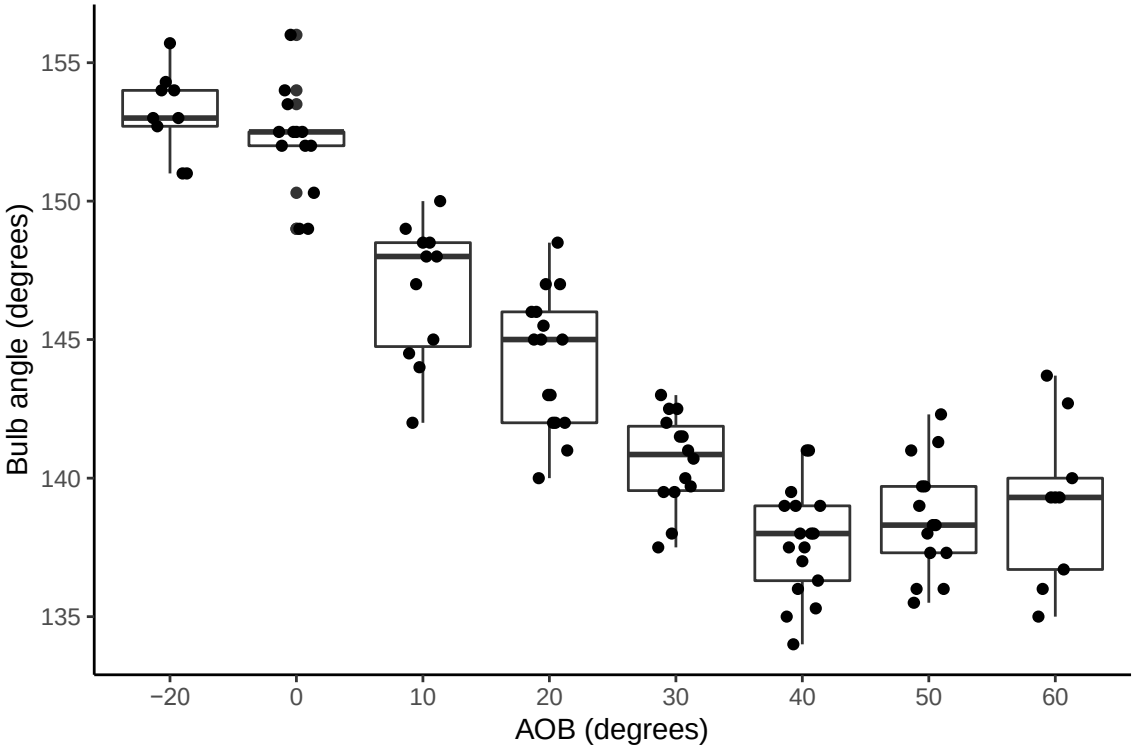

Fig. 3-6 Boxplot showing that bulb angle decreases as angle of blow (AOB) increases for flakes in the drop tower dataset

3.2 Dibble dataset

The same significant relationship between the angle of blow and the bulb angle as measured by both the vector calculation (Kruskal-Wallis test, $H = 25.037$, $p < 0.01$) and the virtual goniometer (Kruskal-Wallis test, $H = 24.698$, $p < 0.01$) methods is observed in the Dibble dataset (Fig.3-7, Table Appx-II.2 in Appendix II). Using the vector calculation method, the average bulb angle is 150.3 (± 5.4) degrees for flakes in the zero angle of blow group and is 135.3 (± 6.1) degrees for flakes in the 40-degree angle of blow group. Using the virtual goniometer method, the average bulb angle is 152.8 (± 4.7) degrees for flakes in the zero angle of blow group and is 134.3 (± 8.4) degrees for flakes in the 40-degree angle of blow group. Overall, the vector calculation method tends to return a smaller average bulb angle value than the virtual goniometer method (Fig.3-8, see also Table Appx-II.2 in Appendix II). It should be noted that the standard deviation of bulb angle in the Dibble dataset is bigger than that in the drop tower dataset (Table Appx-II.1 and

Table Appx-II.2 in Appendix II). Unlike with the drop tower dataset, the maximum angle of blow represented in the Dibble dataset is 40 degrees. As such, we were not able to examine if the bulb angle reaches a plateau once the angle of blow tilts beyond 40 degrees.

The regression models used to predict bulb angle calculated using both the vector calculation and the virtual goniometer methods can be found in Appendix II. For the vector calculation bulb angle model, the overall regression was statistically significant (R^2 = 0.50, F (3, 49) = 16.31, $p < 0.001$). Both the angle of blow ($p < 0.001$) and platform depth ($p = 0.01$) were shown to significantly predict bulb angle. However, these two variables are correlated in the Dibble data set. For the virtual goniometer bulb angle model, the overall regression was statistically significant (R^2 = 0.48, F (3, 49) = 15.24, $p < 0.001$). Only the angle of blow was shown to significantly predict bulb angle ($p < 0.001$). There was also a significant correlation between the angle of blow and platform depth (adj. R^2 = 0.19, F (1, 51) = 13.59, $p < 0.001$).

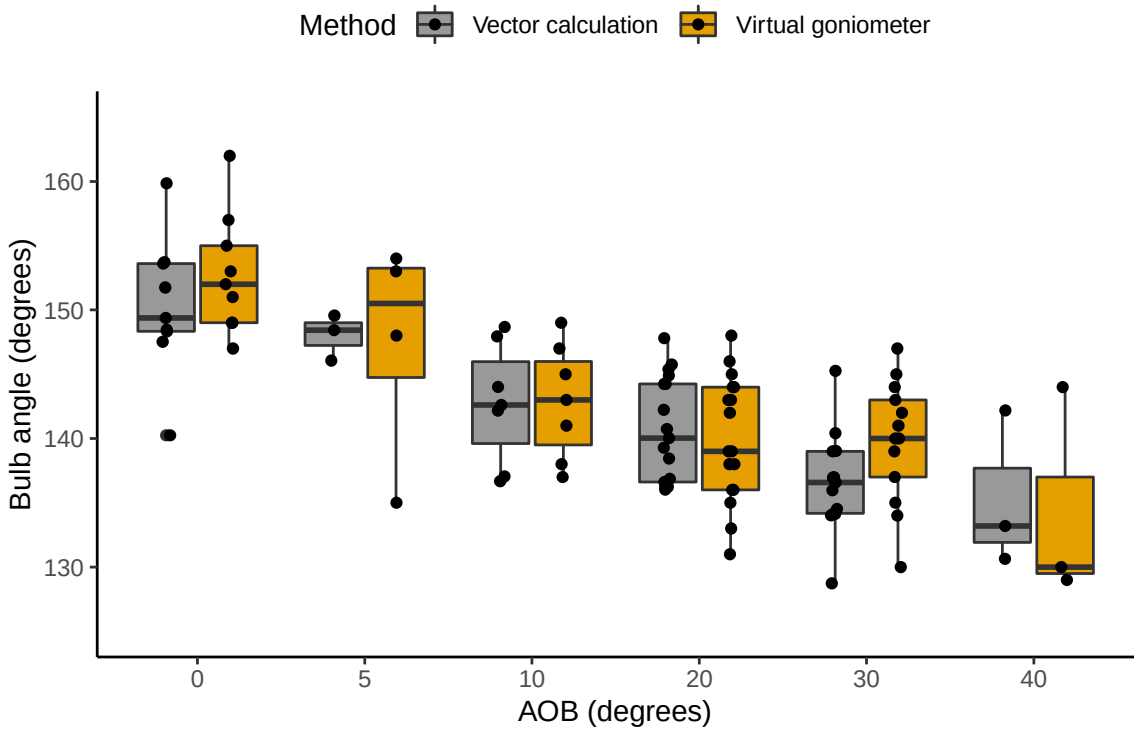

Fig. 3-7 Boxplot summarizing the relationship between bulb angle and angle of blow for flakes in the Dibble dataset. Flakes measured with the vector calculation method

are colored in grey. Flakes measured with the virtual goniometer method are colored in yellow

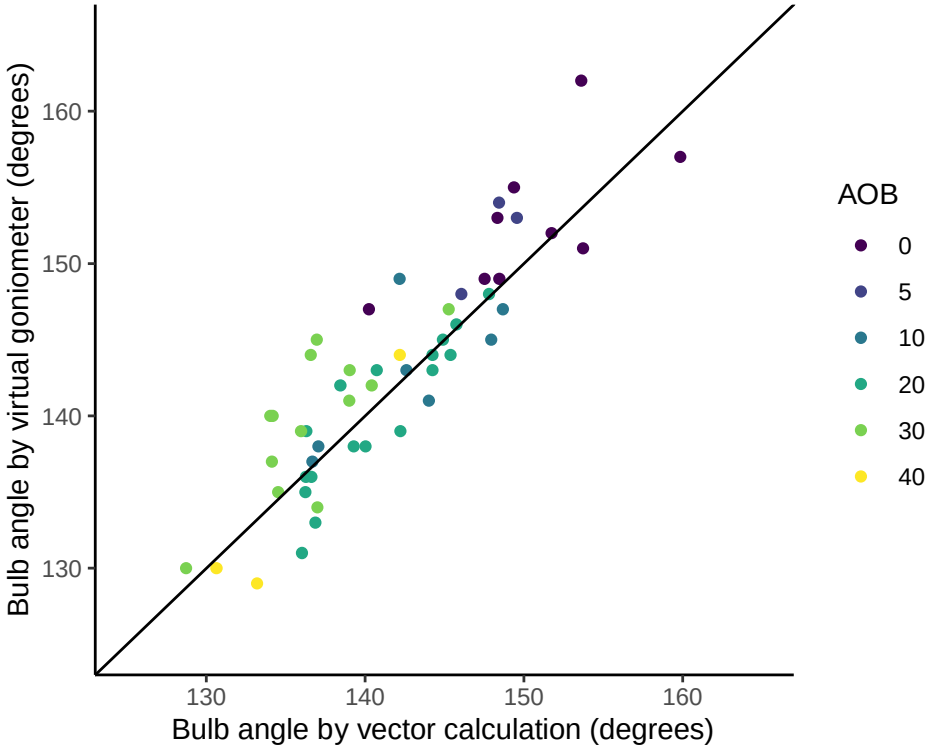

Fig. 3-8 Comparison of the flake bulb angles in the Dibble dataset as measured by the vector calculation method and by the virtual goniometer method. The line represents a 1:1 correspondence

3.3 MPI dataset

For the MPI dataset, the average standard error of the bulb angle is 0.7 degrees (see also Fig.Appx-II.2 in Appendix II). Fig.3-9 shows the distribution of bulb angle measured in this dataset. The average bulb angle for flakes is 132 degrees made with a high angle of blow and is 135.7 degrees for flakes made with a low angle of blow (see also Table Appx-II.3 in Appendix II). There is a significant difference in bulb angle between the knapper-assigned high and low angle of blow groups (Fig.3-10, Kruskal-Wallis test, H = 9.11, $p < 0.01$).

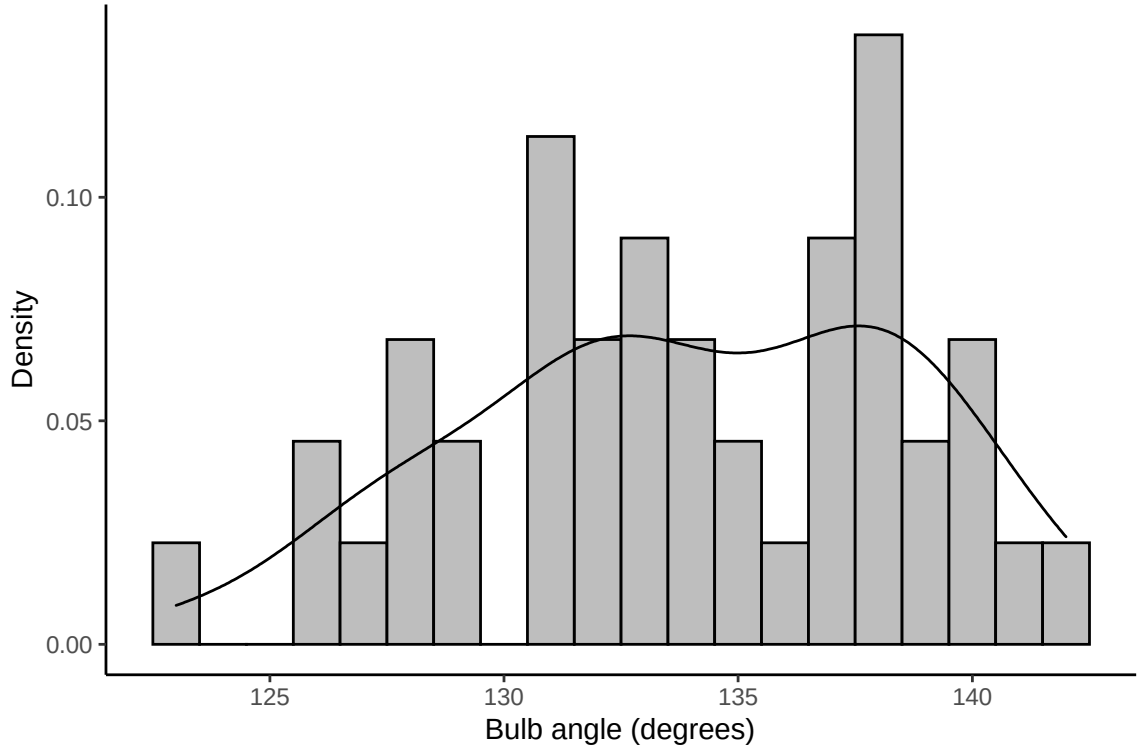

Fig. 3-9 Histogram showing the distribution of bulb angle with overlaying density curve for all flakes analyzed in the MPI dataset

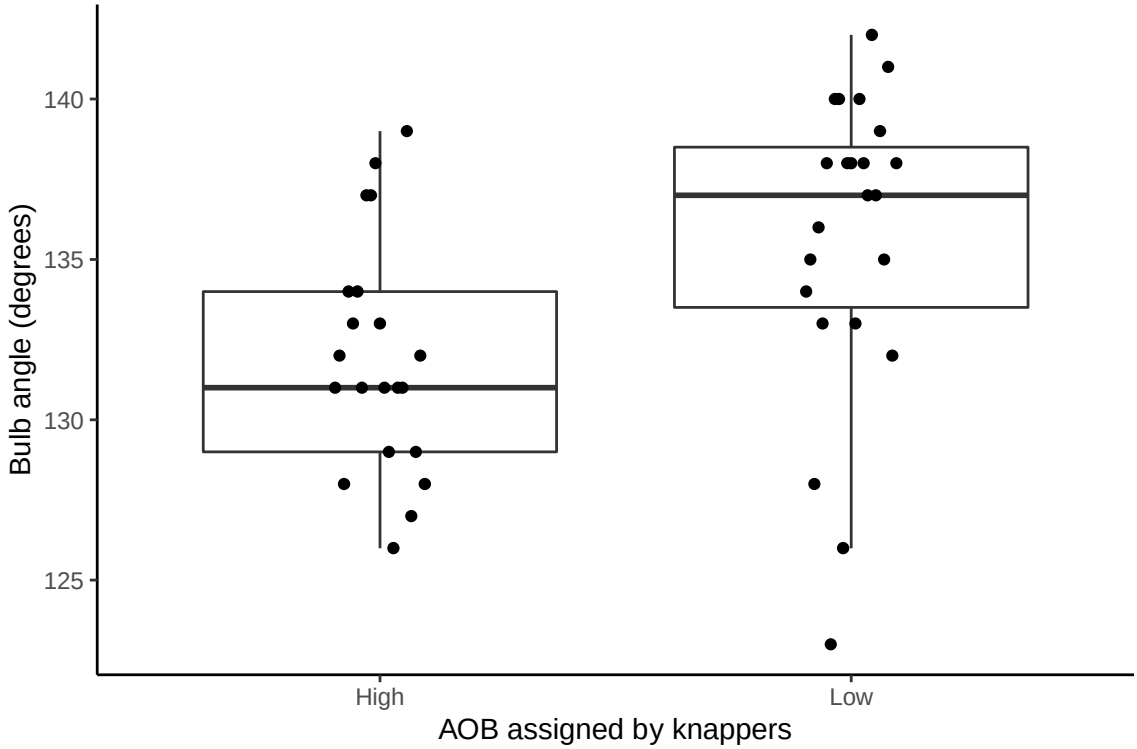

Fig. 3-10 Boxplot showing the result of the angle of blow blind test with the MPI dataset

3.4 Linear modeling

Using flakes from the Dibble dataset, Fig.3-11a compares the actual flake mass to those predicted by the baseline EPA-PD model (Table 3-1). While the baseline model performs relatively well ($R^2 = 0.59$), it is clear that the flakes made with a lower angle of blow tend to have their mass underestimated, and the flakes made with a higher angle of blow tend to have their mass overestimated by the EPA-PD model. In comparison, when the known angle of blow is included as a predictor in addition to EPA and PD, the explanatory power of the model increased considerably ($R^2 = 0.81$), and predicted flake masses are much closer to their actual values (Fig.3-11b). An ANOVA test shows the addition of angle of blow to the EPA-PD model significantly improves the model's performance ($p < 0.001$).

Fig.3-11c and Fig.3-11d show the relationship between the actual versus the predicted flake mass based on the EPA-PD model and the inclusion of the bulb angles measured by the two methods. While the improvement in R^2 is not as strong

as what we observed earlier with the use of the actual angles of blow values, the addition of the bulb angles still substantially increased the explanatory power of the linear model (Table 3-1). This observation is reflected by the ANOVA tests showing that adding the bulb angle as a predictor to EPA and PD does significantly increase the amount of flake mass variation accountable by the linear model ($p < 0.001$).

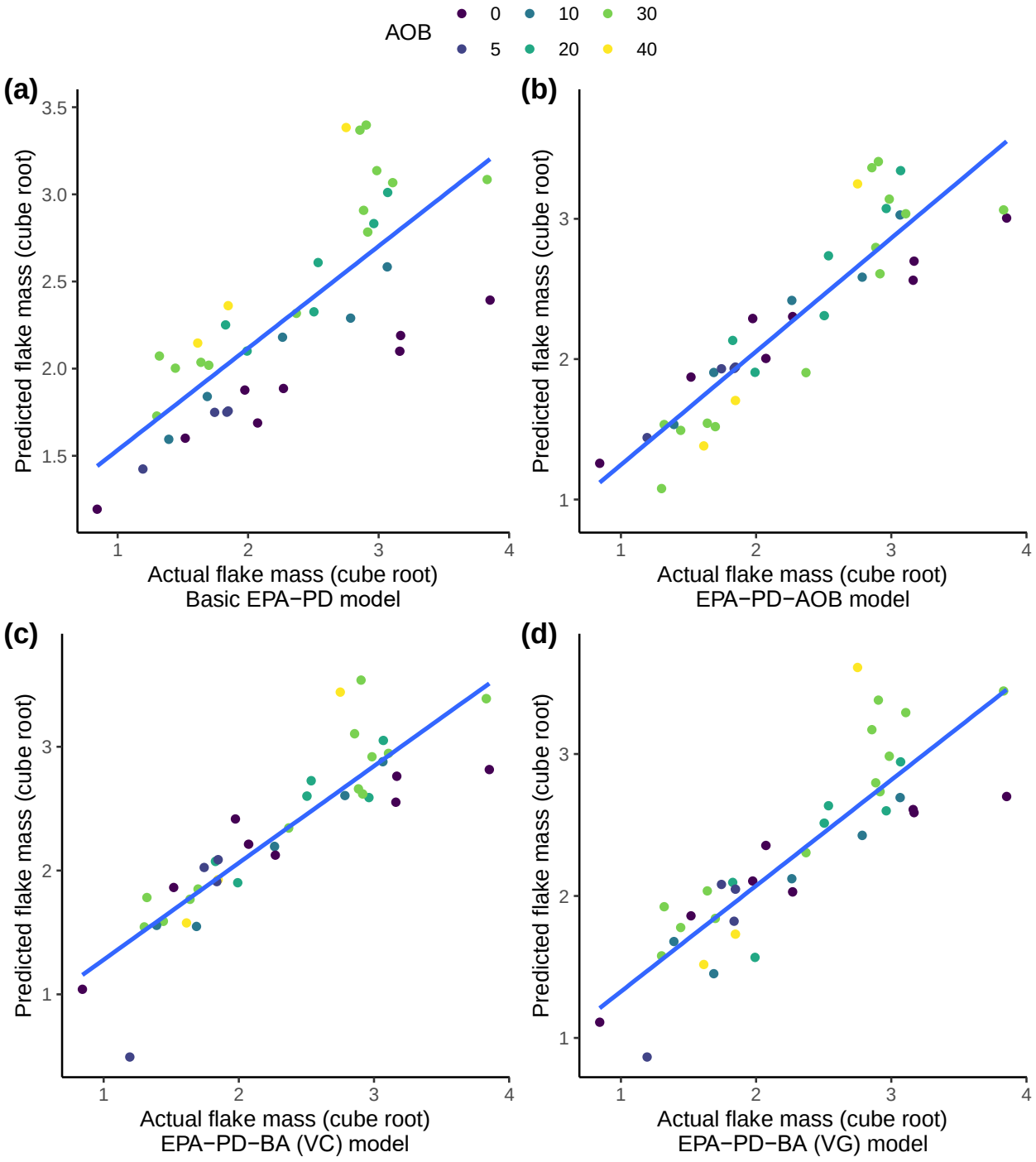

Fig. 3-11 Comparison of the actual flake mass and modeled flake mass in the Dibble dataset, n = 53. (a) Actual to predicted flake mass using the basic EPA-PD model, (b) actual to predicted flake mass using the EPA-PD-AOB model, (c) actual to predicted flake mass using the EPA-PD-BA (vector calculation) model, and (d) actual to predicted flake mass using the EPA-PD-BA (virtual goniometer) model.

Table 3-1 Summary statistics of the different EPA-PD models

	Basic EPA-PD model	EPA-PD-AOB model	EPA-PD-BA (VC) model	EPA-PD-BA (VG) model
R^2	0.59	0.81	0.78	0.75
Adj. R^2	0.56	0.79	0.76	0.72
F statistics	25.41(2,36)	49(3,35)	42.04(3,35)	34.17(3,35)
p value	*< 0.001*	*< 0.001*	*< 0.001*	*< 0.001*

4 Discussion

Reconstructing the knapping gestures from the archaeological record is an important path to understanding the early knappers' tool behavior. Up to now the angle of blow has been considered to be archaeologically invisible (Magnani et al., 2014). In this study, we hypothesized that the angle of blow can in fact be gauged by the immediate angle between the striking platform and the protruding side of the Hertzian cone, what we referred to as the bulb angle. The results across all three datasets examined here support the hypothesis by showing that the bulb angle does indeed correlate with the angle of blow. Increasing the angle of blow during flake removal (i.e., greater tilt) causes the bulb angle to decrease, while a lower angle of blow (i.e., more direct) results in higher bulb angle values. Importantly, this relationship is consistent among flakes made from different raw materials (soda-lime glass and flint) and under both mechanical and flintknapping experiments, suggesting that the correlation between the bulb angle and the angle of blow can be generalized to other flake formation settings.

The relationship between the bulb angle and the angle of blow is warranted by the fracture mechanics of Hertzian cone formation (Gorham and Salman, 2005;

Kocer and Collins, 1998; Marimuthu et al., 2016; Zeng et al., 1992a). Despite its close relevance to flake formation, the field of fracture mechanics has had relatively little impact on lithic studies, likely owing to its mathematically laden nature and possibly to diverging goals. As previously discussed, earlier fracture mechanics-based controlled lithic experiments in the 70s and 80s emphasized testing ideas that directly come from the fracture mechanics literature. Unfortunately, results from these studies were not well applied to the actual archaeological record (Cotterell et al., 1985; Cotterell and Kamminga, 1987; Speth, 1972). Although several studies have incorporated the orientation of the Hertzian cone to infer handedness of the knappers (Bargalló and Mosquera, 2014; Dominguez-Ballesteros and Arrizabalaga, 2015; Rugg and Mullane, 2001), they did not establish a direct link between features of the Hertzian cone and the relevant knapping gestures. Instead, more recent controlled experiments have largely focused on assessing the empirical effects on flaking outcomes from knapping parameters that are under the direct control of knappers (Dibble and Pelcin, 1995; Dibble and Rezek, 2009; Dibble and Whittaker, 1981; Dogandžić et al., 2020; Leader et al., 2017; Magnani et al., 2014; Mraz et al., 2019; Pelcin, 1996; Rezek et al., 2011). This knapper-guided approach aims to establish statistical relationships between independent factors (e.g., EPA and PD) and dependent flake attributes, which can then be applied to infer past technological patterns from archaeological finds.

Here we expand on this knapper-guided approach by taking previous observations about the effect of the angle of blow and then incorporating fracture mechanics theory to help develop and test a hypothesis about the relationship between the angle of blow and the bulb angle. Importantly, the fracture mechanic model of Hertzian cone formation allowed us to make simple yet explicit predictions about what the bulb angles should be under different angles of blow. To this end, the experimental results show a relatively good agreement with these predicted values. For example, in the drop tower dataset, the average bulb angle on soda-lime glass flakes made with a zero angle of blow is 152 degrees, which is close to our theoretical prediction of 158 degrees based on the empirical value of the Hertzian cone angle for soda-line glass. In comparison, the bulb angle values among the Dibble dataset associated with a zero angle of blow are lower (148.4 and 150.3 degrees). While the reason for this discrepancy is currently unclear, it may be

possible that the use of the 3D models for the Dibble dataset involved additional sources of error associated with the scanning and model processing procedure. In particular, the area of the flake at which the bulb angle was measured has a relatively complex morphology, such that minor variation in scan quality and levels of smoothing may substantially influence the measurements taken. Future studies should evaluate the influence of scan quality on the accuracy and precision of the bulb angle measurement.

For the drop tower dataset, the bulb angle stabilized at around 138 degrees once the angle of blow reached 40 degrees and beyond. This angle is close to the constant Hertzian cone angle of 136 degrees in soda-lime glass. As we outlined earlier in Fig.3-2b, this minimum bulb angle likely represents the maximum tilt that the Hertzian cone can achieve when one side of the cone comes up against the platform surface. When the angle of blow reaches past 40 degrees, the Hertzian cone cannot tilt up any farther and the bulb angle becomes plateaued at a value that is close to the Hertzian cone angle constant. However, we were not able to verify this hypothesis further with the Dibble dataset, as the sample size of the flakes in the Dibble dataset made with an angle of blow larger than 40 degrees is too small to allow meaningful statistical comparison. Future studies should thus investigate whether there is a similar threshold in the angle of blow at which point the bulb angle stabilizes under different knapping conditions and raw materials. There are also other differences between the Dibble dataset and the drop tower experiment that may influence the Hertzian cone formation. While most fracture mechanics studies that investigate Hertzian cone formation are conducted with spherical indenters (Chaudhri and Chen, 1989; Fischer-Cripps, 2007; Frank and Lawn, 1967; Marimuthu et al., 2016), a flat-bevel ended hammer was used in the experiments that created the Dibble dataset. The non-spherical hammer tip may cause additional complications in the Hertzian cone formation (Fischer-Cripps, 2007).

For both the drop tower dataset and Dibble dataset, the bulb angle linear models show that the angle of blow is the only variable that could significantly predict bulb angle, for the most part. The only exception is that in the Dibble dataset, platform depth appears to also influence bulb angle (when measured using the vector calculation method) in addition to the angle of blow. However, it should be noted that there is a significant correlation between the angle of blow and platform

depth in the Dibble dataset because of the way the experiments were structured in the first place (i.e., not all angles of blow were attempted for all platform depths). For this reason, platform depth also correlates with bulb angle, and there is no reason to think that platform depth influences bulb angle.

Though the results of the blind test on the MPI data show that bulb angles on high and low angles of blow flakes differ from each other on average, it is clear that relaxing the controls of the previous experiments makes the differences less apparent. One point of caution concerns the use of hammerstones in the experiment. These were not strictly controlled between strikes. While the size of the hammer does not change the Hertzian cone angle for a particular raw material type, it may influence how the cone responds to changes in the strike angle. Similarly, changes in the platform surface morphology may also alter the intended angle of blow. We also think it is likely that despite their intention to use specifically either a low or high angle of blow, the knappers might differ in their consistency as they rotated the core or adjusted their swing such that the angle changed in the opposite direction of their intention. It is possible, for instance, that while the arrangement of the core and overall arm movement should have led to a high angle of blow, for instance, small adjustments in the wrist orientation at strike may have lowered the angle.

It is important to emphasize here that the Hertzian cone angle varies by raw material. Specifically, it seems that the Hertzian cone angle is related to the mechanical properties of the material, such as the Poisson's ratio (Frank and Lawn, 1967; Kocer and Collins, 1998; Roesler, 1956). Raw materials with a larger Poisson's ratio, or those that are stiffer, have a larger cone angle (Olivi-Tran et al., 2020). As a result, we expect that the bulb angle produced when striking a core with a zero angle of blow will vary by raw material type. A larger Hertzian cone angle will result in a larger bulb angle for any given angle of blow. Similarly, the point at which the bulb angle plateaus with the angle of blow will vary as well. In fact, raw materials with larger Hertzian cone angles should plateau sooner, and the range of angles of blow that can be measured on these materials will be more limited. On the contrary, raw materials with smaller Hertzian cone angles will allow a greater range of angles of blow to be measured. This potential discrepancy in the range of bulb angle variation in different raw materials could further complicate our interpretation of

actual archaeological assemblages where raw material types vary. For now, until the Hertzian cone angle is known for the appropriate raw material types, comparisons in bulb angles are best done within a given raw material type.

The linear model results show that the angle of blow is an important knapping parameter that can help improve our ability to explain flake variation using independent flake variables, such as EPA and PD. The current EPA-PD model of flake formation derived from the controlled experiments by Dibble and colleagues (Dibble and Rezek, 2009; Dogandžić et al., 2020; Leader et al., 2017; Magnani et al., 2014; McPherron et al., 2020; Rezek et al., 2011) only addresses a portion of the variation in flake size and shape. In their paper on the topic, Dibble and Rezek (2009) found that exterior platform angle, platform depth, and angle of blow all influenced flake mass, yet the angle of blow was mostly dropped from subsequent presentations of the model because the parameter could not be measured on the flakes themselves. Our results show that the inclusion of the angle of blow into the EPA-PD model significantly improved the model performance. More importantly, we further showed that substituting the angle of blow by the bulb angles resulted in a similar improvement in model R^2, indicating that the bulb angle is a useful proxy for gauging the angle of blow on flakes.

5 Conclusions

Our findings, for the first time, demonstrate a quantitative method for measuring the angle at which knappers strike the hammer during flake removal, or the angle of blow, from a measurable flake attribute – the bulb angle. While both researchers and modern knappers have long noted the significance of this parameter in successful flake removal and in learning skill of knapping, up to now the variable has been largely considered to be invisible in the archaeological record. The ability to gauge the angle of blow among archaeological flakes by using the bulb angle opens a range of new research opportunities to study how hominins managed this important component of force delivery in knapping stone flakes over the past 2-3 million years. Importantly, given that the angle of blow has been repeatedly shown to be an important factor in the learning of stone working among modern knappers,

quantifying changes in the angle of blow among Paleolithic flake assemblages may offer new insights into the evolution of human technology and cultural transmission.

It is important to keep in mind that the bulb angle measurement may be complicated by other sources of variation. Not only is the bulb angle a small-sized feature that can be prone to measurement error, but factors such as raw material, hammer size and shape, and the initial nodule condition may also all contribute to variation in the bulb angle. As with any newly developed methods, we urge for more studies to test the reliability of the bulb angle, especially under more diverse experimental settings. Lastly, our study shows that incorporating fracture mechanics provides promising insights and inspirations to translate different knapping behaviors to tangible flake attributes (McPherron et al., 2020). To this end, exploring force delivery variables such as striking force and hammer size and velocity from a fundamental perspective of flaking mechanics can be a fruitful avenue forward, helping to establish connections between quantitative flake attributes with the dynamic manual gesture and knapping techniques of past hominins.

Acknowledgments:

The project has received funding from the European Research Council (ERC) under the European Union's Horizon 2020 research and innovation programme (grant agreement No. 714658, STONECULT project). LL received funding from the Leakey Foundation Research Grant. We would like to thank our colleagues Alexander Schnapper and Christof Binder from the metal workshop and Thomas Nieß and Karin Rein from the glass workshop at the University of Tübingen for their help in building the drop tower setup and preparing the glass cores. SPM thanks Jean-Jacques Hublin and the Max Planck Society for their continued support of his research. We would like to thank Alicia Walsh, Aylar Abdolahzadeh, and Tamara Dogandžić for scanning the flakes of the Dibble dataset, and also Tamara Dogandžić and Karen Ruebens for their help in landmarking the 3D flake models of the Dibble dataset. We would like to thank Katrina Yezzi-Woodley, Peter J. Olver, and Jeff Calder for their help in making the virtual goniometer work for the OS used by LL at the time when the paper was written. Thanks, as well to David Braun and Zeljko Rezek for many helpful conversations about these data along the way. Lastly, we

acknowledge the late Harold Dibble for the foundational work he laid out in the controlled lithic experiments. Our work could not have been done without it.

CHAPTER 4 Did early hominins control their hammer strike angles when making stone tools?

This chapter includes the following manuscript that will be submitted to the *Journal of Human Evolution*:

Li, L., Braun. D.R, Lin, S.C., Reeves, J.S., McPherron, S.P. Did early hominins control their hammer strike angles when making stone tools?

Author contributions

Conceptualization: Li Li, Jonathan S. Reeves, Shannon P. McPherron

Data curation: Li Li, Jonathan Reeves, Shannon P. McPherron

Writing – original draft: Li Li, Shannon P. McPherron, Sam C. Lin, Jonathan S. Reeves

Writing – review and editing: Li Li, David R. Braun, Sam C. Lin, Jonathan S. Reeves, Shannon P. McPherron

Abstract

The emergence and development of stone technology have shaped the trajectory of human evolution. Stone artifacts are one of the most important pieces of evidence for studying hominin behavior and cognition because of their sheer quantity and indestructible nature. Technical decision making is a central focus of Oldowan research as it provides a path to examine hominins' cognitive capabilities from the archaeological record. Our understanding of early hominins' technical decisions is limited to evidence that is preserved in the lithic record. We have a good understanding of early hominins' knapping strategies from different aspects such as raw material selection, core management, hammer selection, and platform preparation. However, whether and how early hominins control their hammerstone strike angle, or the angle of blow – a force delivery variable of the knapping process that plays a key role in determining the flaking outcome – is poorly understood. The angle of blow plays a significant role in determining the knapping outcome. In this study, we use a newly developed method to measure the angle of blow. We then examine diachronic variation in early hominins' control over the angle of blow. Our dataset consists of flakes from 12 early Pleistocene assemblages that are dated from 1.95 Ma to 1.4 Ma. Our results show that towards the Oldowan-Acheulean transition, early hominins started to develop a more comprehensive understanding of the role of the angle of blow in flake formation and were likely adjusting their striking angle to make flakes of different sizes.

1 Introduction

The knowledge that early stone knappers possessed to make sharp-edged stone flakes is one of the most pressing questions to answer in order to understand the origin and evolution of hominin tool use. At the heart of this question is the notion of control – how did early humans control the knapping process to produce the desired flake outcomes, and how did these knapping capabilities change over the course of human evolution? One of the primary approaches that archaeologists have employed to answer these questions is to characterize the reduction sequence of past stone production to understand the ways in which hominins shaped the core for flake removals. We have gained much knowledge about the different aspects of

early hominins' lithic reduction sequences from both artifact analysis (e.g., flake scar direction, refitting elements, reduction intensity, etc.) and replicative or actualistic experiments (Braun et al., 2008b; Delagnes and Roche, 2005; Douglass et al., 2021; Harmand, 2007; Nonaka et al., 2010; Sharon, 2009; Stout et al., 2009, 2010; Toth and Schick, 2009, 2019). For example, Oldowan hominins followed certain technical rules for flake removal such as exploiting acute platform angles, rotating cores in specific directions, and adjusting reduction intensity based on types of the raw material (Braun et al., 2008b, 2008a; de la Torre, 2004; Delagnes and Roche, 2005; Goldman-Neuman and Hovers, 2009; Harmand, 2007; Reti, 2016; Stout et al., 2005, 2009, 2010; Toth, 1982, 1985). Acheulean hominins followed specific removal sequences and used different percussion techniques for the shaping of bifaces and other large cutting tools (LCTs) (Bradley and Sampson, 1986; de la Torre et al., 2008; Newcomer, 1971; Sharon, 2009; Shipton, 2018, 2016; Toth and Schick, 2019).

However, beyond reduction sequence and core morphology, how percussive force is applied to remove a flake is an important factor in flaking control. Modern knapping experiments have demonstrated the importance of manual gestures in the percussion delivery for successful flake removals, from the placement and support of the core to the trajectory of the arm swing and the angle at which the hammer impacts the core (Biryukova et al., 2005; Biryukova and Bril, 2008; Bril et al., 2010; Cueva-Temprana et al., 2019; Nonaka et al., 2010; Rein et al., 2013; Vernooij et al., 2015; Williams-Hatala et al., 2021). These findings not only signal the importance of technical gestures in learning to knap stone but also imply that knapping gestures would have been constrained biomechanically by the hand and wrist morphology, which varied among hominin species over time (Biryukova et al., 2000; Bril et al., 2010; Marzke, 2013; Susman, 1998; Williams et al., 2012, 2010; Williams-Hatala et al., 2021). Thus, reconstructing how past knappers controlled knapping gestures during flake production is paramount if we are to fully understand the evolution of lithic technology in relation to evolutionary changes in hominin biology and cognition.

A key parameter of manual knapping gesture is the hammer strike angle, or the angle of blow (AOB). Modern knappers have observed that changing the angle of blow can substantially alter the flaking outcome (Johnson, 1975; Whittaker, 1994). Namely, striking a hammer perpendicularly straight into the core carries the risk of crushing the platform or generating step fractures while tilting the core to change the

angle of blow can help facilitate flake detachment (Whittaker, 1994). Under identical core morphologies, altering the angle of blow alone can produce very different flaking outcomes. This observation is supported by controlled flaking experiments, which showed that tilting the angle of blow to make it oblique relative to the platform tends to produce flakes that are smaller, shorter, and have a less prominent bulb of percussion (Fig.4-1) (Dibble and Rezek, 2009; Magnani et al., 2014; Speth, 1975). Given that the amount of percussive force required for detaching flakes is correlated with flake size (Dibble and Rezek, 2009; Dogandžić et al., 2020; Mraz et al., 2019), these findings imply that tilting the angle of blow also reduces the amount of percussive force required to detach a flake from a given platform. In addition, the angle of blow also influences the prominence of the bulb of percussion and the occurrence of platform lipping on flakes (Bataille and Conard, 2018; Hellweg, 1984; Schmid et al., 2019, 2021; Soriano et al., 2007).

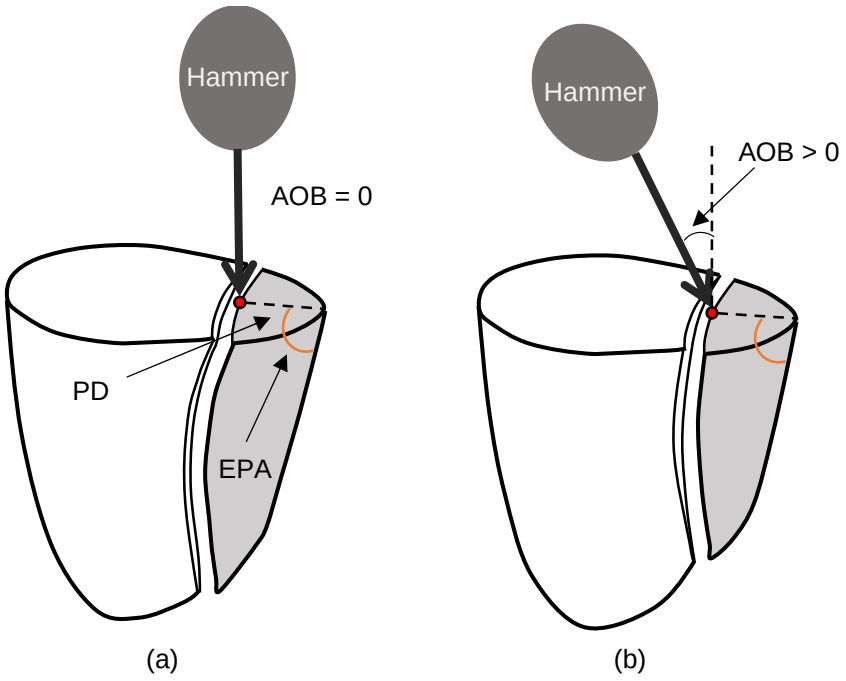

Fig. 4-1 Schematic illustration of the effect of the angle of blow (AOB) on flaking. The angle of blow is measured as the angle between the hammer striking direction and the perpendicular of the platform surface (marked by the black arc in b), the red dot refers to the point of percussion. (a) Shows the scenario when the angle of blow is

perpendicular to the platform (equal to zero), (b) shows the scenario when the angle of blow is oblique (or is positive)

Being able to control and apply the appropriate angle of blow has also been suggested to be crucial for certain lithic technologies. For example, an acute or oblique angle of blow is found to be preferred for the making of Oldowan-like choppers or chopping tools and Acheulean-like handaxes (Cueva-Temprana et al., 2019). Biface thinning is commonly said to involve tilting the angle of blow such that the hammer strikes ‘inward’ to the biface on the platform edge (Shipton, 2018). Boëda (1993) specified the need for hammers to strike perpendicularly to the platform surface in order for the fracture to travel parallel to the plane of intersection between the two hemispheric surfaces for the classic Levallois flake removal. In contrast, tilting the angle of blow to strike ‘tangentially’ or ‘outward’ to the core has often been associated with blade production technologies in the Late Pleistocene, often in relation to soft hammer percussion (Clark, 2012; Crabtree, 1972b; Newcomer, 1975).

Evidence from both actualistic and controlled experimental studies has shown the importance of the angle of blow in determining the flaking outcome. It thus stands to reason that controlling the angle of blow during knapping at some point became an integral part of the hominin technological repertoire. One possibility is that the capacity to adjust the angle of blow may have already been well-expressed among the earliest hominin tool makers, who systematically produced flakes with sharp edges by exploiting suitable platform locations of percussion (Braun et al., 2019; Režek et al., 2018). Alternatively, hominins’ ability to control the angle of blow may have emerged later in time, which in turn enabled them to develop novel knapping patterns to produce new forms of stone tools, such as Acheulean bifaces and Levallois products. These two hypotheses stem from the different views of hominins’ cognitive and technological capacities along their evolutionary trajectory (Cueva-Temprana et al., 2022; Morgan et al., 2015; Shipton and Nielsen, 2015; Snyder et al., 2021; Stout et al., 2010, 2019; Tennie et al., 2016, 2017, 2020). Some argue that early hominins (such as those from the Oldowan) were already cognitively capable of acquiring the necessary skills to produce the stone artifacts via a human-like cultural

transmission (Morgan et al., 2015; Pargeter et al., 2021; Stout et al., 2019). Others, to the contrary, contend that early hominins were more likely to rely on spontaneous and individual abilities to produce the stone artifacts (Cueva-Temprana et al., 2022; Snyder et al., 2021; Tennie et al., 2016, 2017).

However, it is difficult to test the aforementioned hypotheses because there is no obvious feature on stone flakes that reflects the angle of blow. As such, the angle of blow has been either considered 'archaeologically invisible' or combined with discussion of soft hammer use in relation to the occurrence of platform lipping (Schmid et al., 2019, 2021). A recent study by Li (Under Review) presented a new method to quantify the angle of blow from archaeological flakes. The method is based on the principle that, in conchoidal fracture, the direction of the hammer blow can cause the Hertzian cone to tilt in different ways after fracture initiation (Chaudhri, 2015; Chaudhri and Chen, 1989; Lawn et al., 1984; Salman et al., 1995; Suh et al., 2006). The variation in the tilt of the Hertzian cone can be measured on a feature of the flake's bulb of percussion, termed the 'bulb angle' (Fig.4-2) (Li et al., Under Review). More specifically, as the angle of blow becomes more oblique relative to the platform surface, the resulting bulb angle on a flake becomes smaller. In other words, a large bulb angle indicates a more direct angle of blow relative to the platform, and a small bulb angle indicates a more oblique angle of blow relative to the platform (Fig.4-2). Tested using several experimental datasets produced under both controlled and flintknapping settings, Li et al. (Under Review) showed that bulb angle can be a reliable and direct proxy for capturing the angle of blow during flake production.

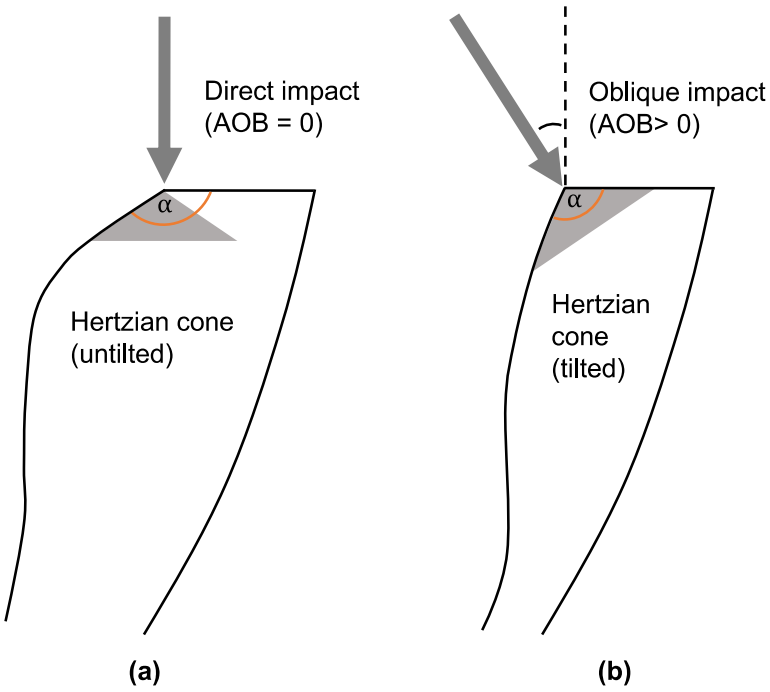

Fig. 4-2 Schematic illustration of bulb angle on a flake from its profile view, bulb angle is marked by the orange arc and α refers to the Hertzian cone angle. (a) shows the orientation of the Hertzian cone when the angle of blow is zero, the theoretical bulb angle is 90° + 0.5α; (b) shows the case when the Hertzian cone is completely pushed onto the platform by an oblique (positive) angle of blow, the theoretical bulb angle is equal to α

We know that early hominins understood the basics of knapping and produced flakes in a systematic manner (Braun et al., 2008b; Delagnes and Roche, 2005; Roche et al., 1999). But how they carried out specific knapping gestures such as adjusting the angle of blow needs further investigation. Measuring bulb angle on archaeological flakes provides us an opportunity to reconstruct early hominins' control over the angle of blow. Modern knappers are known to adjust the angle of blow to facilitate the removal of flakes (Crabtree, 1975; Geribàs et al., 2010; Ranere and Browman, 1978; Whittaker, 1994), often in conjunction with adjusting exterior platform angle and platform depth. If hominin knappers were able to control the angle of blow, we may expect to see a correlation between bulb angle and exterior platform angle and platform depth.

Exterior platform angle and platform depth are the two essential attributes of platform preparation. Exterior platform angle reflects how the edge of the core is set up and platform depth shows how far into a core's platform a knapper chooses to hit for flake removal (Fig.4-1a). It has been repeatedly shown in controlled flaking experiments that increasing either or both these two variables will result in a larger flake (Dibble and Pelcin, 1995; Dibble and Rezek, 2009; Dibble and Whittaker, 1981; Dogandžić et al., 2020; Leader et al., 2017; Magnani et al., 2014; Rezek et al., 2011). Importantly too, the relationship is such that at higher exterior platform angles, equivalent changes in platform depth have proportionately greater impacts on flake outcomes. Archaeological evidence shows that hominins became more aware of the effect of exterior platform angle and platform depth and more capable of manipulating them to achieve different results through time (Braun, 2012; Braun et al., 2019; Dibble, 1997; Lin et al., 2013; Režek et al., 2018; Roche, 2005). But we do not know whether the same diachronic progression can be applied to hominins' control over the angle of blow. At present we do not yet have a clear comprehension of when (or if) early hominins understood the effect of the angle of blow and could control it.

We propose two possible scenarios of early hominins' understanding and control over the angle of blow in relation to their platform preparation strategies. First, early hominins developed a more comprehensive understanding of the mechanics of the angle of blow in flaking together with exterior platform angle and platform depth through time. As a result, we expect to observe stronger correlations between bulb angle as a proxy for the angle of blow and exterior platform angle and platform depth from later times in the archaeological record. Second, or in the null hypothesis, early hominins did not understand how the angle of blow works in flake formation, or they did not control the angle of blow in any systematic fashion. And as a result, we would then expect a normal distribution of bulb angle with no correlation with exterior platform angle or platform depth, or other flake attributes.

In this study, we apply the bulb angle method to analyze a series of Early Pleistocene assemblages to examine if early hominin toolmakers controlled the angle of blow during stone tool manufacture. We also include a much later in time Middle Paleolithic assemblage produced by Neandertals as a point of comparison to help contextualize changes observed in the Early Pleistocene assemblages.

Including the Middle Paleolithic dataset allows us to evaluate the level of competence in knapping of these Early Pleistocene knappers against Neandertals, who are known as capable knappers.

2 Materials and Methods

We studied complete and unretouched flakes from 12 Early Pleistocene assemblages from the Koobi Fora Formation (Fm.), East Turkana, Kenya, and one Middle Paleolithic assemblage Roc de Marsal (RDM) from France. The 12 Early Pleistocene assemblages are curated in the Nairobi National Museum in Kenya. The Middle Paleolithic assemblage is currently curated in Campagne, France.

The Koobi Fora Fm. is an ideal location to investigate technological decision making through time as it possesses a well-documented and chronologically understood Early Pleistocene lithic record that spans from the Oldowan to the appearance of the Acheulean (Fig.4-3). Moreover, this sedimentary package contains three named industries in stone tool production known as the Oldowan, Karari, and Acheulean. The temporal range of the Oldowan in this region spans from around 1.95 Ma to 1.56 Ma (Archer et al., 2014; Braun et al., 2010; Brown et al., 2006). The Oldowan technology is characterized by the dominance of simple cores and flakes with an emphasis on the least-effort production of sharp edges (Schick and Toth, 2006, 1994; Toth, 1985). The Oldowan gives way to a local industry called the Karari (Harris, 1978), which is defined by the predominance of single platform cores (G. L. Isaac and Isaac, 1997). This local industry is eventually replaced by the Acheulean by about 1.4 Ma (Brown et al., 2006; Isaac and Isaac, 1997; Presnyakova et al., 2018). A vast majority of stone artifacts from the Koobi Fora Fm. were produced on *basalt.* Basalt cobbles were transported to the center of the east side of the Turkana Basin by rivers and streams (Braun et al., 2009a). Whole and split river cobbles were the primary blanks used in core reduction throughout the Oldowan and Karari. During the Acheulean, large flakes and elongated cobbles were predominantly used in large cutting tools (LCT) production (G. L. Isaac and Isaac, 1997; Presnyakova et al., 2018). The Koobi Fora Fm. is, therefore, a single geographic location that can provide an ideal collection of assemblages for studying

changes in the technical decision-making of early hominins through time while controlling for the influence of mechanical properties of the raw material.

Fig. 4-3 Locations of the assemblages analyzed in the study. The Oldowan assemblages are colored and labeled in blue, the Karari assemblages are colored and labeled in yellow, and the Acheulean assemblages are colored and labeled in red

2.1 An overview of the study sites

2.1.1 The Early Pleistocene assemblages

The 12 Early Pleistocene assemblages in this study are categorized into three groups based on the technological industry they belong to. The Oldowan Industry includes localities FwJj 20, FxJj 1, FxJj 3, FxJj 10, and FxJj 82 (Archer et al., 2014; Braun and Harris, 2009, 2003; Braun et al., 2010). FwJj 20 is dated to about 1.95 Ma and is from the Upper Burgi Member (Mbr.) (Archer et al., 2014; Braun et al., 2010). FxJj 1, FxJj 3, FxJj 10, and FxJj 82 are from the KBS Mbr. in the Karari region (Braun and Harris, 2009, 2003), they are dated between 1.87 and 1.6 Ma (Braun and Harris, 2009; Brown et al., 2006; Isaac and Behrensmeyer, 1997; Lepre and Kent, 2010; Toth, 1985) (Fig.4-3). FwJj 20 is located in Area 41 of the Koobi Fora Fm. (Braun et al., 2010). Both FxJj 1 and FxJj 3 are located in Area 105, FxJj 10 is located in Area 118, and FxJj 82 is located in Area 130 of the Koobi Fora Fm. (Fig.4-3) (Braun and Harris, 2009). We analyzed all unretouched flakes from these localities.

The Karari Industry includes localities FxJj 16, FxJj 18IH, FxJj 20E, and FxJj 50 (Harris, 1978; Isaac and Harris, 1997; Kaufulu, 1983). They are from the Lower Okote Mbr and are dated to between around 1.6 and 1.5 Ma (Bunn, 1997; Isaac and Behrensmeyer, 1997). FxJj 18IH (Ingrid Herbich Site) is the youngest location of the FxJj 18 site complex (Harris, 1978; Kaufulu, 1983). Because the excavation at FxJj 18IH yielded a large number of artifacts, we randomly sampled the complete and unretouched flakes with a clear bulb angle to reach a sample size of at least 40. FxJj 20E (East) belongs to the FxJj 20 site complex (Harris, 1978; Hlubik et al., 2017; B. Isaac and Isaac, 1997). FxJj 16 and FxJj 18 are from Area 130, FxJj 20E and FxJj 50 are from Area 131 of the Koobi Fora Fm. (Fig.4-3) (Braun et al., 2009a; Bunn et al., 1980; Harris, 1978; Isaac and Harris, 1997). We analyzed all unretouched flakes from the remaining three Karari localities.

The Acheulean includes localities FxJj 37, FxJj 63, and FxJj 65 (Isaac and Harris, 1997; Liljestrand, 1980; Presnyakova, 2019; Presnyakova et al., 2018). FxJj 37 belongs to the Okote Mbr. and FxJj 63 and FxJj 65 are situated within the Chari Mbr. They are dated to around 1.4 Ma (Isaac and Harris, 1997; Presnyakova, 2019; Presnyakova et al., 2018). All three localities are located in Area 131 of the Koobi

Fora Fm. (Fig.4-3) (Isaac and Harris, 1997). We analyzed all unretouched flakes from these three localities.

2.1.2 Roc de Marsal

Roc de Marsal is a small south-facing cave site located in a tributary valley of the Vézère River, southwest of Les Eyzies, France (Fig.4-3). The lower layers (Layer 9-5) at RDM are characterized by Levallois blank production (Lin et al., 2015; Sandgathe et al., 2011b). In this study, we analyzed unretouched Levallois flakes from Layers 9 through 7 (Lin et al., 2015; Sandgathe et al., 2011b). We limited the analysis to flint flakes only to avoid potential variation in bulb angle that can be introduced by the raw material (Li et al., Under Review). Because of the large number of artifacts in these three layers, we randomly sampled the collection to measure flakes with a clear bulb angle to reach a sample size of at least 50 for each layer. However, due to difficulties in measuring exterior platform angle and platform depth from some of these flakes, the final sample size was further reduced.

2.2 Attribute measurements

Only unretouched flakes with a clear platform and bulb of percussion were measured for the purpose of this study (Table 4-1) (Li et al., Under Review). We also excluded flakes with platform lipping. As a result, only a small portion of flakes from the archaeological assemblages have a well-preserved bulb angle that can be measured and used in the analysis. Attributes that were measured included bulb angle (BA), exterior platform angle (EPA), platform depth (PD), and flake mass. Both bulb angle and exterior platform angle were measured using a goniometer with a one-degree precision, platform depth was measured using a digital caliper with a 0.01mm precision, and flake mass was measured using a digital scale with a 0.01g precision. Measurements of both exterior platform angle and platform depth followed the protocols outlined in Dibble and Rezek (2009). Exterior platform angle was measured as the angle between the platform and the exterior surface of the flake (see also Dibble and Whittaker, 1981). Platform depth was measured from the point of percussion to the exterior edge of the platform. Bulb angle was measured as the

angle between the flake's platform and the protruding side of the Hertzian cone before it extends to form the bulb of percussion (Li et al., Under Review) (Fig.4-2).

We took several steps to minimize the measurement error in bulb angle. First, we only measured unlipped flakes with a complete platform and a clear bulb of percussion. Second, we measured the bulb angle of each flake on two separate occasions and used the average in the analysis. Third, we calculated the difference between the two bulb angle measurements and excluded the ones that are above the 95% percentile, which is 5 degrees (see Fig.Appx-III.1 in Appendix III). Last, for the east African assemblages, we only included flakes made from basalt, which is the dominant raw material at the Koobi Fora Fm., to avoid introducing additional confounding factors in the raw material properties. For the Middle Paleolithic assemblage, we only included flakes made from flint because it is the dominant raw material.

Bulb angle varies by raw material type due to the mechanical properties of the Hertzian cone (Olivi-Tran et al., 2020). That is, the range of variation of a raw material's bulb angle is determined by its Hertzian cone angle (Fig.4-2). As a result, raw materials with a larger Hertzian cone angle have a smaller range of variation for bulb angle and vice versa. Fracture mechanics studies show that the Hertzian cone angle of a specific type of raw material is largely affected by its Poisson's ratio (Olivi-Tran et al., 2020; Zeng et al., 1992a, 1992b). We obtain the Poisson's ratio of both basalt and flint from several studies to estimate the Hertzian cone angle and therefore the range of bulb angle variation we expect to see (Aliyu et al., 2017; Ji et al., 2019; Schultz, 1993). We estimate that the range of variation in bulb angle (from the theoretical Hertzian cone angle) is 108° – 144° (±6°) for basalt and 110° – 125° (±10°) for flint (Olivi-Tran et al., 2020). Although theoretically speaking that the two raw materials (basalt and flint) used in this study have a different overall range of bulb angle variation determined by their Hertzian cone angle, it should be noted that we are only doing an inter-dataset comparison and analysis on the same raw material of the relationships between bulb angle and other flake attributes. Moreover, RDM is used as a control group for us to compare the characteristics of the knapping strategies between Neandertals and early hominins, which does not concern the absolute value of bulb angle.

LL measured bulb angle on all flakes from both the Early Pleistocene assemblages and RDM. Flake platform attributes (exterior platform angle and platform depth) and flake mass from the Early Pleistocene assemblages were collected by LL and JSR following the protocols described above. Flake platform attributes and flake mass from RDM were collected by different individuals (including SPM) over several years as a part of the analysis of that site. All of these basic attributes were collected following the same protocols as described above to minimize the measurement error (Debénath and Dibble, 2015).

Table 4-1 Summary of flakes with bulb angle measured from the 13 archaeological localities in chronological order from young to old

Industry	Geological Mbr/ Time period	Locality (site) name	N
Levallois	Middle Paleolithic	RDM (Layers 9-7)	22
Acheulean	Upper Okote and Chari (1.48-1.38 Ma)	FxJj 37	58
		FxJj 63	47
		FxJj 65	33
Karari	Lower Okote (1.56-1.48 Ma)	FxJj 16	25
		FxJj 18 IH	46
		FxJj 20E	85
		FxJj 50	21
Oldowan	KBS (1.87 – 1.56 Ma)	FxJj 1	24
		FxJj 3	5
		FxJj 10	39
		FxJj 82	25
	Upper Burgi (1.98-1.87 Ma)	FwJj 20	78

2.3 Statistical comparison

The archaeological data are analyzed in three steps. First, we summarize the overall bulb angle distribution across the four chronological groups. We use one-way ANOVA to examine whether there is a significant difference in bulb angle between

the three Early Pleistocene groups. We then conduct a post hoc Tukey test to find how bulb angle differs between the different technological groups.

Second, we examine the relationship between bulb angle and the basic flake attributes – exterior platform angle and platform depth using ordinary least squares linear regression. We use bulb angle as the response variable and exterior platform and platform depth as the independent variables in the linear regression model (formula: bulb angle ~ exterior platform angle + platform depth). If the early hominins systematically varied the angle of blow based on exterior platform angle and/or platform depth to achieve different flaking outcomes, we should expect to find that either one or both of these two variables can predict bulb angle. That is, results from the linear models should return small (< 0.05) *p* values for the relationships between bulb angle and exterior platform angle and/or platform depth. We identify influential cases using Cook's distance and find no significant difference between models using all data and models with the influential cases excluded. To more clearly present the pattern of platform depth and bulb angle relationship, we use a boxplot to display the average bulb angle by intervals of platform depth.

Third, we use one-way ANOVA tests to compare the difference in flake mass by intervals of bulb angle. Grouping flakes by intervals of bulb angle allows us to examine how mass varies within particular bulb angle intervals. All data analyses in this study are conducted in R version 4.1.1 (R Core Team, 2020).

3 Results

For the same raw material, a small bulb angle indicates that an oblique angle of blow was used to remove the flake. On the other hand, a big bulb angle indicates that a direct angle of blow was used to remove the flake (Fig.4-4) (Li et al., Under Review).

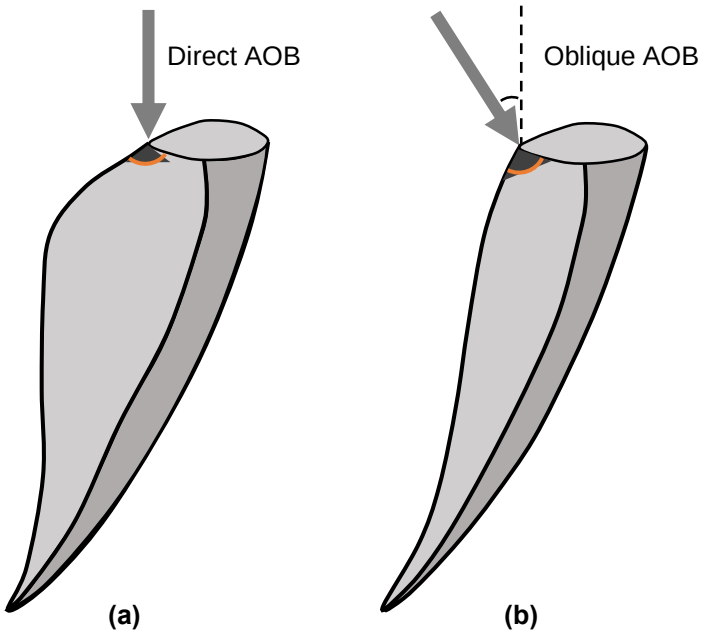

Fig. 4-4 Profile view of the flake made from different angles of blow, bulb angle is marked by the orange arc and the Hertzian cone is represented by the dark grey triangle. (a) Shows the case when the flake is made with a direct angle of blow and has a big bulb angle, (b) shows the case when the flake is made with an oblique angle of blow and has a small bulb angle

3.1 The Early Pleistocene assemblages

Fig.4-5 shows the bulb angle distribution of the Early Pleistocene assemblages grouped by technology (see also Table 4-2). Comparisons between Early Pleistocene industries show significant differences in bulb angle (ANOVA, F statistic = 9.744, $p < 0.001$). A post hoc Tukey test shows that the average bulb angle is the lowest for flakes from the Karari assemblages and it is also significantly different from the average bulb angle from the Oldowan and the Acheulean assemblages. Compared to the Karari and Acheulean assemblages, flakes from the Oldowan assemblages have the highest variance for bulb angle (Table 4-2).

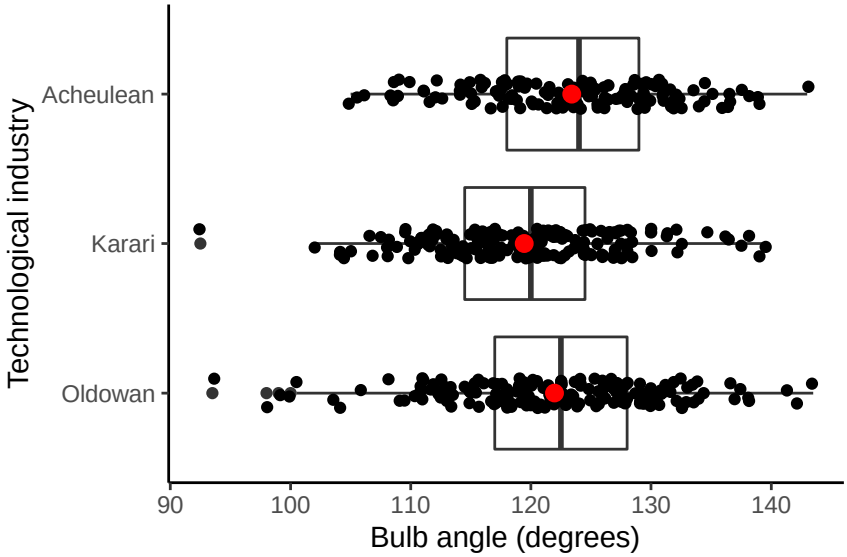

Fig. 4-5 Boxplot showing the bulb angle distribution of the four Early Pleistocene groups, the red dot in each boxplot indicates the average bulb angle. The groups on the y axis are in chronological order from young to old (top to bottom)

Table 4-2 Summary statistics of the bulb angle distribution for the Early Pleistocene dataset

	Bulb angle (degrees)			
Industry	**Mean**	**SD**	**Variance**	**N**
Oldowan	122.0	8.7	75.3	171
Karari	119.4	7.7	59.0	177
Acheulean	123.4	7.9	62.9	138

Results of the linear regression models show that there is a significant positive correlation between bulb angle and both exterior platform angle and platform depth for flakes from the Acheulean assemblages (R^2 = 0.15, *p[PD] < 0.001*, *p[EPA] = 0.015*, Fig. 4-6). For flakes from the Karari assemblages, there is a significant relationship between bulb angle and platform depth only (R^2 = 0.06, *p[PD] = 0.014*, *p[EPA] = 0.29*, Fig. 4-6). For flakes from the Oldowan assemblages, there is not a significant relationship between bulb angle and either exterior platform angle or platform depth (Fig.4-6).

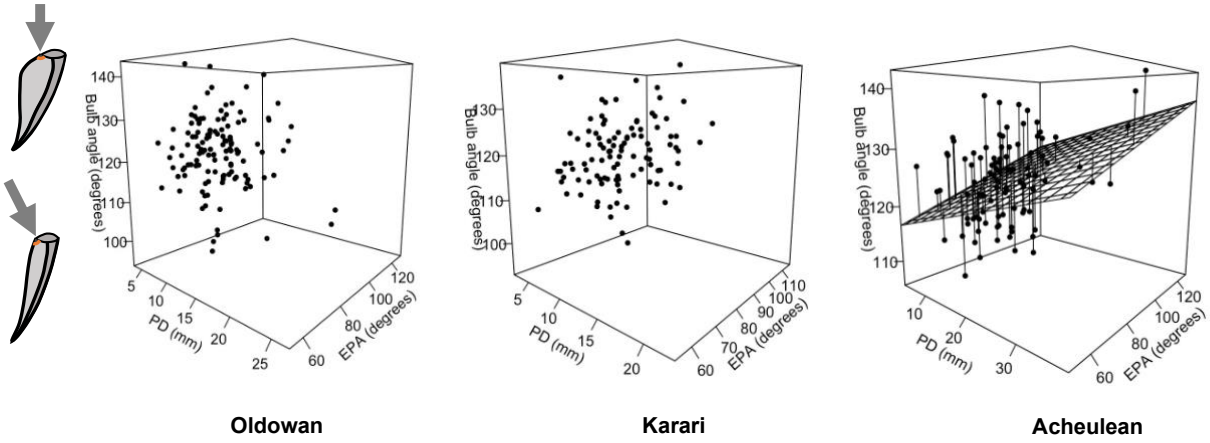

Fig. 4-6 3D scatterplots of the regression results using exterior platform angle (EPA) and platform depth (PD) to predict bulb angle for flakes from Early Pleistocene assemblages grouped by technological industry. The regression plane for flakes from the Acheulean assemblages is displayed

We also examine the relationship between bulb angle and platform depth alone. Results of the linear regression models show that there is a significant positive relationship between bulb angle and platform depth for flakes from the Karari ($R^2 = 0.13$, $p < 0.001$) and the Acheulean ($R^2 = 0.06$, $p = 0.002$) assemblages (Fig.4-7). This platform depth and bulb angle relationship indicates that smaller platform depths are associated with more oblique angles of blow and bigger platform depths are associated with more direct angles of blow. We further use 15 mm as the upper cutoff to standardize platform depth across the three Early Pleistocene groups. The relationship between platform depth and bulb angle remains significant for flakes from the Karari ($R^2 = 0.06$, $p = 0.003$) and the Acheulean assemblages ($R^2 = 0.08$, $p = 0.007$, see also Fig.Appx-III.2 in Appendix II).

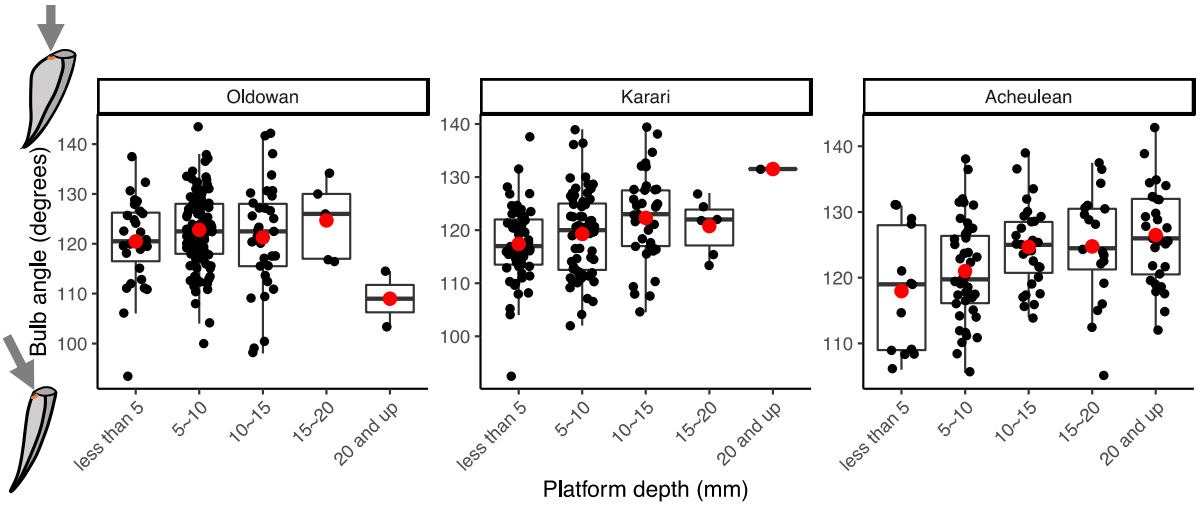

Fig. 4-7 Boxplots of the relationship between platform depth and bulb angle for flakes from the Early Pleistocene assemblages. The red dot represents the average bulb angle within each platform depth interval

Comparisons between the bulb angle intervals show significant differences in mass for flakes from the Oldowan (ANOVA, F statistic = 2.94, $p = 0.015$), Karari (ANOVA, F statistic = 8.71, $p < 0.001$), and Acheulean (ANOVA, F statistic = 4.69, $p < 0.001$) assemblages. Both the average and the range of variation of flake mass increases with bulb angle for flakes from the Acheulean and Karari assemblages but this is not the case for flakes from the Oldowan assemblages (Fig.4-8). That is, for the Acheulean and Karari assemblages, the more oblique angles of blow are mostly associated with lighter flakes and the range of flake mass significantly increases with more direct angles of blow. Using 100 g as the upper cutoff value to standardize flake mass, we still observe the same significant relationship between bulb angle and flake mass on flakes from the Karari (ANOVA, F statistic = 6.81, $p < 0.001$) and Acheulean (ANOVA, F statistic = 4.85, $p < 0.001$) assemblages (see also Fig.Appx-III.3 in Appendix II).

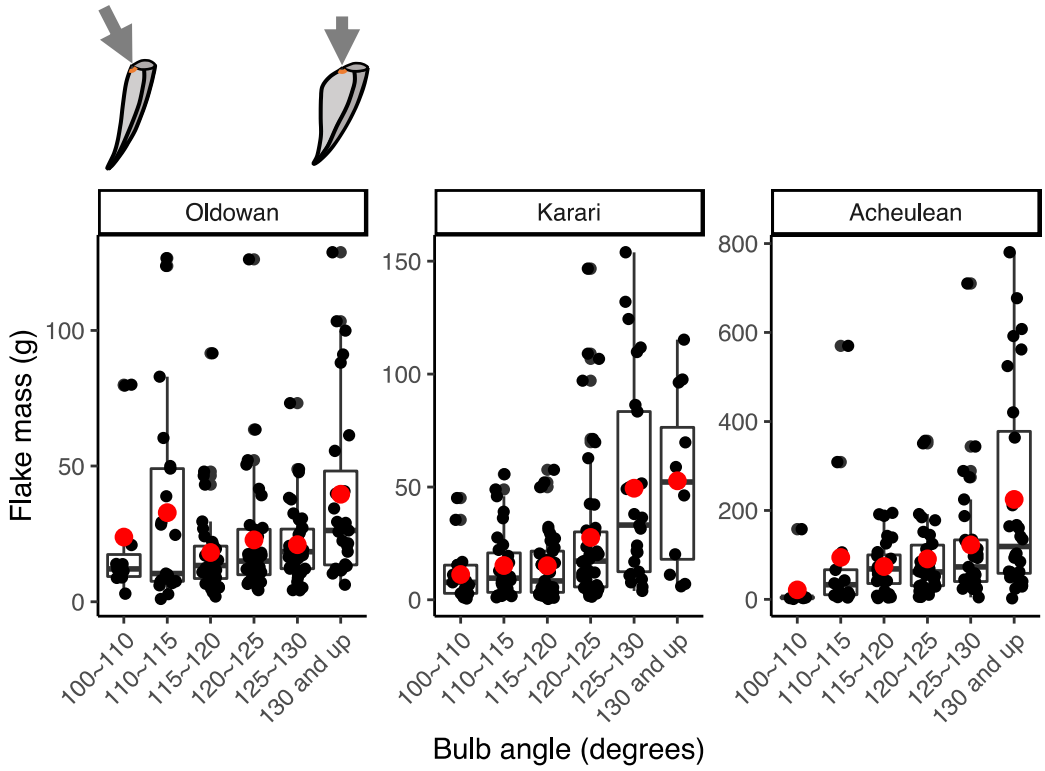

Fig. 4-8 Boxplots of the relationship between bulb angle and flake mass for flakes from the Early Pleistocene assemblages grouped by the technological industry. The red dot represents the average flake mass within each bulb angle interval

3.2 Roc de Marsal

For the RDM dataset, we observe a similar relationship between platform depth and bulb angle. There is a significant relationship platform depth and bulb angle (R^2 = 0.06, *p = 0.01*, Fig.4-9). Similar to what is observed on flakes from the Karari and Acheulean assemblages, bulb angle increases with platform depth, indicating that the angle of blow becomes more direct as platform depth increases.

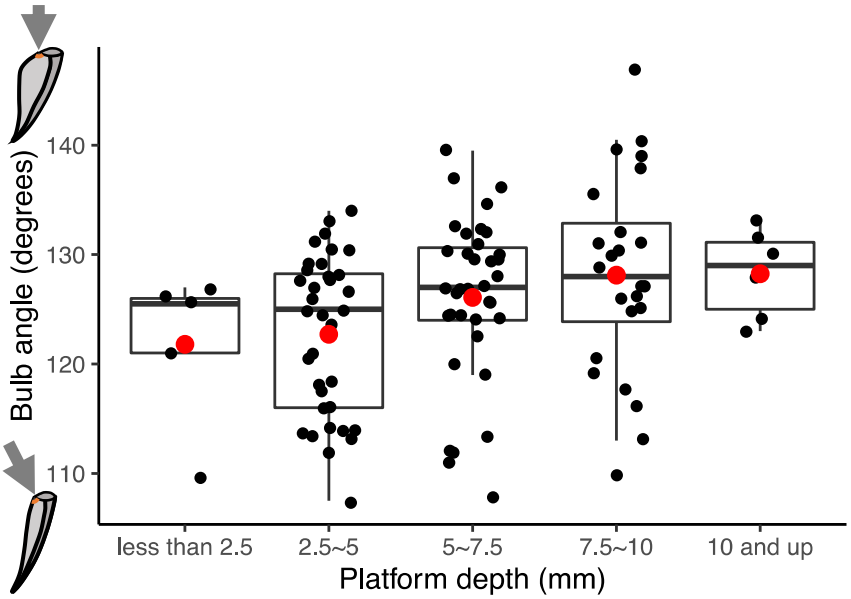

Fig. 4-9 Boxplot of the relationship between platform depth and bulb angle for flakes from RDM. The average bulb angle within each platform depth interval is represented by the red dot

4 Discussion

Measuring bulb angle from archaeological flakes allows us to systematically quantify and reconstruct hominins' control over the angle of blow. The results presented in this study support our first proposed scenario that early hominins developed a more comprehensive understanding of the effect of the angle of blow in flaking through time. This progressive change in early hominins' control over the angle of blow is reflected in the increasingly significant relationship between bulb angle and exterior platform angle and platform depth towards the Oldowan-Acheulean transition. In addition, the high variance in bulb angle on flakes from the Oldowan assemblages (1.98-1.56 Ma) indicates that compared to the Karari (1.56-1.48 Ma) and Acheulean (1.48-1.38 Ma) hominins, the Oldowan hominins used a more spread-out range of angles of blow during knapping (Table 4-2), likely due to their lack of overall control of the angle of blow.

The most significant pattern we discover from the Early Pleistocene dataset is the diachronic change in the relationship between platform depth and bulb angle. For flakes from the Oldowan assemblages, we find no significant relationship between

platform depth and the angle of blow. We start to observe a significant platform depth and angle of blow relationship for flakes from the Karari assemblages and this relationship becomes stronger for flakes from the younger Acheulean assemblages. The Karari and especially Acheulean hominins preferred to use a more oblique angle of blow to remove flakes with a small platform depth and to use a more direct angle of blow to remove flakes with a big platform depth. Moreover, the Acheulean hominins have also started to adjust their angle of blow according to exterior platform angle in addition to platform depth. In other words, the Acheulean hominins had a preference for using a direct angle of blow to remove flakes with both a big platform depth and a big exterior platform angle.

The relationship between bulb angle and flake mass suggests that the Acheulean and Karari hominins chose to mostly use an oblique angle of blow to make smaller flakes and expanded the range of flake size when using a direct angle of blow. They especially preferred to use a direct angle of blow to make the very large flakes. The bulb angle and flake mass relationship can be explained by two reasons. First, the bulb angle and flake mass relationship in part reflects the relationship between platform depth and bulb angle. Put simply, as increasing platform depth (also exterior platform angle) will cause flake size to increase while keeping other variables unchanged (Dibble and Pelcin, 1995; Dibble and Rezek, 2009; Dibble and Whittaker, 1981), the wider range of platform depth associated with the more direct angles of blow will inevitably result in flakes with a much wider size range, as well as a greater average mass. Second, the bulb angle and flake mass relationship to some extent demonstrates the mechanics of the angle of blow in flake formation. It has been shown that a more direct angle of blow will produce flakes that are larger in both their linear dimensions and mass when exterior platform angle and platform depth are held at a constant (Dibble and Rezek, 2009; Magnani et al., 2014).

However, the bulb angle and flake mass relationship reflects more than just the mechanics of platform depth and the angle of blow in flaking. Bulb angle is an indicator for the angle of blow, however, it is not affected by either platform depth or exterior platform angle, in other words these variables can vary independently and represent choices or capacities of ancient knappers (Li et al., Under Review). The bulb angle and platform depth relationship observed in the Acheulean and Karari

assemblages hence reflects a particular knapping strategy carried out by the early hominins rather than the basic mechanics of flaking. Early hominins understood the effect of both platform depth and the angle of blow in flaking and purposely adjusted them to achieve their desired outcomes. Namely, these knappers knew that by hitting further into the platform they could make a bigger flake because of the large platform depth, and by hitting at a more direct angle they could maximize the size of the flake with the chosen platform depth.

We note that compared to the Oldowan and Karari assemblages, flakes from the Acheulean assemblages have a much wider range of variation in platform depth and flake mass, which might be partially driven by large flake exploitation of the Acheulean industry (Sharon, 2010). After standardizing platform depth and flake mass across all three Early Pleistocene industries, we still observe the same significant bulb angle and platform depth/ flake mass relationships. This suggests that the Acheulean hominins' preference for using a more direct angle of blow to make a bigger flake is not just driven by a few extreme cases in the dataset.

The Middle Paleolithic RDM assemblage is used as a point of comparison for us to interpret our observations of the changes in the knapping strategies carried out by the Early Pleistocene hominins. We find that early hominins began to adjust their angles of blow according to platform depth and exterior platform angle towards the Oldowan-Acheulean transition. Neandertals from RDM were also adjusting their angles of blow according to platform depth and exterior platform angle. The Neandertals at RDM had a preference to use more direct angles of blow when making flakes with a big platform depth and a small exterior platform angle. The similarities between the Acheulean and Karari hominins' and Neandertal' control over the angle of blow suggest the possibility that early hominins from these two Early Pleistocene industries might understand the role of the angle of blow in flaking to some degree that is comparable to the Neandertals, who were more competent knappers.

We acknowledge the caveat that the range of variation in bulb angle is dependent on the mechanical properties of the raw material (Olivi-Tran et al., 2020). However, in this study we controlled for the raw material type within the two datasets: only basalt flakes were included in the Early Pleistocene dataset and only

flint flakes were included in the RDM dataset. This allows us to conduct reliable intra-dataset comparisons of the relationships between bulb angle and other flake attributes.

The Oldowan-Acheulean transition encompasses changes in many aspects of hominins' lifeways such as stone tool production and use, dietary breadth, and geographical occupation, as well as possible changes of hominin species (Braun and Harris, 2003; de la Torre et al., 2012; McHenry and de la Torre, 2018; Presnyakova, 2019; Semaw et al., 2009; Ungar et al., 2006; Uno et al., 2018). From a technological point of view, many differences (some rather substantial) are observed in knapping technique, reduction sequence, and raw material selection (Braun and Harris, 2003; De la Torre, 2016; Semaw et al., 2009). From a cognitive point of view, many argue that the Acheulean tool makers are more cognitively advanced compared to their predecessors (De la Torre, 2016; Semaw et al., 2009; Stout et al., 2011, 2015; Toth and Schick, 2018). Our results show that compared to the Oldowan and the Karari hominins, the Acheulean hominins appeared to exert a more systematic control over the angle of blow together with exterior platform angle and platform depth. This gradual change in the relationship between the angle of blow and basic flake attributes (i.e., exterior platform angle, platform depth, and flake mass) from the Oldowan (via the Karari) to the Acheulean assemblages provides new evidence that can contribute to the discussion of the Oldowan-Acheulean transition from both a cognitive and technological perspective (De la Torre, 2016; Semaw et al., 2009).

The change in early hominins' control over the angle of blow observed in our study shows that Acheulean hominins had a rather good understanding of the effect of the angle of blow in flaking. They implemented a systematic control over the angle of blow by adjusting how they struck the platform based on the size of exterior platform angle and where they wanted to strike it (i.e., platform depth). The similarities of the bulb angle and EPA-PD relationships between the Acheulean assemblages and RDM further indicate that the Acheulean hominins understood the role of the angle of blow in flaking to a degree that is comparable to Neandertals, who are often considered more competent prehistoric knappers. Although Oldowan hominins understood the basic fracture mechanics of flaking such as the role of exterior platform angle and platform depth (Gallotti, 2018; Nonaka et al., 2010), they

might not have had a good understanding of other important knapping variables such as the angle of blow. The lack of a significant pattern between bulb angle and other basic flake attributes suggests that Oldowan hominins either did not care about controlling the angle of blow, or they could not implement a more precise control over the variable due to possible physical or cognitive constraints (Stout et al., 2015; Tocheri et al., 2007).

5 Conclusions

In this study, we discover evidence showing that some early hominins might not only understand the role of the angle of blow in flaking but also started to strategically adjust their striking angle towards the Oldowan-Acheulean transition. Using bulb angle as a proxy, we are able to systematically reconstruct the angle blow – a previously archaeologically invisible variable – from the lithic record. Our results indicate that early hominins from the Acheulean favored a more direct angle of blow for making bigger flakes and started to develop a more comprehensive understanding of the effect of the angle of blow, exterior platform angle, and platform depth in flaking to an extent that is comparable to Neandertals. The Early Pleistocene assemblages in our study spread across several hundred thousand years. Our findings of the changes in early hominins' control over the angle of blow during this time period share some temporal overlap with and might even be related to some of the major shifts in hominins' lifeways that happened during the Oldowan-Acheulean transition (Braun and Harris, 2003; de la Torre et al., 2012; McHenry and de la Torre, 2018; Presnyakova, 2019; Semaw et al., 2009; Ungar et al., 2006; Uno et al., 2018). Reconstructing hominins' knapping actions from measurable attributes on the stone artifacts not only allows us to quantify their technical decisions but also is a first step to investigate the evolution of hominins' technical capabilities through time from the archaeological record.

Acknowledgments

LL was awarded a research grant from the Leakey Foundation to complete the field research in this study. LL is funded by European Research Council (ERC)

under European Union’s Horizon 2020 research and innovation programme (grant agreement No.567 714658, STONECULT project). The excavations at Roc de Marsal received financial support from the US National Science Foundation (Grants #0917739 and #0551927), the Leakey Foundation, and the University of Pennsylvania Research Foundation. We thank Claudio Tennie for his helpful comments on the manuscript. We thank the Nairobi National Museum for granting LL permission to analyze the Early Pleistocene assemblages in this study. We thank Sylvia Wemanya for her generous help to LL’s data collection at the Nairobi National Museum.

CHAPTER 5 General discussion

1 Summary of findings

The early stone tools have remained mysterious ever since their discovery. The mysteries surrounding these stone tools are being uncovered one by one (e.g., Braun, 2012; Braun and Hovers, 2009; Carvalho and McGrew, 2012; Panger et al., 2019; Plummer, 2004; Schick and Toth, 1994; Semaw et al., 2009; Stout et al., 2019; Toth and Schick, 2018, 2019). This thesis aims to fulfill a small part of this effort by investigating the evolution of early hominins' knapping strategies using an experimental approach.

The research in this thesis is carried out in three phases, with each phase being a publishable scientific article. The first phase (paper one) is an effort to review and synthesize what we have learned from previous controlled flaking experiments, and to discuss future directions. The second phase (paper two) is a controlled experiment to find solutions that allow us to measure the angle of blow from tangible flake attributes. The last phase (paper three) is investigating how early hominins managed their angles of blow from the archaeological record using the method developed in phase two. Here I will briefly review key findings from each phase of the thesis.

1.1 The EPA-PD flake formation model

Previous controlled flaking experiments have greatly informed us about the mechanics of flake formation from the knapper's perspective. We now have a better quantitative measure of how variables such as platform and core surface morphology, hammer size and material, hammer strike angle, and hammer strike position impact flake size and shape. Among these variables, two have been repeatedly found to have the most significant influence – exterior platform angle and platform depth. As a result of the significant effect of exterior platform angle and platform depth, a flake formation model (the EPA-PD model) is derived from the experimental results. In essence, the EPA-PD model uses exterior platform angle and platform depth to predict flake size.

Several studies have shown that both modern and prehistoric knappers understand the role of exterior platform angle and platform depth in flaking and manipulate them to achieve different flaking outcomes (Braun et al., 2019; Dibble, 1997; Dogandžić et al., 2015; Lin et al., 2013, 2015; Nonaka et al., 2010). Although the EPA-PD model has been applied to interpret several experimental and archaeological assemblages (Braun et al., 2019; Dogandžić et al., 2020, 2015; Lin et al., 2015; Režek et al., 2018), it only explains a portion of the flake variability. Any changes made to variables such as platform and core surface morphology, hammer material, and force application location that alter the "standard" experimental setting will cause the EPA-PD model's performance to decline (Leader et al., 2017; Magnani et al., 2014; McPherron et al., 2020; Rezek et al., 2011). The addition of the angle of blow (AOB) can significantly improve EPA-PD model's explanatory power. However, this updated EPA-PD-AOB model has only been applied to a few experimental assemblages because of the difficulty in obtaining the angle of blow from archaeological flakes. Next, I will discuss results from the controlled experiment conducted in this thesis that allow us to reconstruct the angle of blow from measurable flake attributes.

1.2 Reconstructing the angle of blow from flake attributes

The angle of blow is an important force delivery variable in knapping. Several experimental studies have shown that varying the angle of blow will cause changes in both flake size and its bulb of percussion (Dibble and Rezek, 2009; Magnani et al, 2014; Speth, 1972). More specifically, as the angle of blow becomes more oblique relative to the platform, the flakes will be smaller (Dibble and Rezek, 2009; Hellweg, 1984; Magnani et al., 2014; Speth, 1972, 1975), and have a less prominent bulb of percussion (Soriano et al., 2007; Speth, 1972). Despite its significant effect on flake formation and its direct connection to knapping strategies, the angle of blow has not been included much in lithic studies owing to the difficulty in measuring it on the artifacts. In this thesis, I conducted a controlled flaking experiment (the drop tower experiment) guided by fracture mechanics theory to reconstruct the angle of blow from measurable flake attributes.

Fracture mechanics studies show that the Hertzian cone is tilted by an oblique angle of blow. That is, as the hammer strikes towards the platform surface, the Hertzian

cone pivots into the flake (Fig.5-1). The change in the Hertzian cone's orientation can be recorded by bulb angle, which is the angle between the protruding side of the Hertzian cone on a flake's interior surface and its platform (Fig.5-1). When hitting the platform with an oblique angle of blow, bulb angle will decrease as a result of the Hertzian cone being tilted towards the platform. Results from the drop tower experiment show that there is a significant relationship between the angle of blow and bulb angle. More specifically, the bulb angle on a flake decreases as the angle of blow increases or becomes more oblique. This result is then further validated in two additional experimental datasets, proving that bulb angle can be used as a reliable proxy for the angle of blow.

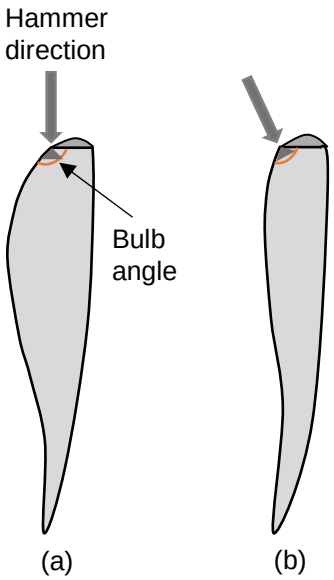

Fig. 5-1 Illustration of bulb angle from a flake's profile view, the dark grey triangle represents the Hertzian cone, and the orange arc marks the bulb angle. (a) Shows when the hammer strike is direct, (b) shows when the hammer strikes the platform at an angle

1.3 Investigating early hominins' control over the angle of blow from the archaeological record

We already have a good understanding of early hominins' knapping strategies from different aspects such as raw material and hammer selection, platform preparation, and reduction sequences (Braun et al., 2008b, 2009b; Delagnes and Roche, 2005;

Roche et al., 1999). The newly developed method to measure the angle of blow allows us to further advance our understanding of early hominins' knapping behaviors. The overarching goal of this thesis is to connect the traditionally invisible aspects of stone tool production, namely, the angle of blow, to tangible lithic attributes to explore the technical decisions made by early hominins. I want to answer the question of whether and how early hominins controlled their angles of blow to produce the artifacts we see in the archaeological record and whether there is a change in their control over the angles of blow through time.

Drawing on data from 12 Early Pleistocene assemblages, I am able to systematically reconstruct the angle of blow used by the Early Pleistocene hominins and integrate them into the analysis of the hominins' knapping strategies with other flake attributes such as exterior platform angle and platform depth. I find that early hominins began to adjust their angle of blow with platform depth (and exterior platform angle) to make flakes of different sizes towards the Oldowan-Acheulean transition. In particular, when making flakes with large platform depths, the Acheulean hominins preferred to use a direct angle of blow.

To summarize, evidence from the Early Pleistocene lithic record indicates that early hominins started to gain more understanding of the angle of blow as well as other basic flake attributes such as platform depth towards the Oldowan-Acheulean transition. A Middle Paleolithic assemblage is included to help contextualize observations made from the Early Pleistocene assemblages by using Neandertals as a point of comparison. The similarities between the relationships between bulb angle and other flake attributes (e.g., platform depth and exterior platform angle) suggest the possibility that early hominins towards the Oldowan-Acheulean transition might have understood the mechanics of the angle of blow in flaking to an extent that is comparable to Neandertals, who are competent knappers.

2 Implications for the evolution of hominin behavior

Whether early stone tools (such as the Oldowan and Acheulean) can be viewed as a representation of what delineates human culture from non-human culture is a hotly debated topic. Here human culture refers to a form of cumulative culture, in which

individuals are capable of learning and producing artifacts by accumulating modification and innovation over generations (Dean et al., 2014; Tennie et al., 2009, 2016). No consensus has been achieved on when cumulative culture appeared in the trajectory of human evolution (Stout et al., 2019; Tennie et al., 2016, 2017). Some argue that early hominins were already producing stone tools under the learning mechanisms similar to that of modern humans (Morgan et al., 2015; Stout et al., 2019), while others argue that early stone artifacts are more likely products of individual learning of the hominins, which is similar to the learning mechanisms of extant non-human primates (Tennie et al., 2016, 2017). One way to address this debate is to move beyond the traditional technological approach that focuses on studying the reduction sequences of flake removals and turn to examine the manual gestures of force delivery during knapping (e.g., the angle of blow).

Knapping is a motor skill that involves complex interactions of different body parts (Biryukova and Bril, 2008; Bril et al., 2010; Geribàs et al., 2010; Nonaka et al., 2010; Rein et al., 2013; Susman, 1998; Williams et al., 2012). To achieve their desired flaking outcome, knappers not only need to understand the mechanics of different knapping variables but also need to coordinate their body parts so they can knap using the most effective gesture. Although we know that skilled knappers such as *Homo sapiens* (including modern knappers) and Neandertals systematically control different flake attributes such as exterior platform angle and platform depth when making flakes (Dibble, 1997; Lin et al., 2015; Nonaka et al., 2010; Režek et al., 2018), how these attributes are transformed into specific knapping actions such as the angle of blow or hammer velocity is yet to be explored.

The controlled experimental approach used in this thesis provides a platform to directly link knapping actions (e.g., the angle of blow) to measurable flake attributes based on the basic fracture mechanics of flake formation. Furthermore, results from the experiments allow us to study manual gestures of knapping from the archaeological record that can provide new pieces of evidence for evaluating the role of flaking mechanics and individual choices of knapping strategies that underlie decisions made by the prehistoric knappers. Investigating changes in hominins' knapping strategies through time can provide insight into understanding the evolution of the learning mechanisms of stone tool production and help clarify the debate over the emergence of cumulative culture in human history.

3 Limitations

A replicative knapping approach with modern knappers is not sufficient for reconstructing features of force delivery during knapping due to the fundamental differences in wrist morphology between early hominins and *Homo sapiens* (Tocheri et al., 2007). A controlled flaking experimental approach, on the other hand, which can examine the effect of individual knapping variables in flaking (Dibble and Rezek, 2009; Dibble and Whittaker, 1981), sometimes lacks a connection between the basic flaking mechanics and the actual knapping actions that generate the observed variation in lithic assemblages. In other words, how to transform results from the controlled flaking experiments into a meaningful interpretation of hominins' knapping behaviors remains a challenging job.

The drop tower and plate glass setup used in this thesis has the advantage of isolating and controlling different knapping variables and a fast turnaround for completing the experiments. However, the setup also has its limitations in its use of the experimental material and artificial mechanics for flake removal. For example, while the plate glass is convenient for being cut into different shapes, the thickness of the glass confines the flake width that can be produced. The size of the steel ball bearings to be used as hammers is also restricted in that too small a hammer cannot generate enough force to remove a flake and too big a hammer will crush the core.

Besides the general experimental setup, we should also recognize the limitations of the experimental results. First, despite the drop tower experiment in this thesis having shown that bulb angle can be used to estimate the angle of blow, how sensitive bulb angle is to changes in the angle of blow needs further investigation. Second, we have yet to investigate the effect of raw material properties and hammer material and shape on bulb angle as these variables may introduce additional complications to our interpretation of the bulb angle and angle of blow relationship. Third, although bulb angle allows us to measure angle of blow from archaeological flakes, we still do not have a clear expectation of how or why the angle of blow should vary in a lithic assemblage due to our lack of knowledge of the Hertzian cone angle of different raw materials. At a more fundamental level, we do not yet know exactly what are the factors that drive changes in the angle of blow carried out by

hominins. In other words, more attention needs to be paid to the reasons behind hominins' manipulation of the angle of blow, or the goals that they wanted to reach via adjusting their angle of blow. We also need to study the relationships between bulb angle and other flake attributes on more archaeological flakes.

While the EPA-PD model (or the EPA-PD relationship) can explain the range of variation in flake formation to some degree (Braun et al., 2019; Dogandžić et al., 2015; Lin et al., 2015, 2013; McPherron et al., 2020; Režek et al., 2018), it is highly susceptible to changes that are made to variables such as hammer material and core morphology (Leader et al., 2017; Li et al., Under Review; Magnani et al., 2014; McPherron et al., 2020; Rezek et al., 2011). There is an urgent need for a more generalized flake formation model that can be effectively applied under a less controlled setting to interpret flake variation in archaeological assemblages.

4 Conclusions

Reconstructing hominins' technical capabilities from the archaeological record is an important path to understanding their tool behavior. Stone artifacts are an important piece of evidence for studying hominin behavior and cognition. Among the various methods that archaeologists have explored to study the stone tool record, controlled experimentation plays an important role as it offers a platform to systematically generate and test hypotheses about past knappers' behaviors under a controlled and reproducible setting. In this thesis, I use an experimental approach to reconstruct an invisible knapping variable, namely the angle of blow, from the Early Pleistocene archaeological record. Results show that early hominins started to develop an understanding of the role of the angle of blow together with other flake attributes (e.g., exterior platform angle and platform depth) in flaking towards the Oldowan-Acheulean transition.

Chapter 2 reviews what we have learned from previous controlled flaking mechanics conducted by Harold Dibble (the Dibble experiments) and colleagues and synthesizes models of flake formation. The Dibble experiments have investigated a number of flaking variables including platform and core surface morphology, hammer material, hammer size and shape, hammer strike angle and location, and raw

material properties. Results of these studies highlight the dominant effect of exterior platform angle and platform depth: while other tested variables all have an influence on the flake size and shape, exterior platform angle and platform depth often overshadow their effect (Dibble and Rezek, 2009; Dogandžić et al., 2020; Leader et al., 2017; Magnani et al., 2014; Rezek et al., 2011). Results from the Dibble experiments also lead to the creation of a flake formation model, namely the EPA-PD model, which uses exterior platform angle and platform depth to predict flake size in the form of mass (Li et al., Under Review, Under Reviewa; McPherron et al., 2020). The EPA-PD model, however, can only explain a portion of flake variability in lithic assemblages. The work from paper two (Chapter 3) now allows us to add another important flaking variable – the angle of blow, to the EPA-PD model, which can greatly improve the model's performance in predicting flake size.

Chapter 3 investigates the effect of the angle of blow using a controlled experimental approach. As discussed in Chapter 2, the angle of blow is an important force delivery variable in knapping that has a significant impact on flake formation, it can also significantly improve the current EPA-PD model. However, the angle of blow has been largely overlooked in many lithic studies because of the difficulty in measuring it on actual artifacts. Drawing on knowledge from fracture mechanics, Chapter 3 sets out to quantify the effect of the angle of blow on measurable flake attributes. Results of drop tower experiment conducted in Chapter 3 show that for the first time, the angle of blow can be estimated from a tangible flake attribute called the bulb angle.

In Chapter 4, I (and collaborators) reconstruct the angle of blow from selected Early Pleistocene assemblages using the method developed in Chapter 3. Our goal is to track whether and how early hominins changed their control over the angle of blow towards the Oldowan-Acheulean transition. We find that early hominins started to show more understanding and control of the angle of blow together with key platform preparation variables (i.e., platform depth and exterior platform angle). In particular, hominins from the later Early Pleistocene assemblages are found to strategically adjust their angles of blow according to platform depth (and exterior platform angle) to make flakes of different sizes.

5 Outlook

As discussed in Chapter 2, controlled flaking experiments have long been critiqued for their artificial setup. Great effort has been done to improve the external validity of the controlled experiments so that the experimental results can be better applied to interpret the archaeological record (Dibble and Pelcin, 1995; Dibble and Rezek, 2009; Dibble and Whittaker, 1981; Dogandžić et al., 2020). It is important to keep in mind that the experimental design and hypothesis formulation should focus on establishing testable causal relationships between the knapper-controlled variables and different flake attributes. In essence, controlled flaking experiments should work to quantify knapping behaviors into measurable flake attributes, which will not only help us better understand the underlying mechanics of different knapping variables but also allow us to reconstruct hominins' knapping actions from the stone artifacts. I will discuss several future lines of research using the controlled experimental approach that I plan to pursue hereafter.

First, as a continuation of the experimental work from this thesis (Chapter 3), the effect of the angle of blow in flaking requires further investigation. Fracture mechanics studies show that the minimum stress required to initiate a crack on the surface of brittle solids is related to the angle of blow. That is, less stress is required for crack initiation with an oblique angle of blow (Suh et al., 2006). However, this has yet to be tested under a controlled flaking setup. The drop tower setup is well equipped to test whether the angle of blow has an impact on the minimum stress required to remove a flake of a certain exterior platform angle and platform depth. Understanding the effect of the angle of blow in flake initiation allows us to interpret hominins' knapping strategies from the perspective of energy conservation.

Second, it is imperative to understand the role of striking force in flaking. Striking force is an important knapping variable that reflects the biomechanics of hominins' arm swing. There is no consensus on how striking force plays a role in flake formation largely owing to the difficulty in controlling this variable in the current experimental setup (Chapter 2). Up to now, striking force has not been studied as an independent variable, it has only been studied in association with flake size in the previous controlled flaking experiments (Dibble and Rezek, 2009; Dogandžić et al., 2020; Mraz et al., 2019). Although we know the general concept that more force is

required to remove a larger flake, the individual effect of striking force is actually not well understood (Dibble and Pelcin, 1995; Dibble and Rezek, 2009; Dogandžić et al., 2020; Mraz et al., 2019). It remains to be examined whether the application of excessive force in addition to what is minimally required to remove a flake with fixed exterior platform angle and platform depth will make any change to the flake form. At a fundamental level, it is necessary to clarify the muddled use of force-related terms such as energy, momentum, load, and pressure in the description of the flake formation process. These terms refer to different mechanics and should not be used interchangeably. Furthermore, understanding the difference between these force terms will greatly benefit the current experimental design to allow testing striking force as an independent variable in the form of hammer mass and/or velocity.

Third, hammer size is another variable that has not been thoroughly investigated in the previous experimental studies. The effect of hammer size has been tested in a few experimental studies and is found to have no significant impact on flake form (Magnani et al., 2014; Pelcin, 1996). Pelcin (1996) showed a possible correlation between hammer radius (for spherical hammers only) and platform ring crack diameter, which is the diameter of the contact area between the hammer and the core platform. However, this relationship between hammer radius and platform ring crack diameter is also affected by the angle of blow and has not been followed up in later studies. I see the importance of systematically examining the effect of hammer radius on platform ring crack diameter. The results have the potential of allowing us to estimate hammer size from measurable flake attributes, which will further our understanding of hominins' knapping behavior from the perspective of hammer selection.

Fourth, results from the controlled experiments up to now have only been applied to a limited number of archaeological assemblages (Braun et al., 2019; Dogandžić et al., 2020; Lin et al., 2013; Režek et al., 2018). With the new discoveries from this thesis, there is an urgent need to extend the application of what we have learned from the controlled experiments to a much bigger pool of archaeological assemblages. Once this is done, we will be able to conduct systematic comparisons of the technological capabilities between different groups of hominins, from both a temporal and a geographical perspective.

At last, results of all current and future experimental studies will contribute to the development of a computer program called ‘Virtual Knapper’ that simulates the production of stone tools under different scenarios from first principles (see also in Orellana Figueroa et al., 2021). The Virtual Knapper program allows unbiased and reproducible flaking experiments to be conducted in a digital environment with a fast turnaround and at an affordable price (Orellana Figueroa et al., 2021). In addition, the program also has the potential of drawing more public attention to field of lithic studies by making such controlled flaking experiments accessible.

Bibliography

Akimune, Y., 1990. Oblique impact of spherical particles onto silicon nitride. J. Am. Ceram. Soc. 73, 3607–3610.

Aldeias, V., Goldberg, P., Sandgathe, D., Berna, F., Dibble, H.L., McPherron, S.P., Turq, A., Rezek, Z., 2012. Evidence for Neandertal use of fire at Roc de Marsal (France). J. Archaeol. Sci. 39, 2414–2423.

Aliyu, M.M., Murphy, W., Lawrence, J.A., Collier, R., 2017. Engineering geological characterization of flints. Q. J. Eng. Geol. Hydrogeol. 50, 133–147.

Allen, H., 1996. Ethnography and prehistoric archaeology in Australia. J. Anthropol. Archaeol. 15, 137–159.

Amick, D.S., Mauldin, R.P., 1989. Experiments in lithic technology. British Archaeological Reports Limited.

Andrefsky Jr, W., 2004. Lithics: Macroscopic Approaches to Analysis 2nd Edition. Cambridge University Press.

Andrefsky, W., 2006. Experimental and archaeological verification of an index of retouch for hafted bifaces. Am. Antiq. 71, 743–757.

Andrefsky, W., 1994. Raw-material availability and the organization of technology. Am. Antiq. 59, 21–34.

Archer, W., Braun, D.R., Harris, J.W., McCoy, J.T., Richmond, B.G., 2014a. Early Pleistocene aquatic resource use in the Turkana Basin. J. Hum. Evol. 77, 74–87.

Archer, W., Pop, C.M., Rezek, Z., Schlager, S., Lin, S.C., Weiss, M., Dogandžić, T., Desta, D., McPherron, S.P., 2018. A geometric morphometric relationship predicts stone flake shape and size variability. Archaeol. Anthropol. Sci. 10, 1991–2003.

Ascher, R., 1961. Analogy in archaeological interpretation. Southwest. J. Anthropol. 17, 317–325.

Baena, J., Moncel, M.-H., Cuartero, F., Navarro, M.G.C., Rubio, D., 2017. Late Middle Pleistocene genesis of Neanderthal technology in Western Europe: The case of Payre site (south-east France). Quat. Int. 436, 212–238.

Baker, T., 2004. The Lithic Containers of the Archaeological Record. URL http://www.ele.net/containers/lithic_containers.htm

Baker, T., 2003. A Theory for Flake Creation, A Status Report of Research Begun April, 1997.

Bamford, M.K., 2011. Late pliocene woody vegetation of area 41, Koobi Fora, East turkana basin, Kenya. Rev. Palaeobot. Palynol. 164, 191–210.

Bargalló, A., Mosquera, M., 2014. Can hand laterality be identified through lithic technology? Laterality Asymmetries Body Brain Cogn. 19, 37–63.

Barsky, D., 2009. An overview of some African and Eurasian Oldowan sites: evaluation of hominin cognition levels, technological advancement and adaptive skills. Interdiscip. Approaches Oldowan 39–47.

Bataille, G., Conard, N.J., 2018. Blade and bladelet production at Hohle Fels Cave, AH IV in the Swabian Jura and its importance for characterizing the technological variability of the Aurignacian in Central Europe. PloS One 13, e0194097.

Biryukova, E., Bril, B., Dietrich, G., Roby-Brami, A., Kulikov, M., Molchanov, P., 2005. The organization of arm kinematic synergies : the case of stone –bead knapping in Khambhat. pp. 73–89.

Biryukova, E.V., Bril, B., 2008. Organization of goal-directed action at a high level of motor skill: The case of stone knapping in India. Motor Control 12, 181–209.

Biryukova, E.V., Roby-Brami, A., Frolov, A.A., Mokhtari, M., 2000. Kinematics of human arm reconstructed from spatial tracking system recordings. J. Biomech. 33, 985–995. https://doi.org/10.1016/S0021-9290(00)00040-3

Bjarke Ballin, T., 2014. Gunflints from Drottningen af Swerige (1745) and Concordia (1786). Arms Armour 11, 44–67.

Boëda, E., 1995. Levallois: a volumetric construction, methods, a technique, in: The Definition and Interpretation of Levallois Technology. Prehistory Press Madison, pp. 41–65.

Boëda, E., 1993. Le débitage discoïde et le débitage Levallois récurrent centripède. Bull. Société Préhistorique Fr. 90, 392–404.

Bonnichsen, R., 1977. Models for deriving cultural information from stone tools. University of Ottawa Press.

Bordes, F., 1971. Essai de préhistoire expérimentale: fabrication d'un épieu de bois. Mélanges Préhistoire D'archéocivilisation D'ethnologie Offer. À André Varagnac 69–73.

Bordes, F., 1969. The Corbiac blade technique and other experiments. Tebiwa 12, 1–22.

Bordes, F., 1953. Notules de typologie paléolithique. I. Outils moustériens à fracture volontaire. Bull. Société Préhistorique Fr. 50, 224–226.

Bordes, F., 1950. Principes dune méthode detude des techniques de débitage et de la typologie du Paleolithique ancien et moyen.

Bordes, F., Lafille, J., 1962. Paleontologie humaine - decouverte dun squelette denfant Mousterien dans le gisement du Roc de Marsal, commune de Campagne-du-Bugue (Dordogne). COMPTES RENDUS Hebd. SEANCES Acad. Sci. 254, 714.

Bradbury, A.P., Carr, P.J., 1995. Flake typologies and alternative approaches: an experimental assessment. Lithic Technol. 100–115.

Bradley, B., Sampson, C., 1986. Analysis by replication of two Acheulean artefact assemblages from Caddington, England, m, G N. Bailey and P. Callow (eds.). Stone Age Prehistory.

Braun, D., Harris, J.W., 2009. Plio-Pleistocene technological variation: a view from the KBS Mbr., Koobi Fora formation. Cut. Edge New Approaches Archaeol. Hum. Orig. Stone Age Inst. Press Gosport 17–32.

Braun, D.R., 2012. What does Oldowan technology represent in terms of hominin behavior. Stone Tools Foss. Bones Debates Archaeol. Hum. Orig. 222.

Braun, D.R., Aldeias, V., Archer, W., Arrowsmith, J.R., Baraki, N., Campisano, C.J., Deino, A.L., DiMaggio, E.N., Dupont-Nivet, G., Engda, B., 2019. Earliest known

Oldowan artifacts at> 2.58 Ma from Ledi-Geraru, Ethiopia, highlight early technological diversity. Proc. Natl. Acad. Sci. 116, 11712–11717.

Braun, D.R., Harris, J.W., 2003. Technological developments in the oldowan of koobi fora: innovatives techniques of artifact analysis. Treb. Arqueol. 117–144.

Braun, D.R., Harris, J.W., Levin, N.E., McCoy, J.T., Herries, A.I., Bamford, M.K., Bishop, L.C., Richmond, B.G., Kibunjia, M., 2010. Early hominin diet included diverse terrestrial and aquatic animals 1.95 Ma in East Turkana, Kenya. Proc. Natl. Acad. Sci. 107, 10002–10007.

Braun, D.R., Harris, J.W.K., Maina, D.N., 2009a. Oldowan Raw Material Procurement and Use: Evidence from the Koobi Fora Formation*. Archaeometry 51, 26–42. https://doi.org/10.1111/j.1475-4754.2008.00393.x

Braun, D.R., Hovers, E., 2009. Introduction: Current issues in Oldowan research. Interdiscip. Approaches Oldowan 1–14.

Braun, D.R., Plummer, T., Ditchfield, P., Ferraro, J.V., Maina, D., Bishop, L.C., Potts, R., 2008a. Oldowan behavior and raw material transport: perspectives from the Kanjera Formation. J. Archaeol. Sci. 35, 2329–2345. https://doi.org/10.1016/j.jas.2008.03.004

Braun, D.R., Plummer, T., Ferraro, J.V., Ditchfield, P., Bishop, L.C., 2009b. Raw material quality and Oldowan hominin toolstone preferences: evidence from Kanjera South, Kenya. J. Archaeol. Sci. 36, 1605–1614. https://doi.org/10.1016/j.jas.2009.03.025

Braun, D.R., Tactikos, J.C., Ferraro, J.V., Arnow, S.L., Harris, J.W., 2008b. Oldowan reduction sequences: methodological considerations. J. Archaeol. Sci. 35, 2153–2163.

Brenet, M., Bourguignon, L., Folgado, M., Ortega, I., 2009. Élaboration d'un protocole d'expérimentation lithique pour la compréhension des comportements techniques et techno-économiques au Paléolithique moyen. Nouv. Archéologie 60–64.

Bril, B., Rein, R., Nonaka, T., Wenban-Smith, F., Dietrich, G., 2010. The role of expertise in tool use: Skill differences in functional action adaptations to task constraints. J. Exp. Psychol. Hum. Percept. Perform. 36, 825–839.

Bril, B., Smaers, J., Steele, J., Rein, R., Nonaka, T., Dietrich, G., Biryukova, E., Hirata, S., Roux, V., 2012. Functional mastery of percussive technology in nut-cracking and stone-flaking actions: experimental comparison and implications for the evolution of the human brain. Philos. Trans. R. Soc. B Biol. Sci. 367, 59–74. https://doi.org/10.1098/rstb.2011.0147

Brown, Francis H., Haileab, B., McDougall, I., 2006. Sequence of tuffs between the KBS Tuff and the Chari Tuff in the Turkana Basin, Kenya and Ethiopia. J. Geol. Soc. 163, 185–204.

Brown, F. H., Haileab, B., McDougall, I., 2006. Sequence of tuffs between the KBS Tuff and the Chari Tuff in the Turkana Basin, Kenya and Ethiopia. J. Geol. Soc. 163, 185–204. https://doi.org/10.1144/0016-764904-165

Buchanan, B., Mraz, V., Eren, M.I., 2016. On identifying stone tool production techniques: an experimental and statistical assessment of pressure versus soft hammer percussion flake form. Am. Antiq. 81, 737–751.

Bunn, H., Harris, J.W., Isaac, G., Kaufulu, Z., Kroll, E., Schick, K., Toth, N., Behrensmeyer, A.K., 1980. FxJj50: an early Pleistocene site in northern Kenya. World Archaeol. 12, 109–136.

Bunn, H.T., 1997. The bone assemblages from the excavated sites. Koobi Fora Res. Proj. 5, 402–444.

Callahan, E., 1985. Experiments with Danish Mesolithic microblade technology. J. Dan. Archaeol. 4, 23–39.

Callahan, E., 1979. The basics of biface knapping in the eastern fluted point tradition: a manual for flintknappers and lithic analysts. Eastern States Archeological Federation.

Carvalho, S., McGrew, W.C., 2012. The origins of the Oldowan: Why chimpanzees (Pan troglodytes) still are good models for technological evolution in Africa. Stone Tools Foss. Bones Debates Archaeol. Hum. Orig. 201–221.

Chaudhri, M.M., 2015. Dynamic fracture of inorganic glasses by hard spherical and conical projectiles. Philos. Trans. R. Soc. Math. Phys. Eng. Sci. 373, 20140135.

Chaudhri, M.M., Chen, L., 1989. The orientation of the Hertzian cone crack in soda-lime glass formed by oblique dynamic and quasi-static loading with a hard sphere. J. Mater. Sci. 24, 3441–3448.

Cignoni, P., Ranzuglia, G., Callieri, M., Corsini, M., Ganovelli, F., Pietroni, N., Tarini, M., 2011. MeshLab.

Clark, J.E., 2012. Stoneworkers' approaches to replicating prismatic blades, in: The Emergence of Pressure Blade Making. Springer, pp. 43–135.

Clarkson, C., Hiscock, P., 2011. Estimating original flake mass from 3D scans of platform area. J. Archaeol. Sci. 38, 1062–1068.

Cotterell, B., Kamminga, J., 1992. Mechanics of pre-industrial technology: an introduction to the mechanics of ancient and traditional material culture. Cambridge University Press.

Cotterell, B., Kamminga, J., 1987. The Formation of Flakes. Am. Antiq. 52, 675–708. https://doi.org/10.2307/281378

Cotterell, B., Kamminga, J., Dickson, F.P., 1985. The essential mechanics of conchoidal flaking. Int. J. Fract. 29, 205–221. https://doi.org/10.1007/BF00125471

Crabtree, D.E., 1975. Comments on lithic technology and experimental archaeology. Lithic Technol. Mak. Using Stone Tools 86, 105.

Crabtree, D.E., 1972a. The cone fracture principle and the manufacture of lithic materials. Tebiwa 15, 29–42.

Crabtree, D.E., 1972b. An introduction to flintworking. Occas. Pap. Mus. Ida. State Univ. 28, 1–98.

Crabtree, D.E., 1970. Flaking Stone with Wooden Implements: Flaked stone artifacts from Palliaike, Chile, suggest that wooden flaking tools were used in the New World. Science 169, 146–153.

Crabtree, D.E., 1966. A stoneworker's approach to analyzing and replicating the Lindenmeier Folsom. Ariel 129, 92–22.

Crabtree, D.E., Davis, E.L., 1968. Experimental manufacture of wooden implements with tools of flaked stone. Science 159, 426–428.

Cueva-Temprana, A., Lombao, D., Morales, J.I., Geribàs, N., Mosquera, M., 2019. Gestures during knapping: a two-perspective approach to Pleistocene Technologies. Lithic Technol. 44, 74–89.

Cueva-Temprana, A., Lombao, D., Soto, M., Itambu, M., Bushozi, P., Boivin, N., Petraglia, M., Mercader, J., 2022. Oldowan Technology Amid Shifting Environments 2.03–1.83 Million Years Ago. Front. Ecol. Evol. 122.

Damlien, H., 2015. Striking a difference? The effect of knapping techniques on blade attributes. J. Archaeol. Sci. 63, 122–135.

Davidson, I., McGrew, W.C., 2005. Stone tools and the uniqueness of human culture. J. R. Anthropol. Inst. 11, 793–817.

Davis, Z.J., Shea, J.J., 1998. Quantifying lithic curation: An experimental test of Dibble and Pelcin's original flake-tool mass predictor. J. Archaeol. Sci. 25, 603–610.

De la Torre, I., 2016. The origins of the Acheulean: past and present perspectives on a major transition in human evolution. Philos. Trans. R. Soc. B Biol. Sci. 371, 20150245.

de la Torre, I., 2011. The early stone age lithic assemblages of Gadeb (Ethiopia) and the developed Oldowan/early Acheulean in East Africa. J. Hum. Evol. 60, 768–812.

de la Torre, I., 2004. Omo Revisited: Evaluating the Technological Skills of Pliocene Hominids. Curr. Anthropol. 45, 439–465. https://doi.org/10.1086/422079

de la Torre, I., Mora, R., Martínez-Moreno, J., 2008. The early Acheulean in Peninj (Lake Natron, Tanzania). J. Anthropol. Archaeol. 27, 244–264.

de la Torre, I.G., McHenry, L.J., Njau, J., Pante, M.D., 2012. The origins of the Acheulean at Olduvai Gorge (Tanzania): a new paleoanthropological project in East Africa. Archaeol. Int.

de Lotbiniere, S., 1984. Gunflint recognition. Int. J. Naut. Archaeol. 13, 206–209.

Dean, L.G., Vale, G.L., Laland, K.N., Flynn, E., Kendal, R.L., 2014. Human cumulative culture: a comparative perspective. Biol. Rev. 89, 284–301.

Debénath, A., Dibble, H.L., 2015. Handbook of Paleolithic typology. University of Pennsylvania Press.

Delagnes, A., Roche, H., 2005. Late Pliocene hominid knapping skills: The case of Lokalalei 2C, West Turkana, Kenya. J. Hum. Evol. 48, 435–472.

Dibble, H.L., 1997. Platform variability and flake morphology: a comparison of experimental and archaeological data and implications for interpreting prehistoric lithic technological strategies. Lithic Technol. 22, 150–170.

Dibble, H.L., Pelcin, A., 1995. The effect of hammer mass and velocity on flake mass. J. Archaeol. Sci. 22, 429–439.

Dibble, H.L., Rezek, Z., 2009. Introducing a new experimental design for controlled studies of flake formation: results for exterior platform angle, platform depth, angle of blow, velocity, and force. J. Archaeol. Sci. 36, 1945–1954.

Dibble, H.L., Whittaker, J.C., 1981. New experimental evidence on the relation between percussion flaking and flake variation. J. Archaeol. Sci. 8, 283–296.

Dogandžić, T., Abdolazadeh, A., Leader, G., Li, L., McPherron, S.P., Tennie, C., Dibble, H.L., 2020. The results of lithic experiments performed on glass cores are applicable to other raw materials. Archaeol. Anthropol. Sci. 12, 44.

Dogandžić, T., Braun, D.R., McPherron, S.P., 2015. Edge length and surface area of a blank: experimental assessment of measures, size predictions and utility. PLoS One 10, e0133984.

Dominguez-Ballesteros, E., Arrizabalaga, A., 2015. Flint knapping and determination of human handedness. Methodological proposal with quantifiable results. J. Archaeol. Sci. Rep. 3, 313–320.

Douglass, M., Davies, B., Braun, D.R., Faith, J.T., Power, M., Reeves, J., 2021. Deriving original nodule size of lithic reduction sets from cortical curvature: An application to monitor stone artifact transport from bipolar reduction. J. Archaeol. Sci. Rep. 35, 102671.

Driscoll, K., García-Rojas, M., 2014. Their lips are sealed: identifying hard stone, soft stone, and antler hammer direct percussion in Palaeolithic prismatic blade production. J. Archaeol. Sci. 47, 134–141.

Eren, M.I., Dominguez-Rodrigo, M., Kuhn, S.L., Adler, D.S., Le, I., Bar-Yosef, O., 2005. Defining and measuring reduction in unifacial stone tools. J. Archaeol. Sci. 32, 1190–1201.

Eren, M.I., Greenspan, A., Sampson, C.G., 2008. Are Upper Paleolithic blade cores more productive than Middle Paleolithic discoidal cores? A replication experiment. J. Hum. Evol. 55, 952–961.

Eren, M.I., Lycett, S.J., 2012. Why Levallois? A morphometric comparison of experimental ‘preferential’Levallois flakes versus debitage flakes. PLoS One 7, e29273.

Eren, M.I., Lycett, S.J., Patten, R.J., Buchanan, B., Pargeter, J., O’Brien, M.J., 2016. Test, model, and method validation: the role of experimental stone artifact replication in hypothesis-driven archaeology. Ethnoarchaeology 8, 103–136.

Eren, M.I., Lycett, S.J., Roos, C.I., Sampson, C.G., 2011. Toolstone constraints on knapping skill: Levallois reduction with two different raw materials. J. Archaeol. Sci. 38, 2731–2739.

Eren, M.I., Roos, C.I., Story, B.A., von Cramon-Taubadel, N., Lycett, S.J., 2014. The role of raw material differences in stone tool shape variation: an experimental assessment. J. Archaeol. Sci. 49, 472–487.

Faulkner, A., 1973. Mechanics of eraillure formation. Newsl. Lithic Technol. 4–12.

Faulkner, A., 1972. Mechanical principles of flintworking. Washington State University.

Fischer-Cripps, A.C., 2007. Introduction to Contact Mechanics. New York: Springer.

Flenniken, J.J., 1978. Reevaluation of the Lindenmeier Folsom: a replication experiment in lithic technology. Am. Antiq. 43, 473–480.

Forestier, H., 1992. Approche technologique de quelques séries dites clactoniennes du nord-ouest de la France et du sud-est de l'Angleterre. Mém. Maîtrise Univ. Paris X Nanterre.

Frank, F.C., Lawn, B., 1967. On the theory of Hertzian fracture. Proc. R. Soc. Lond. Ser. Math. Phys. Sci. 299, 291–306.

Franklin, J.D., Simek, J.F., 2008. Core refitting and the accuracy of aggregate lithic analysis techniques: the case of 3rd Unnamed Cave, Tennessee. Southeast. Archaeol. 108–121.

Frison, G., 1979. Observations on the use of stone tools: dulling of working edges of some chipped stone tools in bison butchering. In (B. Hayden, Ed.) Lithic Use-Wear Analysis. New York: Academic Press.

Gallagher, J.P., 1977. Contemporary stone tools in Ethiopia: implications for archaeology. J. Field Archaeol. 4, 407–414.

Gallotti, R., 2018. Before the Acheulean in East Africa: An overview of the Oldowan lithic assemblages. Emergence Acheulean East Afr. Beyond 13–32.

Geneste, J.-M., 1988. Les industries de la grotte Vaufrey: technologie du débitage, économie et circulation de la matière première lithique. Grotte Vaufrey Paléoenvironnement Chronol. Act. Hum. 441–518.

Geneste, J.-M., 1985. Analyse lithique d'industries moustériennes du Périgord: une approche du comportement des groupes humains au paléolithique moyen (PhD Thesis). Bordeaux 1.

Geribàs, N., Mosquera, M., Vergès, J.M., 2010. The gesture substratum of stone tool making: an experimental approach. Sezione Museol. Sci. E Nat. 6, 155–162.

Goldman-Neuman, T., Hovers, E., 2009. Methodological considerations in the study of Oldowan raw material selectivity: insights from AL 894 (Hadar, Ethiopia), in: Interdisciplinary Approaches to the Oldowan. Springer, pp. 71–84.

Gorham, D.A., Salman, A.D., 2005. The failure of spherical particles under impact. Wear 258, 580–587.

Gowlett, J.A., Goren-Inbar, N., Sharon, G., Equinox, L., 2014. The elements of design form in Acheulean bifaces: modes, modalities, rules, and language. Lucy Lang. Benchmark Pap. 409.

Gowlett, J.A.J., 2015. Variability in an early hominin percussive tradition: the Acheulean versus cultural variation in modern chimpanzee artefacts. Philos. Trans. R. Soc. B Biol. Sci. 370, 20140358.

Gowlett, J.A.J., 1990. Archaeological studies of human origins and early prehistory in Africa. Hist. Afr. Archaeol. 13–38.

Harmand, S., 2007. Harmand, Sonia. "Economic behaviors and cognitive capacities of early hominins between 2.34 Ma and 0.70 Ma in West Turkana, Kenya. Mitteilungen Ges. Für Urgesch.

Harris, J.W.K., 1983. Cultural beginnings: Plio-Pleistocene archaeological occurrences from the Afar, Ethiopia. Afr. Archaeol. Rev. 1, 3–31.

Harris, J.W.K., 1978. The Karari Industry, its place in east African prehistory (PhD Thesis). University of California, Berkeley.

Hayden, B., 2015. Insights into early lithic technologies from ethnography. Philos. Trans. R. Soc. B Biol. Sci. 370, 20140356.

Hayden, B., 2008. What were they doing in the Oldowan? An ethnoarchaeological perspective on the origins of human behavior. Lithic Technol. 33, 105–139.

Hayden, B., Hutchings, W.K., 1989. Whither the billet flake? Amick, DS and Mauldin, RP (eds.) Experiments in lithic technology: 235-257. BAR Int. Ser. 528.

Hayden, B., Nelson, M., 1981. The use of chipped lithic material in the contemporary Maya highlands. Am. Antiq. 46, 885–898.

Hellweg, P., 1984. Flintknapping: The Art of Making Stone Tools. Canyon Publishing Company.

Hiscock, P., Clarkson, C., 2009. The reality of reduction experiments and the GIUR: reply to Eren and Sampson. J. Archaeol. Sci. 36, 1576–1581.

Hiscock, P., Clarkson, C., 2005a. Experimental evaluation of Kuhn's geometric index of reduction and the flat-flake problem. J. Archaeol. Sci. 32, 1015–1022.

Hiscock, P., Clarkson, C., 2005b. Measuring artefact reduction: an examination of Kuhn's Geometric Index of Reduction. Lithics Aust. Perspect. Lithic Reduct. Use Classif.

Hlubik, S., Berna, F., Feibel, C., Braun, D., Harris, J.W., 2017. Researching the nature of fire at 1.5 Mya on the site of FxJj20 AB, Koobi Fora, Kenya, using high-resolution spatial analysis and FTIR spectrometry. Curr. Anthropol. 58, S243–S257.

Hoffman, J.I., 2016. Archive computer code with raw data. Nature 534, 326–326.

Hovers, E., 2012. Invention, reinvention and innovation: the makings of Oldowan lithic technology, in: Developments in Quaternary Sciences. Elsevier, pp. 51–68.

Isaac, B., Isaac, G.L., 1997. Koobi Fora Research Project: Plio-Pleistocene Archaeology/Edited by Glynn Ll. Isaac; Assisted by Barbara Isaac. Clarendon Press.

Isaac, G., Harris, J.W.K., 1997. Sites stratified within the KBS Tuff: reports. Isaac G Assist. Isaac BEds Koobi Fora Res. Proj. 5, 71–114.

Isaac, G.L., 1976. Plio-Pleistocene artifact assemblages from Koobi Fora, Kenya, in: Earliest Man and Environments in the Lake Rudolf Basin. University of Chicago Press Chicago.

Isaac, G.L., Behrensmeyer, A.K., 1997. Geological context and palaeoenvironments. Koobi Fora Res. Proj. 5, 12–70.

Isaac, G.L., Isaac, B., 1997. Koobi Fora Research Project. "Koobi Fora Research Project Vol. 5: Plio-Pleistocene Archaeology. Oxford University Press, Oxford.

Jennings, T.A., Pevny, C.D., Dickens, W.A., 2010. A biface and blade core efficiency experiment: implications for Early Paleoindian technological organization. J. Archaeol. Sci. 37, 2155–2164.

Ji, S., Wang, Q., Li, L., 2019. Seismic velocities, Poisson's ratios and potential auxetic behavior of volcanic rocks. Tectonophysics 766, 270–282.

Johnson, L.L., 1975. Graph theoretic analysis of lithic tools from northern Chile. Lithic Technol. Mak. Using Stone Tools 63–95.

Johnson, L.L., Behm, J.A., Bordes, F., Cahen, D., Crabtree, D.E., Dincauze, D.F., Hay, C.A., Hayden, B., Hester, T.R., Katz, P.R., 1978. A history of flint-knapping experimentation, 1838-1976 [and comments and reply]. Curr. Anthropol. 19, 337–372.

Karavanić, I., Šokec, T., 2003. The Middle Paleolithic percussion or pressure flaking tools? The comparison of experimental and archaeological material from Croatia. Pril. Instituta Za Arheol. U Zagrebu 20, 13–14.

Kaufulu, Z.M., 1983. The geological context of some early archaeological sites in Kenya, Malawi and Tanzania: Microstratigraphy, site formation and interpretation. University of California, Berkeley.

Kenmotsu, N., 1990. Gunflints: a study. Hist. Archaeol. 24, 92–124.

Key, A.J., Dunmore, C.J., 2018. Manual restrictions on Palaeolithic technological behaviours. PeerJ 6, e5399.

Kimura, Y., 2002. Examining time trends in the Oldowan technology at Beds I and II, Olduvai Gorge. J. Hum. Evol. 43, 291–321.

Kocer, C., Collins, R.E., 1998. Angle of Hertzian cone cracks. J. Am. Ceram. Soc. 81, 1736–1742.

Kuhn, S.L., 1990. A geometric index of reduction for unifacial stone tools. J. Archaeol. Sci. 17, 583–593. https://doi.org/10.1016/0305-4403(90)90038-7

Langitan, F.B., Lawn, B.R., 1969. Hertzian fracture experiments on abraded glass surfaces as definitive evidence for an energy balance explanation of Auerbach's law. J. Appl. Phys. 40, 4009–4017.

Lawn, B.R., 1967. Partial cone crack formation in a brittle material loaded with a sliding spherical indenter. Proc. R. Soc. Lond. Ser. Math. Phys. Sci. 299, 307–316.

Lawn, B.R., Wiederhorn, S.M., Roberts, D.E., 1984. Effect of sliding friction forces on the strength of brittle materials. J. Mater. Sci. 19, 2561–2569.

Lawn, B.R., Wilshaw, T.R., Hartley, N.E.W., 1974. A computer simulation study of Hertzian cone crack growth. Int. J. Fract. 10, 1–16.

Leader, G., Abdolahzadeh, A., Lin, S.C., Dibble, H.L., 2017. The effects of platform beveling on flake variation. J. Archaeol. Sci. Rep. 16, 213–223.

Leakey, L.S.B., 1934. Adam's Ancestors: An Up-to-date Outline of what is Known about the Origin of Man. Metheuen and Company, London.

Lepre, C.J., Kent, D.V., 2010. New magnetostratigraphy for the Olduvai Subchron in the Koobi Fora Formation, northwest Kenya, with implications for early Homo. Earth Planet. Sci. Lett. 290, 362–374.

Li, L., Lin, S.C., McPherron, S.P., Abdolahzadeh, A., Chan, A., Dogandžić, T., Iovita, R., Leader, G.M., Magnani, M., Rezek, Z., Dibble, H.L., Under Review. A synthesis of the Dibble et al. controlled experiments into the mechanics of lithic production.

Li, L., Reeves, J.S., Lin, S.C., Tennie, C., McPherron, S.P., Under Review. Quantifying knapping actions: a method for measuring the angle of blow on flakes.

Liljestrand, K., 1980. FxJj 37: a site report including a comparison with other Lower Pleistocene archaeological sites from East Africa (PhD Thesis).

Lin, S.C., McPherron, S.P., Dibble, H.L., 2015. Establishing statistical confidence in Cortex Ratios within and among lithic assemblages: a case study of the Middle Paleolithic of southwestern France. J. Archaeol. Sci. 59, 89–109.

Lin, S.C., Rezek, Z., Abdolahzadeh, A., Braun, D.R., Dogandžić, T., Leader, G.M., Li, L., McPherron, S.P., 2022. The mediating effect of platform width on the size and shape of stone flakes. Plos One 17, e0262920.

Lin, S.C., Rezek, Z., Braun, D., Dibble, H.L., 2013. On the utility and economization of unretouched flakes: the effects of exterior platform angle and platform depth. Am. Antiq. 78, 724–745.

Lin, S.C., Rezek, Z., Dibble, H.L., 2018. Experimental design and experimental inference in stone artifact archaeology. J. Archaeol. Method Theory 25, 663–688.

Lycett, S.J., 2013. Cultural transmission theory and fossil hominin behaviour. Underst. Cult. Transm. Anthropol. Crit. Synth. 26, 102.

Lycett, S.J., Eren, M.I., 2013. Levallois lessons: the challenge of integrating mathematical models, quantitative experiments and the archaeological record. World Archaeol. 45, 519–538.

Lycett, S.J., von Cramon-Taubadel, N., Eren, M.I., 2016. Levallois: potential implications for learning and cultural transmission capacities. Lithic Technol. 41, 19–38.

Macchi, R., Daver, G., Brenet, M., Prat, S., Hugheville, L., Harmand, S., Lewis, J., Domalain, M., 2021. Biomechanical demands of percussive techniques in the context of early stone toolmaking. J. R. Soc. Interface 18, 20201044.

Magnani, M., Rezek, Z., Lin, S.C., Chan, A., Dibble, H.L., 2014. Flake variation in relation to the application of force. J. Archaeol. Sci. 46, 37–49.

Marimuthu, K.P., Rickhey, F., Lee, H., Lee, J.H., 2016. Spherical indentation cracking in brittle materials: An XFEM study, in: 2016 7th International Conference on Mechanical and Aerospace Engineering (ICMAE). IEEE, pp. 267–273.

Marwick, B., 2017. Computational reproducibility in archaeological research: Basic principles and a case study of their implementation. J. Archaeol. Method Theory 24, 424–450.

Marzke, M.W., 2013. Tool making, hand morphology and fossil hominins. Philos. Trans. R. Soc. B Biol. Sci. 368, 20120414.

McHenry, L.J., de la Torre, I., 2018. Hominin raw material procurement in the Oldowan-Acheulean transition at Olduvai Gorge. J. Hum. Evol. 120, 378–401.

McPherron, S.P., Abdolahzadeh, A., Archer, W., Chan, A., Djakovic, I., Dogandžić, T., Leader, G., Li, L., Lin, S., Magnani, M., Reeves, J., Rezek, Z., Weiss, M., 2020. Introducing Platform Surface Interior Angle (PSIA) and Its Role in Flake Formation, Size and Shape. Manuscr. Submitt. Publ.

Moore, M.W., Perston, Y., 2016. Experimental insights into the cognitive significance of early stone tools. PloS One 11, e0158803.

Morgan, T.J., Uomini, N.T., Rendell, L.E., Chouinard-Thuly, L., Street, S.E., Lewis, H.M., Cross, C.P., Evans, C., Kearney, R., de la Torre, I., 2015. Experimental evidence for the co-evolution of hominin tool-making teaching and language. Nat. Commun. 6, 1–8.

Mourre, V., Villa, P., Henshilwood, C.S., 2010. Early use of pressure flaking on lithic artifacts at Blombos Cave, South Africa. science 330, 659–662.

Mraz, V., Fisch, M., Eren, M.I., Lovejoy, C.O., Buchanan, B., 2019. Thermal engineering of stone increased prehistoric toolmaking skill. Sci. Rep. 9, 1–8. https://doi.org/10.1038/s41598-019-51139-3

Muller, A., Clarkson, C., 2016. Identifying major transitions in the evolution of lithic cutting edge production rates. PLoS One 11, e0167244.

Muller, A., Clarkson, C., 2014. Estimating original flake mass on blades using 3D platform area: problems and prospects. J. Archaeol. Sci. 52, 31–38.

Munafò, M., 2016. Open science and research reproducibility. ecancermedicalscience 10.

Newcomer, M.H., 1975. Punch technique" and Upper Paleolithic blades. Lithic Technol. Mak. Using Stone Tools 86, 97.

Newcomer, M.H., 1971. Some quantitative experiments in handaxe manufacture. World Archaeol. 3, 85–94.

Nonaka, T., Bril, B., Rein, R., 2010. How do stone knappers predict and control the outcome of flaking? Implications for understanding early stone tool technology. J. Hum. Evol. 59, 155–167. https://doi.org/10.1016/j.jhevol.2010.04.006

Odell, G.H., 1979. A new and improved system for the retrieval of functional information from microscopic observations of chipped stone tools. Lithic Use-Wear Anal. 329–344.

Olivi-Tran, N., Despetis, F., Faivre, A., 2020. Modeling of deep indentation in brittle materials. Mater. Res. Express 7, 035201.

Orellana Figueroa, J.D., Reeves, J.S., McPherron, S.P., Tennie, C., 2021. A proof of concept for machine learning-based virtual knapping using neural networks. Sci. Rep. 11, 19966. https://doi.org/10.1038/s41598-021-98755-6

Pargeter, J., Khreisheh, N., Stout, D., 2019. Understanding stone tool-making skill acquisition: Experimental methods and evolutionary implications. J. Hum. Evol. 133, 146–166.

Pargeter, J., Liu, J., Kilgore, M.B., Majoe, A., Stout, D., 2021. Testing the social, cognitive, and motor foundations of Paleolithic skill reproduction. OSA.

Pelcin, A.W., 1998. The threshold effect of platform width: a reply to Davis and Shea. J. Archaeol. Sci. 25, 615–620.

Pelcin, A.W., 1997a. The effect of core surface morphology on flake attributes: evidence from a controlled experiment. J. Archaeol. Sci. 24, 749–756.

Pelcin, A.W., 1997b. The effect of indentor type on flake attributes: evidence from a controlled experiment. J. Archaeol. Sci. 24, 613–621.

Pelcin, A.W., 1996. Controlled experiments in the production of flake attributes.

Pelegrin, J., 2006. Long blade technology in the Old World: an experimental approach and some archaeological results. Skilled Prod. Soc. Reprod. 2, 37–68.

Pelegrin, J., 1993. A framework for analysing prehistoric stone tool manufacture and a tentative application to some early stone industries. Use Tools Hum. Non-Hum. Primates 30214.

Pelegrin, J., 1990. Prehistoric lithic technology: some aspects of research. Archaeol. Rev. Camb. 9, 116–125.

Plummer, T., 2004. Flaked stones and old bones: Biological and cultural evolution at the dawn of technology. Am. J. Phys. Anthropol. 125, 118–164. https://doi.org/10.1002/ajpa.20157

Prasciunas, M.M., 2007. Bifacial cores and flake production efficiency: an experimental test of technological assumptions. Am. Antiq. 72, 334–348.

Presnyakova, D., 2019. Landscape perspectives on variability in the Acheulean behavioural system in sub-Saharan Africa: A view from Koobi Fora and Elandsfontein (PhD Thesis). Eberhard Karls Universität Tübingen.

Presnyakova, D., Braun, D.R., Conard, N.J., Feibel, C., Harris, J.W., Pop, C.M., Schlager, S., Archer, W., 2018. Site fragmentation, hominin mobility and LCT variability reflected in the early Acheulean record of the Okote Member, at Koobi Fora, Kenya. J. Hum. Evol. 125, 159–180.

Quinn, C., 2004. An experimental use-wear and functional analysis of gunflints.

R Core Team, 2020. R: A Language and Environment for Statistical Computing. R Foundation for Statistical Computing, Vienna, Austria.

Ranere, A.J., Browman, D.L., 1978. Toolmaking and tool use among the preceramic peoples of Panama. Adv. Andean Archaeol. 41–84.

Rein, R., Bril, B., Nonaka, T., 2013. Coordination strategies used in stone knapping. Am. J. Phys. Anthropol. 150, 539–550.

Reti, J.S., 2016. Quantifying Oldowan Stone Tool Production at Olduvai Gorge, Tanzania. PLOS ONE 11, e0147352. https://doi.org/10.1371/journal.pone.0147352

Režek, Ž., Dibble, H.L., McPherron, S.P., Braun, D.R., Lin, S.C., 2018. Two million years of flaking stone and the evolutionary efficiency of stone tool technology. Nat. Ecol. Evol. 2, 628.

Rezek, Z., Lin, S., Iovita, R., Dibble, H.L., 2011. The relative effects of core surface morphology on flake shape and other attributes. J. Archaeol. Sci. 38, 1346–1359.

Rezek, Z., Lin, S.C., Dibble, H.L., 2016. The role of controlled experiments in understanding variation in flake production.

Roche, H., 2005. From simple flaking to shaping: stone knapping evolution among early hominids.

Roche, H., Delagnes, A., Brugal, J.-P., Feibel, C., Kibunjia, M., Mourre, V., Texier, P.-J., 1999. Early hominid stone tool production and technical skill 2.34 Myr ago in West Turkana, Kenya. Nature 399, 57–60. https://doi.org/10.1038/19959

Roesler, F.C., 1956. Brittle fractures near equilibrium. Proc. Phys. Soc. Sect. B 69, 981.

Rolian, C., Lieberman, D.E., Zermeno, J.P., 2011. Hand biomechanics during simulated stone tool use. J. Hum. Evol. 61, 26–41.

Roussel, M., Bourguignon, L., Soressi, M., 2009. Identification par l'expérimentation de la percussion au percuteur de calcaire au Paléolithique moyen: le cas du façonnage des racloirs bifaciaux Quina de Chez Pinaud (Jonzac, Charente-Maritime). Bull. Société Préhistorique Fr. 219–238.

Rugg, G., Mullane, M., 2001. Inferring handedness from lithic evidence. Laterality Asymmetries Body Brain Cogn. 6, 247–259.

Salman, A.D., Gorham, D.A., 2000. The fracture of glass spheres. Powder Technol. 107, 179–185.

Salman, A.D., Gorham, D.A., Verba, A., 1995. A study of solid particle failure under normal and oblique impact. Wear 186, 92–98.

Sandgathe, D.M., Dibble, H.L., Goldberg, P., McPherron, S.P., 2011a. The Roc de Marsal Neandertal child: A reassessment of its status as a deliberate burial. J. Hum. Evol. 61, 243–253.

Sandgathe, D.M., Dibble, H.L., Goldberg, P., McPherron, S.P., Turq, A., Niven, L., Hodgkins, J., 2011b. On the role of fire in Neandertal adaptations in Western Europe: evidence from Pech de l'Azé IV and Roc de Marsal, France. PaleoAnthropology 2011, 216–242.

Scerri, E.M., Gravina, B., Blinkhorn, J., Delagnes, A., 2016. Can lithic attribute analyses identify discrete reduction trajectories? A quantitative study using refitted lithic sets. J. Archaeol. Method Theory 23, 669–691.

Schick, K., Toth, N., 2006. An overview of the Oldowan industrial complex: the sites and the nature of their evidence. Oldowan Case Stud. Earliest Stone Age 3–42.

Schick, K.D., Toth, N.P., 1994. Making silent stones speak: Human evolution and the dawn of technology. Simon and Schuster.

Schindler, B., Koch, J., 2012. Flakes giving you lip? Let them speak: an examination of the relationship between percussor type and lipped platforms. Archaeol. East. N. Am. 99–106.

Schmid, V.C., Douze, K., Tribolo, C., Martinez, M.L., Rasse, M., Lespez, L., Lebrun, B., Hérisson, D., Ndiaye, M., Huysecom, E., 2021. Middle Stone Age Bifacial Technology and Pressure Flaking at the MIS 3 Site of Toumboura III, Eastern Senegal. Afr. Archaeol. Rev. 1–33.

Schmid, V.C., Porraz, G., Zeidi, M., Conard, N.J., 2019. Blade Technology Characterizing the MIS 5 DA Layers of Sibudu Cave, South Africa. Lithic Technol. 44, 199–236.

Schoville, B.J., Brown, K.S., Harris, J.A., Wilkins, J., 2016. New experiments and a model-driven approach for interpreting Middle Stone Age lithic point function using the edge damage distribution method. PloS One 11, e0164088.

Schultz, R.A., 1993. Brittle strength of basaltic rock masses with applications to Venus. J. Geophys. Res. Planets 98, 10883–10895.

Semaw, S., Rogers, M., Stout, D., 2009. The Oldowan-Acheulian Transition: Is there a “Developed Oldowan” Artifact Tradition?, in: Camps, M., Chauhan, P. (Eds.), Sourcebook of Paleolithic Transitions: Methods, Theories, and Interpretations. Springer, New York, NY, pp. 173–193. https://doi.org/10.1007/978-0-387-76487-0_10

Sharon, G., 2010. Large flake Acheulian. Quat. Int. 223–224, 226–233. https://doi.org/10.1016/j.quaint.2009.11.023

Sharon, G., 2009. Acheulian giant-core technology: a worldwide perspective. Curr. Anthropol. 50, 335–367.

Sharon, G., Goren-Inbar, N., 1999. Soft percussor use at the Gesher Benot Ya ‘aqov Acheulian site. Mitekufat Haeven 28, 55–79.

Shea, J., Davis, Z., Brown, K., 2001. Experimental tests of Middle Palaeolithic spear points using a calibrated crossbow. J. Archaeol. Sci. 28, 807–816.

Shea, J.J., 2017. Occasional, obligatory, and habitual stone tool use in hominin evolution. Evol. Anthropol. Issues News Rev. 26, 200–217.

Sheets, P.D., 1973. Edge abrasion during biface manufacture. Am. Antiq. 38, 215–218.

Sheets, P.D., Muto, G.R., 1972. Pressure blades and total cutting edge: an experiment in lithic technology. Science 175, 632–634.

Shipton, C., 2018. Biface knapping skill in the East African Acheulean: Progressive trends and random walks. Afr. Archaeol. Rev. 35, 107–131.

Shipton, C., 2016. Hierarchical organization in the Acheulean to Middle Palaeolithic transition at Bhimbetka, India. Camb. Archaeol. J. 26, 601–618.

Shipton, C., Nielsen, M., 2015. Before cumulative culture. Hum. Nat. 26, 331–345.

Shott, M., 1986. Technological organization and settlement mobility: an ethnographic examination. J. Anthropol. Res. 42, 15–51.

Shott, M.J., 1989. Bipolar industries: ethnographic evidence and archaeological implications. North Am. Archaeol. 10, 1–24.

Shott, M.J., Bradbury, A.P., Carr, P.J., Odell, G.H., 2000. Flake size from platform attributes: predictive and empirical approaches. J. Archaeol. Sci. 27, 877–894.

Shott, M.J., Seeman, M.F., 2017. Use and multifactorial reconciliation of uniface reduction measures: A pilot study at the Nobles Pond Paleoindian site. Am. Antiq. 82, 723–741.

Snyder, W.D., Reeves, J.S., Tennie, C., 2021. Early knapping techniques do not necessitate cultural transmission.

Soriano, S., Villa, P., Wadley, L., 2007. Blade technology and tool forms in the Middle Stone Age of South Africa: the Howiesons Poort and post-Howiesons Poort at rose Cottage Cave. J. Archaeol. Sci. 34, 681–703.

Speth, J.D., 1981. The role of platform angle and core size in hard-hammer percussion flaking. Lithic Technol. 10, 16–21.

Speth, J.D., 1975. Miscellaneous studies in hard-hammer percussion flaking: the effects of oblique impact. Am. Antiq. 203–207.

Speth, J.D., 1974. Experimental investigations of hard-hammer percussion flaking. Tebiwa.

Speth, J.D., 1972. Mechanical Basis of Percussion Flaking. Am. Antiq. 37, 34–60. https://doi.org/10.2307/278884

Stevens, N.E., Harro, D.R., Hicklin, A., 2010. Practical quantitative lithic use-wear analysis using multiple classifiers. J. Archaeol. Sci. 37, 2671–2678. https://doi.org/10.1016/j.jas.2010.06.004

Stout, D., 2011. Stone toolmaking and the evolution of human culture and cognition. Philos. Trans. R. Soc. B Biol. Sci. 366, 1050–1059.

Stout, D., Bril, B., Roux, V., DeBeaune, S., Gowlett, J.A.J., Keller, C., Wynn, T., Stout, D., 2002. Skill and cognition in stone tool production: an ethnographic case study from Irian Jaya. Curr. Anthropol. 43, 693–722.

Stout, D., Hecht, E., Khreisheh, N., Bradley, B., Chaminade, T., 2015. Cognitive demands of Lower Paleolithic toolmaking. PLoS One 10, e0121804.

Stout, D., Khreisheh, N., 2015. Skill learning and human brain evolution: An experimental approach. Camb. Archaeol. J. 25, 867–875.

Stout, D., Passingham, R., Frith, C., Apel, J., Chaminade, T., 2011. Technology, expertise and social cognition in human evolution. Eur. J. Neurosci. 33, 1328–1338.

Stout, D., Quade, J., Semaw, S., Rogers, M.J., Levin, N.E., 2005. Raw material selectivity of the earliest stone toolmakers at Gona, Afar, Ethiopia. J. Hum. Evol. 48, 365–380.

Stout, D., Rogers, M.J., Jaeggi, A.V., Semaw, S., 2019. Archaeology and the Origins of Human Cumulative Culture: A Case Study from the Earliest Oldowan at Gona, Ethiopia. Curr. Anthropol. World J. Sci. Man 309–340.

Stout, D., Schick, K., Toth, N., 2009. Understanding Oldowan knapping skill: an experimental study of skill acquisition in modern humans. Cut. Edge New Approaches Archaeol. Hum. Orig. 247–266.

Stout, D., Semaw, S., Rogers, M.J., Cauche, D., 2010. Technological variation in the earliest Oldowan from Gona, Afar, Ethiopia. J. Hum. Evol. 58, 474–491. https://doi.org/10.1016/j.jhevol.2010.02.005

Suh, C.-M., Kim, D.-K., Lee, M.-H., 2006. A study on damage behavior of glass by oblique impact of steel ball. Int. J. Mod. Phys. B 20, 4291–4296.

Sullivan, A.P., Rozen, K.C., 1985. Debitage analysis and archaeological interpretation. Am. Antiq. 50, 755–779.

Susman, R.L., 1998. Hand function and tool behavior in early hominids. J. Hum. Evol. 35, 23–46.

Swain, M.V., Lawn, B.R., 1976. Indentation fracture in brittle rocks and glasses, in: International Journal of Rock Mechanics and Mining Sciences & Geomechanics Abstracts. Elsevier, pp. 311–319.

Tabarev, A.V., 1997. Paleolithic wedge-shaped microcores and experiments with pocket devices. Lithic Technol. 22, 139–149.

Tennie, C., Braun, D.R., Premo, L.S., McPherron, S.P., 2016. The Island test for cumulative culture in the Paleolithic, in: The Nature of Culture. Springer, pp. 121–133.

Tennie, C., Call, J., Tomasello, M., 2009. Ratcheting up the ratchet: on the evolution of cumulative culture. Philos. Trans. R. Soc. B Biol. Sci. 364, 2405–2415.

Tennie, C., Hopper, L., van Schaik, C.P., 2020. On the Origin of Cumulative Culture: Consideration of the Role of Copying in Culture- Dependent Traits and a Reappraisal of the Zone of Latent Solutions Hypothesis, in: Chimpanzees in Context: A

Comparative Perspective on Chimpanzee Behavior, Cognition, Conservation, and Welfare. University of Chicago Press.

Tennie, C., Premo, L.S., Braun, D.R., McPherron, S.P., 2017. Early stone tools and cultural transmission: Resetting the null hypothesis. Curr. Anthropol. World J. Sci. Man 652–672.

Texier, P.J., Roche, H., 1995. The impact of predetermination on the development of some Acheulean chaînes opératoires. Evol. Humana En Eur. Los Yacim. Sierra Atapuerca 2, 403–420.

Titton, S., Barsky, D., Bargalló, A., Serrano-Ramos, A., Vergès, J.M., Toro-Moyano, I., Sala-Ramos, R., Solano, J.G., Jimenez Arenas, J.M., 2020. Subspheroids in the lithic assemblage of Barranco León (Spain): Recognizing the late Oldowan in Europe. PloS One 15, e0228290.

Tocheri, M.W., Orr, C.M., Larson, S.G., Sutikna, T., Saptomo, E.W., Due, R.A., Djubiantono, T., Morwood, M.J., Jungers, W.L., 2007. The primitive wrist of Homo floresiensis and its implications for hominin evolution. Science 317, 1743–1745.

Toth, N., 1985. The Oldowan reassessed: a close look at early stone artifacts. J. Archaeol. Sci. 12, 101–120.

Toth, N., Schick, K., 2019. Why did the Acheulean happen? Experimental studies into the manufacture and function of Acheulean artifacts. L'Anthropologie 123, 724–768.

Toth, N., Schick, K., 2018. An overview of the cognitive implications of the Oldowan Industrial Complex. Azania Archaeol. Res. Afr. 53, 3–39.

Toth, N., Schick, K., 2009. The importance of actualistic studies in Early Stone Age research: some personal reflections. Cut. Edge New Approaches Archaeol. Hum. Orig. 267–344.

Toth, N.P., 1982. The stone technologies of early hominids at Koobi Fora, Kenya: an experimental approach (PhD Thesis). University of California, Berkeley.

Tringham, R., Cooper, G., Odell, G., Voytek, B., Whitman, A., 1974. Experimentation in the formation of edge damage: a new approach to lithic analysis. J. Field Archaeol. 1, 171–196.

Tsirk, A., 2014. Fractures in knapping. Archaeopress Oxford.

Turq, A., 1979. L'évolution du Moustérien de type Quina au Roc de Marsal et en Périgord: modifications de l'équilibre technique et typologique. Ecole des Hautes études en sciences sociales.

Turq, A., Dibble, H., Faivre, J.-P., Goldberg, P., McPherron, S.P., Sansgathe, D., 2008. Le moustérien récent du Périgord Noir: Quoi de Neuf?, in: Les Sociétés Du Paléolithique Dans Un Grand Sud-Ouest de La France| Nouveaux Gisements, Nouveaux Résultats, Nouvelles Méthodes; Journées SPF, Université Bordeaux 1, Talence, 24-25 Novembre 2006. Société Préhistorique Française, pp. 83–94.

Ungar, P.S., Grine, F.E., Teaford, M.F., 2006. Diet in early Homo: a review of the evidence and a new model of adaptive versatility. Annu Rev Anthr. 35, 209–228.

Uno, K.T., Rivals, F., Bibi, F., Pante, M., Njau, J., de la Torre, I., 2018. Large mammal diets and paleoecology across the Oldowan–Acheulean transition at Olduvai Gorge, Tanzania from stable isotope and tooth wear analyses. J. Hum. Evol. 120, 76–91.

Van Peer, P., 2021. A mechanical framework of conchoidal flaking and its place in lithic systematics. J. Paleolit. Archaeol. 4, 1–35.

Van Rossum, G., Drake, F.L., 2011. The python language reference manual. Network Theory Ltd.

Vernooij, C.A., Mouton, L.J., Bongers, R.M., 2015. Learning to control orientation and force in a hammering task. Z. Für Psychol.

Vicente-Saez, R., Martinez-Fuentes, C., 2018. Open Science now: A systematic literature review for an integrated definition. J. Bus. Res. 88, 428–436.

Whallon Jr, R., 1978. Threshing sledge flints. A distinctive pattern of wear. Paleorient 319–324.

White, S.W., 1975. Gunflints: Their Possible Significance for the Northwest. Northwest Anthropol. Res. Notes 9, 51–69.

Whittaker, J., 1996. Athkiajas: a Cypriot flintknapper and the threshing sledge industry. Lithic Technol. 21, 108–120.

Whittaker, J., Kamp, K., Yilmaz, E., 2009. Çakmak revisited: Turkish flintknappers today. Lithic Technol. 34, 93–110.

Whittaker, J.C., 1994. Flintknapping: making and understanding stone tools. University of Texas Press.

Wilkinson, M.D., Dumontier, M., Aalbersberg, Ij.J., Appleton, G., Axton, M., Baak, A., Blomberg, N., Boiten, J.-W., da Silva Santos, L.B., Bourne, P.E., 2016. The FAIR Guiding Principles for scientific data management and stewardship. Sci. Data 3, 1–9.

Williams, E.M., Gordon, A.D., Richmond, B.G., 2012. Hand pressure distribution during Oldowan stone tool production. J. Hum. Evol. 62, 520–532.

Williams, E.M., Gordon, A.D., Richmond, B.G., 2010. Upper limb kinematics and the role of the wrist during stone tool production. Am. J. Phys. Anthropol. 143, 134–145.

Williams-Hatala, E.M., Hatala, K.G., Key, A., Dunmore, C.J., Kasper, M., Gordon, M., Kivell, T.L., 2021. Kinetics of stone tool production among novice and expert tool makers. Am. J. Phys. Anthropol. 174, 714–727.

Wilson, J., Andrefsky, W., 2008. Exploring retouch on bifaces: Unpacking production, resharpening, and hammer type. Lithic Technol. Meas. Prod. Use Curation 86–105.

Yezzi-Woodley, K., Calder, J., Olver, P.J., Cody, P., Huffstutler, T., Terwilliger, A., Melton, J.A., Tappen, M., Coil, R., Tostevin, G., 2021. The virtual goniometer: demonstrating a new method for measuring angles on archaeological materials using fragmentary bone. Archaeol. Anthropol. Sci. 13, 1–16.

Zeng, K., Breder, K., Rowcliffe, D.J., 1992a. The Hertzian stress field and formation of cone cracks—I. Theoretical approach. Acta Metall. Mater. 40, 2595–2600.

Zeng, K., Breder, K., Rowcliffe, D.J., 1992b. The Hertzian stress field and formation of cone cracks—ii. determination of fracture toughness. Acta Metall. Mater. 40, 2601–2605.

Appendix I Chapter 2 Supplementary Information

1 Statistical analysis

1.1 EPA-PD linear model

1.1.1 Summary statistics of the EPA-PD model

Call:
lm(formula = flake_mass_cbrt ~ platthick * epa, data = lm_model)
Residuals:

Min	1Q	Median	3Q	Max
-0.67207	-0.15750	0.02198	0.14393	0.61056

Coefficients:

	Estimate	Std. Error	t value	Pr(>|t|)
(Intercept)	-0.020923	0.855880	-0.024	0.981
platthick	0.063811	0.117180	0.545	0.588
epa	0.010427	0.012545	0.831	0.409
platthick:epa	0.002140	0.001805	1.185	0.240

Residual standard error: 0.2774 on 72 degrees of freedom
Multiple R-squared: 0.8036, Adjusted R-squared: 0.7954
F-statistic: 98.17 on 3 and 72 DF, p-value: < 2.2e-16

1.1.2 Summary statistics of the EPA-PD-AOB model:

Call:
lm(formula = flake_mass_cbrt ~ platthick * epa + aob, data = lm_model)
Residuals:

Min	1Q	Median	3Q	Max
-0.55112	-0.10528	0.01444	0.09568	0.61352

Coefficients:

	Estimate	Std. Error	t value	Pr(>|t|)
(Intercept)	-0.400954	0.571987	-0.701	0.4856
platthick	0.087193	0.078160	1.116	0.2684
epa	0.017977	0.008401	2.140	0.0358 *
aob	-0.024644	0.002583	-9.539	2.39e-14 ***
platthick:epa	0.002634	0.001205	2.186	0.0321 *

Signif. codes: 0 '***' 0.001 '**' 0.01 '*' 0.05 '.' 0.1 ' ' 1
Residual standard error: 0.185 on 71 degrees of freedom
Multiple R-squared: 0.9139, Adjusted R-squared: 0.9091
F-statistic: 188.4 on 4 and 71 DF, p-value: < 2.2e-16

2 Figures from the Dibble experiments

With this synthesis paper, we will be sharing the data produced by the Dibble and colleague experiments (at www.pennlithicexp.net). The database from the experiments was maintained over the years by Dibble. On his passing, we obtained a copy. However, this database includes a lot of cases (flakes and cores) and variables that were never used in the papers published by Dibble and colleagues for various reasons. As for the cases, for instance, some experiments did not work properly, or some flakes represented only tests of the experimental setup. As for the unpublished variables, again, some of these measures just did not yield interesting results. The main complication is that there was not a list of which cases were used in which papers, and as the experiments continued, some cases were naturally used in multiple papers.

Our approach to solving this problem was to filter the database based on our collective knowledge of the experiments and their results, and then one of us (LL with some help from SPM) replicated the figures and main results of each of the experimental papers. When we compare the results presented here with the published papers, we find individual differences, but the overall pattern is the same. In other words, we cannot be sure to have included exactly the same set of cases in each instance, but our results are in line with the previously published results.

2.1 Dibble and Rezek (2009)

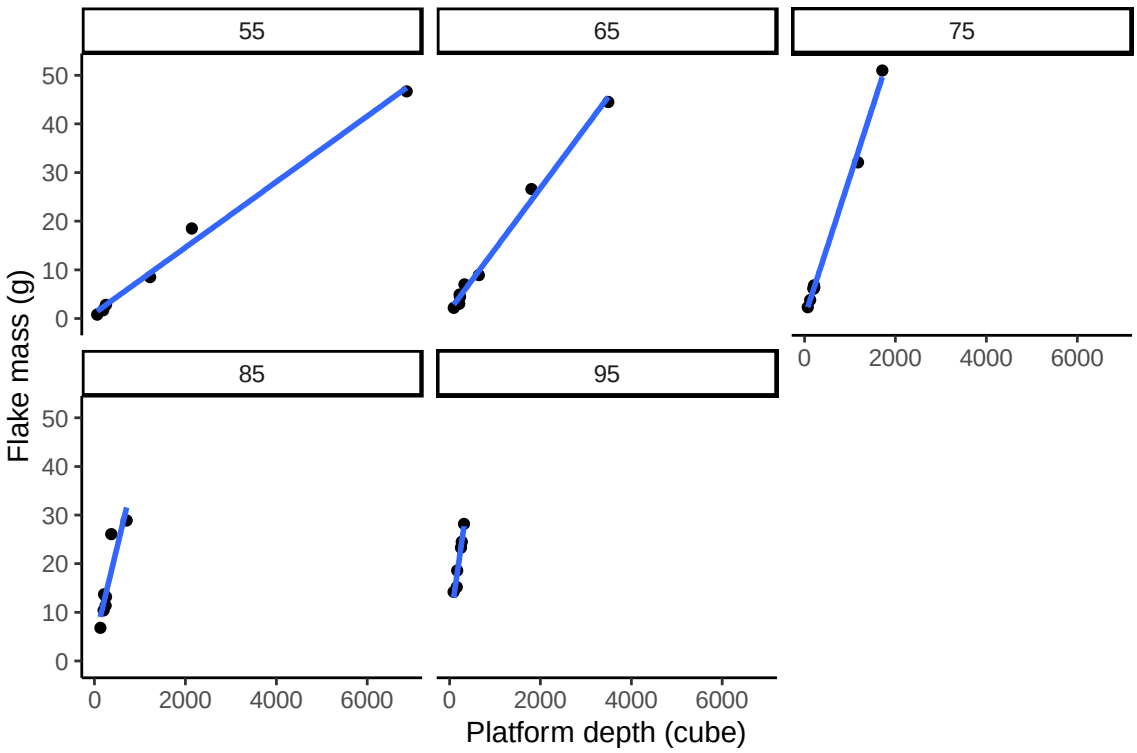

Fig.Appx-I. 1 Relationship between flake mass and PD (cubed)

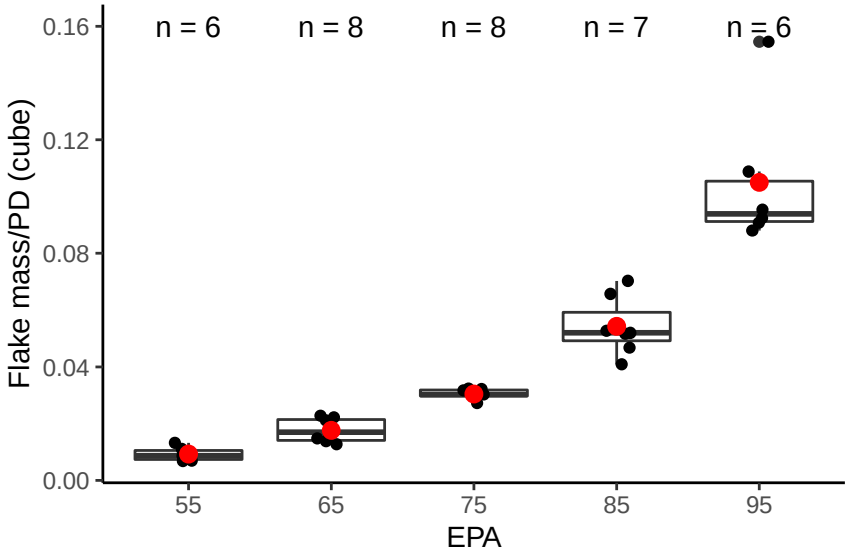

Fig.Appx-I. 2 Box plot showing relationship between flake mass standardized by PD (cubed) and EPA

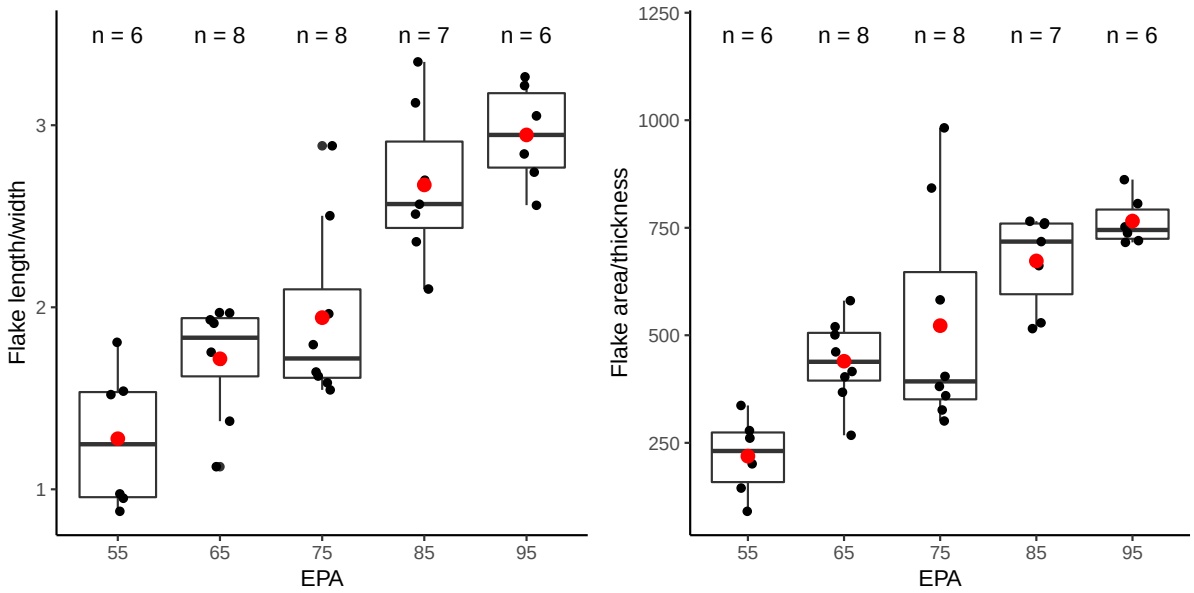

Fig.Appx-I. 3 Boxplot showing changes in flake shape (left: length to width, right: area to thickness) as affected by different values of EPA

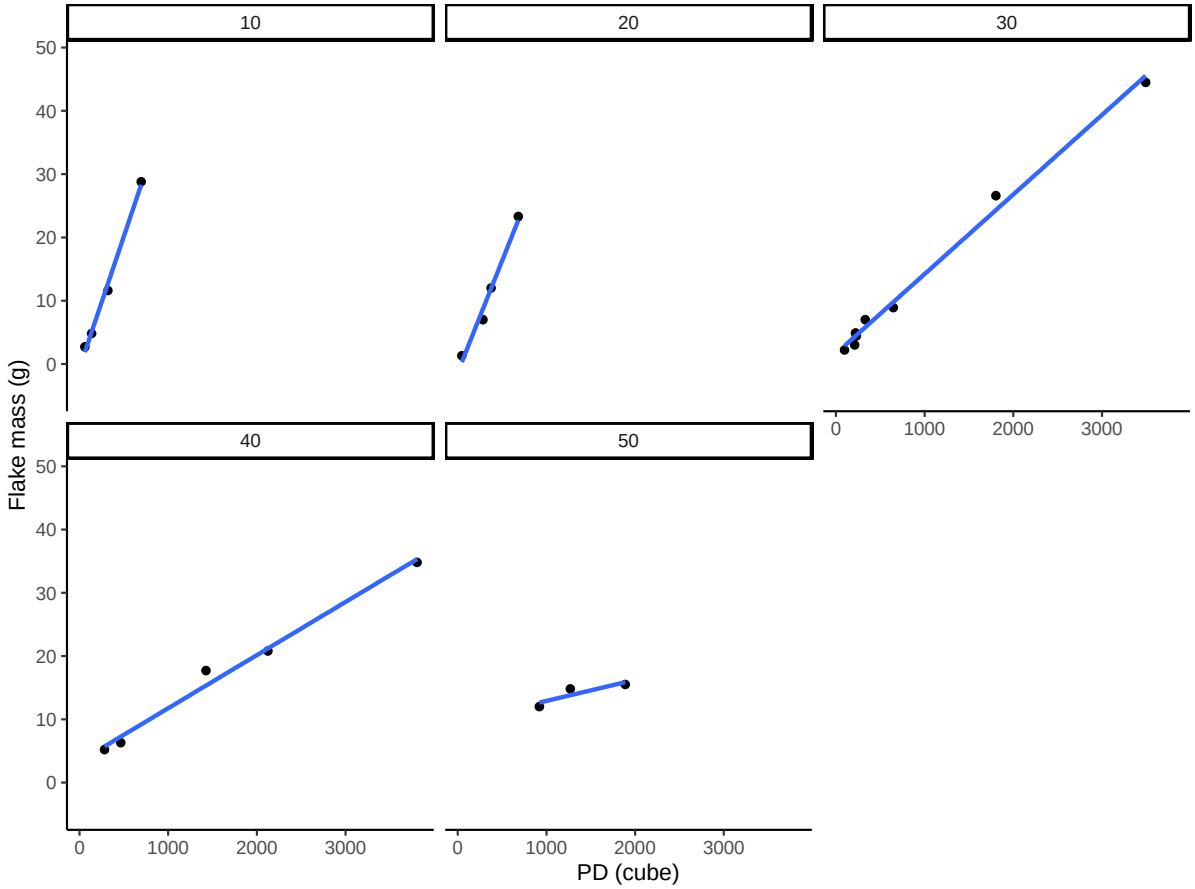

Fig.Appx-I. 4 Relationship between flake mass and PD (cubed) for different AOBs

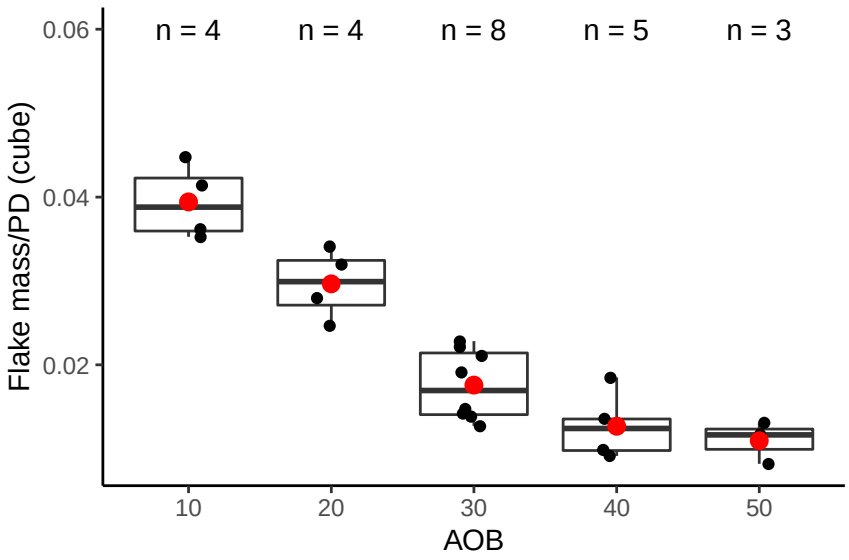

Fig.Appx-I. 5 Boxplot showing relationship between flake mass standardized by PD (cubed) for different AOBs

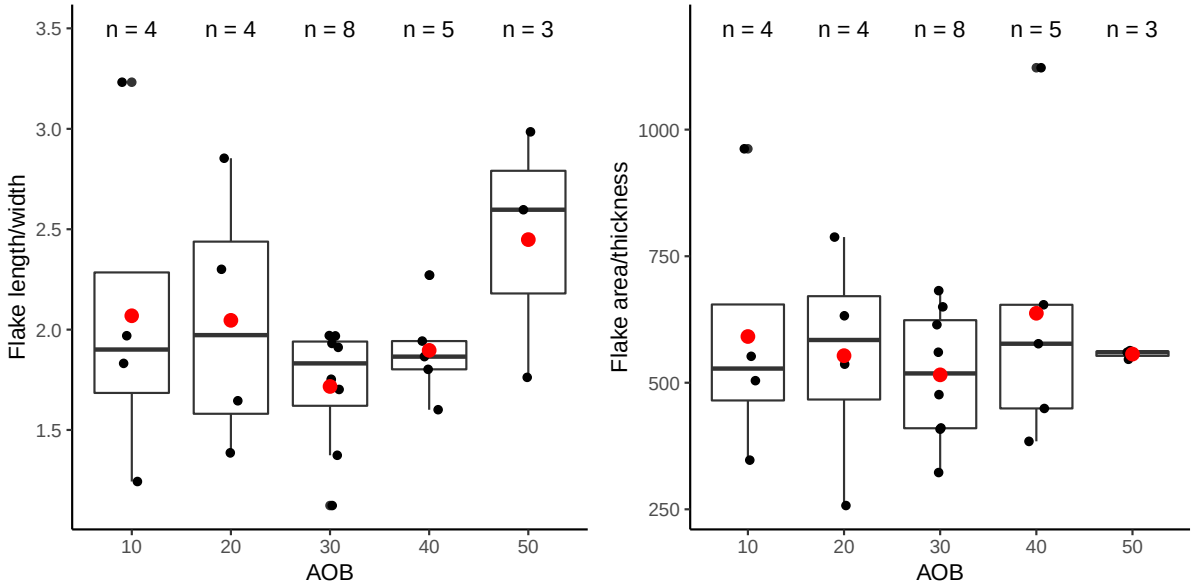

Fig.Appx-I. 6 Boxplot showing changes in flake shape (left: length to width, right: area to thickness) as affected by different AOBs

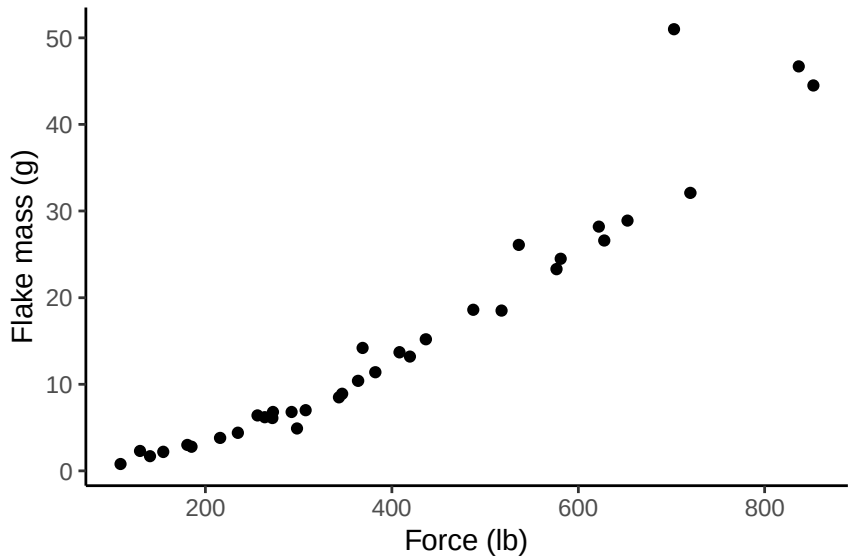

Fig.Appx-I. 7 Flake mass as a function of force

2.2 Rezek et al. (2011)

Table.Appx-I. 1 Dataset overview, breakdown of the number of flakes by core morphology and EPA

Core type	55	65	75
SEMISPHERICAL	7	4	7
CENTERRIDGE	4	8	6
CONVERGENT	12	3	7
DIVERGENT	5	5	6
PARALLEL	5	8	6

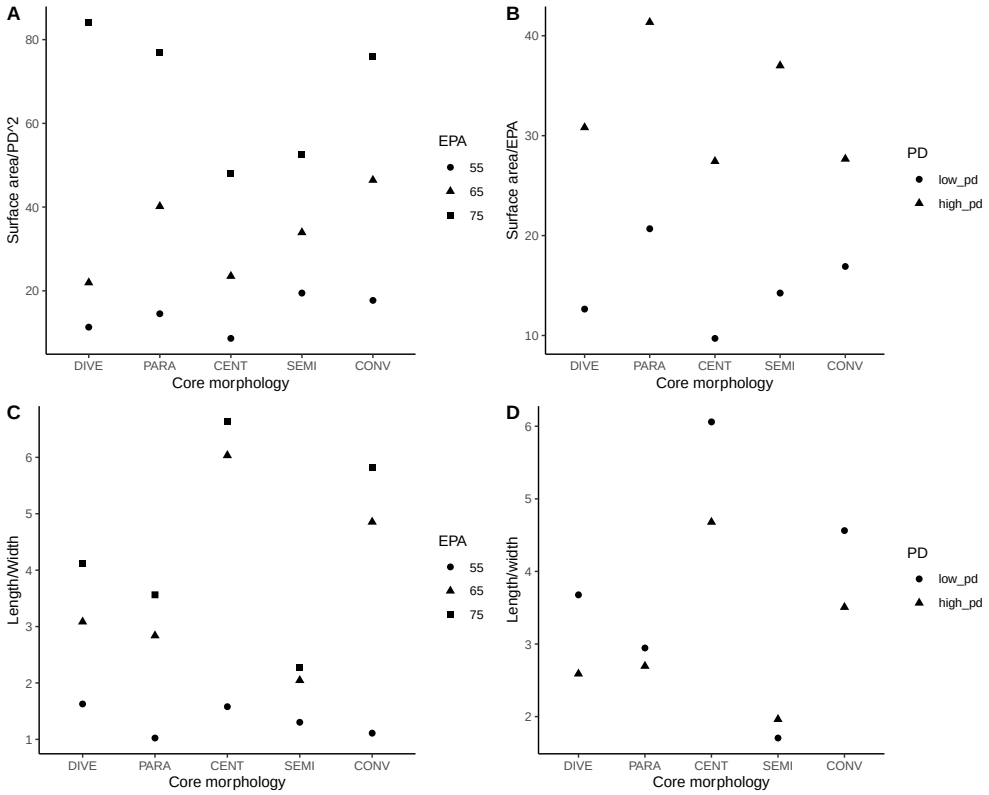

Fig.Appx-I. 8 Graphs of both intra- and inter-Core variability on flake surface area, either controlling for PD (graph A) or EPA (graph B) and length/width (graphs C and D)

2.3 Magnani et al. (2014)

Table.Appx-I. 2 Presence or absence of lipping by hammer material. Includes EPA = 55, 65, and 75, all values of AOB, and both locations of force (strikes both on the platform surface and the exterior edge of the platform)

Hammer material	Platform lipping	% Lipped
BONE50	50	98.04%
COPPER	35	56.45%
STEEL	20	33.90%

Table.Appx-I. 3 Presence or absence of lipping by EPA, including flakes struck with both copper and steel hammers, both force locations, and a full range of AOBs. The lack of association with EPA holds even if AOB or location of force is controlled

EPA	Lipped	Not lipped	% Lipped
55	4	1	80.00%

65	37	49	43.02%
75	14	16	46.67%

Table.Appx-I. 4 Presence or absence of lipping by location of force. All flakes were produced with the copper hammer, EPA = 65, a full range of AOBs are included

Force type	Lipped	Not lipped	% Lipped
Platform surface	5	11	31.25%
Exterior platform edge	20	13	60.61%

Table.Appx-I. 5 Presence or absence of lipping by AOB. All flakes were produced with copper hammer and EPA = 65. Flakes produced by both locations of force (on edge or on platform) are included

AOB	Lipped	Not lipped	% Lipped
Negative AOB	20	6	76.92%
Positive AOB	5	18	21.74%

Table.Appx-I. 6 Relationship between location of force and the ratio of platform area to flake area, broken down by the presence or absence of lipping (EPA = 65, AOB = 5, all hammer types included)

Lipping	Force type	Mean	Count	SD
NO	Platform surface	0.034	6	0.008
NO	Exterior platform edge	0.010	4	0.006
YES	Platform surface	0.027	3	0.006
YES	Exterior platform edge	0.014	4	0.003

Table.Appx-I. 7 Mean values and sample size (N) of various dimension ratios by shape and size of the hammer (EPA = 65, AOB = 0, steel hammers). The first three entries of the table refer to the hammers with rounded tips

Hammer end	N	Len/Wid	Len/Thick	Wid/Thick	Len/PD	Wid/PD	Thick/PD	Weight (cube)/PD
3.2 mm	3	1.59	16.50	9.52	10.51	6.63	0.74	0.08
6.47 mm	3	1.32	11.16	8.05	9.37	7.02	0.92	0.08
9.61 mm	3	1.54	15.18	8.56	8.68	6.29	0.84	0.06
FLAT	2	1.32	15.81	10.87	14.57	10.36	0.98	0.18
EDGE	2	1.96	14.88	7.58	12.81	6.36	0.84	0.10

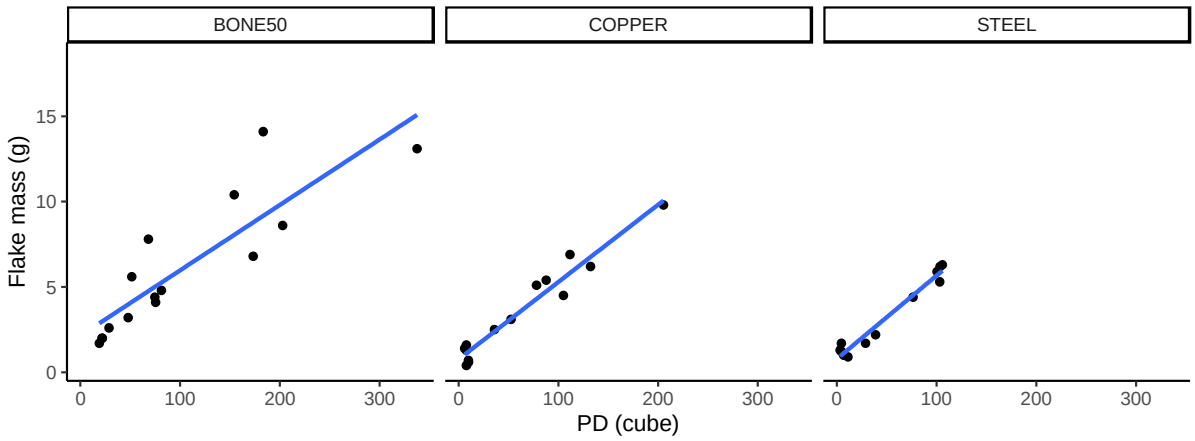

Fig.Appx-I. 9 Scatter diagrams and correlations between flake weight and platform depth cubed by hammer material (EPA = 65, AOB = 5, both platform surface-struck and edge-struck flakes are included)

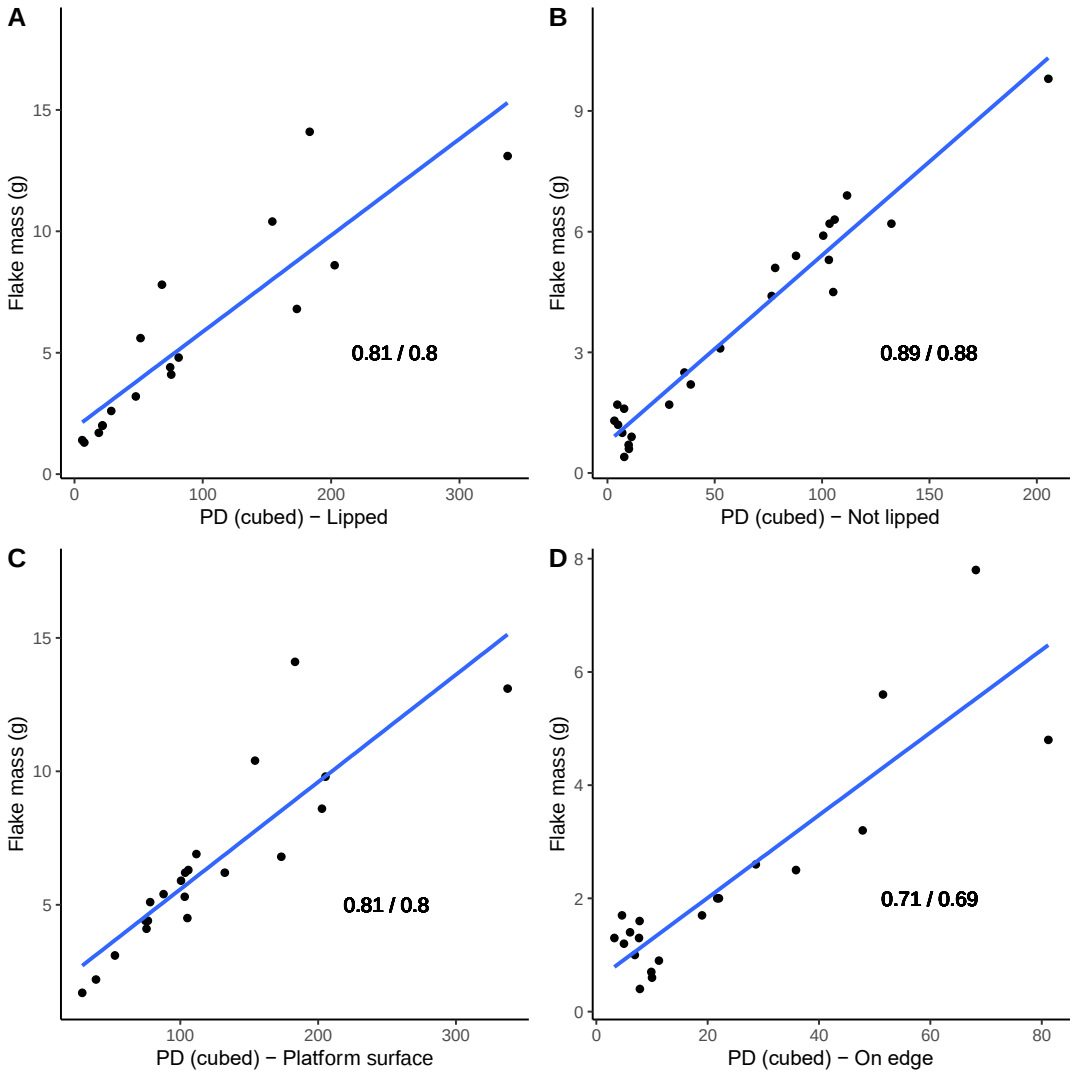

Fig.Appx-I. 10 Correlations between flake weight and platform depth cubed for lipped and unlipped flakes, both platform-struck and edge-struck flakes are included. AOB = 5, EPA = 65, R^2 and adjusted R^2 are displayed on each plot

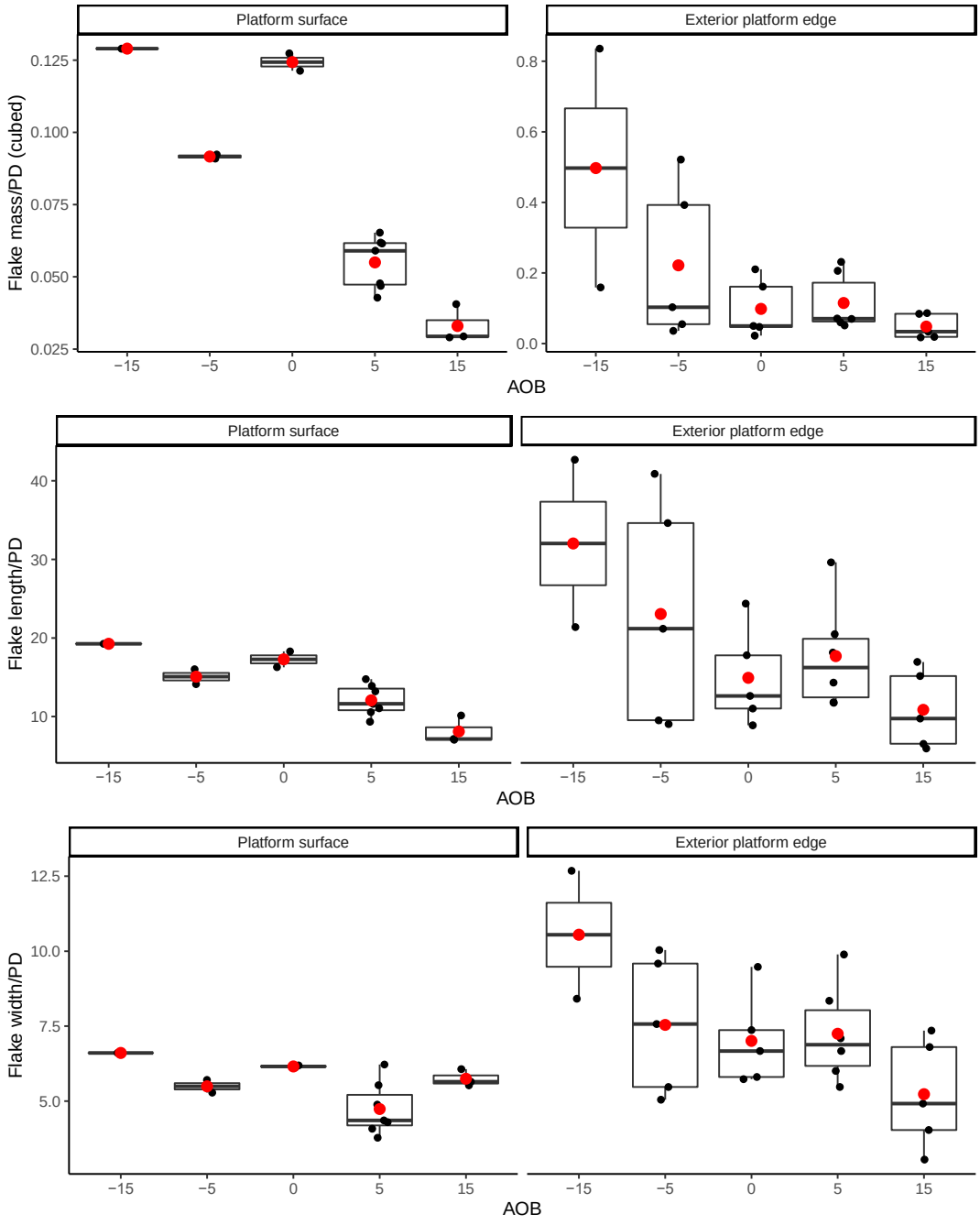

Fig.Appx-I. 11 Flake weight relative to platform depth cubed by angle of blow (EPA = 65, copper hammer). Note that the means of weight/platform depth cubed between edge-struck and platform-struck are not significantly different, except in the case of AOB = 5

2.4 Leader et al. (2017)

Table.Appx-I. 8 Basic descriptive statistics and tests among different both platform depth and initial platform depth

Bevel type	N	Weight/PD (cube)	Weight/Initial PD(cube)
CONCAVE_2	7	0.129	0.039
CONCAVE_4	8	0.405	0.032
CONCAVE_6	8	1.136	0.030
FLAT_2	9	0.213	0.064
FLAT_4	6	0.178	0.033
FLAT_6	3	0.481	0.003
UNBEVELED_75	11	0.061	0.061
UNBEVELED_90	5	0.182	0.182

Table.Appx-I. 9 Averages of bevel width, G2 refers to the 2mm bevel, G4 refers to the 4mm bevel, G4-8 refers to the narrow 4mm bevel, G4-30 refers to the wide 4mm bevel, G6 refers to the 6mm bevel

Bevel type	N	Bevel width
G2	7	13.90
G4	8	18.32
G4-30	6	27.11
G4-8	7	7.72
G6	8	20.61

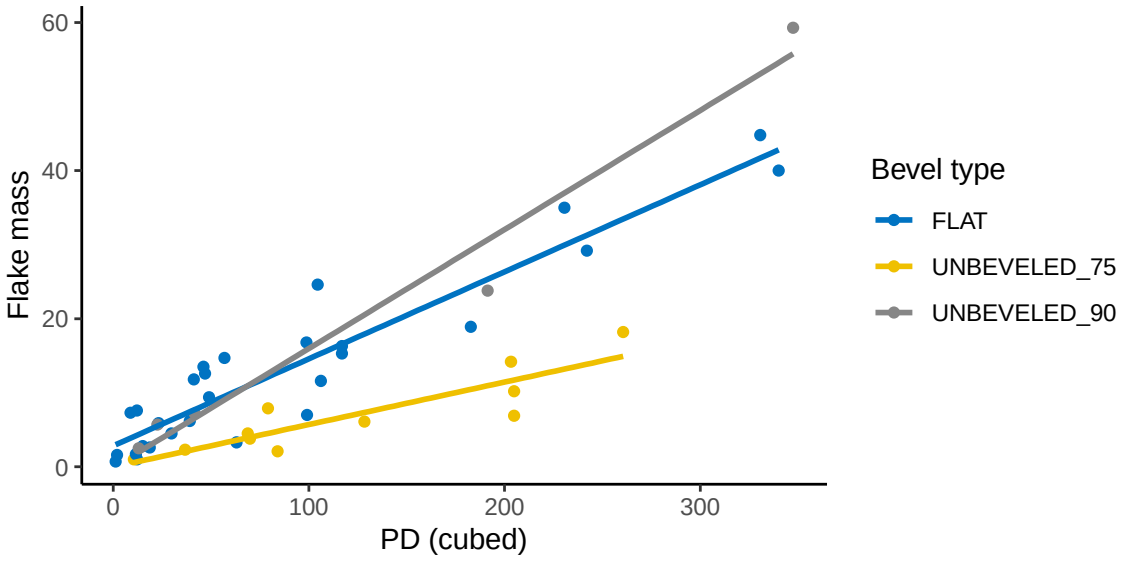

Fig.Appx-I. 12 Scatter plot of flake weight and platform depth cubed for combined sample of flat-beveled flakes and unbeveled flakes produced with EPA of 75 and 90. In the bevel field, GRINDER represents concave bevel, SANDER represents flat bevel, and NONE represents either no bevel or lateral bevel

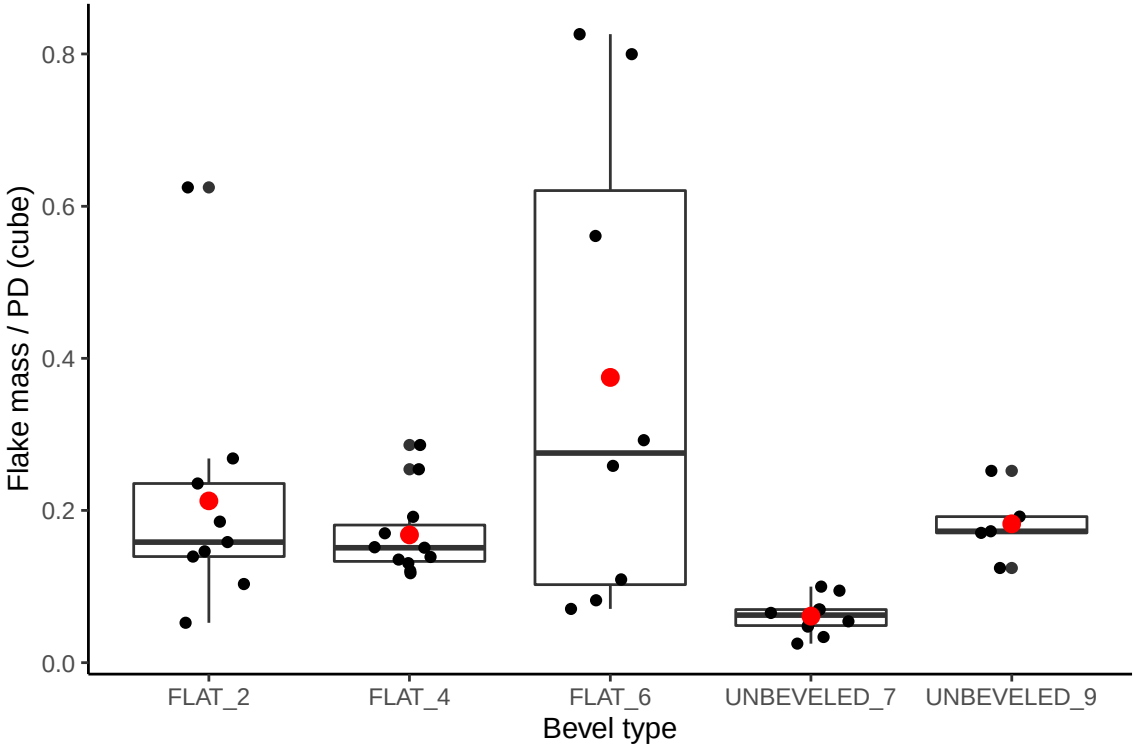

Fig.Appx-I. 13 Boxplot of the ratio of flake weight to platform depth cubed for flat-beveled flakes compared with unbeveled flakes with EPA of 75 and 90

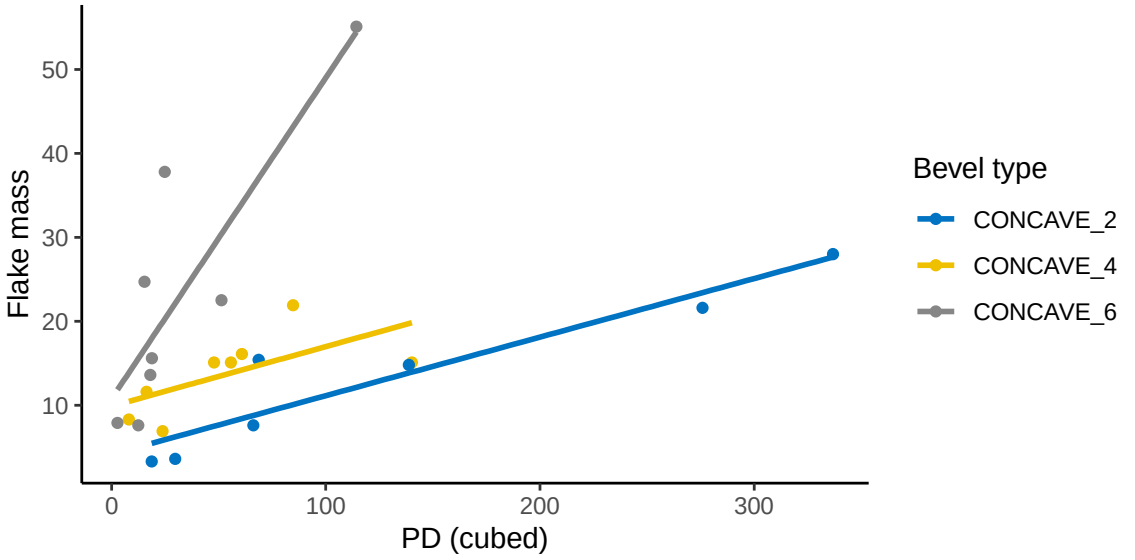

Fig.Appx-I. 14 Scatter plot of flake weight and platform depth cubed for combined sample of concave-beveled flakes and unbeveled flakes produced with EPA of 75 and 90

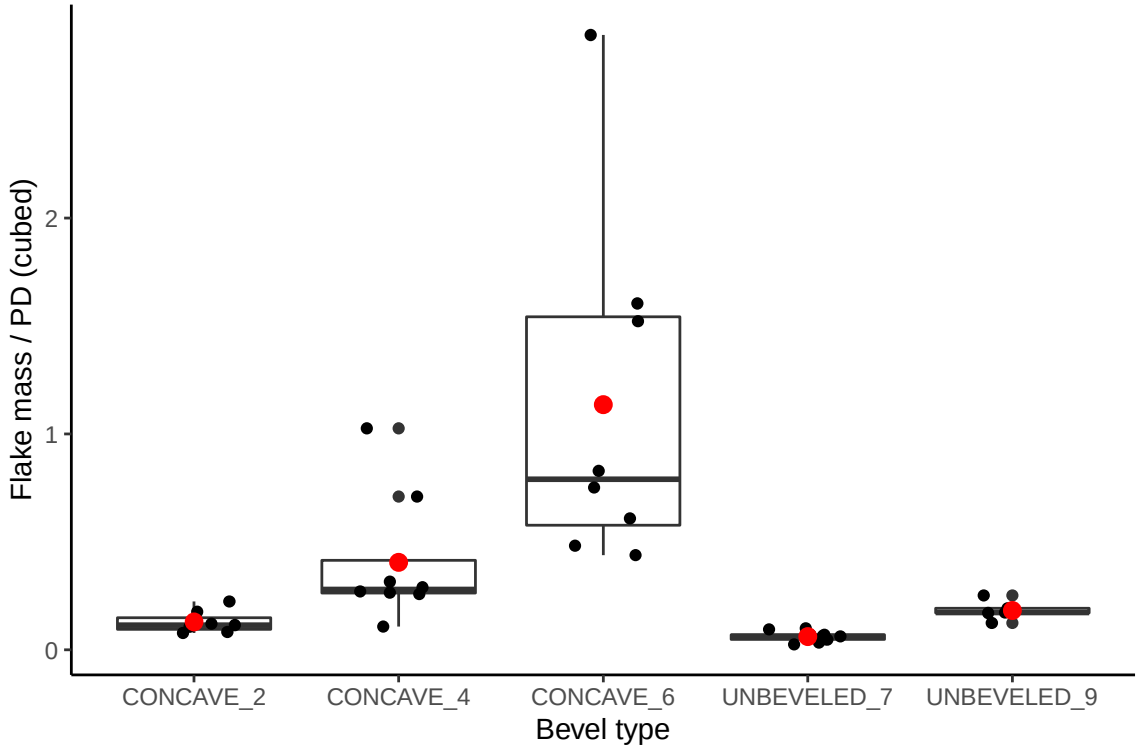

Fig.Appx-I. 15 Boxplots of the ratio of flake weight to platform depth with unbeveled flakes with EPA of 75 and 90

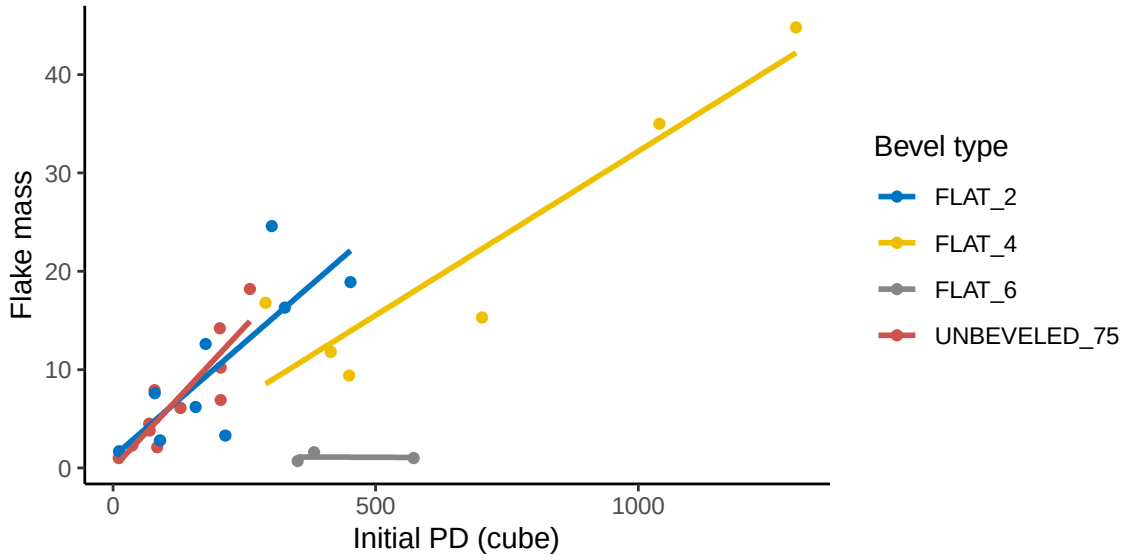

Fig.Appx-I. 16 Scatter plot of flake weight and initial platform depth cubed for flat-beveled flakes of different bevel depths and unbeveled flakes produced with EPA = 75

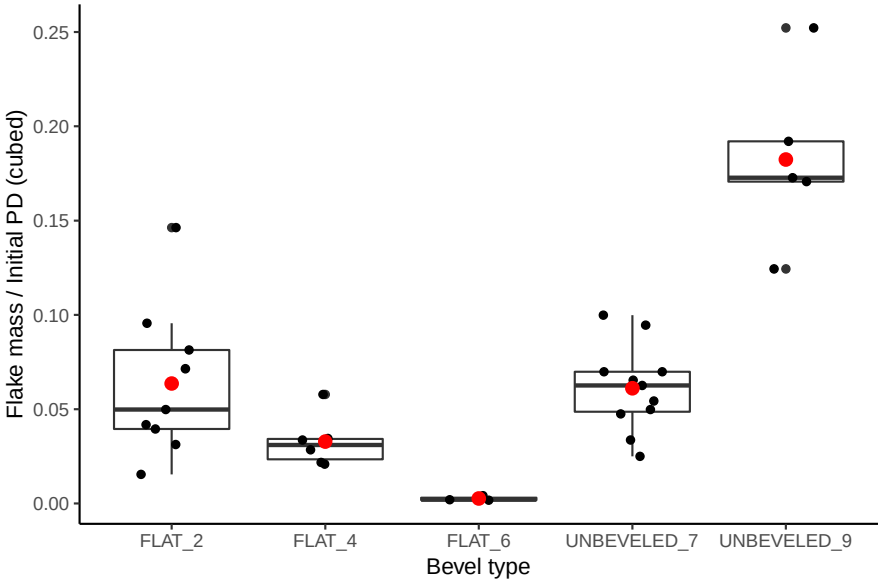

Fig.Appx-I. 17 Boxplot of the ratio of flake weight to initial platform depth cubed for flat-beveled flakes compared with unbeveled flakes, EPA = 75 and 90

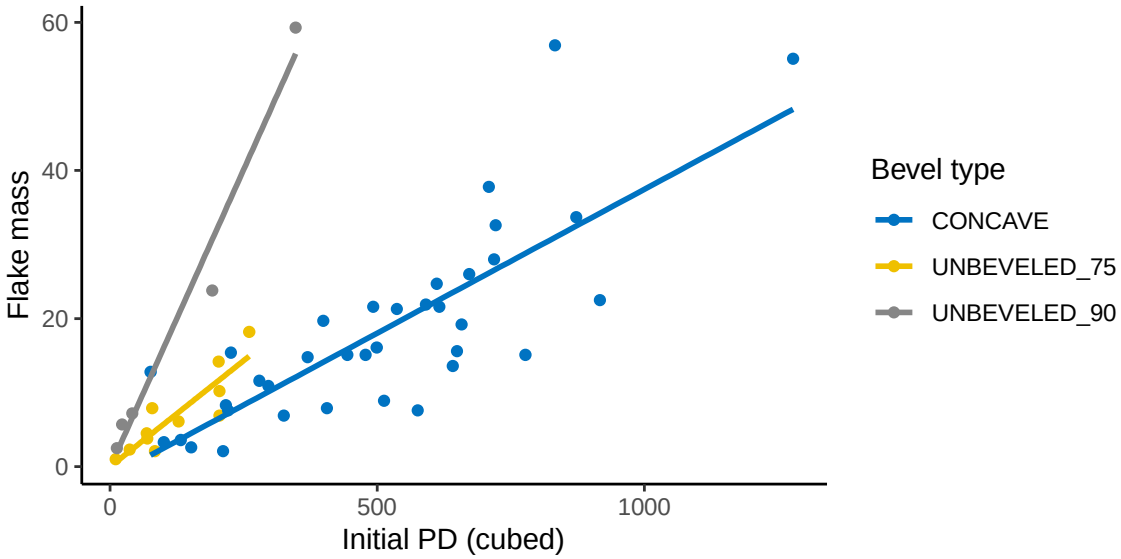

Fig.Appx-I. 18 Scatterplot of flake weight and initial platform depth cubed for concave-beveled flakes of different bevel depths and unbeveled flakes produced with EPA = 75 and 90

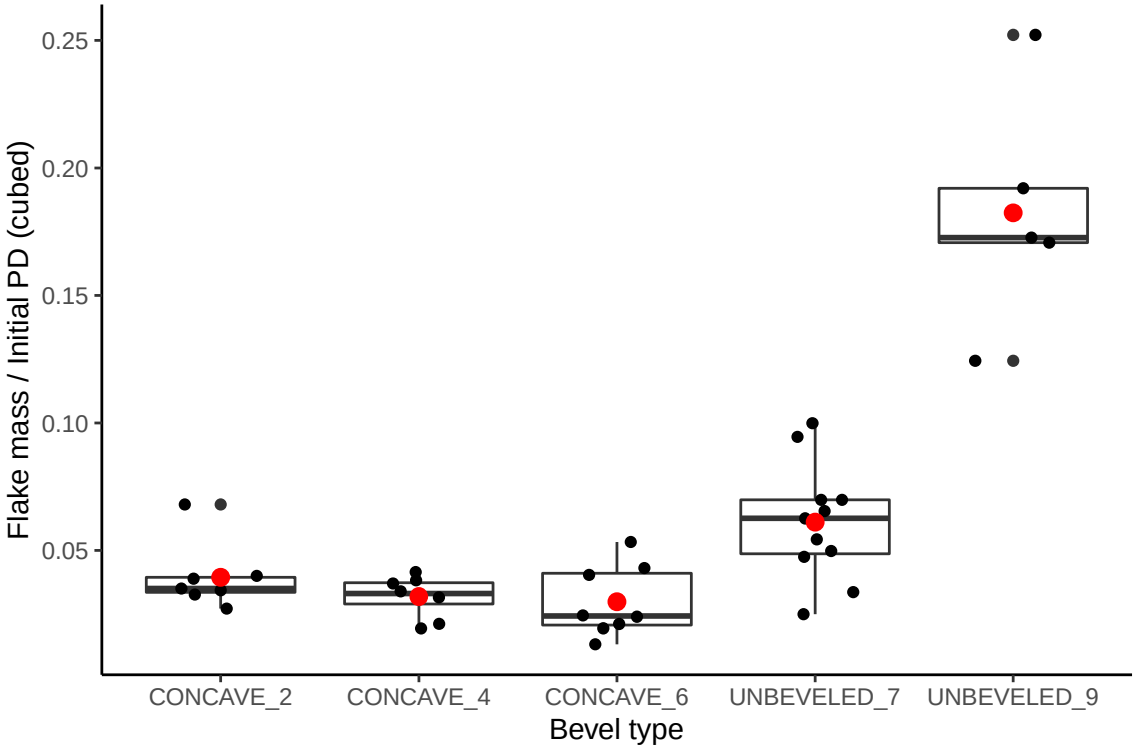

Fig.Appx-I. 19 Boxplot of the ratio of flake weight to initial platform depth cubed for concave-beveled flakes compared with unbeveled flakes, with EPA = 75 and 90

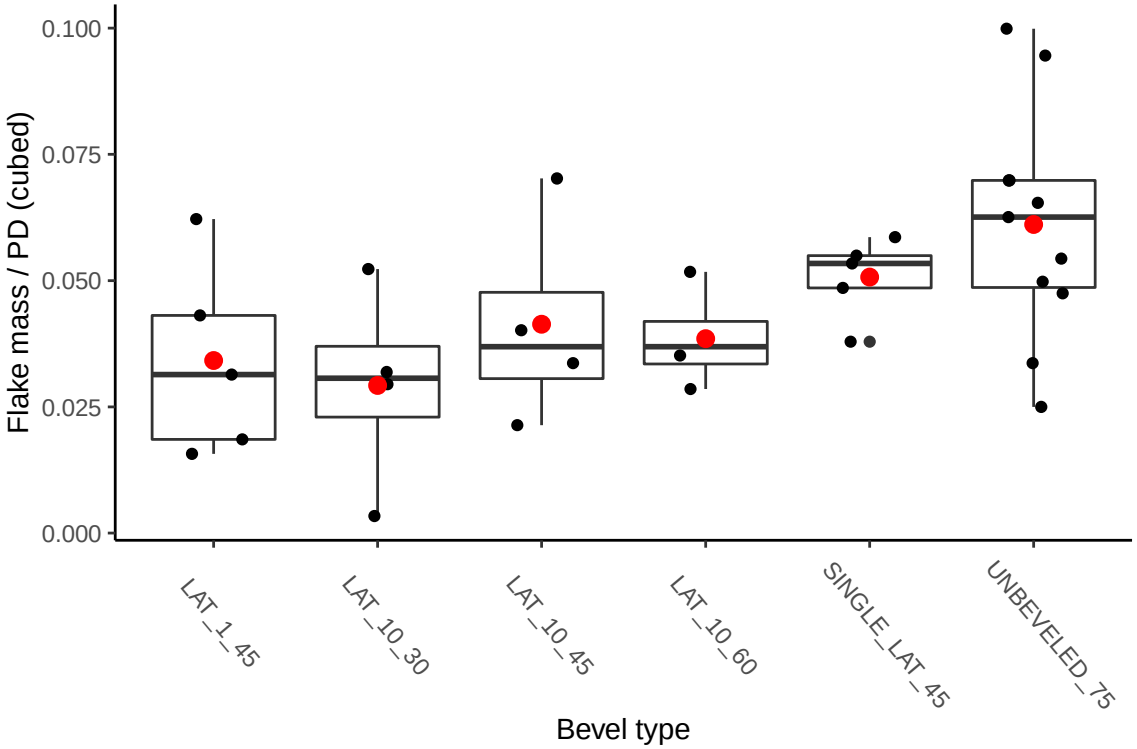

Fig.Appx-I. 20 Boxplot of the ratio of flake weight to platform depth cubed for various classes of laterally-beveled flakes compared with unbeveled flakes with EPA = 75

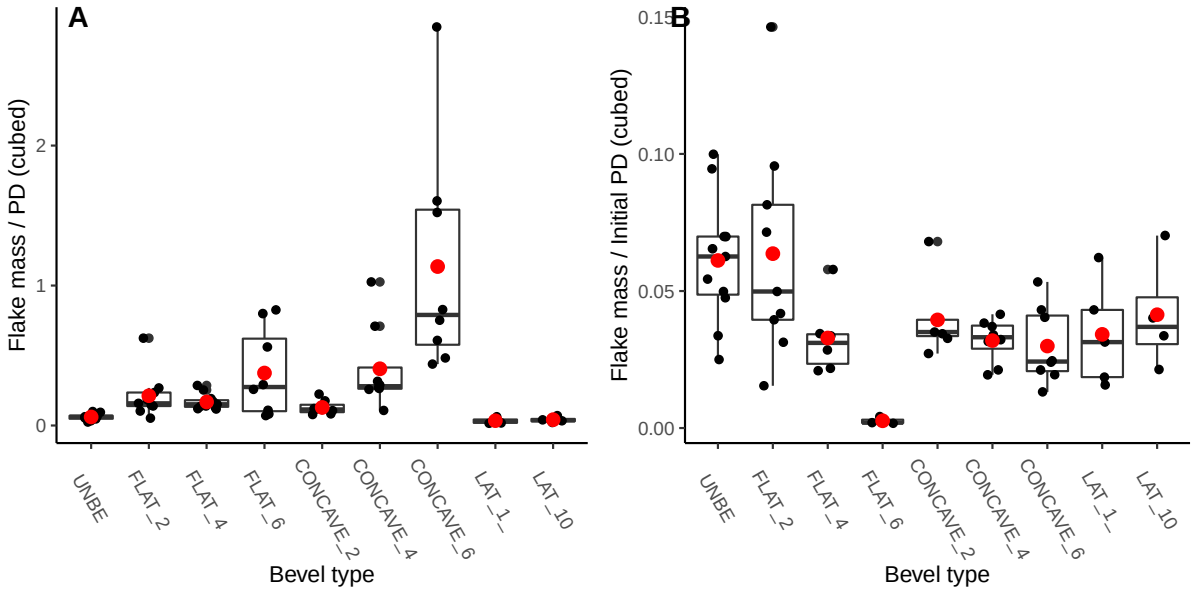

Fig.Appx-I. 21 Boxplots showing ratios of (A) flake weight to platform depth and (B) flake weight to initial platform depth for various classes of bevels

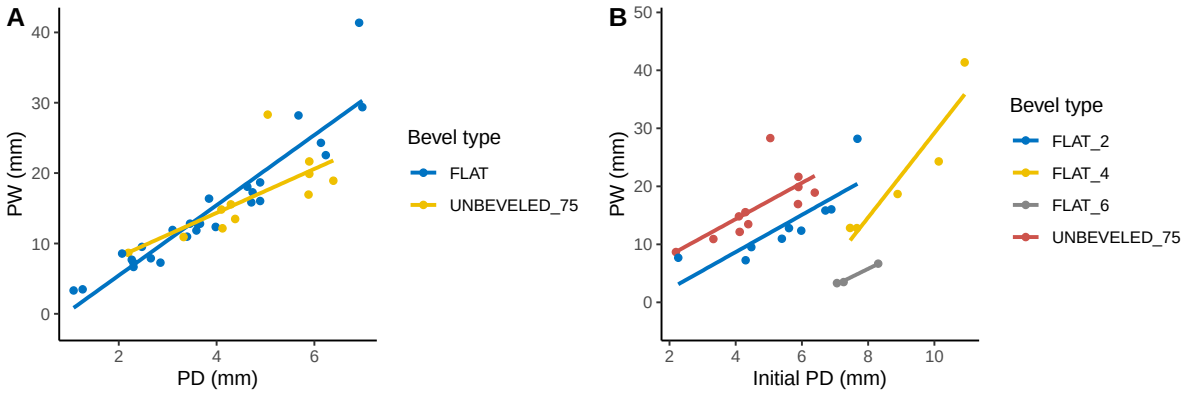

Fig.Appx-I. 22 Scatterplots showing (A) platform width to platform depth for all bevel depths of flat-beveled flakes, (B) platform width vs. initial platform depth for each bevel depth of flat- beveled flakes

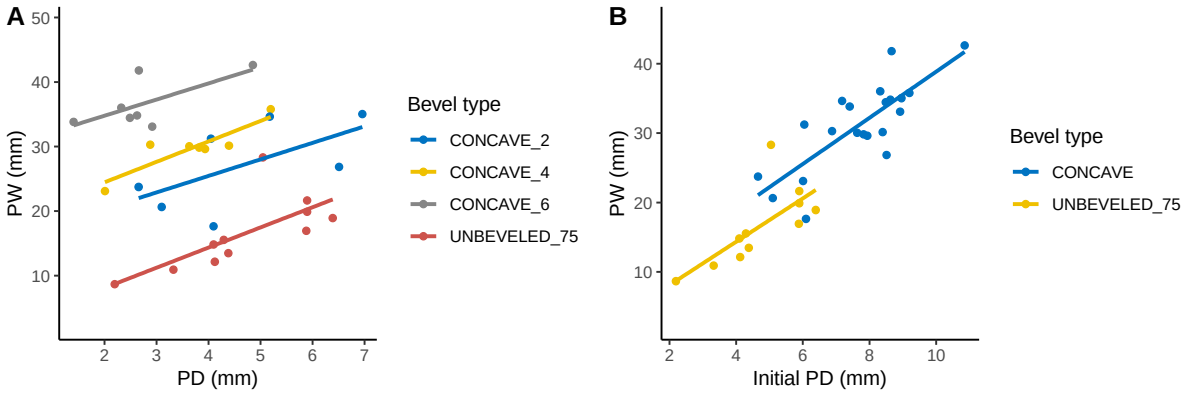

Fig.Appx-I. 23 Scatter plots showing (A) platform width to platform depth for each bevel depth of concave-beveled flakes, (B) platform width vs. initial platform depth for all bevel depths of concave-beveled flakes

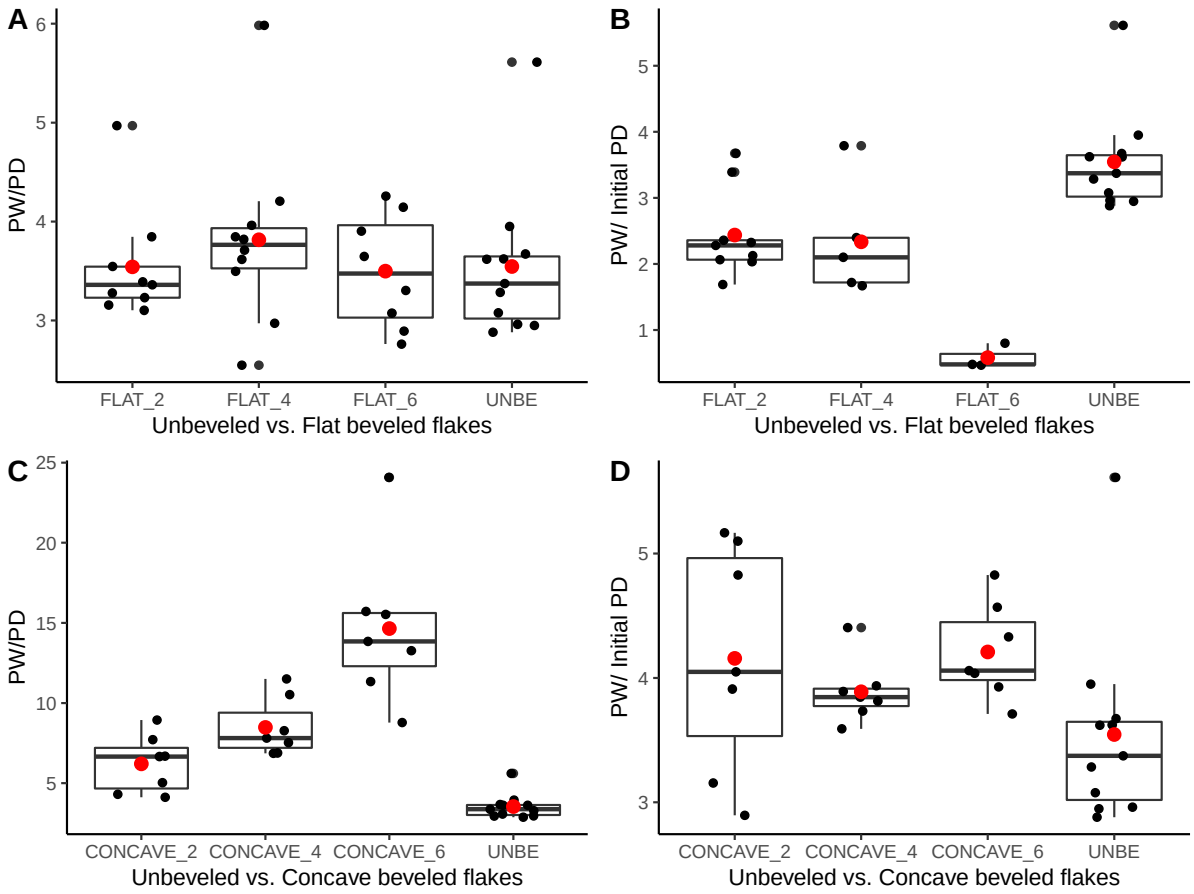

Fig.Appx-I. 24 Boxplots of ratios of platform width to both platform depth and initial platform depth. (A) Platform width to platform depth, flat-beveled flakes; (B) Platform width to initial platform depth, flat-beveled flakes; (C) Platform width to platform depth, concave-beveled flakes; (D) Platform width to initial platform depth, concave-beveled flakes

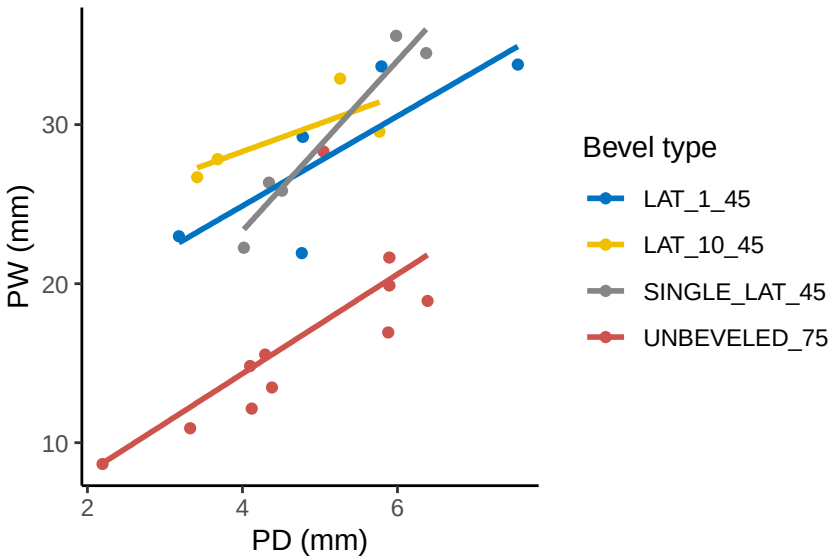

Fig.Appx-I. 25 Relationship between platform width and platform depth for unbeveled cores, laterally-beveled cores with 1 mm and 10 mm platform surface, and cores with single lateral bevels. All bevel angles at 45° relative to the platform surface

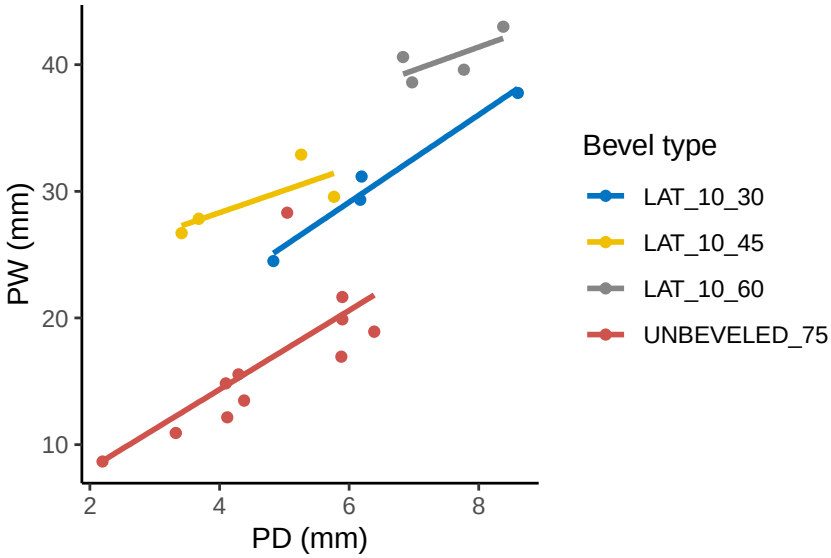

Fig.Appx-I. 26 Relationship between platform width and platform depth for unbeveled cores and laterally-beveled cores with bevel angles at 30°, 45°, and 60° relative to platform surface. All platform surfaces of the beveled cores have a width of 10 mm

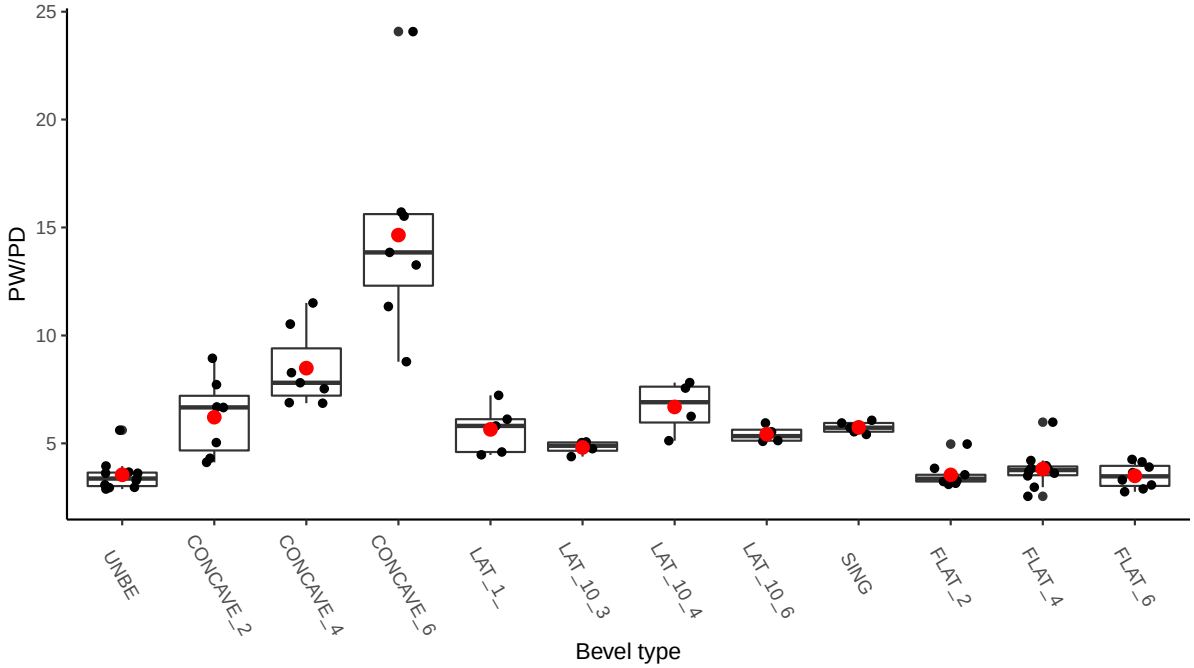

Fig.Appx-I. 27 Boxplots of ratio of platform width to platform depth for all of major bevel classes described above

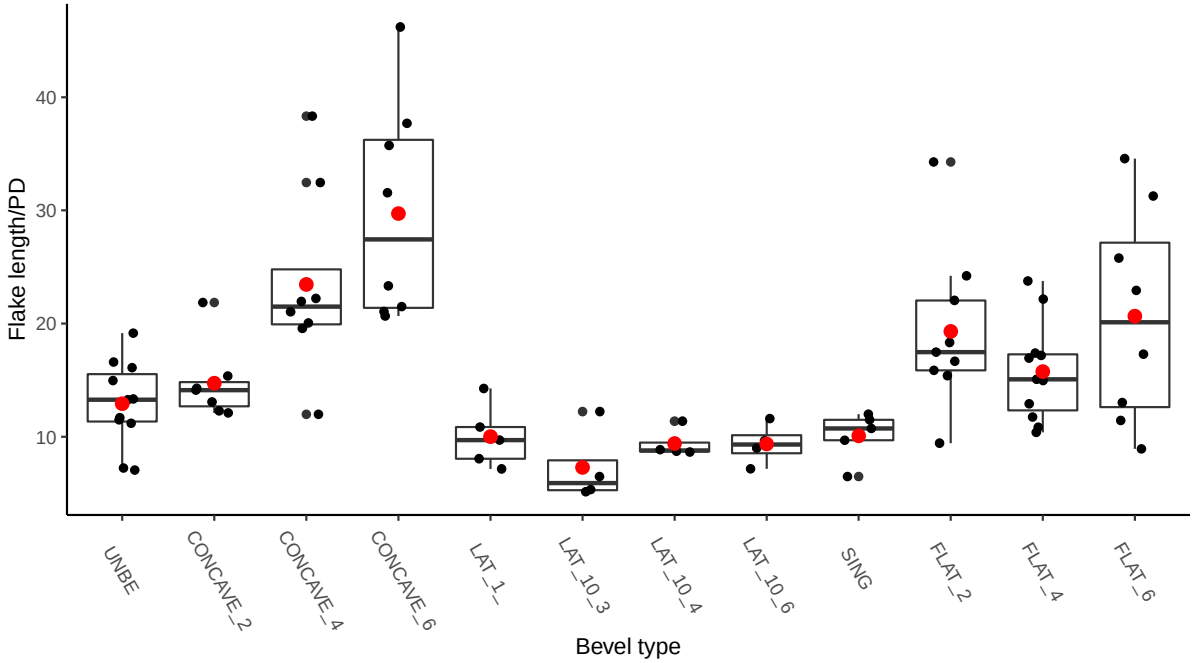

Fig.Appx-I. 28 Box plots of ratio of flake length to platform depth for all major bevel classes described above

2.5 Dogandžić et al. (2020)

Table.Appx-I. 10 Sample size by raw material and by EPA

EPA	Glass	Basalt	Flint	Obsidian
65	4	5	5	5
75	4	7	6	6
85	3	4	4	4

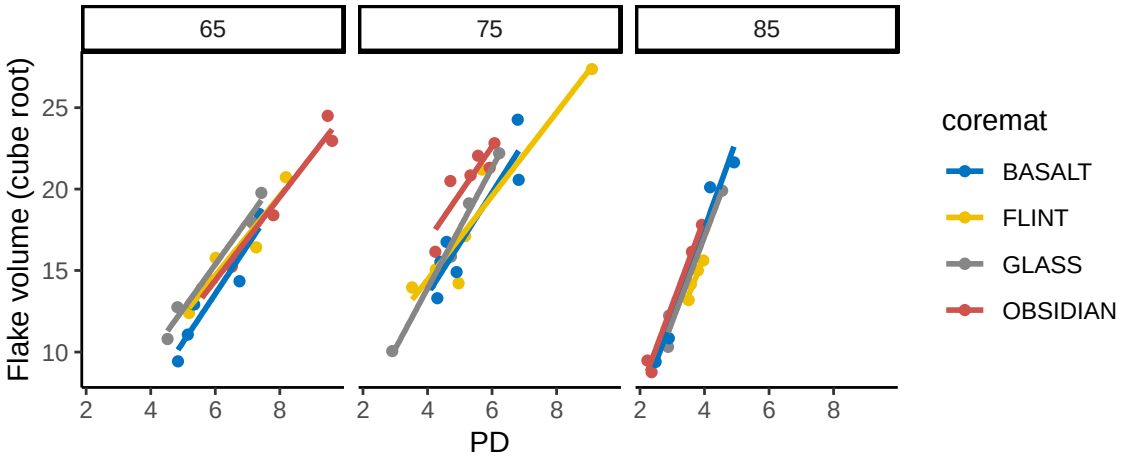

Fig.Appx-I. 29 Volume (cube root) as a function of platform depth for each EPA group, by raw material

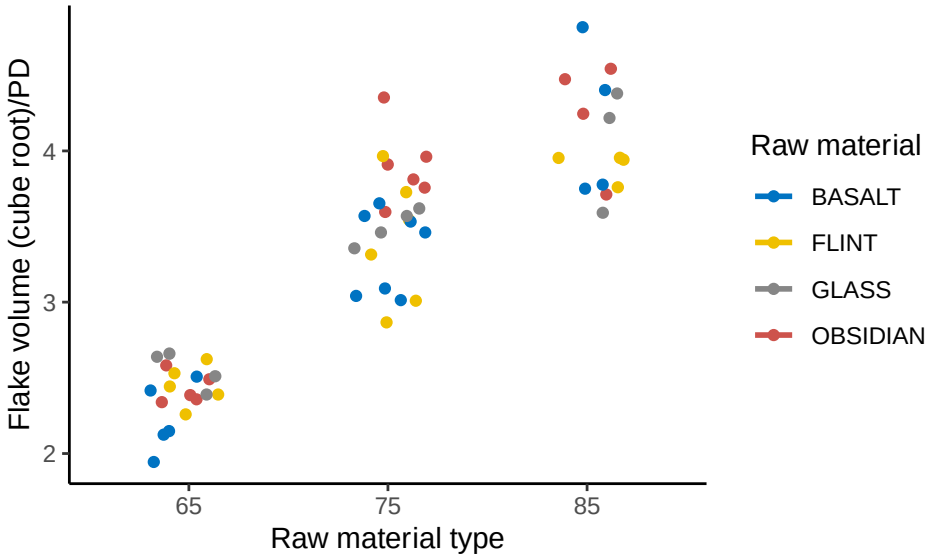

Fig.Appx-I. 30 Dotplot showing the effect of EPA on flake volume (cube root of volume is standardized by platform depth) for different raw materials

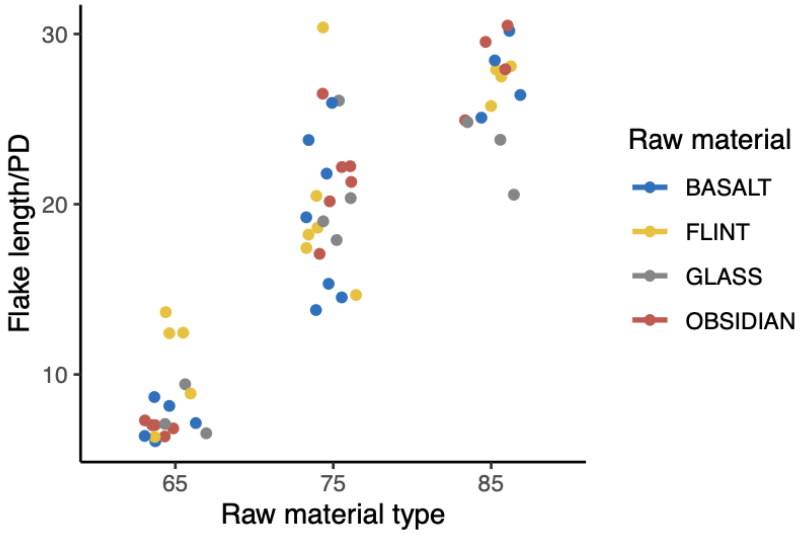

Fig.Appx-I. 31 Dotplot showing the effect of EPA on flake length (standardized by platform depth) for different raw materials

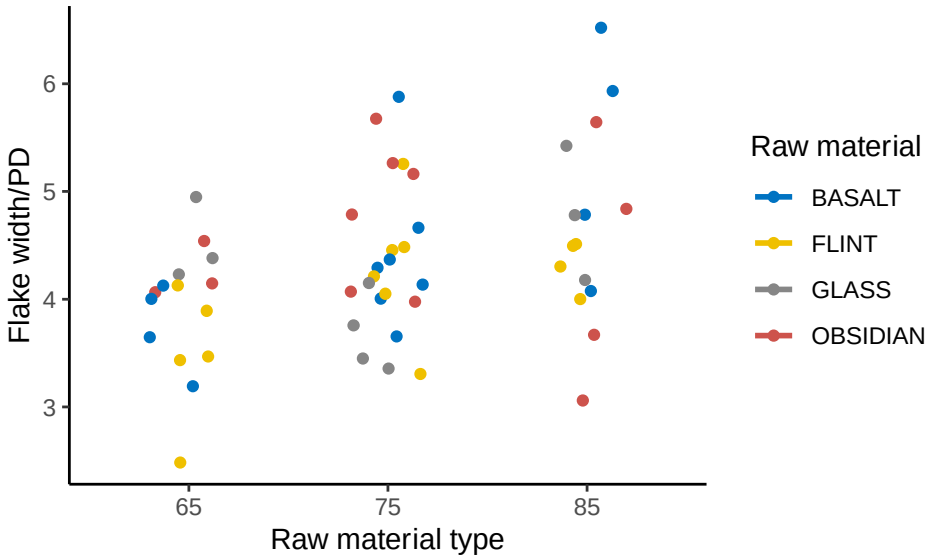

Fig.Appx-I. 32 Dotplot showing the effect of EPA on flake width (standardized by platform depth) for different raw materials

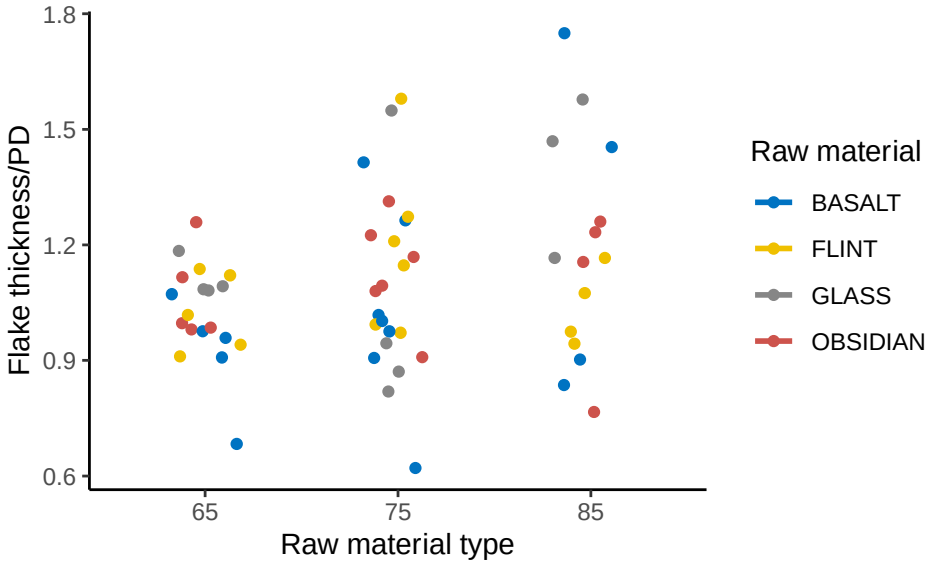

Fig.Appx-I. 33 Dotplot showing the effect of EPA on flake thickness (standardized by platform depth) for different raw materials

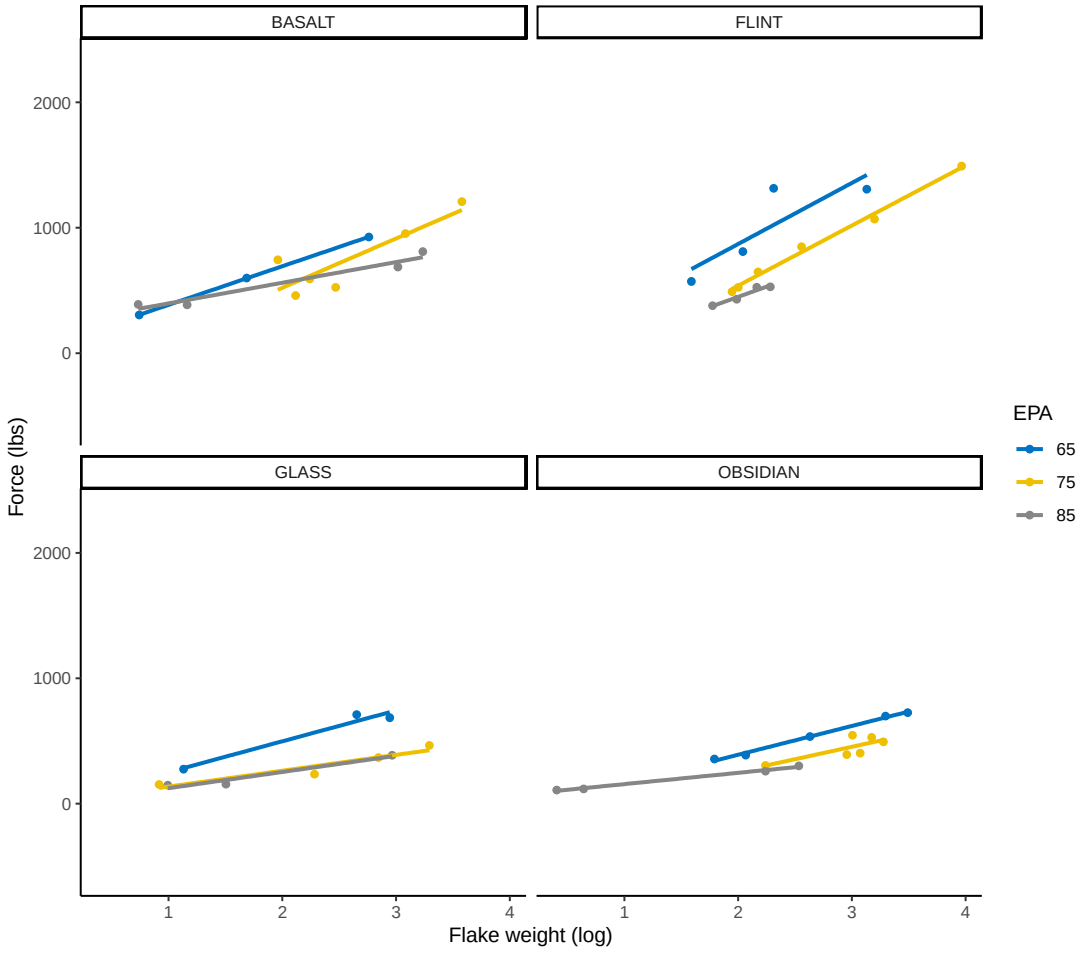

Fig.Appx-I. 34 Relationship of force required to remove flakes by weight (log transformed) for different raw materials and varying EPAs

3 A description of each of the variables in the controlled experiment dataset

3.1 Experimental design

[Caliper measurement] Caliper measurements were done with digital calipers with .01 mm precision.

[Electronic scales] Various types of electronic scales were used to weigh the flakes and cores. These were precise to .1 grams. Scales were not cabled directly to the data collection computers.

[Angle measurements] These were done with analog goniometers with 1-degree markings.

[Microscribe measurement] These refer to measurements taken with the Microscribe instrument. This instrument consists of an arm that can move freely in three dimensions. A stylus is attached to the end of this arm, and sensors throughout the arm are able to track its movement and exact orientation. The result of a measurement is an XYZ coordinate. We are unsure which particular Microscribe model was used in the Dibble lab, but we think the model used has an accuracy of less than .1 millimeters and that measurements were recorded with a precision of .01 millimeters.

[SQUID] All ID numbers consist of the letter E (for experiment) followed by a running sequence of numbers. Gaps in this series correspond mainly to the flakes or cores that were later considered unsuitable for inclusion in the experiments (e.g., they were tests or some aspect of the experiment failed).

[EXPERIMENT] Experimental design. Valid entries are BEVEL2016, COREMOPHOLOGY, ECONOMIC, HAMMER, RawMat, and blank. BEVEL2016: the Leader et al. (2017) study, COREMORPHOLOGY: the Rezek et al. (2011) study, ECONOMIC and the blank entries: the Dibble & Rezek (2009) study, HAMMER: the Magnani et al. (2014) study, and RawMat: the Dogandžić et al. (2020) study.

3.2 The independent variables tested in the experiments

[CORETYPE] Experimental design. Valid entries are CENTERRIDGE, CONVERGENT, DIVERGENT, PARALLEL, and SEMISPHERICAL.

CENTERRIDGE: cores with an external surface with a central ridge; CONVERGENT: cores with a center ridge on the exterior surface and two side ridges that meet at the distal end; DIVERGENT: cores with a center ridge and two side ridges that meet at the proximal end; PARALLEL: cores with three parallel ridges on the exterior surface; SEMISPHERICAL: cores with a smooth and half spherical exterior surface. For more information see Rezek et al. (2011:1348) and Dibble & Rezek (2009:1946).

[HMAT] Experimental design. Hammer material, valid entries are BONE50, COPPER, and STEEL. BONE50: synthetic bone; COPPER: copper; STEEL: steel. For more information see Magnani et al. (2014:39).

[FORCETYPE] Experimental design. Force type, valid entries are DYNAMIC, ON-EDGE, PUNCH. DYNAMIC and PUNCH: the hammer strikes directly on the platform with a fast velocity at some distance away from the core exterior surface; ON-EDGE: the hammer strikes on the exterior platform edge at a negative AOB (Magnani et al, 2014:38).

[HEND]. Experimental design. Hammer end, valid entries are 3.2, 6.47, 9.6, EDGE, FLAT, and ROUND. The numbers refer to the width of the steel hammer tips used in Magnani et al. (2014). For more information see Magnani et al. (2014:44).

[AOB] Experimental design. Angle measurement. Degrees. The angle at which the hammer strikes the platform. A perpendicular strike is 0 degrees. A strike angled into the core is negative degrees. A strike angled back towards the core surface is positive degrees. AOB values range from -20 to 50 at 5-degree intervals with the exceptions of 25, 35, and 45 degrees. See Dibble & Rezek (2009) and Magnani et al. (2014:38) for more information.

[EPA] Angle measurement. Degrees. EPA is the angle between the core surface and the platform surface recorded at the point of percussion (see Dibble & Rezek 2009: Fig.2). In these experiments, the platform surface was always flat, and the core surface immediately below the platform edge was also flat. Different EPAs were obtained by cutting platforms at the required angle using a diamond blade wet saw (Dibble & Rezek 2009:1949). EPA values range from 55 to 95 in 5-degree intervals

with the exception that 60 degrees and 80 degrees are not represented. EPAs of 75 and 65 degrees are by far the best represented in the dataset.

[BEVEL] Experimental design. Valid entries are GRINDER, NONE, and SANDER. GRINDER: flakes with concave bevels produced by a cylindrical grinding wheel; NONE: flakes with no bevels, or flakes with the lateral bevels only; SANDER: flakes with flat bevels produced by a sander. See Leader et al. (2017) for more information.

[NLATBEVELS] Experimental design. Valid entries are 1, 2, and NA. The numbers refer to the number of lateral bevels cut from the platform (Leader et al. 2017:214-215, Fig.3c).

[BEVELCUT] Experimental design. Bevel cut, this refers to the depth of the concave or flat bevels. Valid entries are 0, 2, 4, 6, and NA. The numbers refer to the depth of the bevel cut in millimeters. See Leader et al. (2017) for more information.

[BEVELCODE] Experimental design. Bevel code, valid entries are 0, 90, EC55, EC65, EC75, EC85, EC95, G2, G4, G4-30, G4-8, G6, P1, P10-30, P10-45, P10-60, P40, S2, S4, S6. G stands for the grinder bevel, and the number after represents the bevel depth in millimeters. For G4-30 and G4-8, 30 and 8 refer to the width of the concave bevel (with depth of 4 mm) in millimeters. S stands for the sander bevel, and the number after represents the bevel depth in millimeters. P stands for platform, and the number immediately after represents the different platform width intervals at which were the lateral bevels cut (1 mm, 20 mm, and 40 mm); the number behind the hyphen for P10 refers to the angle at which the lateral bevel was cut relative to the platform surface (Leader et al. 2017:214). See Leader et al. (2017) for more information. EC65, EC75, EC85, EC95 refer to the corresponding EPA value of the flakes.

[COREMAT] Experimental design. Core material, valid entries are BASALT, FLINT, GLASS, OBSIDIAN. This refers to the type of core raw material.

[APPARATUS] Experimental design. The apparatus used to run the experiment. valid entries are IGOR and SUPER_IGOR. IGOR refers to the experimental device that uses a pneumatic cylinder, SUPER_IGOR refers to the experimental device that uses a Servohydraulic press.

3.3 Results

[TERMINATION] Observation. Valid entries are EXPLODED, FEATHER, HINGE, OVERSHOT, and STEP. EXPLODED: terminations of flakes that shatter; FEATHER: normal terminations where the flake cleanly and smoothly exits the core surface; HINGE: flakes that end abruptly and hinge to the core surface; OVERSHOT: flakes exit the back of the core; STEP: flakes that end abruptly and step to the core surface.

[LENGTH] Caliper measurement. Millimeters. Distance from the point of percussion to the most distal point following the Jelinek method (Dogandžić et al., 2015).

[WIDTH] Caliper measurement. Millimeters. Distance across the flake at the midpoint of the length measurement and perpendicular to the length measurement (Dogandžić et al., 2015).

[THICK] Caliper measurement. Millimeters. Thickness is measured at the midpoint of the length measurement (Dogandžić et al., 2015).

[PLATWIDTH] Caliper measurement. Millimeters. Width of the platform measured box style between the most distant lateral points. By box style we mean that it is not the direct line distance between these two points. Rather it represents the width of a hypothetical rectangle or box placed on the platform and aligned with the interior of the flake (meaning also that it is aligned with the platform depth).

[PLATTHICK] Caliper measurement. Millimeters. Platform thickness (or platform depth, PD) is measured from the point of percussion directly back to the exterior face of the flake. In other words, platform thickness is not the maximum thickness, but rather the thickness at the point of percussion.

[FWEIGHT] Electronic scale measurement. Grams. Flake weight.

[BEVELWIDTH] Caliper measurement. Millimeters. Bevel width.

[FORCEAMT] Load cell measurement. Pounds (lbf). The maximum force recorded by the load cell during a flake removal event.

[SURFACEAREA] Microscribe measurement. Square Millimeters. Surface area is a measure of the area of a flake's interior surface. It was measured by tracing the edge with the stylus on the Microscribe.

[LIPPING] Observation. Valid entries are N/A, NO, YES. This refers to the presence of lipping on a flake.

[PLATFORMAREA] Microscribe measurement. Square Millimeters. Platform area is a measure of the area of a flake's platform. It was measured by tracing the edge of the platform with the stylus of the Microscribe.

[INITIALPLATTHICK] Caliper measurement. Millimeters. Initial platform thickness is the distance between the point of percussion and original platform surface before the bevel was cut (Leader et al. 2017:214).

[FVOLUME] Cubic millimeters. Flake volume is calculated by dividing flake mass with the density of the core material (Dogandžić et al., 2020).

Note: Flakes with SQUID between E-2001 and E-2112 (the low force flakes) from the Leader et al. (2017) experiment have a lower force-to-mass ratio that stands out from the rest of the flakes in the dataset. There are two possible explanations for this discrepancy in the force-mass relationship: 1) the load cell was incorrectly calibrated when recording the striking force for the low force flakes; 2) the platform beveling on some of these low force flakes might cause changes in the force-mass relationship that are yet to be investigated and understood. Given that the force-mass relationship among the low force flakes is internally consistent despite the differences in their beveling conditions, we think the first alternative is more plausible.

Appendix II Chapter 3 Supplementary Information

1 The drop tower setup

The drop tower used in our experiment is made of a vertical stand with an adjustable pole. An electromagnet switch controls the release of the hammer attached to a lever that can move along the supporting pole to adjust the hammer's drop height. To test the precision of the hammer strike, we dropped ball bearings onto targets drawn on carbon paper and compared the position of the mark made by the ball bearing and the original targets. The drop tower setup can achieve a precision of around 2 mm for aiming the striking target.

2 Supplementary figures

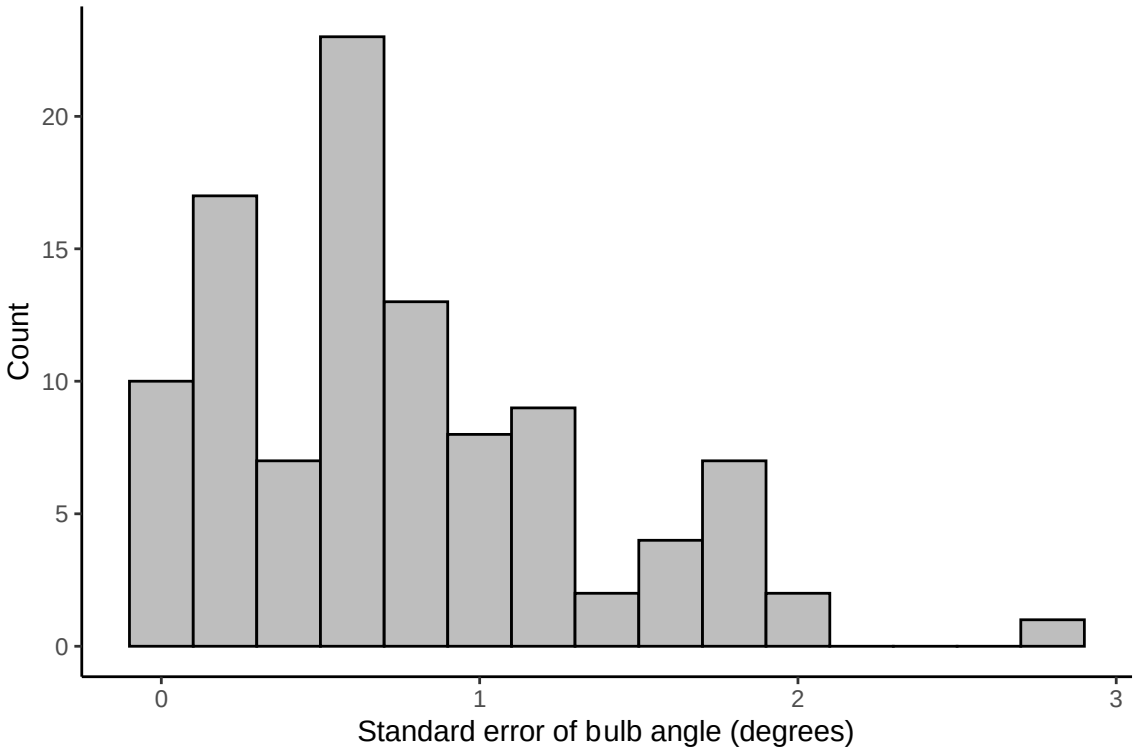

Fig.Appx-II. 1 Histogram showing the distribution of the standard error of the three bulb angle measurements for each flake in the drop tower dataset

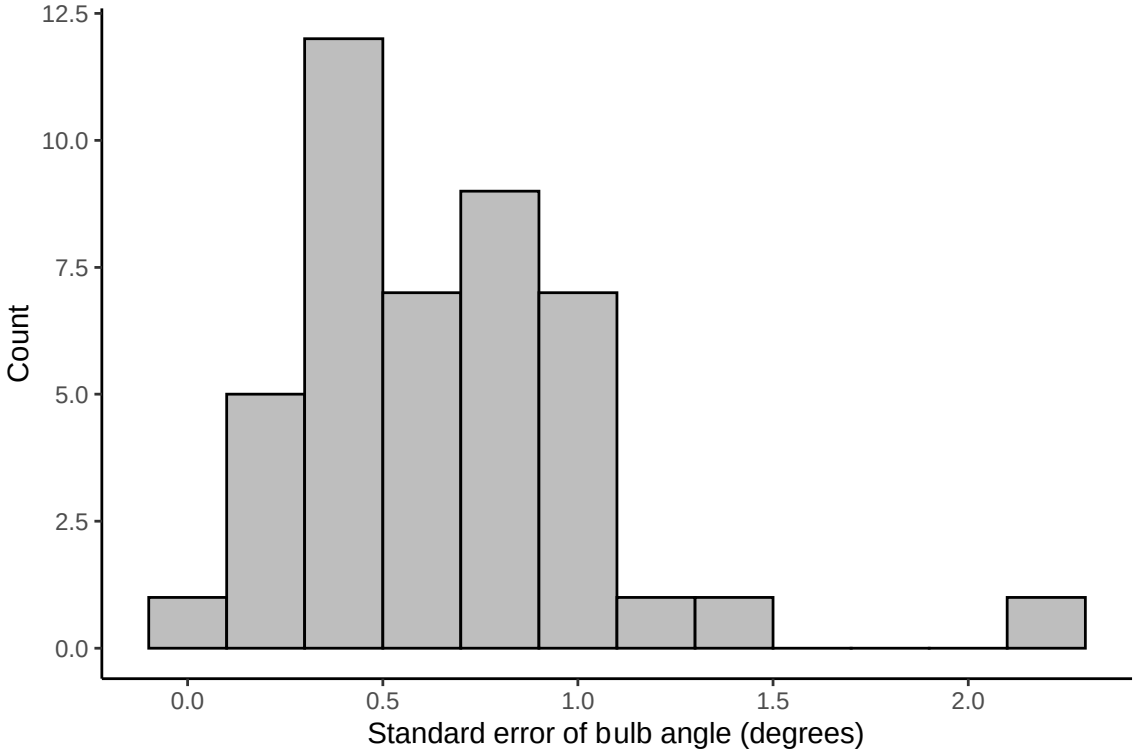

Fig.Appx-II. 2 Histogram showing the distribution of the standard error of the four bulb angle measurements for each flake in the MPI dataset

3 Supplementary tables

Table.Appx-II. 1 Summary statistics of bulb angle by angle of blow for the drop tower dataset (n = 103)

AOB	Count	Bulb angle (mean)	SD	Variance
-20	9	153.2	1.53	2.34
0	13	152.1	1.91	3.66
10	11	146.8	2.51	6.32
20	16	144.2	2.44	5.97
30	14	140.6	1.68	2.82
40	17	137.7	1.98	3.91
50	14	138.6	2.08	4.33
60	9	139.7	2.9	8.40

Table.Appx-II. 2 Summary of bulb angle by angle of blow based on the measurement method, VG refers to the virtual goniometer method and VC refers to the vector calculation method (the Dibble dataset, n = 70)

	Vector calculation		Virtual goniometer		
AOB	**Bulb angle (mean)**	**SD**	**Bulb angle (mean)**	**SD**	**Count**
0	150.3	5.4	152.8	4.7	9
5	142.0	12.1	147.5	8.7	4
10	142.7	4.7	142.9	4.5	7
20	140.7	4.1	140.0	4.8	17
30	136.6	3.9	139.8	4.8	13
40	135.3	6.1	134.3	8.4	3

Table.Appx-II. 3 Summary of angle blow prediction for all flakes in the MPI dataset

AOB assigned by knappers	**Average bulb angle**	**SD of bulb angle**	**Count**
High	132.0	3.61	21
Low	135.7	4.82	23

4 Statistical analysis

4.1 The drop tower dataset

Kruskal-Wallis test checking the difference in bulb angle by angle of blow for flakes in the drop tower dataset:

```
Kruskal-Wallis rank sum test
data:  bulb_angle by factor(AOB)
Kruskal-Wallis chi-squared = 84.709, df = 7, p-value = 1.503e-15
```

Linear regression to examine the effect of angle of blow and platform depth on bulb angle for flakes in the drop tower dataset:

```
Call:
lm(formula = bulb_angle ~ AOB + pd_mm, data = drop_tower_data)
Residuals:
 Min              1Q       Median  3Q       Max
-6.4598          -1.9173  0.1068  1.6500   7.9277
Coefficients:
                 Estimate          Std. Error          t value          Pr(>|t|)
```

(Intercept)	148.07148	0.75724	195.542	<2e-16 ***
AOB	-0.22362	0.01207	-18.534	<2e-16 ***
pd_mm	0.09445	0.05895	1.602	0.112

Signif. codes: 0 '***' 0.001 '**' 0.01 '*' 0.05 '.' 0.1 ' ' 1
Residual standard error: 2.759 on 98 degrees of freedom
(2 observations deleted due to missingness)
Multiple R-squared: 0.7802, Adjusted R-squared: 0.7757
F-statistic: 173.9 on 2 and 98 DF, p-value: < 2.2e-16

4.2 The Dibble dataset

Kruskal-Wallis test checking the difference in bulb angle (measured with the vector calculation method) by angle of blow for flakes in the Dibble dataset:

Kruskal-Wallis rank sum test
data: bulb_angle_vc by factor(aob)
Kruskal-Wallis chi-squared = 25.037, df = 5, p-value = 0.0001371

Linear regression to examine the effect of angle of blow, exterior platform angle, and platform depth on bulb angle (measured with the vector calculation method) for flakes in the Dibble dataset:

Call:

lm(formula = bulb_angle_vc ~ aob + platthick + epa, data = dibble_data)
Residuals:

Min	1Q	Median	3Q	Max
-20.5964	-2.2564	0.3315	3.2732	10.1760

Coefficients:

	Estimate	Std. Error	t value	Pr(>|t|)
(Intercept)	150.37597	7.47665	20.113	< 2e-16 ***
aob	-0.43329	0.06918	-6.263	9.19e-08 ***
platthick	0.92110	0.35241	2.614	0.0119 *
epa	-0.09841	0.10185	-0.966	0.3387

Signif. codes: 0 '***' 0.001 '**' 0.01 '*' 0.05 '.' 0.1 ' ' 1
Residual standard error: 5.028 on 49 degrees of freedom
Multiple R-squared: 0.4997, Adjusted R-squared: 0.469
F-statistic: 16.31 on 3 and 49 DF, p-value: 1.75e-07

Linear regression to examine the correlation between the angle of blow and platform depth in the Dibble dataset:

```
Call:
lm(formula = platthick ~ aob, data = dibble_data)
Residuals:
 Min      1Q  Median      3Q     Max
-4.2387 -1.3219 -0.2363  1.2620  4.8556
Coefficients:
             Estimate Std. Error t value Pr(>|t|)
(Intercept)  4.49304    0.50711   8.860  6.75e-12 ***
aob          0.08766    0.02378   3.686  0.000552 ***
---
Signif. codes:  0 '***' 0.001 '**' 0.01 '*' 0.05 '.' 0.1 ' ' 1
Residual standard error: 2.05 on 51 degrees of freedom
Multiple R-squared:  0.2104,    Adjusted R-squared:  0.1949
F-statistic: 13.59 on 1 and 51 DF,  p-value: 0.0005522
```

Kruskal-Wallis test checking the difference in bulb angle (measured with the virtual goniometer method) by angle of blow for flakes in the Dibble dataset:

```
Kruskal-Wallis rank sum test
data:  bulb_angle_vg by factor(aob)
Kruskal-Wallis chi-squared = 24.698, df = 5, p-value = 0.0001594
```

Linear regression to examine the effect of angle of blow, exterior platform angle, and platform depth on bulb angle (measured with the virtual goniometer method) for flakes in the Dibble dataset:

```
Call:
lm(formula = bulb_angle_vg ~ aob + epa + platthick, data = dibble_data)
Residuals:
Min      1Q  Median      3Q     Max
-12.708  -3.415   0.405   3.886  11.754
Coefficients:
             Estimate Std. Error t value Pr(>|t|)
(Intercept) 160.05965    8.03598  19.918  < 2e-16 ***
aob          -0.40944    0.07436  -5.506  1.34e-06 ***
epa          -0.17600    0.10947  -1.608   0.114
platthick     0.37066    0.37877   0.979   0.333
---
Signif. codes:  0 '***' 0.001 '**' 0.01 '*' 0.05 '.' 0.1 ' ' 1
Residual standard error: 5.404 on 49 degrees of freedom
Multiple R-squared:  0.4827,    Adjusted R-squared:  0.4511
F-statistic: 15.24 on 3 and 49 DF,  p-value: 3.893e-07
```

4.3 The MPI dataset

Kruskal-Wallis tests comparing the difference in bulb angle by angle of blow (the MPI

dataset):

Kruskal-Wallis rank sum test
data: Bulb_angle by factor(AOB_assigned)
Kruskal-Wallis chi-squared = 9.1067, df = 1, p-value = 0.002547

4.4 The EPA-PD model comparison

ANOVA test comparing the EPA-PD model and the EPA-PD-AOB model:

Analysis of Variance Table
Model 1: fweight_cbrt ~ platthick + epa
Model 2: fweight_cbrt ~ platthick + epa + aob

	Res.Df	RSS	Df	Sum of Sq	F	Pr(>F)
1	36	8.8933				
2	35	4.1241	1	4.7691	40.474	2.584e-07 ***

Signif. codes: 0 '***' 0.001 '**' 0.01 '*' 0.05 '.' 0.1 ' ' 1

ANOVA test comparing the EPA-PD model and the EPA-PD-BA model:

Analysis of Variance Table
Model 1: fweight_cbrt ~ platthick + epa
Model 2: fweight_cbrt ~ platthick + epa + bulb_angle_vc

	Res.Df	RSS	Df	Sum of Sq	F	Pr(>F)
1	36	8.8933				
2	35	4.6590	1	4.2343	31.809	2.303e-06 ***

Signif. codes: 0 '***' 0.001 '**' 0.01 '*' 0.05 '.' 0.1 ' ' 1

Analysis of Variance Table
Model 1: fweight_cbrt ~ platthick + epa
Model 2: fweight_cbrt ~ platthick + epa + bulb_angle_vg

	Res.Df	RSS	Df	Sum of Sq	F	Pr(>F)
1	36	8.8933				
2	35	5.4581	1	3.4352	22.028	4.036e-05 ***

Signif. codes: 0 '***' 0.001 '**' 0.01 '*' 0.05 '.' 0.1 ' ' 1

Appendix III Chapter 4 Supplementary Information

1 Supplementary figures

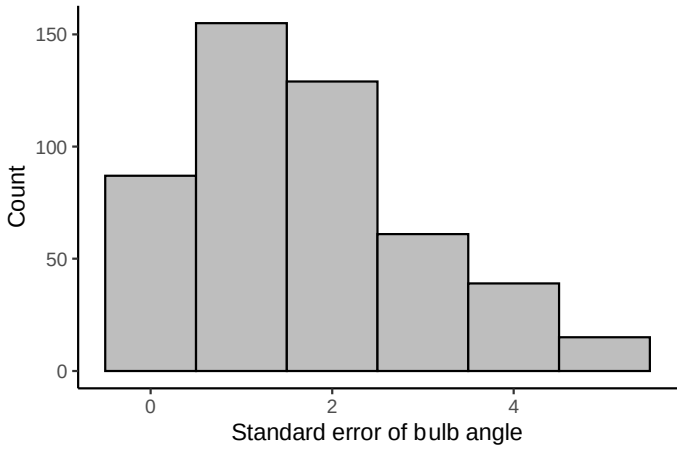

Fig.Appx-III. 1 Histogram of bulb angle standard error for flakes from the Early Pleistocene dataset

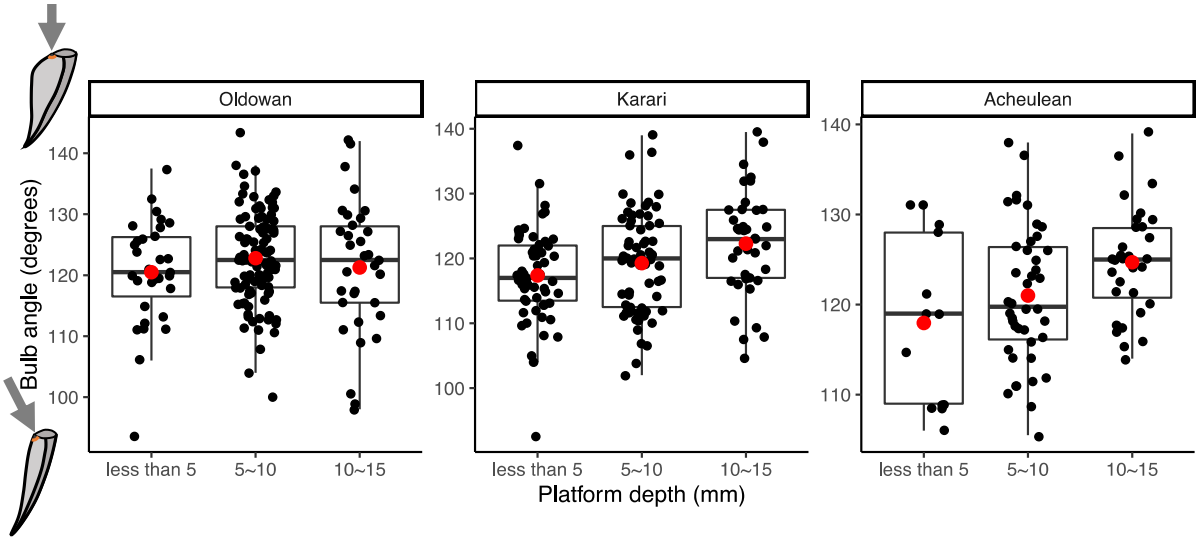

Fig.Appx-III. 2 Boxplots of the relationship between platform depth and bulb angle, using 15 mm as the upper cutoff to standardize platform depth. The red dot represents the average platform depth within each bulb angle group

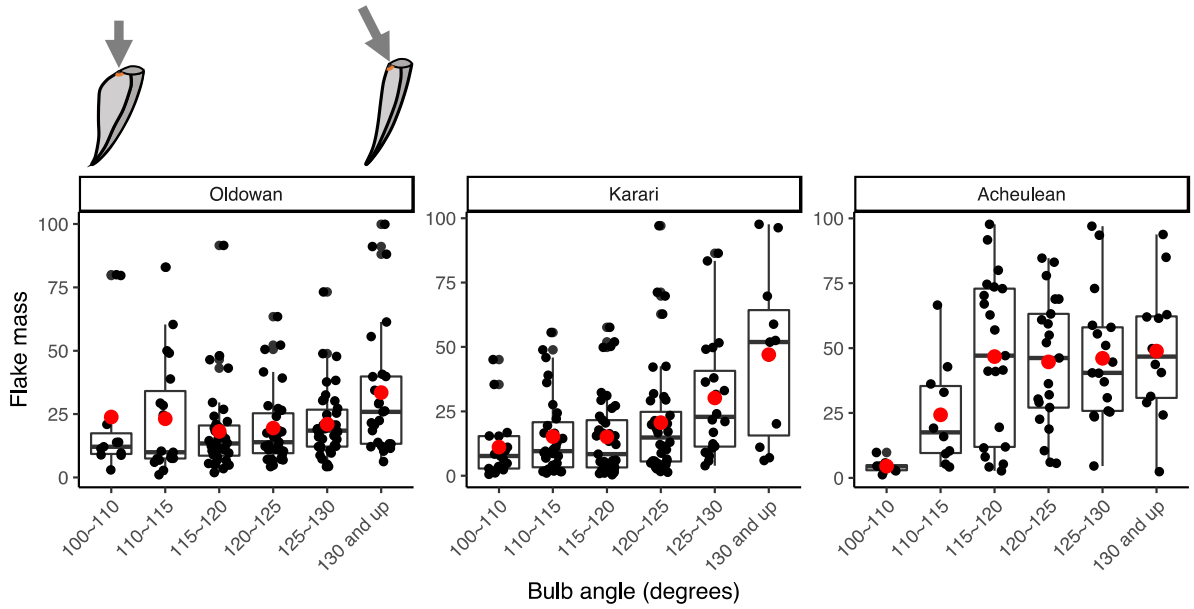

Fig.Appx-III. 3 Boxplots of the relationship between bulb angle and flake mass, using 100 g as the upper cutoff to standardize flake mass. The red dot represents the average flake mass within each bulb angle group